Quantum Master Equations for Spin Chemistry

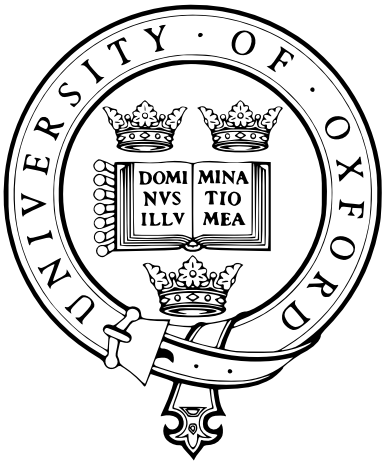

Thomas P. Fay

Corpus Christi College

University of Oxford

A thesis submitted for the degree of

Doctor of Philosophy

Michaelmas 2020

Quantum Master Equations for Spin Chemistry

Thomas P. Fay

Corpus Christi College

University of Oxford

A thesis submitted for the degree of

Doctor of Philosophy

Michaelmas 2020

Abstract

It is a remarkable fact that the interactions between electron and nuclear spins, and their interactions with a magnetic field, can have a profound effect on chemical reactivity, despite the fact that the characteristic interaction energies are orders of magnitude smaller than thermal energy. These observations are explained by the existence of long-lived quantum coherences between spins in certain molecular species (in particular radical pairs), and the study of these spin effects constitutes the field of *spin chemistry*, a field which spans a wide range of systems, from biochemical reactions to device physics.

Because spin chemistry involves subtle quantum effects, many intuitive models used by Physical Chemists, in particular classical kinetic equations, cannot be universally applied. On the other hand, complete first principles modelling of reactions involving spin effects comes at an impossibly high computational cost in complex systems, and often offers little physical insight. In order to address the shortcomings of these approaches, *quantum master equations* (QMEs) are employed to describe spin chemical phenomena. These are equations that describe a reduced set of degrees of freedom quantum mechanically, accounting for the effects of remaining degrees freedom implicitly.

In this thesis I explore the use of QME techniques to resolve a range of problems in spin chemistry. These techniques can be used to obtain the correct radical pair spin QME, resolving questions about the role of quantum measurement in these systems. As well as aiding the development of the theory of spin chemistry, QMEs provide a practical tool for modelling radical pair reactions including spin relaxation effects, as I also demonstrate. As a final study of QME techniques in spin chemistry, I use these methods to show when the classical kinetic description of radical pair reactions is and is not valid.

Publication List

Much of the work in this thesis is based on published peer-reviewed papers, which are listed below. Additional papers have also been published over as part of my DPhil research, but which do not directly form a part of this thesis, are also listed below.

Published work relevant to this thesis

T. P. Fay, L. P. Lindoy, and D. E. Manolopoulos, "Spin-selective electron transfer reactions of radical pairs: Beyond the Haberkorn master equation", J. Chem. Phys. **149**, 064107 (2018) [*The work presented in chapters 3, 4 and 5 is an expanded version of the work originally published in this paper.*]

T. P. Fay, L. P. Lindoy, and D. E. Manolopoulos, "Electron spin relaxation in radical pairs: Beyond the Redfield approximation", J. Chem. Phys. **151**, 154117 (2019) [*Some numerical studies on perturbative master equations in chapter 6, and the majority of the work presented in chapters 7 was originally published in this paper.*]

T. P. Fay and D. E. Manolopoulos, "Radical pair intersystem crossing: Quantum dynamics or incoherent kinetics?", J. Chem. Phys. **150**, 151102 (2019) [*The work presented in chapter 8 is an expanded version of the research originally published in this paper.*]

Additional published work

A. M. Lewis, T. P. Fay, D. E. Manolopoulos, C. Kerpal, S. Richert, and C. R. Timmel, "On the low magnetic field effect in radical pair reactions", J. Chem. Phys. **149**, 034103 (2018)

T. P. Fay, L. P. Lindoy, D. E. Manolopoulos, and P. J. Hore, "How quantum is radical pair magnetoreception?", Faraday Discuss. **221**, 77 (2019)

L. P. Lindoy, T. P. Fay, and D. E. Manolopoulos, "Quantum mechanical spin dynamics of a molecular magnetoreceptor", J. Chem. Phys. **152**, 164107 (2020)

Additional unpublished work

T. P. Fay, L. P. Lindoy, and D. E. Manolopoulos, "Spin relaxation in radical pairs from the stochastic Schrödinger equation", submitted [*The stochastic Scrödinger equation results in chapter 7 will be published here.*]

Acknowledgements

Whilst my narcissistic tendencies compel me to claim that I – and I alone – am responsible for the crafting of this tome over the past three years, I am honour-bound to acknowledge that such a task would not have been possible without the support of those around me, and here I will endeavour to thank each of them in the most (in)appropriate way.

Before I degenerate (further) into silliness, I should start with the serious acknowledgements.

First and foremost I would like to thank my supervisor, David Manolopoulos. I am grateful to him for his relentless enthusiasm, and for giving me the flexibility and encouragement to pursue my own interests. Subtlety is not a word commonly associated with David, but his subtle guidance, questioning and insight over the past years have been invaluable to me. Although I fear I may now have permanent hearing damage in my left ear from the thunderous way in which he announces his presence in the group office.

Secondly I would like to thank my comrades in the Manolopoulos group. I have learned much from our many fun discussions over the years (a few of which were about work). Special thanks go to Joe (whose deep physical insight has been inestimably valuable to me, although I think he may be responsible for the hearing loss in my *right* ear) and Lachlan (the coding savant whose energy is only matched by the bizarreness of his sleeping habits).

I would also like to thank Peter Hore, for sharing his wisdom through many enlightening discussions, as well as the many other members of the Spin Chemistry groups in Oxford for their experimental insights.

I must also thank all the tutors and teachers who have guided me along my academic trajectory, especially Kim, Jim, Grant, Rachel, Ann and Martin (who has also taught me much in the less academic pursuit of Karaoke).

The tea breaks and pub trips (in the Before Times) with the Theoretical Chemists have

formed an essential part of postgraduate study – I will sorely miss sharing the astringent coffee, mediocre beer and goofy conversations with all of you. (Max M deserves special credit for his persistence in rallying us.)

Without the companionship and support (in whatever colourful form that takes) of my many friends (one of whom is sadly no longer with us) the last few years would have quite frankly been hell, for even I can only tolerate so much Theoretical Chemistry. Specific thanks go to Ben S (for his gentle nonsense), Ben W, Katharine and Laura (for their astrological *and* psychoanalytical insights), Will, Max H, Jennifer, Tess, Dasha, Sam, Kesia, Rex and Jonathan, the many vibrant Corpuscles, and Angela (for your friendship in the strangeness of the post-Covid era). You have all enriched the past four years of my life in numerous ways (although perhaps not morally).

Finally, thank you Mum and Dad for the 26 years of love, kindness and support.

Contents

List of Figures

1 Introduction

Weak interactions between spins are not commonly thought of as a driving force in chemical processes, but in surprisingly many systems these weak spin interactions in fact play a decisive role.[3–8] The study of these effects is known as *spin chemistry*, and the paradigmatic system in which spin chemical effects manifest is the radical pair.[3,5–7] Radical pairs are important intermediates in a whole range of systems, ranging from light-harvesting molecular devices[9–11] to biological processes that underpin life on Earth,[12–17] but what perhaps makes radical pairs most fascinating (at least to the chemical physicist) is that they display quantum coherence effects at ambient temperatures in the condensed phases.[3,8] The long lived spin coherence in radical pairs is evidenced by the remarkable sensitivity of their reactions to extremely weak magnetic interactions between spins. This sensitivity can be exploited in many experiments as a probe of these systems[3–7,18–20] and magnetic field effects on radical pairs may even form the basis of certain biological functions.[7,21–24] Here I will give a brief overview of spin, radical pair reactions, and the theory used to describe them, setting the stage for the rest of the work presented in this thesis.

1.1 Spin

Electrons, and other particles like the nuclei of atoms, possess an intrinsic angular momentum referred to as spin. The spin angular momentum $\hat{\mathbf{S}}$ is a vector quantity, with operators $\hat{S}_x$, $\hat{S}_y$ and $\hat{S}_z$ corresponding to its three Cartesian vector components. These operators obey

the commutation relations,

$$[\hat{S}_x, \hat{S}_y] = i\hbar\hat{S}_z,\ [\hat{S}_y, \hat{S}_z] = i\hbar\hat{S}_x,\ [\hat{S}_z, \hat{S}_x] = i\hbar\hat{S}_y, \tag{1.1}$$

and from these commutation relations it can be shown that the total square spin angular momentum $\hat{S}^2 = \hat{\mathbf{S}} \cdot \hat{\mathbf{S}}$ commutes with each of its components,

$$[\hat{S}^2, \hat{S}_\alpha] = 0. \tag{1.2}$$

It is thus possible to specify a set of simultaneous eigenstates of $\hat{S}^2$ and $\hat{S}_z$, denoted $|S, M_s\rangle$, which satisfy

$$\hat{S}^2 |S, M_S\rangle = \hbar^2 S(S+1) |S, M_S\rangle \tag{1.3}$$

$$\hat{S}_z |S, M_S\rangle = \hbar M_S |S, M_S\rangle . \tag{1.4}$$

The total angular momentum quantum number S can take non-negative integer and half-integer values, and the projection quantum number M_S takes values from $-S$ to S in integer steps. Due to the frequency with which they are encountered, the $S = 1/2$ spin states are often specially denoted $|\alpha\rangle$ and $|\beta\rangle$,

$$|\alpha\rangle = \left|\frac{1}{2}, +\frac{1}{2}\right\rangle,\ |\beta\rangle = \left|\frac{1}{2}, -\frac{1}{2}\right\rangle. \tag{1.5}$$

Particles in nature often possess a well defined total spin angular momentum, for example electrons and ^{1}H nuclei (protons) are $S = 1/2$ particles and ^{14}N nuclei are $S = 1$ particles.

For a system composed of two spins, with spin operators $\hat{\mathbf{S}}_i$ where $i = 1$ or 2, the total angular momentum $\hat{\mathbf{S}} = \hat{\mathbf{S}}_1 + \hat{\mathbf{S}}_2$ is itself an angular momentum operator, meaning it obeys the commutation relations in Eq. (1.1), so there exists a set of eigenstates obeying Eqs. (1.3) and (1.4). If the total angular momentum quantum numbers of spins 1 and 2 are S_1 and S_2, the total angular momentum quantum number S can only take values in integer steps between $S_1 + S_2$ and $|S_1 - S_2|$. This means that for a pair of electron spins, there are two sets of total angular momentum states: one with $S = 0$, the singlet state $|\mathrm{S}\rangle$, and one with

$S = 1$, the triplet states $|\mathrm{T}_m\rangle$, which can be written in terms of the uncoupled states as

$$|\mathrm{S}\rangle = \frac{1}{\sqrt{2}}\Big(|\alpha_1\beta_2\rangle - |\beta_1\alpha_2\rangle \Big) \tag{1.6a}$$

$$|\mathrm{T}_+\rangle = |\alpha_1\alpha_2\rangle \tag{1.6b}$$

$$|\mathrm{T}_0\rangle = \frac{1}{\sqrt{2}}\Big(|\alpha_1\beta_2\rangle + |\beta_1\alpha_2\rangle \Big) \tag{1.6c}$$

$$|\mathrm{T}_-\rangle = |\beta_1\beta_2\rangle\,. \tag{1.6d}$$

These coupled electron spin states will be of central importance in understanding spin coherence effects in radical pairs.

1.2 Radical pair reactions

A radical is a chemical fragment which contains an unpaired electron, and therefore possesses a net electron spin angular momentum. Radicals are typically highly reactive and therefore generally only exist transiently as intermediates in some chemical reactions. One observation that has sparked much intrigue is the large effect that applied magnetic fields can have on reactions between pairs of radicals.[3–7] The source of this intrigue is that chemical reactivity is normally governed by energy differences between states relative to thermal energy, $k_\mathrm{B}T$.[7] Magnetic field effects on radical pair reactions typically greater than 10% can been seen with magnetic field strengths as low as 1 mT at room temperature,[3–7,25–30] (although magnetic field effects as large as 2600% have recently been observed in 1 T fields[31]) but remarkably under these conditions the Zeeman splitting of the electron spin energy levels is only $10^{-6}k_\mathrm{B}T$, so one would only expect changes in thermal populations of spin states of about 0.0001%. How then can magnetic field effects as large as 10% be observed on these reactions? The answer lies in the unique properties of the radical pair intermediate, and therefore this mechanism by which magnetic field effects are produced is referred to as the *radical pair mechanism*.

The radical pair mechanism has its origin in (i) the spin state selectivity of the reactions of a radical pair intermediate, (ii) the small energetic separation of spin states in spatially separated radical pairs, (iii) the highly non-equilibrium nature of the radical pair interme-

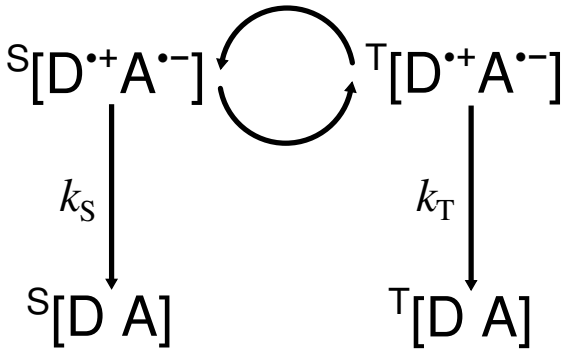

Figure 1.1: A diagrammatic representation of the radical pair mechanism for a $D^{\bullet+}A^{\bullet-}$ radical pair.

diate, and (iv) the slow rate of thermalisation of the spins. In a reaction between a pair of radicals the total electron spin state is conserved, and in the absence of strong spin-orbit coupling (as is the case in many reactions of organic radicals[7]) the products of the radical pair reaction have a well-defined total electronic spin angular momentum; they are either $S = 0$ singlets or $S = 1$ triplets. Conservation of spin angular momentum in the reaction process means that only radical pairs where the electrons are in a singlet state can recombine to give a singlet product.[3,7] Similarly only triplet radical pairs can react to give a triplet product. This reaction mechanism is summarised in Fig. 1.1 for a radical pair consisting of a excited donor-acceptor radical ion pair, $D^{\bullet+}A^{\bullet-}$, recombining to give either a singlet ^{S}[D A] or triplet ^{T}[D A] product.

If the radicals spend most of their time relatively well separated in space, then the average exchange interaction between them will be very weak, typically much smaller than $k_B T$.[3,7] This means that very weak magnetic interactions between the electron spins and nuclear spins or an external magnetic field can mix singlet and triplet electron spin states of the radical pair. Because these magnetic interactions are so weak, the spins are usually only very weakly coupled to other thermalised degrees of freedom in the chemical system, such as vibrations and rotations of the radicals and any surrounding solvent, so the thermalisation of spins to equilibrium is slow, and quantum coherences between spin states are long lived.[3,7] This means that weak magnetic interactions can control intersystem crossing in the radical pair which can be translated into magnetic field effects on quantum yields of competing reaction pathways and rates of reaction.[3–7] This coherent interconversion process is represented in Fig. 1.1 by the curved arrows between the radical pair singlet and triplet states.

1.2.1 Quantum dynamics

The existence of long lived coherences between spin degrees of freedom in radical pairs means that the mathematical description of the radical pair must explicitly include these coherences, however it is unfeasible (and unnecessary) to include all spin, electronic, vibrational and rotation degrees of freedom in the description of the radical pair. Instead the radical pair is described with an effective spin density operator $\hat{\rho}(t)$ for the electron and nuclear spins in the radical pair. The time evolution of this is normally described by the phenomenological Haberkorn master equation,[3,32–34]

$$\frac{\mathrm{d}}{\mathrm{d}t}\hat{\rho}(t) = -\frac{i}{\hbar}\left[\hat{H}, \hat{\rho}(t)\right] - \left\{\hat{K}, \hat{\rho}(t)\right\}. \tag{1.7}$$

The weak magnetic interactions which generate coherent spin dynamics are all contained in the effective spin Hamiltonian $\hat{H}$, and $[\cdot,\cdot]$ denotes the commutator, so the first term describes the coherent spin dynamics of the radical pair. The second term in this equation describes the evolution of the spin density operator due to the spin selective reactions, where $\{\cdot,\cdot\}$ denotes the anticommutator and $\hat{K}$ is the Haberkorn reaction operator, which is given by[32]

$$\hat{K} = \frac{k_\mathrm{S}}{2}\hat{P}_\mathrm{S} + \frac{k_\mathrm{T}}{2}\hat{P}_\mathrm{T}, \tag{1.8}$$

in which k_S and k_T and the first order singlet and triplet radical pair reaction rate constants, and $\hat{P}_\mathrm{S}$ and $\hat{P}_\mathrm{T}$ are projection operators onto the singlet and triplet electron spin states.

The time dependent spin density operator can then be used to obtain observables of the radical pair reaction, for example the time dependent singlet and triplet populations of the radical pair, $\langle P_\mathrm{S}(t)\rangle$ and $\langle P_\mathrm{T}(t)\rangle$, are given by

$$\langle P_\mathrm{S}(t)\rangle = \mathrm{Tr}\left[\hat{P}_\mathrm{S}\hat{\rho}(t)\right] \tag{1.9a}$$

$$\langle P_\mathrm{T}(t)\rangle = \mathrm{Tr}\left[\hat{P}_\mathrm{T}\hat{\rho}(t)\right], \tag{1.9b}$$

where $\mathrm{Tr}[\cdots]$ denotes the trace over spin degrees of freedom. Further details of the spin density operator description of radical pair are given in chapters 2, 3 and 6.

The initial condition for the spin density operator is dictated by how the radical pair is

formed.[3,7] A commonly encountered case is where the radical pair is formed by a series of spin conserving electron transfer reactions initiated by photoexcitation of a singlet ground state, therefore the spin density operator initially corresponds to a singlet electronic state, with the nuclear spins in thermal equilibrium, so $\hat{\rho}(0) \propto \hat{P}_{\mathrm{S}}$.[3,7]

Although Eq. (1.7) has been used for many years to describe radical pair reactions,[3] it was originally proposed based on phenomenological arguments,[32] and in recent years its validity has been called into question, with alternative quantum measurement based descriptions of the spin density operator evolution being proposed.[35–38] In chapter 3 this is addressed in detail, by starting from fundamental chemical reaction rate theory, but for the purpose of introducing radical pair reactions and the role of magnetic interactions in their dynamics Eq. (1.7) will suffice.

1.2.2 Spin interactions

The effective spin Hamiltonian describes all of the weak magnetic interactions of spins in the radical pair, and here I will provide a brief overview of the most important magnetic interactions in the context of radical pair reactions. Firstly the spin Hamiltonian can be split into an electron spin term $\hat{H}_{\mathrm{e}}$ and two single radical hyperfine coupling Hamiltonians $\hat{H}_{\mathrm{hfc},i}$,

$$\hat{H} = \hat{H}_{\mathrm{e}} + \hat{H}_{\mathrm{hfc},1} + \hat{H}_{\mathrm{hfc},2}. \tag{1.10}$$

The electron spin term can be written as follows

$$\hat{H}_{\mathrm{e}} = \mu_{\mathrm{B}}\mathbf{B}\cdot\mathbf{g}_1\cdot\hat{\mathbf{S}}_1 + \mu_{\mathrm{B}}\mathbf{B}\cdot\mathbf{g}_2\cdot\hat{\mathbf{S}}_2 - 2J\hat{\mathbf{S}}_1\cdot\hat{\mathbf{S}}_2 + \hat{\mathbf{S}}_1\cdot\mathbf{D}\cdot\hat{\mathbf{S}}_2. \tag{1.11}$$

The first two terms in this equation describe the Zeeman interaction of the radical electron spins, where μ_{B} is the Bohr magneton, $\mathbf{B}$ is the external magnetic field vector, $\mathbf{g}_i$ is the g tensor for radical i, and $\hat{\mathbf{S}}_i$ is the unitless[a] electron spin operator for radical i.[3,7] Spin orbit interactions in the radicals lead to deviations in the radical g tensors from the free electron g tensor of $\mathbf{g}_{\mathrm{e}} = g_{\mathrm{e}}\mathbf{1}$, where $\mathbf{1}$ is an identity matrix. The deviations from the free electron g tensor can be split into an isotropic part $(g_i - g_{\mathrm{e}})\mathbf{1}$ and an anisotropic part $\Delta\mathbf{g}_i$,

[a]From this point on I will exclusively use unitless spin operators, so the factors of $\hbar$ in section 1.1 are dropped in the definitions of the spin operators. This means that J and $\mathbf{D}$ have units of energy.

which is a real symmetric traceless matrix.[3,7,39] The third term in $\hat{H}_{\mathrm{e}}$ describes the scalar interaction between electron spins, where J is the isotropic scalar coupling constant, which is a combination of the direct exchange interaction between the radicals, and long range superexchange coupling interactions.[3,7] The final term describes the anisotropic magnetic dipole coupling between the two radical electron spins, where $\mathbf{D}$ is the real symmetric dipolar coupling tensor.[3,7]

The hyperfine coupling Hamiltonians $\hat{H}_{\mathrm{hfc},i}$ describe the magnetic interactions between the N_i nuclear spins in each radical, with corresponding spin operators $\hat{\mathbf{I}}_{ik}$, and the electron spin in each radical. These Hamiltonians are given by

$$\hat{H}_{\mathrm{hfc},i} = \sum_{k=1}^{N_i} \hat{\mathbf{S}}_i \cdot \mathbf{A}_{ik} \cdot \hat{\mathbf{I}}_{ik}, \tag{1.12}$$

where the total hyperfine coupling tensor for a given nuclear spin $\mathbf{A}_{ik}$ is given by $\mathbf{A}_{ik} = a_{ik}\mathbf{1} + \Delta\mathbf{A}_{ik}$.[3,7,40] a_{ik} is the isotropic hyperfine coupling constant for nuclear spin k in radical i, the strength of which is controlled by the Fermi contact interaction, which is the magnetic interaction of the electron spin density within the nucleus with the nuclear spin.[3,7,40] $\Delta\mathbf{A}_{ik}$ is the traceless anisotropic coupling tensor that describes the dipolar interaction between the electron spin density in radical i with nuclear spin k.[40] For radical pairs tumbling freely in solution, the anisotropic dipolar coupling terms, $\Delta\mathbf{A}_{ik}$ and $\mathbf{D}$, and the anisotropic components of $\mathbf{g}_i$ all average to zero, leaving only the isotropic coupling terms in the spin Hamiltonian.[7]

Here I have only briefly described the important spin interactions, more detailed discussion of the origins of these terms will be given in chapter 3. It should be noted that this description of the radical pair spin Hamiltonian ignores nuclear Zeeman and nuclear spin-nuclear spin coupling, an assumption that is normally justified because these interactions are much weaker than those described above, so these nuclear spin interactions have a negligible effect on the spin dynamics.[3,7] This can be understood by noting that the magnetic interactions are all proportional to the gyromagnetic ratios of the spins involved, and since the nuclear gyromagnetic ratios are typically much smaller than the electronic gyromagnetic ratio, nuclear Zeeman terms and nuclear spin coupling terms can be safely

neglected.

1.2.3 Magnetic field effects

In order to understand magnetic field effects on radical pair reactions, we first need to assess which terms in the spin Hamiltonian do not commute with $\hat{S}^2$, since these lead to interconversion between singlet and triplet electron spin states. Because $[\hat{S}^2, \hat{S}_{i\alpha}] \neq 0$ the hyperfine coupling terms cause transitions between singlet and triplet states, so these terms give rise to the hyperfine coupling mechanism of radical pair intersystem crossing.[3] Similarly, if the g tensors of the radicals are isotropic, so $\mathbf{g}_i = g_i\mathbf{1}$ where g_i is the isotropic g factor for radical i, and $\mathbf{B}$ is aligned along the z axis, the difference between the electron g factors, $\Delta g = g_1 - g_2$, gives rise to a term which couples $|\mathrm{S}\rangle$ and $|\mathrm{T}_0\rangle$ states.[3] This mechanism for radical pair intersystem crossing is referred to as the Δg mechanism.

The presence of the electron spin Zeeman interaction in radical pairs means that applied magnetic fields can affect the interconversion of singlet and triplet radical pairs, thereby altering lifetimes and singlet and triplet product yields. These magnetic field effects can be understood by considering the eigenstates of $\hat{H}_\mathrm{e}$ for a system without anisotropic couplings, and when $g_1 = g_2 = g_\mathrm{e}$ and $\mathbf{B} = (0, 0, B)^\mathsf{T}$. In this case, $\hat{H}_\mathrm{e}$ commutes with $\hat{S}^2$, and also $\hat{S}_z$, so the eigenstates of $\hat{H}_\mathrm{e}$ are simply the coupled electron spin eigenstates $|\mathrm{S}\rangle$ and $|\mathrm{T}_m\rangle$, with energy eigenvalues given by

$$E_\mathrm{S} = \frac{3}{2}J \tag{1.13a}$$

$$E_{\mathrm{T}_m} = -\frac{1}{2}J + m g_\mathrm{e}\mu_\mathrm{B}B. \tag{1.13b}$$

The magnetic field alters the energy gap between singlet and triplet states, which thus changes the rate of intersystem crossing between these states. In particular when $B = \pm 2J/(g_\mathrm{e}\mu_\mathrm{B})$ the $|\mathrm{S}\rangle$ and $|\mathrm{T}_\pm\rangle$ states will have the same energy, as is illustrated in the left hand panel of Fig. 1.2. At this resonance, the rate of interconversion induced by the hyperfine coupling terms between these states will be maximised, which causes product yields and radical pair lifetimes to go through either a maximum or a minimum at this applied field strength.[3,5]

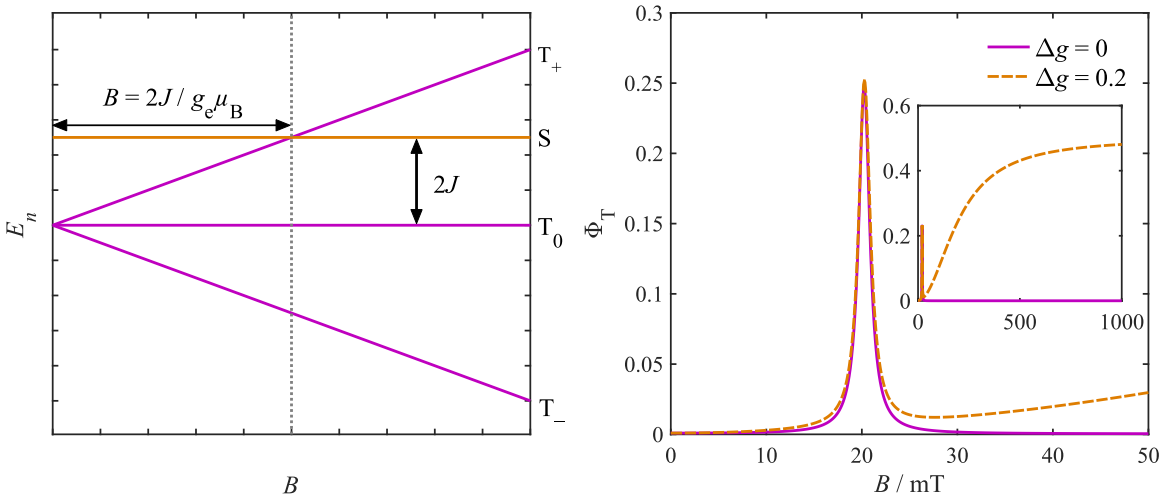

Figure 1.2: Left panel: the singlet and triplet energies in the absence of Δg and hyperfine coupling effects. Right panel: triplet quantum yields for a singlet-born one proton radical pair with $2J/g_e\mu_B$ = 20 mT, $a/g_e\mu_B$ = 1 mT and $k_S = k_T$ = 10 μs^{-1}, as a function of applied magnetic field strength, for two different values of Δg.

A second type of magnetic field effect arises from the Δg mechanism. When the difference in isotropic g factors between the two radicals, Δg, is non-zero, the coupling between $|S\rangle$ and $|T_0\rangle$ states introduced is $\mu_B \Delta g B/2$. This means that as the applied magnetic field strength is increased, the rate of transitions between $|S\rangle$ and $|T_0\rangle$ states increases, which can also lead to changes in product yields and the radical pair lifetime. Because the coupling is proportional to B, the Δg mechanism of intersystem crossing becomes more significant at higher applied field strengths.[5,7]

The magnetic field effect on the triplet product quantum yield is shown for a model calculation in the right hand panel of Fig. 1.2 for a singlet-born ($\hat{\rho}(0) = \hat{P}_S/2$) radical pair with one hyperfine coupled proton and $2J/g_e\mu_B$ = 20 mT. A resonance effect in the triplet quantum yield at $B = 2J/g_e\mu_B$ can clearly be seen, where it passes through a maximum as at this field strength there is efficient interconversion between the initial S state and the T_+ state of the radical pair. When $\Delta g \neq 0$ there is also an increase in the triplet quantum yield with applied field strength, an effect which plateaus at very high fields (as is shown in the insert of the right panel of Fig. 1.2), due to interconversion between S and T_0 states induced by the Δg mechanism. The plateauing of Φ_T when $\Delta g \neq 0$ at large field strengths occurs when the singlet-triplet interconversion is much faster than the reaction rates of the singlet and triplet states.

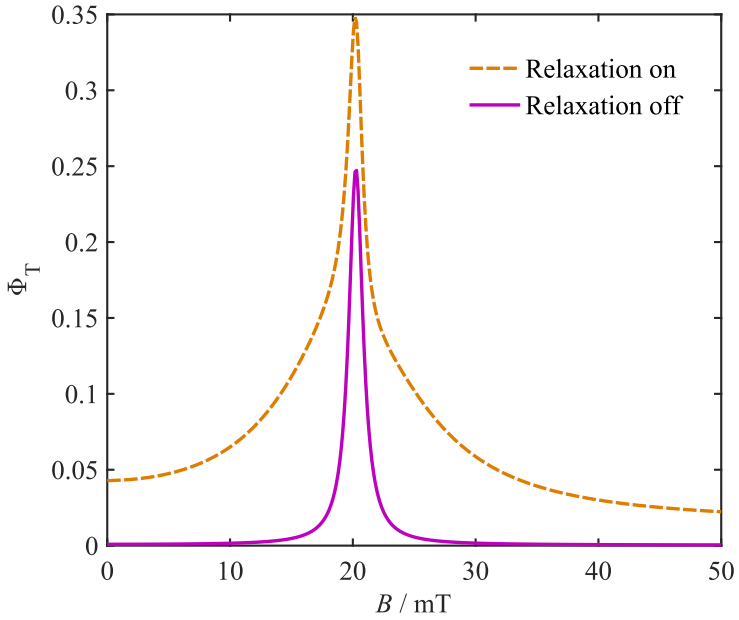

Figure 1.3: The triplet quantum yield of a model one proton radical pair with and without spin relaxation effects. In this case the spin relaxation mechanism included is modulation of anisotropic hyperfine coupling between the proton and electron spin by isotropic rotational Brownian motion. This model uses the same parameters as in Fig. 1.2, with relaxation parameters $\Delta A/g_e\mu_B = 1$ mT and $\tau_R = 1$ ns. Details of the simulation method can be found in chapter 6.

A more subtle magnetic field effect appears at low field strengths when J is close to zero. In this case the rate of singlet triplet interconversion increases with a very small applied field strength, even though the T_+ and T_- states move away from the S state in energy with the application of a field.[6,7] This low magnetic field effect arises due to symmetry breaking in the spin Hamiltonian caused by the application of a field, which creates new pathways for interconversion of S and T_0, which then increases the rate of mixing between these states.[41,42] Although the low magnetic field effect is important in many systems, in the applications considered in this thesis in chapters 7 and 8, the magnetic field effects observed can be understood just in terms of the resonance effect and the Δg mechanism.

1.2.4 Spin relaxation

The spin density operator description of the radical pair given above treats the spin coupling parameters as constants, but in a real physical system molecular vibrations and rotations modulate these parameters.[3,43] This modulation induces transitions between spin states, and leads to decoherence, relaxing the spin system to thermal equilibrium.[3,44–48] These spin relaxation effects are often as important as the coherent spin state interconversion effects, so for the quantitative interpretation of experimental data it is important to include relaxation.[47–53] As a simple demonstration of the importance of spin relaxation effects, in

Fig. 1.3 the triplet quantum yield of a singlet-born one proton radical pair is shown with and without spin relaxation from modulation of the proton-electron dipolar coupling by rotational Brownian motion. In this example we see that the inclusion of spin relaxation increases the triplet quantum yield and significantly broadens the magnetic field effect resonance. This topic will be discussed in more detail in chapter 6.

1.3 Quantum master equations

As mentioned above, it is unfeasible to include all vibrational, electronic, rotational and spin degrees of freedom in the description of radical pair dynamics, so instead we work with a reduced number of degrees of freedom, in this case the spin degrees of freedom of the radical pair, and treat the remaining degrees of freedom in some other way. The equations that govern the dynamics of the reduced description of a problem are called *quantum master equations*[54–56] and therefore the equation for the spin density operator $\hat{\rho}(t)$ given by Eq. (1.7) is an example of a quantum master equation, which in this case was originally obtained phenomenologically.

There exists a large set of techniques for deriving both exact and approximate quantum master equations starting from a full description of a given system.[54,55,57–65] These techniques form the basis of much of the work in this thesis, where they will be applied to solve many problems associated with radical pair dynamics. The starting point for much of this work is the Nakajima-Zwanzig equation, a formally exact quantum master equation which is derived using projection operator techniques.[57–59] For now however I will leave a detailed discussion of quantum master equations to chapter 2, and move on to consider some important systems involving radical pair intermediates.

1.4 Applications

Radical pairs play an important role in many chemical processes, especially in molecules which use light energy to drive chemical reactions. An overview of several of these systems is given below.

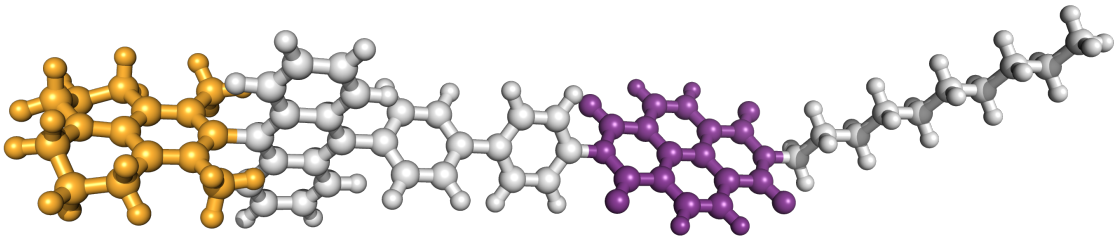

Figure 1.4: An example D – B – A system, DMJ – An – Ph_2 – NDI. The electron donor DMJ is highlighted in orange and the electron acceptor NDI is highlighted in purple.

1.4.1 Light-harvesting molecular devices

A common method for turning light energy into chemical energy, is to use photoexcitation to drive electron transfers.[9,26,48,50,66–68] This process of photoexcitation followed by electron transfer from a donor to an acceptor generates radical ion pairs.[9] The fate of the radical ion pair intermediates is often dictated by spin interactions, and the properties and dynamics of these systems can therefore be probed through magnetic field effects.[26,48,50,66–68] It has been proposed that these types of light-harvesting molecules could form the basis of many useful devices, including artificial photosynthetic reaction systems,[9,48,50] photovoltaics with improved efficiency,[69] magnetic field sensors,[25] and potentially even molecular qubits for quantum computation[11,70–72] and other spintronic devices.[73,74]

The most common setup for these systems is the D – B – A system, where D is an electron donor, A is an electron acceptor, and B is some molecular bridge covalently bonded to D and A which facilitates efficient electron transfer between the two. One of these fragments acts as a chromophore, absorbing light to create a local excitation, normally from the HOMO to LUMO of that fragment, in which there is a high energy electron, and a low energy electron vacancy. This initiates transfer of an electron from D to A, for example if D is initially excited, then the high energy electron will transfer into a lower energy unoccupied orbital on A, often via an intermediate in which B is charged. This is the typical process by which $D^{\bullet+}-B-A^{\bullet-}$ radical ion pairs are formed in these devices. These radical ion pairs can then in principle used to drive other processes, for example to act as sensors or drive other chemical reactions. The two examples that will be studied in chapters 7 and 8 are D – B – A systems of this type.[26,67] An example of one such molecule, which is examined

in more detail in chapter 7, is the DMJ – An – Ph_2 – NDI which is shown in Fig. 1.4,[67] with the electron donor, DMJ, in orange and the electron acceptor, NDI, in purple.

1.4.2 Biological electron transfers

Many important biological electron transfer processes involve radical ion pairs, for example in photosynthetic reaction systems, the first step in transforming light energy into chemical energy involves the formation of a radical ion pair in the reaction centre of photosystems.[12–17] Another example in which radical pairs play an important role in biology is in the formation of reactive oxygen species in Cryptochromes,[75–77] which may form the basis of signalling mechanisms for various processes in plants.[78–80]

The presence of radical pairs in these biological electron transfer processes is evidenced by magnetic field effects.[13,14] In such complex systems it can be difficult to directly observe or extract information about short lived intermediates in a specific and selective manner. However, since only reactions involving paramagnetic species, such as radical pairs, are affected by magnetic fields, magnetic field effects provide a powerful tool for probing these intermediates. Examples of such experiments include the detection of field induced nuclear spin hyperpolarisation with NMR[14,19], or using optical spectroscopy to detect magnetic field effects on concentrations of intermediates.[81,82]

1.4.3 Avian magnetoreception

One subject on which much recent research into radical pair reactions has been focussed is avian magnetoreception.[7,22,23,44–46,49,84–91] It is known from behavioural studies of migratory birds that they possess a magnetic compass sense, sensitive to the Earth's magnetic field, which they use for navigation.[21,22,84] This research has also shown that this magnetic compass sense is light dependent; in particular in certain birds it has been shown that this compass sense only works when blue/green light is present.[92] These observations have led to the hypothesis that radical pair reactions may form the physical basis of this compass sense. This is because radical pair reactions can have an orientation dependent magnetic field response due to anisotropic coupling terms in the spin Hamiltonian, and they are often formed by photoexcitation, which can only occur for certain wavelengths of incident

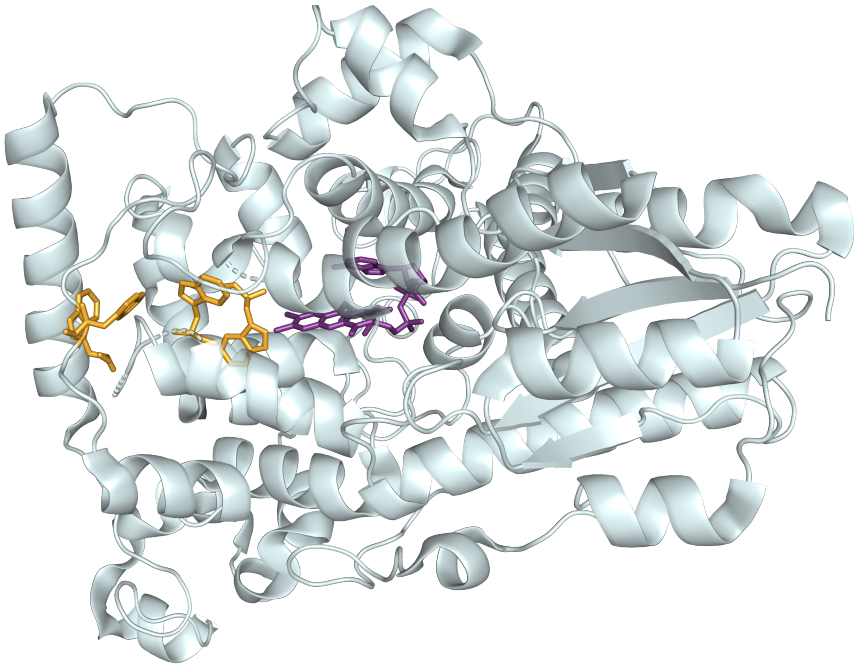

Figure 1.5: The drosophila melanogaster cryptochrome crystal structure (Protein Databank entry 4GU5[83]) with the FAD cofactor highlighted in purple and the tryptophan tetrad highlighted in orange.

light.[21,88]

In particular it has been proposed that radical pairs may be formed in cryptochrome proteins in the bird's eye.[21,93] Cryptochromes contain a bound flavin adenine dinucleotide (FAD) cofactor, which is known to absorb light in the blue/green region of the spectrum.[94] Also it is known that in many cryptochromes, after photoexcitation of the fully oxidised FAD, an electron transfer reaction occurs with a neighbouring tryptophan residue (Trp), reducing the FAD to $FAD^{\bullet -}$, and oxidising the Trp to $Trp^{\bullet +}$.[94] After this initial electron transfer, a sequence of electron transfers occurs along either a triad or tetrad of Trp residues, eventually forming a well-separated radical ion pair.[94] The structure of one such cryptochrome, *drosophila melanogaster* cryptochrome, which is known to form a radical ion pair,[95,96] is shown in Fig. 1.5, with the FAD cofactor in purple and the Trp tetrad in orange. The recombination of this radical pair to the singlet ground state competes with spin-independent deprotonation of the $Trp^{\bullet +}$ radical, and therefore the yield of these two reactions is magnetic field dependent.[21,22] It has been proposed that the magnetic field orientation dependence of the quantum yields of these competing reactions could form the basis of avian magnetoreception.[21,93]

Whilst the $FAD^{\bullet-} - Trp^{\bullet+}$ radical pair is known to form in many cryptochromes, it may not be the radical pair directly responsible for the sensing of the Earth's magnetic field. Alternative radical pairs have also been proposed which may be formed from this initial radical pair, such as FAD-tyrosine,[21,97] FAD-ascorbyl,[98] and FAD-superoxide.[99,100] It has also been suggested that a hypothetical radical triad could display a much higher sensitivity to magnetic fields than any of these radical pairs.[85,86,89] In all of these hypotheses, the key magnetic field sensing process relies on spin coherence between radicals and the spin-dependent reactions, and although the work is this thesis does not directly explore this problem, the theoretical results presented are all applicable to spin chemical effects in biological systems.

1.5 Outline of thesis

This thesis focusses on the application of quantum master equations in spin chemistry, with a specific focus on radical pair reactions. The framework of quantum master equations will been shown to provide a powerful tool for understanding radical pair reactions, such as resolving theoretical questions about the role of quantum measurement theory in spin chemistry, and developing new methods for accurately modelling real radical pair reactions.

Chapter 2 will provide an overview of the general theory of quantum master equations, including several useful techniques for deriving approximate master equations. The main result that will be discussed is the Nakajima-Zwanzig equation, a formally exact master equation applicable to arbitrary systems, which forms the foundation for much of the work presented in the following chapters.

In chapters 3, I will then present an application of these techniques to derive a radical pair quantum master equation which is consistent with the well-established theory of electron transfer reactions. The resulting quantum master equation and its derivation provides insights into the role of quantum measurement theory in radical pair reactions, which has been disputed for some time. Analysis of the quantum master equations using a set of classical approximations is presented in chapter 4, and numerical tests of the theory on a model problem are presented in chapter 5. Following on from this, in chapter 6 the

generalisation of this to include relaxation effects within the Stochastic Liouville equation (SLE) formalism will also be presented. In this chapter I will also discuss how to apply quantum master equation techniques to find accurate approximate solutions to the SLE.

The work that will be presented in chapters 7 and 8 focusses on using master equations to simulate real radical pair reactions, allowing us to gain new understanding of different spin-chemical effects in these systems. In chapter 7 I will describe a method for finding accurate approximate solutions to the radical pair Stochastic Liouville equation using a combination of perturbative master equation techniques and a semiclassical approximation for the spin dynamics. This is applied to investigate the role of spin relaxation effects in $DMJ^{\bullet+}-An-Ph_n-NDI^{\bullet-}$ radical pairs, in a level of detail that cannot be achieved through simple examination of the experimental data. Then in chapter 8 Nakajima-Zwanzig theory will be applied to derive a kinetic master equation for describing radical pair reactions, which provides a theoretical basis to recent attempts to interpret experiments on radical pair reactions using this scheme. The kinetic master equation is then used to investigate the role of coherence and relaxation effects in $PTZ^{\bullet+}-Ph_n-PDI^{\bullet-}$ radical pairs.

Finally in chapter 9 I will reflect on the role of quantum master equations in spin chemistry, and discuss new avenues for potential future research. Appendices of derivation details, additional equations and/or data applicable to results in a given chapter can be found at the end of that chapter, rather than at the end of the thesis.

2 Quantum Master Equations

In this chapter I outline the quantum master equation formalism for describing dynamics of complex quantum systems; this is the theory which forms the foundations of the work presented in this thesis. Starting from the density operator formalism, I begin with a description of the concept of the quantum master equation, and how to derive approximate QMEs for a wide range of problems using projection operator techniques. The focus of this chapter is on the Nakajima-Zwanzig equation, but some alternative approaches are also outlined towards the end.

2.1 Density operators

The state of an isolated quantum system in a pure quantum state, $|\psi\rangle$, is described by a vector in the Hilbert space of all possible states of the system, $\mathcal{H}$. For every observable, O, of the system there is a corresponding linear operator $\hat{O}$ on $\mathcal{H}$, and the expectation value of measurements of this observable for the system in a given state $|\psi\rangle$ is given by the inner product of $|\psi\rangle$ with $\hat{O}\,|\psi\rangle$ (assuming $\langle\psi|\psi\rangle = 1$),

$$\langle O\rangle = \langle\psi|\hat{O}|\psi\rangle\,. \tag{2.1}$$

So in principle all we need to know is the state $|\psi\rangle$ for the system, and from this we can predict all of its experimentally observable behaviour. Real physical systems however are often composed of many identical, independent but distinguishable copies of the system, for example there are typically in the order of $N_{\mathrm{A}} \approx 6\times10^{22}$ identical molecules in solution

phase experiments, so often what is observed in experiments is the statistical average over an ensemble of identical systems. If we have such an ensemble consisting of N copies of the system, each of which is in a state $|\psi_n\rangle$, then the ensemble expectation value of an observable is simply an average of the observable for each constituent system,

$$\langle O \rangle = \frac{1}{N} \sum_{n=1}^{N} \langle \psi_n | \hat{O} | \psi_n \rangle \,. \tag{2.2}$$

Our aim now is to find a more concise description of this ensemble.

We start by defining the quantum mechanical trace of an operator $\hat{A}$ on a Hilbert space $\mathcal{H}$ as,

$$\mathrm{Tr}\big[\hat{A}\big] = \sum_{k} \langle k | \hat{A} | k \rangle \,, \tag{2.3}$$

where the set of $|k\rangle$ forms a basis of the Hilbert space $\mathcal{H}$. Using this, we can write the expectation value of the observable of the ensemble in this notation as

$$\begin{aligned} \langle O \rangle &= \frac{1}{N} \sum_{n=1}^{N} \langle \psi_n | \hat{O} \hat{1} | \psi_n \rangle \\ &= \frac{1}{N} \sum_{n=1}^{N} \langle \psi_n | \hat{O} \sum_{k} | k \rangle\langle k | \psi_n \rangle \\ &= \sum_{k} \langle k | \frac{1}{N} \sum_{n=1}^{N} | \psi_n \rangle\langle \psi_n | \, \hat{O} | k \rangle \\ &= \mathrm{Tr}\left[\frac{1}{N} \sum_{n=1}^{N} | \psi_n \rangle\langle \psi_n | \, \hat{O} \right]. \end{aligned} \tag{2.4}$$

We see that any observable of the ensemble is determined fully by the operator $\hat{\rho}$,

$$\hat{\rho} = \frac{1}{N} \sum_{n=1}^{N} | \psi_n \rangle\langle \psi_n | \,. \tag{2.5}$$

This is the density operator for the ensemble.[56,101] For an ensemble which contains just one sub-system in the quantum state $|\psi\rangle$, or for an ensemble where every sub-system is in the same quantum state, the density operator is simply $\hat{\rho} = |\psi\rangle\langle\psi|$. So we can say that the density operator describes the average state for an ensemble of identical, non-interacting sub-systems.

The space of all linear operators on $\mathcal{H}$, in which all density operators exist, is called the Liouville space, $\mathcal{L}_{\mathcal{H}}$. The Liouville space can equivalently be seen the direct product space of the dual space $\mathcal{H}^*$ (the space spanned by the bras $\langle k|$) and $\mathcal{H}$ itself (the space spanned by the kets $|j\rangle$) with its , i.e. $\mathcal{L}_{\mathcal{H}} = \mathcal{H}^* \otimes \mathcal{H}$, and just like the underlying Hilbert space of quantum states, the Liouville space is a vector space equipped with an inner product. In this thesis I will interchangeably denote an element of Liouville space either by $\hat{\rho}$ or by $|\rho\rangle\rangle$, depending on which notation offers the most clarity in a given context. We can construct basis vectors for the Liouville space given a set of basis states $|k\rangle$ for $\mathcal{H}$, as $|jk\rangle\rangle = |j\rangle\langle k|$, so we can write any density operator as

$$|\rho\rangle\rangle = \sum_{j,k} \rho_{jk} |jk\rangle\rangle \text{ or equivalently } \hat{\rho} = \sum_{j,k} \rho_{jk} \, |j\rangle\langle k| \, . \tag{2.6}$$

We define the inner product in Liouville space as

$$\langle\langle \rho|\sigma\rangle\rangle = \mathrm{Tr}\left[\hat{\rho}^\dagger \hat{\sigma}\right] = \sum_{jk} \rho^*_{jk} \sigma_{jk}, \tag{2.7}$$

and with this we can write the expectation value of an operator, $\hat{A}$, for a given density matrix as

$$\langle A\rangle = \mathrm{Tr}\left[\hat{A}\hat{\rho}\right] = \langle\langle A^\dagger|\rho\rangle\rangle. \tag{2.8}$$

2.1.1 Properties of the density operator

From the above definition of the density operator as an average state of a set of independent identical systems, it is clear that the physically allowed density operators must be Hermitian,[54]

$$\hat{\rho} = \hat{\rho}^\dagger. \tag{2.9}$$

Also, because any state in the ensemble described above has to be normalised such that $\langle\psi_n|\psi_n\rangle = 1$, we can deduce that[54]

$$\mathrm{Tr}[\hat{\rho}] = 1. \tag{2.10}$$

Similarly, using the definition of the density operator as an ensemble average state as in Eq. (2.5), it can be shown that physically allowed density operators are positive semi-definite.[54] This means that for any $|\varphi\rangle \in \mathcal{H}$,

$$\langle\varphi|\hat{\rho}|\varphi\rangle \geq 0. \tag{2.11}$$

This follows from

$$\begin{aligned}\langle\varphi|\hat{\rho}|\varphi\rangle &= \frac{1}{N}\sum_{n=1}^{N}\langle\varphi|\psi_n\rangle\langle\psi_n|\varphi\rangle \\ &= \frac{1}{N}\sum_{n=1}^{N}|\langle\varphi|\psi_n\rangle|^2 \\ &\geq 0,\end{aligned} \tag{2.12}$$

where that last line follows from the fact that $|\langle\varphi|\psi_n\rangle|^2 \geq 0$ for every $|\psi_n\rangle$. From the Cauchy-Schwarz inequality, we know that $|\langle\varphi|\psi_n\rangle|^2 \leq \langle\psi_n|\psi_n\rangle\langle\varphi|\varphi\rangle$, and therefore from this it also follows that for any normalised $|\varphi\rangle \in \mathcal{H}$,[54]

$$\langle\varphi|\hat{\rho}|\varphi\rangle \leq 1. \tag{2.13}$$

We now choose $|\varphi\rangle = |\varphi_\lambda\rangle$, where $|\varphi_\lambda\rangle$ is a normalised eigenstate of $\hat{\rho}$ with eigenvalue λ, i.e. $\hat{\rho}|\varphi_\lambda\rangle = \lambda|\varphi_\lambda\rangle$. With this choice of $|\varphi\rangle$, it follows that the eigenvalues of $\hat{\rho}$ are always be bounded between 0 and 1, since $\langle\varphi_\lambda|\hat{\rho}|\varphi_\lambda\rangle = \lambda$, and $\hat{\rho}$ is Hermitian.[54]

The eigenvalues of the density operator, λ_n, must sum to 1, which can be deduced from Eq. (2.10) by expanding the trace in the eigenbasis of $\hat{\rho}$,

$$\sum_n \lambda_n = 1. \tag{2.14}$$

Similarly it follows that the $\mathrm{Tr}\left[\hat{\rho}^2\right]$ is given by the following

$$\mathrm{Tr}\left[\hat{\rho}^2\right] = \sum_n \lambda_n^2 = \sum_{n,m}\lambda_n\lambda_m - \sum_{n,m\neq n}\lambda_n\lambda_m = 1 - \sum_{n,m\neq n}\lambda_n\lambda_m. \tag{2.15}$$

From the first equality it follows that $\mathrm{Tr}\left[\hat{\rho}^2\right] \geq 0$ and from the final equality it follows that

$\mathrm{Tr}\left[\hat{\rho}^2\right] \leq 1$ and therefore

$$0 \leq \mathrm{Tr}\left[\hat{\rho}^2\right] \leq 1. \tag{2.16}$$

If $\hat{\rho} = |\psi\rangle\langle\psi|$ then $\hat{\rho}^2 = \hat{\rho}$ and $\mathrm{Tr}\left[\hat{\rho}^2\right] = 1$. In this case, the ensemble is said to be in a *pure state*, since this corresponds to every subsystem in the ensemble being in the same quantum state $|\psi\rangle$. Any ensemble state which cannot be written in the form is called a *mixed state*. With this in mind, we call $\mathrm{Tr}\left[\hat{\rho}^2\right]$ the *purity* of the density operator. For a pure state it is exactly 1 and for a mixed state it is less than 1.[54]

We can obtain a tighter lower bound on $\mathrm{Tr}\left[\hat{\rho}^2\right]$ for a system with a finite Hilbert space dimensionality, d, by minimising $\mathrm{Tr}\left[\hat{\rho}^2\right]$ with respect to each λ_n subject to the constraint that $\mathrm{Tr}[\hat{\rho}] = 1$. We do this using the method of Lagrange multipliers, by finding the stationary point of the function

$$L(\boldsymbol{\lambda}, \alpha) = \mathrm{Tr}\left[\hat{\rho}^2\right] + \alpha \left(\mathrm{Tr}[\hat{\rho}] - 1\right). \tag{2.17}$$

Differentiating with respect to λ_n gives

$$\lambda_n = \frac{1}{2\alpha} \tag{2.18}$$

and differentiating with respect to the Lagrange multiplier α gives the constraint,

$$1 = \sum_{n=1}^{d} \lambda_n = \frac{d}{2\alpha} \tag{2.19}$$

so the minimum value of the purity is

$$\mathrm{Tr}\left[\hat{\rho}^2\right] = \frac{1}{d}. \tag{2.20}$$

and in this case the density operator is

$$\hat{\rho} = \frac{1}{d}\hat{1}. \tag{2.21}$$

This state is called the *maximally mixed state*,[54] because in this state, the purity is minimised.

A commonly encountered density operator is the thermal density operator.[54,56] In this case we assume each system of the ensemble of N systems is in an eigenstate of the system

Hamiltonian $\hat{H}$, $|E_j\rangle$ with energy eigenvalue E_j. The number of systems in state $|E_j\rangle$ is given by the Boltzmann probability times the total number of systems in the ensemble,

$$n_j = Np_j = N\frac{e^{-\beta E_j}}{Z(T)}, \tag{2.22}$$

where $\beta = 1/(k_{\mathrm{B}}T)$ and $Z(T)$ is the partition function,

$$Z(T) = \sum_{j=0}^{\infty} e^{-\beta E_j} = \mathrm{Tr}\left[e^{-\beta\hat{H}}\right]. \tag{2.23}$$

The thermal density operator is therefore given by

$$\hat{\rho} = \frac{1}{N}\sum_{j=0}^{\infty} n_j \,|E_j\rangle\langle E_j| = \frac{1}{Z(T)}\sum_{j=0}^{\infty} e^{-\beta E_j}\,|E_j\rangle\langle E_j| = \frac{1}{Z(T)}e^{-\beta\hat{H}}. \tag{2.24}$$

The maximally mixed density operator defined above corresponds to the $T \to \infty$ limit of this. For now I will leave behind these ideas of pure, mixed and thermal states, although they will become important in later chapters.

2.1.2 Time evolution

We have established that the average state of an ensemble of identical, non-interacting systems is encoded in the density operator $\hat{\rho}$. In order to determine dynamical properties of the ensemble, i.e. how observables change with time, we need an equation governing the time evolution of $\hat{\rho}$. To obtain this equation, we start by noting that each composite system evolves according to the time-dependent Schrödinger equation,

$$\frac{\mathrm{d}}{\mathrm{d}t}|\psi(t)\rangle = -\frac{i}{\hbar}\hat{H}\,|\psi(t)\rangle\,, \tag{2.25}$$

where $\hat{H}$ is the system Hamiltonian. Using this we can straightforwardly derive the equation governing the dynamics of $\hat{\rho}(t)$ as follows,[54,56,101]

$$\begin{aligned}\frac{\mathrm{d}}{\mathrm{d}t}\hat{\rho}(t) &= \frac{1}{N}\sum_{n=1}^{N}\frac{\mathrm{d}}{\mathrm{d}t}\left(|\psi_n(t)\rangle\langle\psi_n(t)|\right)\\ &= \frac{1}{N}\sum_{n=1}^{N}\left[\left(\frac{\mathrm{d}}{\mathrm{d}t}|\psi_n(t)\rangle\right)\langle\psi_n(t)| + |\psi_n(t)\rangle\left(\frac{\mathrm{d}}{\mathrm{d}t}\langle\psi_n(t)|\right)\right]\\ &= \frac{1}{N}\sum_{n=1}^{N}\left[-\frac{i}{\hbar}\hat{H}|\psi_n(t)\rangle\langle\psi_n(t)| + \frac{i}{\hbar}|\psi_n(t)\rangle\langle\psi_n(t)|\hat{H}\right]\\ &= -\frac{i}{\hbar}\left(\hat{H}\hat{\rho}(t) - \hat{\rho}(t)\hat{H}\right).\end{aligned} \tag{2.26}$$

Defining the commutator of two operators as $[\hat{A},\hat{B}] = \hat{A}\hat{B} - \hat{B}\hat{A}$, we obtain the Liouville-von Neuman equation for the density operator,[54,56,101]

$$\frac{\mathrm{d}}{\mathrm{d}t}\hat{\rho}(t) = -\frac{i}{\hbar}\left[\hat{H},\hat{\rho}(t)\right]. \tag{2.27}$$

This equation fully governs the time evolution of the density operator and therefore also all observables of the ensemble. The initial conditions for $\hat{\rho}(t)$ depend on the physical system which we are describing. We note that this equation is linear in $\hat{\rho}(t)$ and therefore it can be written more succinctly with the Liouvillian superoperator

$$\mathcal{L} = -\frac{i}{\hbar}[\hat{H},\,\cdot\,]. \tag{2.28}$$

The term *superoperator* is given to a linear function that acts on $\mathcal{L}_{\mathcal{H}}$. With this, the Liouville-von Neumann equation can be written as

$$\frac{\mathrm{d}}{\mathrm{d}t}\hat{\rho}(t) = \mathcal{L}\hat{\rho}(t). \tag{2.29}$$

The formal solution to this equation is simply

$$\begin{aligned}\hat{\rho}(t) &= e^{\mathcal{L}t}\hat{\rho}(0)\\ &= e^{-i\hat{H}t/\hbar}\hat{\rho}(0)e^{-i\hat{H}t/\hbar},\end{aligned} \tag{2.30}$$

and using this we see that for any operator that commutes with $\hat{H}$, i.e. if $[\hat{A}, \hat{H}] = 0$, then $\langle A(t) \rangle$ does not change with time,

$$\begin{aligned} \langle A(t) \rangle &= \mathrm{Tr}\Big[\hat{A} e^{-i\hat{H}t/\hbar} \hat{\rho}(0) e^{-i\hat{H}t/\hbar}\Big] \\ &= \mathrm{Tr}\Big[\hat{A} e^{-i\hat{H}t/\hbar} e^{-i\hat{H}t/\hbar} \hat{\rho}(0)\Big] \\ &= \mathrm{Tr}\big[\hat{A}\hat{\rho}(0)\big] \\ &= \langle A(0) \rangle \,. \end{aligned} \tag{2.31}$$

This clearly holds for $\hat{A} = \hat{1}$, so one important corollary of this is that the trace of $\hat{\rho}(t)$ is conserved by the dynamics.

2.1.3 Open quantum systems and reduced density operators

Often the full quantum system is composed of multiple coupled systems. In some cases, the full Hilbert space can be constructed as a direct product of a *system* Hilbert space and a *bath* Hilbert space,

$$\mathcal{H} = \mathcal{H}_\mathrm{s} \otimes \mathcal{H}_\mathrm{b}. \tag{2.32}$$

This is often called an *open quantum system*, because the quantum system of interest is coupled to a bath with which it can exchange energy, and as such it behaves in a fundamentally different way to the *closed* quantum system evolving in the absence of the bath. In later chapters I will give specific examples of this partitioning, but for now I will only discuss the general case.

Given basis states for $\mathcal{H}_\mathrm{s}$ and $\mathcal{H}_\mathrm{b}$ denoted $|k_\mathrm{s}\rangle_\mathrm{s}$ and $|k_\mathrm{b}\rangle_\mathrm{b}$ respectively, we can construct a basis for $\mathcal{H}$ with the following direct product states,

$$|k_\mathrm{s} k_\mathrm{b}\rangle = |k_\mathrm{s}\rangle_\mathrm{s} \otimes |k_\mathrm{b}\rangle_\mathrm{b} \,, \tag{2.33}$$

and therefore the trace over full system Hilbert space can be decomposed into partial traces

over the system and bath,

$$\begin{aligned}\mathrm{Tr}\big[\hat{A}\big] &= \sum_{k_\mathrm{s},k_\mathrm{b}} \langle k_\mathrm{s} k_\mathrm{b}|\hat{A}|k_\mathrm{s}k_\mathrm{b}\rangle \\ &= \sum_{k_\mathrm{s}} \langle k_\mathrm{s}| \sum_{k_\mathrm{b}} \langle k_\mathrm{b}|\hat{A}|k_\mathrm{b}\rangle_\mathrm{b} |k_\mathrm{s}\rangle_\mathrm{s} \\ &= \mathrm{Tr}_\mathrm{s}[\mathrm{Tr}_\mathrm{b}[\hat{A}]],\end{aligned} \tag{2.34}$$

where the partial traces are given by

$$\mathrm{Tr}_\mathrm{s}[\hat{A}] = \sum_{k_\mathrm{s}} \langle k_\mathrm{s}|\hat{A}|k_\mathrm{s}\rangle_\mathrm{s}\,, \tag{2.35a}$$

$$\mathrm{Tr}_\mathrm{b}[\hat{A}] = \sum_{k_\mathrm{b}} \langle k_\mathrm{b}|\hat{A}|k_\mathrm{b}\rangle_\mathrm{b}\,. \tag{2.35b}$$

By the same arguments, we can also write $\mathrm{Tr}\big[\hat{A}\big] = \mathrm{Tr}_\mathrm{b}[\mathrm{Tr}_\mathrm{s}[\hat{A}]]$. For an observable just of the system, O_s, we can use the fact that $\hat{O}_\mathrm{s}$ only acts of the system degrees of freedom (i.e. $\hat{O}_\mathrm{s}(|\psi\rangle_\mathrm{s} \otimes |\varphi\rangle_\mathrm{b}) = (\hat{O}_\mathrm{s}\,|\psi\rangle_\mathrm{s}) \otimes |\varphi\rangle_\mathrm{b}$) to evaluate its expectation value for an ensemble described by the density operator $\hat{\rho}$ as

$$\begin{aligned}\langle O_\mathrm{s}\rangle &= \mathrm{Tr}\big[\hat{O}_\mathrm{s}\hat{\rho}\big] \\ &= \mathrm{Tr}_\mathrm{s}[\hat{O}_\mathrm{s}\,\mathrm{Tr}_\mathrm{b}[\hat{\rho}]].\end{aligned} \tag{2.36}$$

We call the object $\hat{\sigma}_\mathrm{s} = \mathrm{Tr}_\mathrm{b}[\hat{\rho}]$ the *reduced density operator* for the system. This operator contains all information about the *system* observables, but does not directly contain any information about bath observables.

In the theoretical analysis of quantum systems, and in computational simulation of their dynamics, the reduced description of the problem is very appealing for two main reasons. Firstly, it offers a simpler, and often physically enlightening description of the system dynamics. Working with only a handful of variables of interest gives a clearer picture of the behaviour of the system than working with the, often unwieldy, full density operator. Secondly, from a computational simulation perspective, the reduced description contains far fewer variables, and as such it is typically much more computationally efficient to work with than the full density operator. These two advantages of the reduced description of a problem make this approach especially useful in directly applying theoretical models to

interpret experimental data. Given this, our aim now is to find a description of the dynamics of the reduced density operator that depends only on itself, and not on the full density operator including the bath degrees of freedom. In other words we want to find a *quantum master equation* for $\hat{\sigma}_{\mathrm{s}}(t)$ of the form

$$\frac{\mathrm{d}}{\mathrm{d}t}\hat{\sigma}_{\mathrm{s}}(t) = f(\hat{\sigma}_{\mathrm{s}}(t), t). \tag{2.37}$$

The remainder of this chapter is devoted to finding such quantum master equations.

Before continuing, it should be noted that we can generalise this approach to describing a full quantum system with a reduced set of variables. Suppose we are interested only in some set of N expectation values of operators of the full quantum system, $\langle A_n \rangle = \langle\langle A_n|\rho\rangle\rangle$. In this case we seek a quantum master equation for these expectation values that depends only on this set of expectation values,

$$\frac{\mathrm{d}}{\mathrm{d}t}\left\langle A_n(t)\right\rangle = f_n(\left\langle A_1(t)\right\rangle, \ldots, \left\langle A_N(t)\right\rangle, t). \tag{2.38}$$

One example of such a set of operators is the set of population operators for system states in some basis, i.e. $\hat{A}_{n_{\mathrm{s}}} = |n_{\mathrm{s}}\rangle\langle n_{\mathrm{s}}|_{\mathrm{s}} \otimes \hat{1}_{\mathrm{b}}$. The reduced density operator defined above can also be written in this form by choosing $\hat{A}_{j_{\mathrm{s}}k_{\mathrm{s}}} = |j_{\mathrm{s}}\rangle\langle k_{\mathrm{s}}|_{\mathrm{s}} \otimes \hat{1}_{\mathrm{b}}$ in which case $\langle A_{j_{\mathrm{s}}k_{\mathrm{s}}}\rangle = \langle j_{\mathrm{s}}|\hat{\sigma}_{\mathrm{s}}|k_{\mathrm{s}}\rangle_{\mathrm{s}}$.

2.2 Exact quantum master equations

In this section the theory of how to obtain quantum master equations (QMEs) for our reduced description of the full quantum system is outlined. This is based on Nakajima-Zwanzig theory.[57,58] We lay the foundations of this by first describing Liouville space projection operators, and then show how these can be used to obtain quantum master equations. Two commonly used approximations used to obtain QMEs of practical use are also described.

2.2.1 Projection operators

In the following we will use projection superoperators to obtain quantum master equations.[54,56,58] An operator on Liouville space is a projection operator if it is idempotent,

i.e.

$$\mathcal{P}^2 = \mathcal{P}. \tag{2.39}$$

With this, the identity operator on Liouville space can be decomposed into a sum of $\mathcal{P}$ and its complementary projection superoperator $\mathcal{Q} = 1 - \mathcal{P}$,

$$1 = \mathcal{P} + \mathcal{Q}. \tag{2.40}$$

In the following we will require projection superoperators that contain the generalised reduced description, which means we need the projection superoperator to satisfy

$$\langle A_n \rangle = \langle\langle A_n | \mathcal{P} | \rho \rangle\rangle = \mathrm{Tr}\big[\hat{A}_n^\dagger \mathcal{P} \hat{\rho}\big] \tag{2.41}$$

for all $\langle A_n \rangle$ in our reduced description of the full quantum system.

The first step in obtaining quantum master equations for the reduced description will generally be to define a projection superoperator with the above two properties. A general form for a projection superoperator satisfying these conditions, which covers all cases considered in this thesis, is

$$\mathcal{P} = \sum_n |A_n \rho_n\rangle\rangle\langle\langle A_n| = \sum_n \hat{A}_n \hat{\rho}_n \,\mathrm{Tr}\big[\hat{A}_n^\dagger \cdot\,\big] \tag{2.42}$$

where $\hat{\rho}_n$ is an operator which is chosen such that $|A_n \rho_n\rangle\rangle$ satisfies

$$\langle\langle A_m | A_n \rho_n \rangle\rangle = \mathrm{Tr}\big[\hat{A}_m^\dagger \hat{A}_n \hat{\rho}_n\big] = \delta_{n,m}, \tag{2.43}$$

in which $\delta_{n,m}$ is the Kronecker delta. Provided that Eq. (2.43) is satisfied, there are no formal restrictions on the choice of $\hat{\rho}_n$, although when approximations are made to obtain quantum master equations, some choices of $\hat{\rho}_n$ will be better than others. We see that with this general form of the projection operator, equations (2.39) and (2.41) are automatically satisfied. It is always sensible to include the identity operator $\hat{1}$ in the set of operators $\hat{A}_n$ and as such we will assume this from now on.

To illustrate these ideas, we consider the reduced density operator defined in the previous section. To construct an appropriate projection operator we choose $\hat{A}_{j_s k_s} = |j_s\rangle\langle k_s| \otimes \hat{1}_b$ and

$\hat{\rho}_{j_s k_s} = \hat{\rho}_b$ where $\hat{\rho}_b$ is any bath operator with trace equal to 1. In this case we find that $\mathcal{P}\hat{\rho}$ is

$$\begin{aligned}\mathcal{P}\hat{\rho} &= \sum_{j_s,k_s} |j_s\rangle\langle k_s|_s \, \hat{\rho}_b \, \mathrm{Tr}\big[|k_s\rangle\langle j_s|_s \, \hat{\rho}\big] \\ &= \hat{\rho}_b \sum_{j,k} |j_s\rangle\langle k_s| \; \langle j_s|\hat{\sigma}_s|k_s\rangle \\ &= \hat{\rho}_b \hat{\sigma}_s.\end{aligned} \tag{2.44}$$

Clearly any matrix element of the reduced density operator is given by $\langle\langle A_{j_s k_s}|\mathcal{P}|\rho\rangle\rangle$ or alternatively the complete reduced density operator is given by

$$\hat{\sigma}_s = \mathrm{Tr}_b[\hat{\rho}] = \mathrm{Tr}_b[\mathcal{P}\hat{\rho}]. \tag{2.45}$$

So if we are interested in obtaining equations for the reduced density operator dynamics, we can define a projection superoperator as above which preserves $\hat{\sigma}_s$, but which removes unwanted information about the bath. In this case we can more succinctly write the projection operator $\mathcal{P}$ as

$$\mathcal{P} = \hat{\rho}_b \, \mathrm{Tr}_b[\,\cdot\,]. \tag{2.46}$$

The aim of what follows is to find a general equation for $\frac{\mathrm{d}}{\mathrm{d}t}\mathcal{P}|\rho(t)\rangle\rangle$, for any $\mathcal{P}$ satisfying the above properties. From this we can directly obtain a quantum master equation for the reduced description using the fact that

$$\frac{\mathrm{d}}{\mathrm{d}t}\langle A_n(t)\rangle = \langle\langle A_n|\frac{\mathrm{d}}{\mathrm{d}t}\mathcal{P}|\rho(t)\rangle\rangle. \tag{2.47}$$

2.2.2 The Nakajima-Zwanzig equation

We are now in a position to derive an exact quantum master equation for $\frac{\mathrm{d}}{\mathrm{d}t}\mathcal{P}\hat{\rho}(t)$. Here we assume that $\mathcal{P}$ (and therefore also its complement $\mathcal{Q}$) is independent of time. Projecting the Liouville-von Neumann equation, Eq. (2.29), with the projection superoperator $\mathcal{P}$, and

using Eq. (2.40), we can obtain

$$\begin{aligned}\frac{\mathrm{d}}{\mathrm{d}t}\mathcal{P}\hat{\rho}(t) &= \mathcal{P}\mathcal{L}\hat{\rho}(t)\\ &= \mathcal{P}\mathcal{L}(\mathcal{P}+\mathcal{Q})\hat{\rho}(t)\\ &= \mathcal{P}\mathcal{L}\mathcal{P}\hat{\rho}(t) + \mathcal{P}\mathcal{L}\mathcal{Q}\hat{\rho}(t).\end{aligned} \tag{2.48}$$

We can repeat this with the complementary projection operator $\mathcal{Q}$ to obtain

$$\frac{\mathrm{d}}{\mathrm{d}t}\mathcal{Q}\hat{\rho}(t) = \mathcal{Q}\mathcal{L}\mathcal{Q}\hat{\rho}(t) + \mathcal{Q}\mathcal{L}\mathcal{P}\hat{\rho}(t). \tag{2.49}$$

Our strategy now is to solve Eq. (2.49) for $\mathcal{Q}\hat{\rho}(t)$, which can then be substituted into Eq. (2.48) to obtain an equation for $\mathcal{P}\hat{\rho}(t)$. We do this by first rearranging Eq. (2.49) to collate terms depending on $\mathcal{Q}\hat{\rho}(t)$, and then we pre-multiply Eq. (2.49) by the integrating factor $e^{-\mathcal{Q}\mathcal{L}t}$ which gives

$$\begin{aligned}e^{-\mathcal{Q}\mathcal{L}t}\mathcal{Q}\mathcal{L}\mathcal{P}\hat{\rho}(t) &= e^{-\mathcal{Q}\mathcal{L}t}\frac{\mathrm{d}}{\mathrm{d}t}\mathcal{Q}\hat{\rho}(t) - e^{-\mathcal{Q}\mathcal{L}t}\mathcal{Q}\mathcal{L}\mathcal{Q}\hat{\rho}(t)\\ &= \frac{\mathrm{d}}{\mathrm{d}t}\left(e^{-\mathcal{Q}\mathcal{L}t}\mathcal{Q}\hat{\rho}(t)\right),\end{aligned} \tag{2.50}$$

and finally integrating this gives

$$\begin{aligned}\int_0^t \mathrm{d}\tau\, e^{-\mathcal{Q}\mathcal{L}\tau}\mathcal{Q}\mathcal{L}\mathcal{P}\hat{\rho}(\tau) &= \int_0^t \mathrm{d}\tau\, \frac{\mathrm{d}}{\mathrm{d}\tau}\left(e^{-\mathcal{Q}\mathcal{L}\tau}\mathcal{Q}\hat{\rho}(\tau)\right)\\ &= e^{-\mathcal{Q}\mathcal{L}t}\mathcal{Q}\hat{\rho}(t) - \mathcal{Q}\hat{\rho}(0).\end{aligned} \tag{2.51}$$

We rearrange this to obtain $\mathcal{Q}\hat{\rho}(t)$ in terms of $\mathcal{P}\hat{\rho}(t)$

$$\mathcal{Q}\hat{\rho}(t) = \int_0^t \mathrm{d}\tau\, e^{\mathcal{Q}\mathcal{L}(t-\tau)}\mathcal{Q}\mathcal{L}\mathcal{P}\hat{\rho}(\tau) + e^{\mathcal{Q}\mathcal{L}t}\mathcal{Q}\hat{\rho}(0). \tag{2.52}$$

Finally, we substitute Eq. (2.52) into Eq. (2.48) to obtain the Nakajima-Zwanzig equation for $\mathcal{P}\hat{\rho}(t)$,

$$\frac{\mathrm{d}}{\mathrm{d}t}\mathcal{P}\hat{\rho}(t) = \mathcal{P}\mathcal{L}\mathcal{P}\hat{\rho}(t) + \int_0^t \mathrm{d}\tau\, \mathcal{K}(t-\tau)\mathcal{P}\hat{\rho}(\tau) + \hat{\imath}(t). \tag{2.53}$$

The kernel $\mathcal{K}(t)$ is given by

$$\mathcal{K}(t) = \mathcal{P}\mathcal{L}\mathcal{Q}e^{\mathcal{Q}\mathcal{L}t}\mathcal{Q}\mathcal{L}\mathcal{P} \tag{2.54}$$

and the inhomogeneous term $\hat{\imath}(t)$ is given by

$$\hat{\imath}(t) = \mathcal{P}\mathcal{L}e^{\mathcal{Q}\mathcal{L}t}\mathcal{Q}\hat{\rho}(0). \tag{2.55}$$

We can often choose $\mathcal{P}$ such that $\mathcal{P}\hat{\rho}(0) = \hat{\rho}(0)$ and in such cases the inhomogeneous term $\hat{\imath}(t)$ vanishes. At the very least, since the set of reduced operators $\hat{A}_n$ includes the identity operator, we know that $\mathrm{Tr}[\mathcal{P}\hat{\rho}(t)] = \mathrm{Tr}[\hat{\rho}(t)]$, and also for the inhomogeneous term we find that

$$\begin{aligned}\mathrm{Tr}[\hat{\imath}(t)] &= \mathrm{Tr}\Big[\mathcal{P}\mathcal{L}e^{\mathcal{Q}\mathcal{L}t}\mathcal{Q}\hat{\rho}(0)\Big] \\ &= -\frac{i}{\hbar}\,\mathrm{Tr}\Big[[\hat{H}, e^{\mathcal{Q}\mathcal{L}t}\mathcal{Q}\hat{\rho}(0)]\Big] \\ &= 0.\end{aligned} \tag{2.56}$$

This property will become important in our analysis of approximate master equations later.

The Nakajima-Zwanzig equation (Eq. (2.53)) is a formally exact quantum master equation for the projected density operator $\mathcal{P}\hat{\rho}(t)$, but it in fact is no easier to solve than the Liouville-von Neumann equation for the full system due to the complexity of the kernel $\mathcal{K}(t)$ and the inhomogeneous term $\hat{\imath}(t)$. However the Nakajima-Zwanzig equation does provide a useful starting point for deriving approximate quantum master equations, as will now be explored.

2.3 Approximate quantum master equations

Having described the exact quantum master equation formalism, I shall now examine two main techniques for deriving approximate quantum master equations: the Markovian approximation and the use of perturbation theory.

2.3.1 The Markovian approximation

The first approximation to Eq. (2.53) I will describe is the Markovian approximation. The full Nakajima-Zwanzig equation is non-Markovian, meaning that $\frac{\mathrm{d}}{\mathrm{d}t}\mathcal{P}\hat{\rho}(t)$ depends not only on $\mathcal{P}\hat{\rho}(t)$ at the current point in time, but also on $\mathcal{P}\hat{\rho}(\tau)$ for $0 \leq \tau \leq t$, given the equation involves a time-convolution of the kernel $\mathcal{K}(t)$ and $\mathcal{P}\hat{\rho}(t)$. Here I will show how this

equation can be simplified to a Markovian equation, one where $\frac{\mathrm{d}}{\mathrm{d}t}\mathcal{P}\hat{\rho}(t)$ depends only on $\mathcal{P}\hat{\rho}(t)$ at the current point in time.

We start by defining the Fourier-Laplace transform[a] of a function $f(t)$ as

$$\mathsf{F}[f(t)](\omega) = \tilde{f}(\omega) = \lim_{\eta\to 0^+} \int_0^\infty f(t) e^{+i\omega t - \eta t}\,\mathrm{d}t\,. \tag{2.57}$$

The η is present in the definition to ensure that the transform is well defined for all real ω.[102] The inverse of this transform is given by[102]

$$\mathsf{F}^{-1}[\tilde{f}(\omega)](t) = f(t) = \frac{1}{2\pi}\int_{-\infty}^\infty \tilde{f}(\omega) e^{-i\omega t}\,\mathrm{d}\omega\,. \tag{2.58}$$

Using integration by parts, it is straightforward to show that

$$\mathsf{F}\left[\frac{\mathrm{d}}{\mathrm{d}t}f(t)\right](\omega) = -i\omega\tilde{f}(\omega) - f(0), \tag{2.59}$$

and by a change of variables in the integral, we can show that

$$\mathsf{F}\left[\int_0^t f(t-\tau)g(\tau)\,\mathrm{d}\tau\right](\omega) = \tilde{f}(\omega)\tilde{g}(\omega). \tag{2.60}$$

Taking the Fourier-Laplace transform of the Nakajima-Zwanzig equation, Eq. (2.53), we obtain

$$-i\omega\mathcal{P}\tilde{\hat{\rho}}(\omega) - \mathcal{P}\hat{\rho}(0) = \mathcal{P}\mathcal{L}\mathcal{P}\tilde{\hat{\rho}}(\omega) + \tilde{\mathcal{K}}(\omega)\mathcal{P}\tilde{\hat{\rho}}(\omega) + \tilde{\hat{\imath}}(\omega). \tag{2.61}$$

Now if the reduced system dynamics are much slower than the full system dynamics, then the Fourier-Laplace transformed kernel $\tilde{\mathcal{K}}(\omega)$ will contain a broader range of frequency components than $\mathcal{P}\tilde{\hat{\rho}}(\omega)$. This means $\tilde{\mathcal{K}}(\omega)$ will vary much more slowly with ω than $\mathcal{P}\tilde{\hat{\rho}}(\omega)$, which will be sharply peaked around $\omega = 0$ and thus we can replace $\tilde{\mathcal{K}}(\omega)\mathcal{P}\tilde{\hat{\rho}}(\omega)$ in the above equation with $\tilde{\mathcal{K}}(0)\mathcal{P}\tilde{\hat{\rho}}(\omega)$. We can also apply this approximation to the inhomogeneous term, replacing $\tilde{\hat{\imath}}(\omega)$ with $\tilde{\hat{\imath}}(0)$. Transforming back to the time-domain, the approximate equation for $\mathcal{P}\hat{\rho}(t)$ is

$$\frac{\mathrm{d}}{\mathrm{d}t}\mathcal{P}\hat{\rho}(t) = \mathcal{P}\mathcal{L}\mathcal{P}\hat{\rho}(t) + \tilde{\mathcal{K}}(0)\mathcal{P}\hat{\rho}(t) + \tilde{\hat{\imath}}(0)\delta(t), \tag{2.62}$$

[a] We can relate this to the Laplace transform $\mathsf{L}[f(t)](s) = \int_0^\infty f(t)e^{-st}\,\mathrm{d}t$ by simply replacing s with $-i\omega + \eta$, i.e. $\mathsf{L}[f(t)](-i\omega+\eta) = \mathsf{F}[f(t)](\omega)$.

where $\delta(t)$ is the Dirac delta function.[b] This equation is now Markovian, and when $\hat{\imath}(t) = 0$ it is time homogeneous. When the inhomogeneous term is non-zero, it just gives an instantaneous change in $\mathcal{P}\hat{\rho}(t)$ at $t = 0$, effectively just perturbing the initial conditions. This approximation is equivalent to assuming $\mathcal{K}(t) \approx \tilde{\mathcal{K}}(0)\delta(t)$, i.e. that the kernel decays to zero on a much faster time scale than the reduced dynamics.

In this derivation of the Markovian approximation, we have effectively just truncated the Taylor series for $\tilde{\mathcal{K}}(\omega)$ and $\tilde{\imath}(\omega)$ at the ω^0 term. For such an approximation to be valid for the dynamics at finite times, we certainly need $\tilde{\mathcal{K}}(\omega)$ to be finite (i.e. all $b_n\omega^{-n}$ terms, for $n > 0$, in its Laurent series around $\omega = 0$ must be zero). We further require that if $\|\tilde{\mathcal{K}}(\omega)\| \neq 0$ then $\tilde{\mathcal{K}}(\omega) = O(\omega^0)$ as $\omega \to 0$, otherwise the dynamics will always be non-Markovian. The dynamics may still not be well described by the Markovian approximation even if these conditions hold, specifically if $\tilde{\mathcal{K}}(\omega)$ is not dominated by the $\tilde{\mathcal{K}}(0)$ for relevant frequencies in the problem. This suggests a simple criterion for the validity of the Markovian approximation is that the coefficient of the ω^1 term in the Taylor series for $\tilde{\mathcal{K}}(\omega)$ should be small. Ignoring the inhomogeneous term for now, and noting that $\tilde{\mathcal{K}}'(\omega)$ is dimensionless, our crude condition for the validity of the Markovian approximation for the dynamics is

$$\left\|\tilde{\mathcal{K}}'(\omega = 0)\right\| \ll 1, \tag{2.63}$$

where $\|\cdot\|$ denotes any appropriate matrix norm. In the following two sections an analysis of this approximation for the long-time limit, and for time integrated properties is presented and a more detailed analysis of the error in the Markovian approximation for finite time dynamics is presented in appendix 2.A.

2.3.2 The long time limit

It is important of course to assess when the Markovian approximation is and is not valid. Before considering more general dynamics, the first limit we consider is the long time limit for expectation values of our reduced system variables $\langle A_n(t)\rangle$. To facilitate this analysis, we need to find a relationship between $\lim_{t\to\infty} f(t)$ and $\tilde{f}(\omega)$. To do this, we start by taking

[b] Here the delta function is strictly a one-sided delta function defined such that $\int_0^\infty \delta(t)f(t)\,\mathrm{d}t = f(0)$.

property (2.59) and let $\omega \to 0$,

$$\lim_{\omega\to 0}(-i\omega)\tilde{f}(\omega) = \lim_{\omega\to 0}\lim_{\eta\to 0^+}\int_0^\infty \frac{\mathrm{d}f(t)}{\mathrm{d}t}e^{+i\omega t-\eta t}\,\mathrm{d}t + f(0). \tag{2.64}$$

Now assuming we can swap the limits and integral (which is true if the integrand is uniformly convergent in ω and bounded according to the Dominated Convergence Theorem, which is true if the derivative of $f(t)$ is bounded), we obtain

$$\begin{aligned}\lim_{\omega\to 0}(-i\omega)\tilde{f}(\omega) &= \int_0^\infty \frac{\mathrm{d}f(t)}{\mathrm{d}t}\,\mathrm{d}t + f(0)\\ &= \lim_{t\to\infty} f(t) - f(0) + f(0).\end{aligned} \tag{2.65}$$

This gives the following relationship between $\tilde{f}(\omega)$ and the long time limit of $f(t)$, which is the well-known Final Value Theorem,

$$\lim_{t\to\infty} f(t) = \lim_{\omega\to 0}(-i\omega)\tilde{f}(\omega). \tag{2.66}$$

In the following we will need the formal solution of Eq. (2.61) for $\mathcal{P}\tilde{\hat{\rho}}(\omega)$, which is

$$\mathcal{P}\tilde{\hat{\rho}}(\omega) = [-i\omega - \mathcal{P}\mathcal{L}\mathcal{P} - \tilde{\mathcal{K}}(\omega)]^{-1}(\mathcal{P}\rho(0) + \tilde{i}(\omega)). \tag{2.67}$$

It should be noted that the inverse here implicitly means the inverse within the subspace of the Liouville space $\mathcal{L}_\mathcal{H}$ which is formed by the projection superoperator $\mathcal{P}$, because otherwise the inverse would not be defined (this is further elaborated in the appendix 2.B). We note that $\mathcal{P}\hat{\rho}(t)$ will be differentiable, and $\mathcal{P}\hat{\rho}(t)$ and its derivative will be bounded, so the Final Value Theorem can be applied, so we see that the long time limit of $\mathcal{P}\hat{\rho}(t)$ is given by,

$$\begin{aligned}\lim_{t\to\infty}\mathcal{P}\hat{\rho}(t) &= \lim_{\omega\to 0}(-i\omega)\mathcal{P}\tilde{\hat{\rho}}(\omega)\\ &= \lim_{\omega\to 0}(-i\omega)[-i\omega - \mathcal{P}\mathcal{L}\mathcal{P} - \tilde{\mathcal{K}}(\omega)]^{-1}(\mathcal{P}\hat{\rho}(0) + \tilde{\tilde{i}}(\omega))\\ &= \lim_{\omega\to 0}(-i\omega)[-i\omega - \mathcal{P}\mathcal{L}\mathcal{P} - \tilde{\mathcal{K}}(0)]^{-1}(\mathcal{P}\hat{\rho}(0) + \tilde{\tilde{i}}(0)).\end{aligned} \tag{2.68}$$

Now let us consider the long time limit of the Markovian Nakajima-Zwanzig equation (assuming that this is exists, i.e. that $\tilde{\mathcal{K}}(\omega \to 0)$ is non-zero and finite). Once again we can

formally solve the Fourier-Laplace transformed version of Eq. (2.62), which gives us

$$\mathcal{P}\tilde{\hat{\rho}}(\omega) = [-i\omega - \mathcal{P}\mathcal{L}\mathcal{P} - \tilde{\mathcal{K}}(0)]^{-1}(\mathcal{P}\hat{\rho}(0) + \tilde{\hat{\imath}}(0)), \tag{2.69}$$

and then the long time limit is given by

$$\lim_{t\to\infty} \mathcal{P}\hat{\rho}(t) = \lim_{\omega\to 0}(-i\omega)[-i\omega - \mathcal{P}\mathcal{L}\mathcal{P} - \tilde{\mathcal{K}}(0)]^{-1}(\mathcal{P}\hat{\rho}(0) + \tilde{\hat{\imath}}(0)). \tag{2.70}$$

which is the same as the last line of Eq. (2.68). So we see that the Markovian approximation gives the long-time limit of our reduced system variables $\langle A_n(t \to \infty)\rangle$ exactly, even if it is not accurate for finite time dynamics.

2.3.3 Time-integrated properties

Having established that the Markovian approximation gives the long-time limit of the reduced system dynamics exactly, we will move on to consider more general dynamics. To start with, we can consider time-integrated properties. If we take one of our generalised reduced system operators $\hat{A}_n$, we can define $\Delta\hat{A}_n = \hat{A}_n - \langle A_n(t \to \infty)\rangle$, and we may be interested in the time integrated average of this observable,

$$\int_0^\infty \langle \Delta A_n(t)\rangle \, \mathrm{d}t = \lim_{\omega\to 0} \langle\langle \Delta A_n | \mathcal{P} | \tilde{\rho}(\omega)\rangle\rangle. \tag{2.71}$$

Assuming that this integral is well-defined and finite, we can evaluate this using Eq. (2.67) as follows

$$\begin{aligned}\int_0^\infty \langle \Delta A_n(t)\rangle \, \mathrm{d}t &= \lim_{\omega\to 0} \langle\langle \Delta A_n | [-i\omega - \mathcal{P}\mathcal{L}\mathcal{P} - \tilde{\mathcal{K}}(\omega)]^{-1} \left(\mathcal{P}|\rho(0)\rangle\rangle + |\tilde{\imath}(\omega)\rangle\rangle\right) \\ &= \lim_{\omega\to 0} \langle\langle \Delta A_n | [-i\omega - \mathcal{P}\mathcal{L}\mathcal{P} - \tilde{\mathcal{K}}(0)]^{-1} \left(\mathcal{P}|\rho(0)\rangle\rangle + |\tilde{\imath}(0)\rangle\rangle\right),\end{aligned} \tag{2.72}$$

which is identical to what is obtained from the Markovian equation to $\mathcal{P}|\rho(t)\rangle\rangle$. This means that the Markovian equation also gives exact time-integrated properties of the reduced system, again even if the dynamics are not given accurately by the Markovian approximation.

2.3.4 Perturbation theory

As mentioned above, evaluating the full kernel is in general no simpler than just solving the full Liouville-von Neumann equation. This problem can be circumvented by the use of perturbation theory.[54–58] In this case we will assume that the Liouvillian $\mathcal{L}$ can be divided into a reference part $\mathcal{L}_0$ and a perturbation $\lambda\mathcal{L}_V$,

$$\mathcal{L} = \mathcal{L}_0 + \lambda\mathcal{L}_V. \tag{2.73}$$

We further assume that the projection operator $\mathcal{P}$ and $\mathcal{L}_0$ commute,

$$\mathcal{L}_0\mathcal{P} = \mathcal{P}\mathcal{L}_0, \tag{2.74}$$

and also that $\mathcal{L}_V$ and $\mathcal{P}$ satisfy

$$\mathcal{P}\mathcal{L}_V\mathcal{P} = 0. \tag{2.75}$$

With these two properties, we obtain the following relations between $\mathcal{L}$, $\mathcal{P}$ and $\mathcal{Q}$

$$\mathcal{P}\mathcal{L}\mathcal{P} = \mathcal{L}_0\mathcal{P} \tag{2.76a}$$

$$\mathcal{P}\mathcal{L}\mathcal{Q} = \lambda\mathcal{P}\mathcal{L}_V \tag{2.76b}$$

$$\mathcal{Q}\mathcal{L}\mathcal{P} = \lambda\mathcal{L}_V\mathcal{P} \tag{2.76c}$$

We are now in a position to use perturbation theory to obtain an approximate master equation from the full Nakajima-Zwanzig equation. We do this by expanding the kernel $\mathcal{K}(t)$ in powers of λ,

$$\mathcal{K}(t) = \sum_{n=0}^{\infty} \lambda^n \mathcal{K}^{(n)}(t) \tag{2.77}$$

The expansion can be be evaluated straightforwardly using the Fourier-Laplace transformed kernel $\tilde{\mathcal{K}}(\omega)$,[102] which can be obtained using the kernel definition, Eq. (2.54), and the Fourier-Laplace transform, Eq. (2.57),

$$\tilde{\mathcal{K}}(\omega) = -\mathcal{P}\mathcal{L}\mathcal{Q}[i\omega + \mathcal{Q}\mathcal{L}]^{-1}\mathcal{Q}\mathcal{L}\mathcal{P}. \tag{2.78}$$

Using the relationships above in Eqs. (2.76), we can expand this as a series in λ

$$\begin{aligned}\tilde{\mathcal{K}}(\omega) &= -\lambda^2 \mathcal{P}\mathcal{L}_V \mathcal{Q}[i\omega + \mathcal{Q}\mathcal{L}_0 + \lambda \mathcal{Q}\mathcal{L}_V]^{-1}\mathcal{Q}\mathcal{L}_V\mathcal{P} \\ &= \lambda^2 \mathcal{P}\mathcal{L}_V \mathcal{Q}[1 - (-i\omega - \mathcal{Q}\mathcal{L}_0)^{-1}\lambda\mathcal{Q}\mathcal{L}_V]^{-1}(-i\omega - \mathcal{Q}\mathcal{L}_0)^{-1}\mathcal{Q}\mathcal{L}_V\mathcal{P} \\ &= \sum_{n=2}^{\infty} \lambda^n \mathcal{P}\mathcal{L}_V \mathcal{Q}[(-i\omega - \mathcal{Q}\mathcal{L}_0)^{-1}\mathcal{Q}\mathcal{L}_V]^{n-2}(-i\omega - \mathcal{Q}\mathcal{L}_0)^{-1}\mathcal{Q}\mathcal{L}_V\mathcal{P}. \end{aligned} \tag{2.79}$$

We can write this in terms of the Fourier-Laplace transform of the reference propagator $\tilde{\mathcal{G}}_0(\omega)$,

$$\begin{aligned}\tilde{\mathcal{G}}_0(\omega) &= \int_0^\infty e^{i\omega t} e^{\mathcal{L}_0 t}\, \mathrm{d}t \\ &= (-i\omega - \mathcal{L}_0)^{-1}, \end{aligned} \tag{2.80}$$

by rewriting $(-i\omega - \mathcal{Q}\mathcal{L}_0)^{-1}$ as

$$\begin{aligned}(-i\omega - \mathcal{Q}\mathcal{L}_0)^{-1} &= \int_0^\infty e^{i\omega t} e^{\mathcal{Q}\mathcal{L}_0 t}\, \mathrm{d}t \\ &= \int_0^\infty e^{i\omega t} \left(e^{\mathcal{L}_0 t}\mathcal{Q} + \mathcal{P} \right) \mathrm{d}t \\ &= \tilde{\mathcal{G}}_0(\omega)\mathcal{Q} + \frac{1}{-i\omega}\mathcal{P}. \end{aligned} \tag{2.81}$$

Using the above expressions, and the properties of $\mathcal{P}, \mathcal{Q}$ and $\mathcal{L}_v$ in Eqs. (2.76), we can write $\tilde{\mathcal{K}}(\omega)$ as a series in λ as follows

$$\tilde{\mathcal{K}}(\omega) = \sum_{n=2}^{\infty} \lambda^n \tilde{\mathcal{K}}^{(n)}(\omega) \tag{2.82}$$

where the superoperators $\tilde{\mathcal{K}}^{(n)}(\omega)$ are given by

$$\tilde{\mathcal{K}}^{(n)}(\omega) = \mathcal{P}\mathcal{L}_V[\tilde{\mathcal{G}}_0(\omega)\mathcal{Q}\mathcal{L}_V]^{n-2}\tilde{\mathcal{G}}_0(\omega)\mathcal{L}_V\mathcal{P}. \tag{2.83}$$

To arrive at the final perturbation expansion for the kernel, we invert the Fourier-Laplace transformed version above using the convolution property Eq. (2.60), to find expressions for $\mathcal{K}^{(n)}(t)$. We see that the first non-zero term is the second order term in λ. To illustrate

this, the first three non-zero terms in the expansion are given below,

$$\mathcal{K}^{(2)}(t) = \mathcal{P}\mathcal{L}_V e^{\mathcal{L}_0 t}\mathcal{L}_V\mathcal{P} \tag{2.84}$$

$$\mathcal{K}^{(3)}(t) = \int_0^t \mathrm{d}t_0\, \mathcal{P}\mathcal{L}_V e^{\mathcal{L}_0(t-t_0)}\mathcal{L}_V e^{\mathcal{L}_0 t_0}\mathcal{L}_V\mathcal{P} \tag{2.85}$$

$$\mathcal{K}^{(4)}(t) = \int_0^t \mathrm{d}t_0 \int_0^{t_0} \mathrm{d}t_1\, \mathcal{P}\mathcal{L}_V e^{\mathcal{L}_0(t-t_0)}\mathcal{L}_V e^{\mathcal{L}_0(t_0-t_1)}\mathcal{Q}\mathcal{L}_V e^{\mathcal{L}_0 t_1}\mathcal{L}_V\mathcal{P}. \tag{2.86}$$

Often we will truncate the expansion at some value of n to obtain the nth order perturbative approximation to $\mathcal{K}(t)$. We can of course do the same thing for the inhomogeneous term, in which case we obtain

$$\tilde{i}(\omega) = \sum_{n=1}^{\infty} \lambda^n \tilde{i}^{(n)}(\omega) \tag{2.87}$$

$$\tilde{i}^{(n)}(\omega) = \mathcal{P}\mathcal{L}_V\mathcal{Q}[\mathcal{G}_0(\omega)\mathcal{Q}\mathcal{L}_V]^{n-1}\mathcal{G}_0(\omega)\mathcal{Q}\hat{\rho}(0). \tag{2.88}$$

For the inhomogeneous term, the first non-zero term is first order in λ.

For the kernel we can expect this series expansion to be convergent if

$$\left\|\tilde{\mathcal{G}}_0(\omega)\mathcal{Q}\mathcal{L}_V\tilde{\mathcal{G}}_0(\omega)\mathcal{L}_V\mathcal{P}\right\| < \left\|\tilde{\mathcal{G}}_0(\omega)\mathcal{L}_V\mathcal{P}\right\|. \tag{2.89}$$

It instructive to consider the long-time limit, which corresponds to the $\omega \to 0$, limit of this,

$$\left\|\mathcal{L}_0^{-1}\mathcal{Q}\mathcal{L}_V\mathcal{L}_0^{-1}\mathcal{L}_V\mathcal{P}\right\| < \left\|\mathcal{L}_0^{-1}\mathcal{L}_V\mathcal{P}\right\|. \tag{2.90}$$

Roughly speaking, what this means is that we need the longest time-scale of the reference dynamics generated by $\mathcal{L}_0$ from the initial state to be shorter than the shortest time-scale of the dynamics generated by the perturbation $\mathcal{L}_V$ from the same initial condition.

2.3.5 The perturbation series for the density operator

The accuracy of truncating the kernel can be assessed using the conventional approach in perturbation theory. We start by expanding the Fourier-Laplace transform of $\mathcal{P}\hat{\rho}(t)$ as a series in λ,

$$\mathcal{P}\tilde{\hat{\rho}}(\omega) = \sum_{n=0}^{\infty} \lambda^n \mathcal{P}\tilde{\hat{\rho}}^{(n)}(\omega). \tag{2.91}$$

Now inserting this, and the perturbative expansion of $\tilde{\mathcal{K}}(\omega)$ and $\tilde{\hat{\imath}}(\omega)$ into the Fourier-Laplace transformed Nakajima-Zwanzig equation, Eq. (2.61), we obtain

$$\begin{aligned} -i\omega \sum_{n=0}^{\infty} \lambda^n \mathcal{P}\tilde{\hat{\rho}}^{(n)}(\omega) - \mathcal{P}\hat{\rho}(0) = \mathcal{L}_0 \sum_{n=0}^{\infty} \lambda^n \mathcal{P}\tilde{\hat{\rho}}^{(n)}(\omega) \\ + \sum_{n=1}^{\infty} \lambda^n \tilde{\hat{\imath}}^{(n)}(\omega) + \sum_{n=0}^{\infty}\sum_{m=2}^{\infty} \lambda^{n+m} \tilde{\mathcal{K}}^{(m)}(\omega)\mathcal{P}\tilde{\hat{\rho}}^{(n)}(\omega). \end{aligned} \tag{2.92}$$

Now equating terms of the same power in λ we obtain

$$(-i\omega - \mathcal{L}_0)\mathcal{P}\tilde{\hat{\rho}}^{(m)}(\omega) = \delta_{m,0}\mathcal{P}\hat{\rho}(0) + \sum_{k=2}^{m} \tilde{\mathcal{K}}^{(k)}(\omega)\mathcal{P}\tilde{\hat{\rho}}^{(m-k)}(\omega) + \tilde{\hat{\imath}}^{(m)}(\omega). \tag{2.93}$$

For a truncation of $\mathcal{K}(t)$ and $\hat{\imath}(t)$ at order n, the equations are identical up to $m = n$. Therefore truncation of $\mathcal{K}(t)$ at order n does indeed give $\mathcal{P}\tilde{\rho}(\omega)$ (and thus also $\mathcal{P}\hat{\rho}(t)$) accurate to $\mathcal{O}(\lambda^{n+1})$, however truncation of $\mathcal{P}\tilde{\rho}(\omega)$ at nth order is not equivalent to the solution to the Nakajima-Zwanzig equation with $\mathcal{K}(t)$ truncated at order n.

2.3.6 Short time analysis of second order perturbation theory

The most commonly used truncation of the perturbative series is to retain only the lowest order λ^2 term, i.e. we make the approximation that

$$\mathcal{K}(t) \approx \lambda^2 \mathcal{K}^{(2)}(t). \tag{2.94}$$

From the above analysis we know that this will give $\mathcal{P}\hat{\rho}(t)$ accurate to $\mathcal{O}(\lambda^3)$ for all times. It is also useful to analyse the short time behaviour. In the following we will also assume that $\mathcal{Q}\hat{\rho}(0) = 0$, as is often found to be the case.

The short time analysis is most straightforward to do in the interaction picture, where $\hat{\rho}^{\mathrm{I}}(t) = e^{-\mathcal{L}_0 t}\hat{\rho}(t)$. In this case the full density operator evolves according to

$$\frac{\mathrm{d}}{\mathrm{d}t}\hat{\rho}^{\mathrm{I}}(t) = \lambda \mathcal{L}_V^{\mathrm{I}}(t)\hat{\rho}^{\mathrm{I}}(t) \tag{2.95}$$

in which

$$\mathcal{L}_V^{\mathrm{I}}(t) = e^{-\mathcal{L}_0 t}\mathcal{L}_V e^{\mathcal{L}_0 t}. \tag{2.96}$$

The Nakajima-Zwanzig equation in this case is

$$\frac{\mathrm{d}}{\mathrm{d}t}\mathcal{P}\hat{\rho}^{\mathrm{I}}(t) = \int_0^t e^{-\mathcal{L}_0 t}\mathcal{K}(t-\tau)e^{\mathcal{L}_0\tau}\mathcal{P}\hat{\rho}^{\mathrm{I}}(\tau)\,\mathrm{d}\tau\,. \tag{2.97}$$

In order to analyse the short time behaviour, we need to expand $\mathcal{P}\hat{\rho}^{\mathrm{I}}(\delta t)$ as a Taylor series about $t = 0$,

$$\mathcal{P}\hat{\rho}^{\mathrm{I}}(\delta t) = \sum_{n=0}^{\infty}\frac{\delta t^n}{n!}\mathcal{P}\frac{\mathrm{d}^n}{\mathrm{d}t^n}\hat{\rho}^{\mathrm{I}}(t)\bigg|_{t=0}. \tag{2.98}$$

For both the Nakajima-Zwanzig equation at any truncation of the $\mathcal{K}(t)$ in λ, and the full Liouville-von Neumann equation, $\frac{\mathrm{d}}{\mathrm{d}t}\mathcal{P}\hat{\rho}^{\mathrm{I}}(t)|_{t=0} = 0$ because $\hat{\rho}(0) = \mathcal{P}\hat{\rho}(0)$ and $\mathcal{P}\mathcal{L}_V\mathcal{P} = 0$, so they agree to at least $\mathcal{O}(\delta t^2)$.

We now consider the δt^2 term. The full second derivative is

$$\frac{\mathrm{d}^2}{\mathrm{d}t^2}\hat{\rho}^{\mathrm{I}}(t) = \lambda(\mathcal{L}_V^{\mathrm{I}}(t)\mathcal{L}_0 - \mathcal{L}_0\mathcal{L}_V^{\mathrm{I}}(t))\hat{\rho}^{\mathrm{I}}(t) + \lambda^2\mathcal{L}_V^{\mathrm{I}}(t)\mathcal{L}_V^{\mathrm{I}}(t)\hat{\rho}^{\mathrm{I}}(t) \tag{2.99}$$

Projecting this with $\mathcal{P}$ and noting that $\mathcal{Q}\hat{\rho}(0) = 0$, $\mathcal{P}\mathcal{L}_0 = \mathcal{L}_0\mathcal{P}$ and $\mathcal{P}\mathcal{L}_V\mathcal{P} = 0$ we obtain

$$\mathcal{P}\frac{\mathrm{d}^2}{\mathrm{d}t^2}\hat{\rho}^{\mathrm{I}}(t)\bigg|_{t=0} = \lambda^2\mathcal{P}\mathcal{L}_V\mathcal{L}_V\mathcal{P}\hat{\rho}(0). \tag{2.100}$$

We will now do the same thing for the Nakajima-Zwanzig equation. Firstly, we note that

$$\frac{\mathrm{d}}{\mathrm{d}t}\int_0^t \mathrm{d}\tau\, f(t,\tau)\bigg|_{t=t_0} = f(t_0,t_0) + \int_0^t \mathrm{d}t\,\frac{\partial}{\partial t}f(t,\tau)\bigg|_{t=t_0} \tag{2.101}$$

$$\implies \frac{\mathrm{d}}{\mathrm{d}t}\int_0^t \mathrm{d}\tau\, f(t,\tau)\bigg|_{t=0} = f(0,0), \tag{2.102}$$

and therefore from the Nakajima-Zwanzig equation we also obtain Eq. (2.100), but we also note that

$$\mathcal{K}(0)\mathcal{P}\hat{\rho}(0) = \mathcal{K}^{(2)}(0)\mathcal{P}\hat{\rho}(0). \tag{2.103}$$

And therefore the second order truncation of the Nakajima-Zwanzig kernel, gives $\mathcal{P}\hat{\rho}(\delta t)$ accurate to $\mathcal{O}(\delta t^3)$. This argument also generalises straightforwardly to the case where $\mathcal{Q}\hat{\rho}(0) \neq 0$.

We have established that truncation of the kernel in the Nakajima-Zwanzig kernel at

lowest order in the perturbation strength λ gives the projected density operator accurate to order λ^2 at all times and in the short time limit it is accurate to order t^2. If we however combine these approximations by both truncating the kernel at lowest order in the perturbation strength and making the Markovian approximation, the short time accuracy of the Nakajima-Zwanzig equation with a truncated kernel is lost. So the second order Markovian Nakajima-Zwanzig equation will only be accurate to λ^2 in the long time limit and for time-integrated properties.

2.4 Other approximate QMEs

Whilst most of the results in this thesis use the Nakajima-Zwanzig quantum master equation, combined with perturbation theory and the Markovian approximation, there also exist a range of alternative master equation approaches. Here I will briefly summarise the main alternatives: the time-convolutionless QME, the cumulant expansion and Redfield theory, and I will also highlight the connections between these approaches and the Nakajima-Zwanzig equation.

2.4.1 The time-convolutionless QME

The Nakajima-Zwanzig equation, Eq. (2.53), derived in section 2.2.2, involves a time-convolution of the memory kernel $\mathcal{K}(\tau)$ and the projected density operator $\mathcal{P}\hat{\rho}(\tau)$ for $\tau < t$. This type of equation can be difficult to solve both numerically and analytically, so we introduced the Markovian approximation to the Nakajima-Zwanzig equation, Eq. (2.62), in section 2.3.1 to eliminate this time-convolution. The price we pay for this is loss of accuracy in higher moments of the reduced system variables $\langle \Delta A_n(t) \rangle$, as is shown in appendix 2.A. There is another way to eliminate the time-convolution, and still end up with a formally exact quantum master equation; this is the *time-convolutionless* (TCL) quantum master equation approach.[54,64,65]

The TCL approach is also based using a formal solution for $\mathcal{Q}\hat{\rho}(t)$ in terms of $\mathcal{P}\hat{\rho}(t)$ to eliminate $\mathcal{Q}\hat{\rho}(t)$ from Eq. (2.48) for $\mathcal{P}\hat{\rho}(t)$. We again use the solution to Eq. (2.49), given by Eq. (2.52), to eliminate $\mathcal{Q}\hat{\rho}(t)$ but into this we insert the formal solution for $\mathcal{P}\hat{\rho}(\tau)$ from

the Liouville-von Neumann equation,

$$\begin{aligned}\mathcal{P}\hat{\rho}(\tau) &= \mathcal{P}e^{-\mathcal{L}(t-\tau)}\hat{\rho}(t) \\ &= \mathcal{P}e^{-\mathcal{L}(t-\tau)}\mathcal{P}\hat{\rho}(t) + \mathcal{P}e^{-\mathcal{L}(t-\tau)}\mathcal{Q}\hat{\rho}(t).\end{aligned} \tag{2.104}$$

Inserting this into Eq. (2.52) gives,

$$\begin{aligned}\mathcal{Q}\hat{\rho}(t) = &\int_0^t \mathrm{d}\tau\, e^{\mathcal{Q}\mathcal{L}(t-\tau)}\mathcal{Q}\mathcal{L}\mathcal{P}e^{-\mathcal{L}(t-\tau)}\mathcal{P}\hat{\rho}(t) \\ &+ \int_0^t \mathrm{d}\tau\, e^{\mathcal{Q}\mathcal{L}(t-\tau)}\mathcal{Q}\mathcal{L}\mathcal{P}e^{-\mathcal{L}(t-\tau)}\mathcal{Q}\hat{\rho}(t) + e^{\mathcal{Q}\mathcal{L}t}\mathcal{Q}\hat{\rho}(0).\end{aligned} \tag{2.105}$$

We define the superoperator $\Sigma(t)$ as

$$\Sigma(t) = \int_0^t \mathrm{d}\tau\, e^{\mathcal{Q}\mathcal{L}(t-\tau)}\mathcal{Q}\mathcal{L}\mathcal{P}e^{-\mathcal{L}(t-\tau)}, \tag{2.106}$$

and with this definition we can solve Eq. (2.105) for $\mathcal{Q}\hat{\rho}(t)$,

$$\mathcal{Q}\hat{\rho}(t) = [1-\Sigma(t)]^{-1}\Sigma(t)\mathcal{P}\hat{\rho}(t) + [1-\Sigma(t)]^{-1}e^{\mathcal{Q}\mathcal{L}t}\mathcal{Q}\hat{\rho}(0). \tag{2.107}$$

Inserting this into Eq. (2.48) gives the following

$$\begin{aligned}\frac{\mathrm{d}}{\mathrm{d}t}\mathcal{P}\hat{\rho}(t) = &\mathcal{P}\mathcal{L}\mathcal{P}\hat{\rho}(t) + \mathcal{P}\mathcal{L}[1-\Sigma(t)]^{-1}\Sigma(t)\mathcal{P}\hat{\rho}(t) \\ &+ \mathcal{P}\mathcal{L}[1-\Sigma(t)]^{-1}e^{\mathcal{Q}\mathcal{L}t}\mathcal{Q}\hat{\rho}(0)\end{aligned} \tag{2.108}$$

Using this we find the time-convolutionless quantum master equation for the projected density operator,

$$\frac{\mathrm{d}}{\mathrm{d}t}\mathcal{P}\hat{\rho}(t) = \mathcal{P}\mathcal{L}\mathcal{P}\hat{\rho}(t) + \mathcal{K}_{\mathrm{TCL}}(t)\mathcal{P}\hat{\rho}(t) + \hat{\imath}_{\mathrm{TCL}}(t) \tag{2.109}$$

where the TCL generator $\mathcal{K}_{\mathrm{TCL}}(t)$ is given by

$$\mathcal{K}_{\mathrm{TCL}}(t) = \mathcal{P}\mathcal{L}[1-\Sigma(t)]^{-1}\Sigma(t)\mathcal{P}, \tag{2.110}$$

and the TCL inhomogeneous term $\hat{\imath}_{\mathrm{TCL}}(t)$ is given by

$$\hat{\imath}_{\mathrm{TCL}}(t) = \mathcal{P}\mathcal{L}[1-\Sigma(t)]^{-1}e^{\mathcal{Q}\mathcal{L}t}\mathcal{Q}\hat{\rho}(0). \tag{2.111}$$

This is another formally exact quantum master equation the projected density operator,

which suffers from the same pathology as the formally exact Nakajima-Zwanzig equation: evaluating $\mathcal{K}_{\mathrm{TCL}}(t)$ and $\hat{\imath}_{\mathrm{TCL}}(t)$ is no easier than solving the full Liouville-von Neumann equation. This means we have to make some approximations to derive useful TCL quantum master equations.

Analogous to when we applied perturbation theory to approximate the memory kernel $\mathcal{K}(t)$ in section 2.3.4, we can also apply perturbation theory to evaluate the TCL generator $\mathcal{K}_{\mathrm{TCL}}(t)$. As before we split the Liouvillian into a reference part $\mathcal{L}_0$ and a perturbation $\lambda\mathcal{L}_V$ and we write the TCL generator as a series in λ

$$\mathcal{K}_{\mathrm{TCL}}(t) = \sum_{n=0}^{\infty} \lambda^n \mathcal{K}^{(n)}_{\mathrm{TCL}}(t). \tag{2.112}$$

Assuming we can write $[1-\Sigma(t)]^{-1} = \sum_{n=0}^{\infty} \Sigma(t)^n$, and writing $\Sigma(t)$ as a perturbation series as well, we can straightforwardly evaluate the perturbation series for $\mathcal{K}_{\mathrm{TCL}}(t)$. Recalling that we define $\mathcal{L}_V$ such that $\mathcal{P}\mathcal{L}_V\mathcal{P} = 0$, the first non-zero term is the second order term which is given by

$$\mathcal{K}^{(2)}_{\mathrm{TCL}}(t) = \int_0^t \mathrm{d}\tau\, \mathcal{P}\mathcal{L}_V e^{\mathcal{L}_0\tau}\mathcal{L}_V e^{-\mathcal{L}_0\tau}\mathcal{P}. \tag{2.113}$$

We can analogously expand the inhomogeneous term,

$$\hat{\imath}^{(0)}_{\mathrm{TCL}}(t) = 0 \tag{2.114a}$$

$$\hat{\imath}^{(1)}_{\mathrm{TCL}}(t) = \mathcal{P}\mathcal{L}_V e^{\mathcal{L}_0 t}\mathcal{Q}\hat{\rho}(0) \tag{2.114b}$$

$$\hat{\imath}^{(2)}_{\mathrm{TCL}}(t) = \int_0^t \mathrm{d}\tau\, \mathcal{P}\mathcal{L}_V e^{\mathcal{L}_0(t-\tau)}\mathcal{L}_V e^{\mathcal{L}_0\tau}\mathcal{Q}\hat{\rho}(0). \tag{2.114c}$$

Further to this, if the integrand in the TCL generator, Eq. (2.113), decays to zero on a time-scale faster than the dynamics of $\mathcal{P}\hat{\rho}(t)$, then we can make the TCL equation time homogeneous by replacing the upper limit of the integral t with ∞. In the special case where $\mathcal{L}_0\mathcal{P} = 0$, this gives a master equation identical to the second order Markovian Nakajima-Zwanzig equation.

The TCL master equation gives an alternative perturbative approach for calculating the reduced system dynamics. We will analyse this more in section 2.4.3, but before that, we will show that the TCL approach is closely related to another approach more commonly

used in spin dynamics: the cumulant expansion.

2.4.2 The cumulant expansion

Another method for obtaining a time-convolutionless quantum master equation is the cumulant expansion.[103] This method is somewhat less general than the Nakajima-Zwanzig equation and the TCL QME described above, because it is limited to the case of a simple system-bath partitioning, as described in section 2.1.3, where we are interested in the reduced density operator for the system $\hat{\sigma}_\mathrm{s}(t) = \mathrm{Tr}_\mathrm{b}[\hat{\rho}(t)]$. In other words we are restricted to projection superoperators of the form $\mathcal{P} = \hat{\rho}_\mathrm{b}\,\mathrm{Tr}_\mathrm{b}[\,\cdot\,]$. We further assume that $\hat{\rho}(0) = \hat{\sigma}_\mathrm{s}(0)\hat{\rho}_\mathrm{b}$, so $\mathcal{Q}\hat{\rho}(0) = 0$. Once again we can partition the full Liouvillian into a reference part and a perturbation, and we also split the reference Liouvillian $\mathcal{L}_0$ into a part that only acts on system degrees of freedom $\mathcal{L}_\mathrm{s}$, and a part that only acts on the bath degrees of freedom $\mathcal{L}_\mathrm{b}$.

We start by transforming to the interaction picture, in which the transformed density operator is defined as

$$\hat{\rho}^\mathrm{I}(t) = e^{-\mathcal{L}_0 t}\hat{\rho}(t), \tag{2.115}$$

and the interaction picture superoperators are defined by

$$\mathcal{A}^\mathrm{I}(t) = e^{-\mathcal{L}_0 t}\mathcal{A}e^{\mathcal{L}_0 t}. \tag{2.116}$$

Under this transformation, the Liouville-von Neumann equation, Eq. 2.29, becomes

$$\frac{\mathrm{d}}{\mathrm{d}t}\hat{\rho}^\mathrm{I}(t) = \lambda\mathcal{L}_V^\mathrm{I}(t)\hat{\rho}^\mathrm{I}(t), \tag{2.117}$$

the formal solution to which is

$$\hat{\rho}^\mathrm{I}(t) = \mathsf{T}\exp\left[\int_0^t \mathrm{d}\tau\,\lambda\mathcal{L}_V^\mathrm{I}(\tau)\right]\hat{\rho}_\mathrm{b}\hat{\sigma}_\mathrm{s}(0), \tag{2.118}$$

where T is the time ordering operator in Liouville space, which chronologically orders interaction picture superoperators from earliest on the right to latest on the left. This

time-ordered superoperator can be expanded as,

$$\begin{aligned}
&\mathsf{T}\exp\left[\int_0^t \mathrm{d}\tau\, \lambda \mathcal{L}_V^{\mathrm{I}}(\tau)\right] \\
&= 1 + \lambda \int_0^t \mathrm{d}\tau_1\, \mathcal{L}_V^{\mathrm{I}}(\tau_1) + \lambda^2 \int_0^t \mathrm{d}\tau_1 \int_0^{\tau_1} \mathrm{d}\tau_2\, \mathcal{L}_V^{\mathrm{I}}(\tau_1)\mathcal{L}_V^{\mathrm{I}}(\tau_2) + \cdots \\
&\quad + \lambda^k \int_0^t \mathrm{d}\tau_1 \int_0^{\tau_1} \mathrm{d}\tau_2 \cdots \int_0^{\tau_{k-1}} \mathrm{d}\tau_k\, \mathcal{L}_V^{\mathrm{I}}(\tau_1)\mathcal{L}_V^{\mathrm{I}}(\tau_2)\cdots\mathcal{L}_V^{\mathrm{I}}(\tau_k) + \cdots .
\end{aligned} \tag{2.119}$$

With this, we can find $\hat{\sigma}_{\mathrm{s}}^{\mathrm{I}}(t)$ by taking the trace over the bath, which gives

$$\hat{\sigma}_{\mathrm{s}}^{\mathrm{I}}(t) = \left\langle \mathsf{T}\exp\left[\int_0^t \mathrm{d}\tau\, \lambda \mathcal{L}_V^{\mathrm{I}}(\tau)\right]\right\rangle_{\mathrm{b}} \hat{\sigma}_{\mathrm{s}}(0), \tag{2.120}$$

where we have defined the bath average as

$$\langle\, \cdot\, \rangle_{\mathrm{b}} = \mathrm{Tr}_{\mathrm{b}}[\, \cdot\, \hat{\rho}_{\mathrm{b}}]. \tag{2.121}$$

We now invoke the cumulant expansion. This is done by writing the system propagator as a time-ordered exponential of the cumulant expansion in the perturbation strength λ,

$$\left\langle \mathsf{T}\exp\left[\int_0^t \mathrm{d}\tau\, \lambda \mathcal{L}_V^{\mathrm{I}}(\tau)\right]\right\rangle_{\mathrm{b}} = \mathsf{T}\exp\left[\sum_{k=1}^{\infty} \lambda^k C_k^{\mathrm{I}}(t)\right]. \tag{2.122}$$

The cumulants, $C_n^{\mathrm{I}}(t)$, can be found by comparing coefficients of λ in the exponentiated form of Eq. (2.122) and the expansion of $\left\langle \mathsf{T}\exp\left[\int_0^t \mathrm{d}\tau\, \lambda \mathcal{L}_V^{\mathrm{I}}(\tau)\right]\right\rangle_{\mathrm{b}}$ using Eq. (2.119). Recalling that $\langle \mathcal{L}_V \rangle_{\mathrm{b}} = 0$, the first two cumulants are,

$$C_1^{\mathrm{I}}(t) = 0 \tag{2.123a}$$

$$C_2^{\mathrm{I}}(t) = \int_0^t \mathrm{d}\tau_1 \int_0^{\tau_1} \mathrm{d}\tau_2 \left\langle \mathcal{L}_V^{\mathrm{I}}(\tau_1)\mathcal{L}_V^{\mathrm{I}}(\tau_2)\right\rangle_{\mathrm{b}} \tag{2.123b}$$

Truncating this cumulant expansion at some order n gives the nth order cumulant expansion for the system density operator. This can be recast into a differential equation for $\hat{\sigma}_{\mathrm{s}}(t)$ by differentiating Eq. (2.122),

$$\frac{\mathrm{d}}{\mathrm{d}t}\hat{\sigma}_{\mathrm{s}}^{\mathrm{I}}(t) = \sum_{k=1}^{\infty} \lambda^k \left[\frac{\mathrm{d}}{\mathrm{d}t} C_k^{\mathrm{I}}(t)\right] \hat{\sigma}_{\mathrm{s}}^{\mathrm{I}}(t) \tag{2.124}$$

which when transformed back to the Schrödinger picture gives

$$\frac{\mathrm{d}}{\mathrm{d}t}\hat{\sigma}_{\mathrm{s}}(t) = \mathcal{L}_{\mathrm{s}}\hat{\sigma}_{\mathrm{s}}(t) + \mathcal{K}_{\mathrm{CE}}(t)\hat{\sigma}_{\mathrm{s}}(t). \tag{2.125}$$

where the cumulant expansion generator is

$$\mathcal{K}_{\mathrm{CE}}(t) = \sum_{k=1}^{\infty} \lambda^k e^{\mathcal{L}_{\mathrm{s}}t} \left[\frac{\mathrm{d}}{\mathrm{d}t}\mathcal{C}_k^{\mathrm{I}}(t)\right] e^{-\mathcal{L}_{\mathrm{s}}t}. \tag{2.126}$$

We see that when the cumulant expansion is truncated at second order we obtain

$$\mathcal{K}_{\mathrm{CE}}^{(2)}(t) = \int_0^t \mathrm{d}\tau \left\langle \mathcal{L}_V e^{\mathcal{L}_0\tau}\mathcal{L}_V e^{-\mathcal{L}_0\tau}\right\rangle_{\mathrm{b}}, \tag{2.127}$$

which is identical to the TCL generator truncated at second order with a system-bath projection superoperator, after tracing out the bath. In general, the cumulant expansion and the TCL generator expansion should give identical master equations for the reduced density operator, so the cumulant expansion can be seen as an alternative to Eq. (2.110) for finding the TCL generator.[55]

2.4.3 Redfield theory

Bloch-Redfield-Wangsness theory[60,61], henceforth simply referred to as Redfield theory,[c] is a commonly used approximate master equation, especially in the field of spin dynamics. It is a Markovian, time-homogeneous quantum master equation for the reduced density operator of a system. The Redfield equation can be arrived at from the cumulant expansion quantum master equation (or the TCL quantum master equation), by taking the second order cumulant expansion (or equivalently the second order TCL master equation) and approximating $\mathcal{K}_{\mathrm{CE}}^{(2)}(t)$ with its long-time limit,

$$\mathcal{K}_{\mathrm{CE}}^{(2)}(t) \approx \lim_{t\to\infty} \mathcal{K}_{\mathrm{CE}}^{(2)}(t). \tag{2.128}$$

This approximation is valid if the time-scale on which $\mathcal{K}_{\mathrm{CE}}(t)$ reaches its long-time limit is much faster than the dynamics of the reduced density operator. This gives the following

[c] In some of the open quantum systems literature, the term Redfield theory is also used to refer to the second order Markovian Nakajima-Zwanzig equation. In this thesis I will use Redfield theory exclusively to refer to the original Bloch-Redfield-Wangsness theory, which is based on the TCL formalism.

quantum master equation for the reduced density operator,

$$\frac{\mathrm{d}}{\mathrm{d}t}\hat{\sigma}_{\mathrm{s}}(t) = \mathcal{L}_{\mathrm{s}}\hat{\sigma}_{\mathrm{s}}(t) + \mathcal{R}_{\mathrm{RF}}\hat{\sigma}_{\mathrm{s}}(t), \tag{2.129}$$

where

$$\mathcal{R}_{\mathrm{RF}} = \int_0^\infty \mathrm{d}\tau \left\langle \mathcal{L}_V e^{\mathcal{L}_0\tau}\mathcal{L}_V e^{-\mathcal{L}_0\tau}\right\rangle_{\mathrm{b}}. \tag{2.130}$$

We can compare this to the second-order Markovian Nakajima-Zwanzig equation for the reduced density operator,

$$\frac{\mathrm{d}}{\mathrm{d}t}\hat{\sigma}_{\mathrm{s}}(t) = \mathcal{L}_{\mathrm{s}}\hat{\sigma}_{\mathrm{s}}(t) + \mathcal{R}_{\mathrm{NZ}}\hat{\sigma}_{\mathrm{s}}(t), \tag{2.131}$$

where

$$\mathcal{R}_{\mathrm{NZ}} = \int_0^\infty \mathrm{d}\tau \left\langle \mathcal{L}_V e^{\mathcal{L}_0\tau}\mathcal{L}_V\right\rangle_{\mathrm{b}}. \tag{2.132}$$

The difference is the presence of a backwards reference propagator in Eq. (2.130) which is absent in Eq. (2.132). Although this difference is small, it will be shown in chapter 6 that it can have a big effect on the accuracy of these equations, but for now we will only briefly discuss the origin of this difference.

The Redfield and second order Markovian Nakajima-Zwanzig equations can be arrived at in a slightly different way to that presented above.[62] We start from the Liouville-von Neumann equation in the interaction picture, Eq. (2.117). Integrating this equation gives

$$\hat{\rho}^{\mathrm{I}}(t) = \hat{\rho}(0) + \int_0^t \mathrm{d}\tau\, \mathcal{L}_V^{\mathrm{I}}(\tau)\hat{\rho}^{\mathrm{I}}(\tau). \tag{2.133}$$

Substituting this back into the interaction picture Liouville-von Neumann equation gives

$$\frac{\mathrm{d}}{\mathrm{d}t}\hat{\rho}^{\mathrm{I}}(t) = \mathcal{L}_V^{\mathrm{I}}(t)\hat{\rho}(0) + \mathcal{L}_V^{\mathrm{I}}(t)\int_0^t \mathrm{d}\tau\, \mathcal{L}_V^{\mathrm{I}}(\tau)\hat{\rho}^{\mathrm{I}}(\tau). \tag{2.134}$$

Taking the trace over the bath of this gives an equation for the reduced density operator

$$\frac{\mathrm{d}}{\mathrm{d}t}\hat{\sigma}_{\mathrm{s}}^{\mathrm{I}}(t) = \int_0^t \mathrm{d}\tau\, \mathrm{Tr}_{\mathrm{b}}[\mathcal{L}_V^{\mathrm{I}}(t)\mathcal{L}_V^{\mathrm{I}}(\tau)\hat{\rho}^{\mathrm{I}}(\tau)]. \tag{2.135}$$

At this stage we can make one of two possible approximations. To obtain Redfield theory,

we approximate the system and bath as being uncorrelated in the interaction picture, and we assume the bath does not evolve, so $\hat{\rho}^{\mathrm{I}}(\tau) \approx \sigma_{\mathrm{s}}^{\mathrm{I}}(\tau)\hat{\rho}_{\mathrm{b}}$. Then assuming a separation of time-scales between $\left\langle \mathcal{L}_V^{\mathrm{I}}(t)\mathcal{L}_V^{\mathrm{I}}(\tau)\right\rangle_{\mathrm{b}}$ and $\sigma_{\mathrm{s}}^{\mathrm{I}}(\tau)$, we also replace $\sigma_{\mathrm{s}}^{\mathrm{I}}(\tau)$ with $\sigma_{\mathrm{s}}^{\mathrm{I}}(t)$, so we make the following replacement,[62]

$$\mathrm{Tr}_{\mathrm{b}}[\mathcal{L}_V^{\mathrm{I}}(t)\mathcal{L}_V^{\mathrm{I}}(\tau)\hat{\rho}^{\mathrm{I}}(\tau)] \approx \left\langle \mathcal{L}_V^{\mathrm{I}}(t)\mathcal{L}_V^{\mathrm{I}}(\tau)\right\rangle_{\mathrm{b}} \hat{\sigma}_{\mathrm{s}}^{\mathrm{I}}(t), \tag{2.136}$$

and then finally after transforming back to the Schrödinger picture, we replace the upper limit of the integral with ∞, again assuming the time-scale on which the integral reaches its long-time limit is very short.

The second possible approximation yields the second order Markovian Nakajima-Zwanzig equation. In this case we transform back to the Schrödinger picture first to give,

$$\frac{\mathrm{d}}{\mathrm{d}t}\hat{\sigma}_{\mathrm{s}}(t) = \mathcal{L}_{\mathrm{s}}\hat{\sigma}_{\mathrm{s}}(t) + \int_0^t \mathrm{d}\tau\, \mathrm{Tr}_{\mathrm{b}}[\mathcal{L}_V e^{\mathcal{L}_0\tau}\mathcal{L}_V\hat{\rho}(t-\tau)]. \tag{2.137}$$

and then we make essentially the same approximations as above but *in the Schrödinger picture*, i.e. we assume the system and bath are uncorrelated, and the bath does not evolve $\hat{\rho}(t-\tau) \approx \hat{\sigma}_{\mathrm{s}}(t-\tau)\hat{\rho}_{\mathrm{b}}$ and we assume $\left\langle \mathcal{L}_V e^{\mathcal{L}_0\tau}\mathcal{L}_V\right\rangle_{\mathrm{b}}$ evolves much faster than $\hat{\sigma}_{\mathrm{s}}(t)$, so we make the following replacement

$$\mathrm{Tr}_{\mathrm{b}}[\mathcal{L}_V e^{\mathcal{L}_0\tau}\mathcal{L}_V\hat{\rho}(t-\tau)] \approx \left\langle \mathcal{L}_V e^{\mathcal{L}_0\tau}\mathcal{L}_V\right\rangle_{\mathrm{b}} \sigma_{\mathrm{s}}(t), \tag{2.138}$$

and again also set the upper limit of the integral to ∞. So we can see the difference between the Redfield and second order Nakajima-Zwanzig approximations as arising from the choice of frame, interaction picture or Schrödinger picture, in which we make the approximation that the system and bath are uncorrelated. It is not immediately obvious why one choice is better than the other, but from the previous analysis, we see that taking the Nakajima-Zwanzig approach gives an equation which is correct to second order in the perturbation at long times and for time-integrated properties, whilst the Redfield approach however does not possess this property.

2.5 Summary

In this chapter I have described the framework for deriving both formally exact and approximate quantum master equations from Nakajima-Zwanzig theory, and I have described some general considerations for when we can expect these approximations to be valid. I have also outlined several other important approximate quantum master equations, and highlighted some of the differences between these approaches and Nakajima-Zwanzig theory. The remainder of this thesis will demonstrate utility of Nakajima-Zwanzig theory in Spin Chemistry, where it finds a range of applications from resolving questions about the fundamental description of radical pair reactions, to providing new tools for efficiently simulating spin chemical phenomena.

Appendix

2.A Appendix: Error of the Markovian approximation

Having established above that the Markovian approximation gives the long-time limit and time integrated properties of the reduced system exactly, here we will estimate the error introduced by the Markovian approximation. In order to evaluate this error, we consider the error in the various moments of $\langle \Delta A_n(t) \rangle$, denoted by $\mu^{(m)}(\Delta A_n)$, which are defined as

$$\mu^{(m)}(\Delta A_n) = \int_0^\infty t^m \, \langle \Delta A_n(t) \rangle \, \mathrm{d}t \, . \tag{2.A.1}$$

From our previous analysis, the Markovian approximation gives the $m = 0$ moment exactly. The first moment that is not be captured exactly by the Markovian approximation is the $m = 1$ moment, so we focus on evaluating the error in $\mu^{(1)}(\Delta A_n)$ introduced by this approximation. Using the definition of the Fourier-Laplace transform, Eq. (2.57), we can relate these moments to mth derivatives of $\left\langle \Delta \tilde{A}_n(\omega) \right\rangle$ as follows

$$\mu^{(m)}(\Delta A_n) = (-i)^m \frac{\mathrm{d}^m}{\mathrm{d}\omega^m} \left\langle \Delta \tilde{A}_n(\omega) \right\rangle \Big|_{\omega=0} . \tag{2.A.2}$$

Thus we need to consider the Taylor series of $\left\langle \Delta \tilde{A}_n(\omega) \right\rangle$ around $\omega = 0$, because from Eq. (2.A.2) this is related to the moments by

$$\left\langle \Delta \tilde{A}_n(\omega) \right\rangle = \sum_{m=0}^{\infty} \frac{1}{m!} (i\omega)^m \mu^{(m)}(\Delta A_n). \tag{2.A.3}$$

Using Eq. (2.67), $\left\langle \Delta\tilde{A}_n(\omega) \right\rangle$ is given exactly by

$$\left\langle \Delta\tilde{A}_n(\omega) \right\rangle = \langle\langle \Delta A_n | [-i\omega - \mathcal{P}\mathcal{L}\mathcal{P} - \tilde{\mathcal{K}}(\omega)]^{-1} \left(\mathcal{P}|\rho(0)\rangle\rangle + |\tilde{\imath}(\omega)\rangle\rangle\right). \tag{2.A.4}$$

We know that the Markovian approximation gives the series expansion about $\omega = 0$ exactly to $O(\omega)$, and also clearly the Markovian approximation correctly gives the limit as $\omega \to \infty$ (noting that $\tilde{\mathcal{K}}(\omega) \to 0$ and $|\tilde{\imath}(\omega)\rangle\rangle \to 0$ in this limit), which is simply $\left\langle \Delta\tilde{A}_n(\omega) \right\rangle \sim (-i\omega)^{-1} \langle \Delta A_n(0) \rangle$. In order to proceed with the error analysis of the Markovian approximation, it is useful to first define the Markovian and non-Markovian parts of the Nakajima-Zwanzig equation, by dividing the generator for the dynamics into its Markovian part, $\mathcal{K}_0$, and non-Markovian part, $\Delta\tilde{\mathcal{K}}(\omega)$, as follows,

$$\mathcal{K}_0 = \mathcal{P}\mathcal{L}\mathcal{P} + \tilde{\mathcal{K}}(0) \tag{2.A.5}$$

$$\Delta\tilde{\mathcal{K}}(\omega) = \tilde{\mathcal{K}}(\omega) - \tilde{\mathcal{K}}(0). \tag{2.A.6}$$

For small ω we can expand $\Delta\tilde{\mathcal{K}}(\omega)$ as

$$\Delta\tilde{\mathcal{K}}(\omega) = \omega\tilde{\mathcal{K}}'(0) + O(\omega^2), \tag{2.A.7}$$

where $\tilde{\mathcal{K}}'(\omega) = \frac{\mathrm{d}}{\mathrm{d}\omega}\tilde{\mathcal{K}}(\omega)$. We define the Markovian propagator and its Fourier-Laplace transform as

$$\mathcal{U}_0(t) = \exp(\mathcal{K}_0 t) \tag{2.A.8}$$

$$\tilde{\mathcal{U}}_0(\omega) = [-i\omega - \mathcal{K}_0]^{-1}. \tag{2.A.9}$$

Now we will assume that $\mathcal{K}_0$ is diagonalisable (within the projected subspace), i.e.

$$\mathcal{K}_0 = \sum_k \lambda_k \Pi_k, \tag{2.A.10}$$

where λ_k are the eigenvalues, the real parts of which we will assume satisfy $\mathrm{Re}[\lambda_k] \leq 0$, and the superoperators Π_k are projection superoperators which satisfy,

$$\Pi_k \Pi_l = \delta_{kl} \Pi_k \tag{2.A.11}$$

$$\mathcal{P} = \sum_k \Pi_k. \tag{2.A.12}$$

Using this, the Markovian propagator, and its Fourier-Laplace transform are

$$\mathcal{U}_0(t) = \sum_k e^{\lambda_k t}\Pi_k \tag{2.A.13}$$

$$\tilde{\mathcal{U}}_0 = \sum_k \frac{1}{-i\omega - \lambda_k}\Pi_k. \tag{2.A.14}$$

Assuming for simplicity that for all initial conditions of the reduced system with $\langle\langle 1|\mathcal{P}\rho(0)\rangle\rangle = 1$ the same long-time limit is reached, there will be a single zero eigenvalue, $\lambda_0 = 0$, and the projector Π_0 must be

$$\Pi_0 = |\rho(t \to \infty)\rangle\rangle\langle\langle 1|. \tag{2.A.15}$$

The longest non-zero time-scale of the Markovian dynamics τ_0 can be defined using the non-zero eigenvalues of $\mathcal{K}_0$ as $\tau_0 = \max_{\lambda_k \neq 0}(1/|\lambda_k|)$.

Since our aim is to find the error in higher moments of reduced system variables introduced by the Markovian approximation, we can recast the solution to Eq. (2.61) in into a sum of the Markovian term, $\mathcal{P}|\tilde{\rho}_0(\omega)\rangle\rangle = \tilde{\mathcal{U}}_0(\omega)\left(|\rho(0)\rangle\rangle + |\tilde{\imath}(0)\rangle\rangle\right)$, and a non-Markovian term using the formal solution (Eq. (2.67)),

$$\begin{aligned}\mathcal{P}|\tilde{\rho}(\omega)\rangle\rangle &= \mathcal{P}|\tilde{\rho}_0(\omega)\rangle\rangle + \tilde{\mathcal{U}}_0(\omega)|\Delta\tilde{\imath}(\omega)\rangle\rangle \\ &+\tilde{\mathcal{U}}_0(\omega)\Delta\tilde{\mathcal{K}}(\omega)[-i\omega - \mathcal{K}_0 - \Delta\tilde{\mathcal{K}}(\omega)]^{-1}\left(|\rho(0)\rangle\rangle + |\tilde{\imath}(\omega)\rangle\rangle\right).\end{aligned} \tag{2.A.16}$$

The first term on the left-hand side is simply the Markovian solution, and therefore the other two terms give rise to non-Markovian dynamics. We can now consider the expansion of the non-Markovian terms in powers of ω to find the error in the first moments of the reduced system variable time-evolution. We note that $\langle\langle 1|\iota(t)\rangle\rangle = 0$ and $|\Delta\tilde{\imath}(\omega)\rangle\rangle = \omega|\tilde{\imath}'(0)\rangle\rangle + O(\omega^2)$. Combining this with $\tilde{\mathcal{U}}_0(\omega) = \sum_k(-i\omega - \lambda_k)^{-1}\Pi_k$ and Eq. (2.A.15) for Π_0 implies that there is no $O(1)$ term in $\tilde{\mathcal{U}}_0(0)|\Delta\tilde{\imath}(\omega)\rangle\rangle$, and therefore this first non-Markovian term can be written as

$$\tilde{\mathcal{U}}_0(\omega)|\Delta\tilde{\imath}(\omega)\rangle\rangle = \omega\tilde{\mathcal{U}}_0(0)|\tilde{\imath}'(0)\rangle\rangle + O(\omega^2) \tag{2.A.17}$$

This leaves the second non-Markovian term, which can be expanded using

$$\tilde{\mathcal{U}}_0(\omega)\Delta\tilde{\mathcal{K}}(\omega)[-i\omega-\mathcal{K}_0-\Delta\tilde{\mathcal{K}}(\omega)]^{-1}=\omega\tilde{\mathcal{U}}_0(0)\tilde{\mathcal{K}}'(0)\tilde{\mathcal{U}}_0(0)+\mathcal{O}(\omega^2). \tag{2.A.18}$$

It should be noted that the contributions from the $\mathcal{O}(1/\omega)$ term in $\tilde{\mathcal{U}}_0(\omega)$ vanish, as is shown in appendix 2.B. Combining these results, the error in the Markovian approximation is given by

$$\begin{aligned}\mathcal{P}|\tilde{\rho}(\omega)\rangle\!\rangle-\mathcal{P}|\tilde{\rho}_0(\omega)\rangle\!\rangle=\omega\tilde{\mathcal{U}}_0(0)\tilde{\mathcal{K}}'(0)\tilde{\mathcal{U}}_0(0)\left(|\rho(0)\rangle\!\rangle+|\tilde{\imath}(0)\rangle\!\rangle\right)\\+\omega\tilde{\mathcal{U}}_0(0)|\tilde{\imath}'(0)\rangle\!\rangle+\mathcal{O}(\omega^2).\end{aligned} \tag{2.A.19}$$

Therefore the Markovian approximation will be valid as long as this term is small. We can relate $\tilde{\mathcal{K}}'(0)$ and $|\tilde{\imath}'(0)\rangle\!\rangle$ to the original kernel and inhomogeneous terms using Eq. (2.A.2),

$$\tilde{\mathcal{K}}'(0)=i\int_0^\infty t\mathcal{K}(t)\,\mathrm{d}t\ \text{ and }|\tilde{\imath}'(0)\rangle\!\rangle=i\int_0^\infty t|\iota(t)\rangle\!\rangle\,\mathrm{d}t \tag{2.A.20}$$

so we see that the error in the first moment of a reduced system variable $\langle\Delta A_n(t)\rangle$ is proportional to the first moments of the kernel and inhomogeneous term. Using Eq. (2.A.20) we can find an expression for the error in the first moment of $\langle\Delta A_n(t)\rangle$ relative to the Markovian approximation, $\mu_0^{(1)}(\Delta A_n)$, in terms of the eigenvalues of $\mathcal{K}_0$ and the projectors Π_k,

$$\begin{aligned}\frac{\Delta\mu^{(1)}(\Delta A_n)}{\mu_0^{(1)}(\Delta A_n)}=&\frac{\sum_{k\neq0}\sum_{l\neq0}\frac{1}{\lambda_k\lambda_l}\langle\!\langle\Delta A_n|\Pi_k\tilde{\mathcal{K}}'(0)\Pi_l\left(|\rho(0)\rangle\!\rangle+|\tilde{\imath}(0)\rangle\!\rangle\right)}{-i\sum_{k\neq0}\frac{1}{\lambda_k^2}\langle\!\langle\Delta A_n|\Pi_k\left(|\rho(0)\rangle\!\rangle+|\tilde{\imath}(0)\rangle\!\rangle\right)}\\&-\frac{\sum_{k\neq0}\frac{1}{\lambda_k}\langle\!\langle\Delta A_n|\Pi_k|\tilde{\imath}'(0)\rangle\!\rangle}{-i\sum_{k\neq0}\frac{1}{\lambda_k^2}\langle\!\langle\Delta A_n|\Pi_k\left(|\rho(0)\rangle\!\rangle+|\tilde{\imath}(0)\rangle\!\rangle\right)}\end{aligned} \tag{2.A.21}$$

In line with the error criterion suggested earlier, this will be small if $\|\bar{\mathcal{K}}'(0)\|\ll1$, and it will also be small if $\||\tilde{\imath}'(0)\rangle\!\rangle\|\ll\tau_0$. Furthermore, it is straightforward to see from this analysis that the error in the mth moment of a reduced system variable will depend on all moments up to and including order m of the kernel and inhomogeneous terms.

Using the framework we have established here can also consider what effect the non-Markovian terms have on the long time dynamics. To do this we should construct an approximation for for the non-Markovian terms that is exact to $\mathcal{O}(\omega^2)$. Motivated by the

above analysis, we do this by truncating the non-Markovian terms at first derivatives of $|\Delta\tilde{\imath}(\omega)\rangle\rangle$ and $\Delta\tilde{\mathcal{K}}(\omega)$, which gives the following

$$\begin{aligned}\tilde{\mathcal{U}}_0(\omega)|\Delta\tilde{\imath}(\omega)\rangle\rangle + \tilde{\mathcal{U}}_0(\omega)\Delta\tilde{\mathcal{K}}(\omega)[-i\omega - \mathcal{K}_0 - \Delta\tilde{\mathcal{K}}(\omega)]^{-1}\left(|\rho(0)\rangle\rangle + |\tilde{\imath}(\omega)\rangle\rangle\right) \\ = \omega\tilde{\mathcal{U}}_0(\omega)|\tilde{\imath}'(0)\rangle\rangle + \omega\tilde{\mathcal{U}}_0(\omega)\tilde{\mathcal{K}}'(0)\tilde{\mathcal{U}}_0(\omega)\left(|\rho(0)\rangle\rangle + |\tilde{\imath}(0)\rangle\rangle\right) + \mathcal{O}(\omega^2).\end{aligned} \tag{2.A.22}$$

This is valid at low frequencies $|\omega|\tau_0 \ll 1$, so with this we can derive an approximate correction to the Markovian dynamics for long times $t \gg \tau_0$. We do this by inverting the Fourier-Laplace transform in Eq. (2.A.22), which for $t \gg \tau_0$ gives the following correction to the Markovian dynamics

$$\begin{aligned}\mathcal{P}|\rho(t)\rangle\rangle - |\rho_0(t)\rangle\rangle \approx i\sum_{k\neq 0} e^{\lambda_k t}(1 + t\lambda_k)\Pi_k\mathcal{K}'(0)\Pi_k|\rho(0)\rangle\rangle \\ + i\sum_{k\neq 0}\lambda_k e^{\lambda_k t}\Pi_k|\tilde{\imath}'(0)\rangle\rangle + i\sum_{k\neq 0}\sum_{l\neq k, l\neq 0}\frac{\lambda_k e^{\lambda_k t} - \lambda_l e^{\lambda_l t}}{\lambda_k - \lambda_l}\Pi_k\mathcal{K}'(0)\Pi_l|\rho(0)\rangle\rangle.\end{aligned} \tag{2.A.23}$$

So we see that the non-Markovian terms lead to terms which have the same time dependence of terms in the Markovian dynamics, depending on $e^{\lambda_k t}$, as well as additional longer lived $t\lambda_k e^{\lambda_k t}$ terms. Again we see that these terms will be small if $\|\bar{\mathcal{K}}'(0)\| \ll 1$ and if $\||\tilde{\imath}'(0)\rangle\rangle\| \ll \tau_0$. This further motivates using these as simple criteria for the validity of the Markovian approximation.

2.B Appendix: The Derivative of $\tilde{\mathcal{K}}(\omega)$

We start by defining $\mathcal{A}(\omega) = \mathcal{K}_0 + \Delta\tilde{\mathcal{K}}(\omega)$, and we note that

$$\mathcal{P} = \mathcal{A}(\omega)^{-1}\mathcal{A}(\omega) \tag{2.B.1}$$

where we recall that the inverses here should just be interpreted as inverses on the projected subspace. To be more concrete in what we mean by this, we can write a projected

superoperator $\mathcal{B}$ as

$$\begin{aligned}\mathcal{B} &= \mathcal{P}\mathcal{B}\mathcal{P} \\ &= \sum_{n,m} |A_n\rho_n\rangle\!\rangle\langle\!\langle A_n|\mathcal{B}|A_m\rho_m\rangle\!\rangle\langle\!\langle A_m| \\ &= \sum_{n,m} |A_n\rho_n\rangle\!\rangle [\boldsymbol{\mathcal{B}}]_{nm}\langle\!\langle A_m|.\end{aligned} \tag{2.B.2}$$

Assuming the matrix $\boldsymbol{\mathcal{B}}$ is invertible, the inverse of $\mathcal{B}^{-1}$ is defined by

$$\mathcal{B}^{-1} = \sum_{n,m} |A_n\rho_n\rangle\!\rangle [\boldsymbol{\mathcal{B}}^{-1}]_{nm}\langle\!\langle A_m|. \tag{2.B.3}$$

Noting that the derivative of $\mathcal{P}$ with respect to ω is zero, by taking derivative of Eq. (2.B.1) we can show the following

$$\begin{aligned}0 &= \frac{\mathrm{d}}{\mathrm{d}\omega}\left(\mathcal{A}(\omega)^{-1}\mathcal{A}(\omega)\right) \\ &= \frac{\mathrm{d}}{\mathrm{d}\omega}\left(\mathcal{A}(\omega)^{-1}\right)\mathcal{A}(\omega) + \mathcal{A}(\omega)^{-1}\frac{\mathrm{d}}{\mathrm{d}\omega}\left(\mathcal{A}(\omega)\right)\end{aligned} \tag{2.B.4}$$

and rearranging this gives

$$\frac{\mathrm{d}}{\mathrm{d}\omega}\left(\mathcal{A}(\omega)\right) = -\mathcal{A}(\omega)\frac{\mathrm{d}}{\mathrm{d}\omega}\left(\mathcal{A}(\omega)^{-1}\right)\mathcal{A}(\omega). \tag{2.B.5}$$

Using this $\tilde{\mathcal{K}}'(0)\Pi_0$ can be found as follows,

$$\begin{aligned}\tilde{\mathcal{K}}'(0)\Pi_0 &= \lim_{\omega\to 0}\frac{\mathrm{d}}{\mathrm{d}\omega}\left(\mathcal{A}(\omega)\right)\Pi_0 \\ &= -\lim_{\omega\to 0}\mathcal{A}(\omega)\frac{\mathrm{d}}{\mathrm{d}\omega}\left(\mathcal{A}(\omega)^{-1}\right)\mathcal{A}(\omega)\Pi_0 \\ &= -\lim_{\omega\to 0}\mathcal{A}(\omega)\frac{\mathrm{d}}{\mathrm{d}\omega}\left(\mathcal{A}(\omega)^{-1}\right)\mathcal{K}_0\Pi_0 \\ &= 0,\end{aligned} \tag{2.B.6}$$

and by the same argument it is also true that $\Pi_0\tilde{\mathcal{K}}'(0) = 0$.

3 The Radical Pair Master Equation: General Theory

In this chapter we explore the theory of radical pair reactions, in particular the use of quantum master equations to explain magnetic field effects on these reactions. In the first part of this chapter the original phenomenological theories of radical pair reactions are described, and in the second part new work elucidating the link between chemical reaction rate theory and the radical pair master equation is presented.

3.1 The radical pair mechanism

Interactions between spins, spin state selective reactions and long-lived coherence between spin states underpin the radical pair mechanism. Because of this, we need to include quantum coherences between spin states in our basic description of the radical pair reaction. This motivates using the *spin density operator* $\hat{\rho}_{\mathrm{S}}(t)$ to describe radical pair reactions, a density operator that contains information about all of the coupled electron and nuclear spins in the radical pair.[32,104,105] In order to describe the radical pair reaction, we need a quantum master equation for the dynamics of this spin density operator. We expect the quantum master equation to contain a term that describes the coherent evolution of the spins under the effective spin Hamiltonian $\hat{H}_{\mathrm{S}}$, as well as a term that describes the spin state selective reactions of the radical pair. We assume therefore that the quantum master

equation for the spin density operator takes the following form,

$$\frac{\mathrm{d}}{\mathrm{d}t}\hat{\rho}_\mathrm{s}(t) = -\frac{i}{\hbar}\left[\hat{H}_\mathrm{s}, \hat{\rho}_\mathrm{s}(t)\right] + \mathcal{K}_\mathrm{r}[\hat{\rho}_\mathrm{s}(t)]\,. \tag{3.1}$$

The first term clearly describes the coherent spin evolution, and we have introduced $\mathcal{K}_\mathrm{r}[\,\cdot\,]$ as a general superoperator which describes the spin-selective reaction process.[32,36,104,105]

The precise form of the reaction superoperator $\mathcal{K}_\mathrm{r}[\,\cdot\,]$ has been debated for some time.[32,33,35–38,106–113] We can however reasonably suggest certain properties that the correct superoperator should satisfy. Firstly, it should preserve the hermiticity and positivity of the spin density operator, so that populations of spin states of the radical pair remain real-valued and positive.[32] However $\mathcal{K}_\mathrm{r}[\,\cdot\,]$ need not preserve the norm of the spin density operator, $\mathrm{Tr_s}[\hat{\rho}_\mathrm{s}(t)]$ where the trace is over all spin degrees of freedom, because the radical pair reacts and population is lost. Secondly, the master equation for the singlet and triplet electron spin state populations should reduce to simple first order kinetic equations in the absence of spin interactions, so the reaction superoperator should satisfy[32,35,36]

$$\mathrm{Tr_s}\left[\hat{P}_\mathrm{S}\mathcal{K}_\mathrm{r}[\hat{\rho}_\mathrm{s}(t)]\right] = -k_\mathrm{S}\,\mathrm{Tr_s}[\hat{P}_\mathrm{S}\hat{\rho}_\mathrm{s}(t)] \tag{3.2a}$$

$$\mathrm{Tr_s}\left[\hat{P}_\mathrm{T}\mathcal{K}_\mathrm{r}[\hat{\rho}_\mathrm{s}(t)]\right] = -k_\mathrm{T}\,\mathrm{Tr_s}[\hat{P}_\mathrm{T}\hat{\rho}_\mathrm{s}(t)]. \tag{3.2b}$$

Here $\hat{P}_\mathrm{S}$ is a projection operator onto singlet electron spin states, and similarly $\hat{P}_\mathrm{T}$ is a projection operator onto triplet electron spin states, and therefore the singlet radical pair population is $\langle P_\mathrm{S}(t)\rangle = \mathrm{Tr_s}[\hat{P}_\mathrm{S}\hat{\rho}_\mathrm{s}(t)]$, and the triplet population is $\langle P_\mathrm{T}(t)\rangle = \mathrm{Tr_s}[\hat{P}_\mathrm{T}\hat{\rho}_\mathrm{s}(t)]$. k_S and k_T are the total first order singlet and triplet reaction rate constants. There is a plethora of superoperators that possess these properties, but which produce different dynamics for the radical pair spin system, because they lead to different equations of motion for the singlet-triplet coherences. In the rest of this section I will briefly describe three such superoperators, each of which has been proposed based on different arguments.

3.1.1 The Haberkorn master equation

The original form of radical pair reaction term, commonly known as the "Haberkorn" master equation, was originally proposed in the 1970s[32,104,105] by Johnson & Merrifield[105], and for

nearly 40 years it was used successfully to describe spin-selective reactions of radical pairs. In this approach the Haberkorn reaction superoperator is

$$\mathcal{K}_{\mathrm{r}}[\hat{\rho}_{\mathrm{s}}(t)] = -\left\{\hat{K}, \hat{\rho}_{\mathrm{s}}(t)\right\}, \tag{3.3}$$

where $\{\hat{A}, \hat{B}\}$ denotes the anti-commutator, $\hat{A}\hat{B} + \hat{B}\hat{A}$, and the Haberkorn reaction operator $\hat{K}$ is defined in terms of the spin-selective reaction rate constants as

$$\hat{K} = \frac{k_{\mathrm{S}}}{2}\hat{P}_{\mathrm{S}} + \frac{k_{\mathrm{T}}}{2}\hat{P}_{\mathrm{T}}. \tag{3.4}$$

This form of the reaction superoperator can be arrived at through the following phenomenological arguments, as was explained by Haberkorn in 1976[32]. Firstly, if the spin selective reactions can be described as simple first-order rate processes, then the singlet population elements of the spin density operator, $\hat{P}_{\mathrm{S}}\hat{\rho}_{\mathrm{s}}(t)\hat{P}_{\mathrm{S}}$, should decay at a rate k_{S}, and similarly the triplet population elements $\hat{P}_{\mathrm{T}}\hat{\rho}_{\mathrm{s}}(t)\hat{P}_{\mathrm{T}}$ should decay at rate k_{T}, so this means that the change of the density operator in a short time δt due to the reaction processes should be

$$\delta\hat{\rho}(t)|_{\mathrm{reaction}} = -k_{\mathrm{S}}\hat{P}_{\mathrm{S}}\hat{\rho}_{\mathrm{s}}(t)\hat{P}_{\mathrm{S}}\delta t - k_{\mathrm{T}}\hat{P}_{\mathrm{T}}\hat{\rho}_{\mathrm{s}}(t)\hat{P}_{\mathrm{T}}\delta t. \tag{3.5}$$

This evolution however fails to preserve positivity of the spin density operator, which leads to unphysical negative populations of spin states. In order to preserve positivity, the coherence elements of the spin density operator must also decay at a rate of at least $(k_{\mathrm{S}} + k_{\mathrm{T}})/2$. Assuming the decoherence rate takes its minimum possible value, this means we should correct the above expression for the change in the density operator due to the reaction process,

$$\begin{aligned}\delta\hat{\rho}(t)|_{\mathrm{reaction}} = &-k_{\mathrm{S}}\hat{P}_{\mathrm{S}}\hat{\rho}_{\mathrm{s}}(t)\hat{P}_{\mathrm{S}}\delta t - k_{\mathrm{T}}\hat{P}_{\mathrm{T}}\hat{\rho}_{\mathrm{s}}(t)\hat{P}_{\mathrm{T}}\delta t \\ &- \frac{k_{\mathrm{S}} + k_{\mathrm{T}}}{2}\left(\hat{P}_{\mathrm{S}}\hat{\rho}_{\mathrm{s}}(t)\hat{P}_{\mathrm{T}} + \hat{P}_{\mathrm{T}}\hat{\rho}_{\mathrm{s}}(t)\hat{P}_{\mathrm{S}}\right)\delta t.\end{aligned} \tag{3.6}$$

By noting that $\delta\hat{\rho}(t)|_{\mathrm{reaction}} = \mathcal{K}_{\mathrm{r}}[\hat{\rho}_{\mathrm{s}}(t)]\delta t$, and $\hat{1} = \hat{P}_{\mathrm{S}} + \hat{P}_{\mathrm{T}}$, we arrive at the Haberkorn reaction operator as given in Eq. (3.3). Interestingly the Haberkorn master equation preserves pure states, meaning that if the density operator starts in a pure state $\hat{\rho}_{\mathrm{s}}(0) =$

$|\psi(0)\rangle\langle\psi(0)|$, then it will remain in a pure state given by $\hat{\rho}_s(0) = |\psi(t)\rangle\langle\psi(t)|$, where $|\psi(t)\rangle = e^{-i\hat{H}_s t/\hbar - \hat{K}t}|\psi(0)\rangle$.

A derivation of this reaction superoperator from Weisskopf-Wigner theory for spontaneous emission[114], was originally alluded to by Evans *et al.* in 1973[104], but it was not presented in full until 2010 by Ivanov *et al.*[33]. Using this theory the Haberkorn master equation can be obtained, but the model is somewhat limited and difficult to directly relate to the well established general theory of reaction rates. In particular it assumes that both reactant and product states have the same harmonic potential energy surfaces, which is a somewhat unphysical scenario in the context of chemical reactions.

3.1.2 The Jones-Hore measurement master equation

In 2010 an alternative form of the reaction superoperator was proposed by Jones & Hore based on quantum measurement theory[36]. This approach yielded the following reaction superoperator

$$\mathcal{K}_r[\hat{\rho}_s(t)] = -\left\{\hat{K}, \hat{\rho}_s(t)\right\} - k_D\left(\hat{P}_S\hat{\rho}_s(t)\hat{P}_T + \hat{P}_T\hat{\rho}_s(t)\hat{P}_S\right). \tag{3.7}$$

The first term is just the Haberkorn reaction term, as in Eq. (3.3), and the second term is an additional decoherence term, which results from assuming the reaction processes act as complete projective measurements. Based on the original theory[36] the rate of this additional decoherence k_D is $k_D = (k_S + k_T)/2$.

The reaction superoperator above is derived based on the assumption that a single spin-selective reaction event acts as a complete projective quantum measurement on the radical pair spin density operator. Such a complete projective measurement projects the spin density operator onto the singlet and triplet states,[36]

$$\hat{\rho}_s \rightarrow \hat{P}_S\hat{\rho}_s\hat{P}_S + \hat{P}_T\hat{\rho}_s\hat{P}_T. \tag{3.8}$$

Assuming this reaction event is completely efficient, this will also remove population from the density operator, for example if it is a singlet selective reaction event, then the singlet portion of the density operator will also be removed, so overall this reaction event changes

the spin density operator as follows,

$$\hat{\rho}_s \rightarrow \hat{P}_S\hat{\rho}_s\hat{P}_S + \hat{P}_T\hat{\rho}_s\hat{P}_T - \hat{P}_S\hat{\rho}_s\hat{P}_S = \hat{P}_T\hat{\rho}_s\hat{P}_T. \tag{3.9}$$

Within the Jones-Hore approach, the spin selective reaction processes as described above are assumed to happen continuously at rates k_S and k_T, so in a short time δt a fraction $k_S\delta t$ of the radical pairs undergo a singlet reaction process, and a fraction $k_T\delta t$ undergo a triplet reaction process, and the remaining fraction evolves coherently, so the density operator evolves according to

$$\begin{aligned}\hat{\rho}_s(t+\delta t) = (1 - k_S\delta t - k_T\delta t)\left(\hat{\rho}_s(t) - i[\hat{H}_s, \hat{\rho}_s(t)]\delta t\right) \\ + k_S\delta t\hat{P}_T\hat{\rho}_s(t)\hat{P}_T + k_T\delta t\hat{P}_S\hat{\rho}_s(t)\hat{P}_S.\end{aligned} \tag{3.10}$$

Rearranging this and noting that we can ignore $O(\delta t^2)$ terms gives

$$\begin{aligned}\hat{\rho}_s(t+\delta t) = \hat{\rho}_s(t) - i[\hat{H}_s, \hat{\rho}_s(t)]\delta t \\ - k_S\delta t\left(\hat{\rho}_s(t) - \hat{P}_T\hat{\rho}_s(t)\hat{P}_T\right) - k_T\delta t\left(\hat{\rho}_s(t) - \hat{P}_S\hat{\rho}_s(t)\hat{P}_S\right).\end{aligned} \tag{3.11}$$

We identity the second term on the right-hand side of this equation as the coherent evolution term, so the third and fourth terms must be the reaction terms, which we can rearrange to find the change in the density operator due to the reaction processes. This gives the Jones-Hore reaction superoperator as

$$\mathcal{K}_r[\hat{\rho}_s(t)] = -\left\{\hat{K}, \hat{\rho}_s(t)\right\} - k_D\left(\hat{P}_S\hat{\rho}_s(t)\hat{P}_T + \hat{P}_T\hat{\rho}_s(t)\hat{P}_S\right). \tag{3.12}$$

The first term is just the Haberkorn reaction term, as in Eq. (3.3), and the second term is an additional decoherence term, which results from assuming the reaction processes act as complete projective measurements. Assuming the reaction acts as a complete projective measurement as above, the rate of this additional decoherence k_D is $k_D = (k_S + k_T)/2$.

Later Jones *et al.* generalised this approach to account for "how strongly" the reaction processes act as quantum measurements[37], in which case k_D becomes a parameter related to the strength of the measurement. In the "weak measurement" limit, $k_D = 0$ and their reaction term reduces to the Haberkorn reaction term, whereas in the "strong measurement" limit it is given by $k_D = (k_S + k_T)/2$[37]. In contrast to the Haberkorn master equation,

the Jones-Hore master equation does not preserve pure states, because the measurement operation transforms pure states into mixed states.

The Jones-Hore reaction term gives first order rate equations for the populations of the spin states, and preserves the positivity of the spin density operator, but because this reaction term gives different evolution for the singlet-triplet coherences, it predicts different spin dynamics and reaction yields to the Haberkorn equation. The appearance of the additional decoherence k_{D} based on how strongly the reaction "measures" the spin state of the radical pair creates the problem that one must define some criteria for determining the strength of the measurement process. One criterion suggested in Ref. [109] for electron transfer reactions is the adiabaticity of the reaction. It was suggested that electron transfer reactions close to the adiabatic limit (where the coupling between electron transfer states is large) may act to strongly measure the spin state, whereas those close to the non-adiabatic limit (where the coupling between electron transfer states is small) may only weakly measure the spin state. I will revisit this idea later in more detail, but for now I will briefly describe one additional measurement based approach to treating spin selective reactions of radical pairs.

3.1.3 The Kominis measurement master equation

One final quantum measurement theory based reaction term that has been suggested is the Kominis term.[35,38,110,111,113] As with the Jones-Hore reaction term, the Kominis reaction term was proposed based on the assumption that the spin-selective reactions continuously measure the spin state of the radical pair, but in contrast the with the Jones-Hore approach, this measurement process only affects the "coherent part" of the density operator.[38] I will avoid rehearsing the full argument behind the Kominis reaction term, and simply state its proposed form,

$$\mathcal{K}_{\mathrm{r}}[\hat{\rho}_{\mathrm{s}}(t)] = -\left\{\hat{K}[\hat{\rho}_{\mathrm{s}}(t)], \hat{\rho}_{\mathrm{s}}(t)\right\} - k_{\mathrm{D}}[\hat{\rho}_{\mathrm{s}}(t)]\left(\hat{P}_{\mathrm{S}}\hat{\rho}_{\mathrm{s}}(t)\hat{P}_{\mathrm{T}} + \hat{P}_{\mathrm{T}}\hat{\rho}_{\mathrm{s}}(t)\hat{P}_{\mathrm{S}}\right). \tag{3.13}$$

This form of the reaction term closely resembles the Jones-Hore term, only now the reaction operator $\hat{K}[\hat{\rho}_{\mathrm{s}}(t)]$ and decoherence rate $k_{\mathrm{D}}[\hat{\rho}_{\mathrm{s}}(t)]$ are functionals of the spin density operator, so the Kominis reaction term gives a *non-linear* equation of motion for the spin

density operator. Kominis proposed that these terms should depend on "how coherent" the radical pair state is at a particular moment in time, which means these terms depend explicitly on $\hat{\rho}_\mathrm{s}(t)$. The proposed functional forms of these terms are

$$\begin{aligned}\hat{K}[\hat{\rho}_\mathrm{s}(t)] = &\left(\frac{k_\mathrm{S}}{2}(1 - p_\mathrm{coh}[\hat{\rho}_\mathrm{s}(t)]) + \frac{\mathrm{Tr}\big[(k_\mathrm{S}\hat{P}_\mathrm{S} + k_\mathrm{T}\hat{P}_\mathrm{T})\hat{\rho}_\mathrm{s}(t)\big]}{2\,\mathrm{Tr}[\hat{\rho}_\mathrm{s}(t)]}p_\mathrm{coh}[\hat{\rho}_\mathrm{s}(t)]\right)\hat{P}_\mathrm{S} \\ &+ \left(\frac{k_\mathrm{T}}{2}(1 - p_\mathrm{coh}[\hat{\rho}_\mathrm{s}(t)]) + \frac{\mathrm{Tr}\big[(k_\mathrm{S}\hat{P}_\mathrm{S} + k_\mathrm{T}\hat{P}_\mathrm{T})\hat{\rho}_\mathrm{s}(t)\big]}{2\,\mathrm{Tr}[\hat{\rho}_\mathrm{s}(t)]}p_\mathrm{coh}[\hat{\rho}_\mathrm{s}(t)]\right)\hat{P}_\mathrm{T}\end{aligned} \tag{3.14}$$

$$k_\mathrm{D}[\hat{\rho}_\mathrm{s}(t)] = \frac{k_\mathrm{S} + k_\mathrm{T}}{2}p_\mathrm{coh}[\hat{\rho}_\mathrm{s}(t)] + \frac{\mathrm{Tr}\big[(k_\mathrm{S}\hat{P}_\mathrm{S} + k_\mathrm{T}\hat{P}_\mathrm{T})\hat{\rho}_\mathrm{s}(t)\big]}{\mathrm{Tr}[\hat{\rho}_\mathrm{s}(t)]}(1 - p_\mathrm{coh}[\hat{\rho}_\mathrm{s}(t)]), \tag{3.15}$$

in which $p_\mathrm{coh}[\hat{\rho}_\mathrm{s}(t)]$ is a"measure of coherence" between singlet and triplet states.[38]

We can see that the three main reaction terms which have been proposed are all clearly related; they all involve a term which causes decay of the radical pair spin states which preserves positivity of the density operator, but measurement based approaches gives rise to additional decoherence terms between singlet and triplet states. In order to highlight the differences between the three reaction terms, I have calculated the triplet quantum yields of a set of simple model radical pair reactions as a function of the applied magnetic field, the results of which are shown in Fig. 3.1. The triplet yield Φ_T is calculated from the radical pair density operator with

$$\Phi_\mathrm{T} = k_\mathrm{T}\int_0^\infty \mathrm{Tr}\big[\hat{P}_\mathrm{T}\hat{\rho}_\mathrm{s}(t)\big]\,\mathrm{d}t\,. \tag{3.16}$$

In these models there is a single proton hyperfine coupled to one of the radical electron spins with an isotropic coupling constant of $a/\hbar\gamma_\mathrm{e} = 1$ mT, the electron spins couple to an external applied field of strength B with the isotropic free electron g-tensor, and the radical pair is initialised in the singlet state $\hat{\rho}_\mathrm{s}(0) = \hat{P}_\mathrm{S}/2$. In (a), (c) and (e) the scalar coupling between the radical electron spins is $J/\hbar\gamma_\mathrm{e} = 0$ mT, in (b), (d) and (f) the coupling is $J/\hbar\gamma_\mathrm{e} = -5$ mT. The spin selective recombination rate constants are $k_\mathrm{S} = k_\mathrm{T}/10 = 100\ \mu\mathrm{s}^{-1}$ (a) and (b), $k_\mathrm{S} = k_\mathrm{T}/10 = 10\ \mu\mathrm{s}^{-1}$ in (c) and (d), and $k_\mathrm{S} = k_\mathrm{T}/10 = 1\ \mu\mathrm{s}^{-1}$ in (e) and (f).

The results where $J = 0$ (the left hand column of Fig. 3.1) all show the low field effect at low recombination rates, where there is enhancement of transfer from the singlet state to T_0-triplet state (and therefore an increased triplet yield) as a field is applied.[41,42,115] In

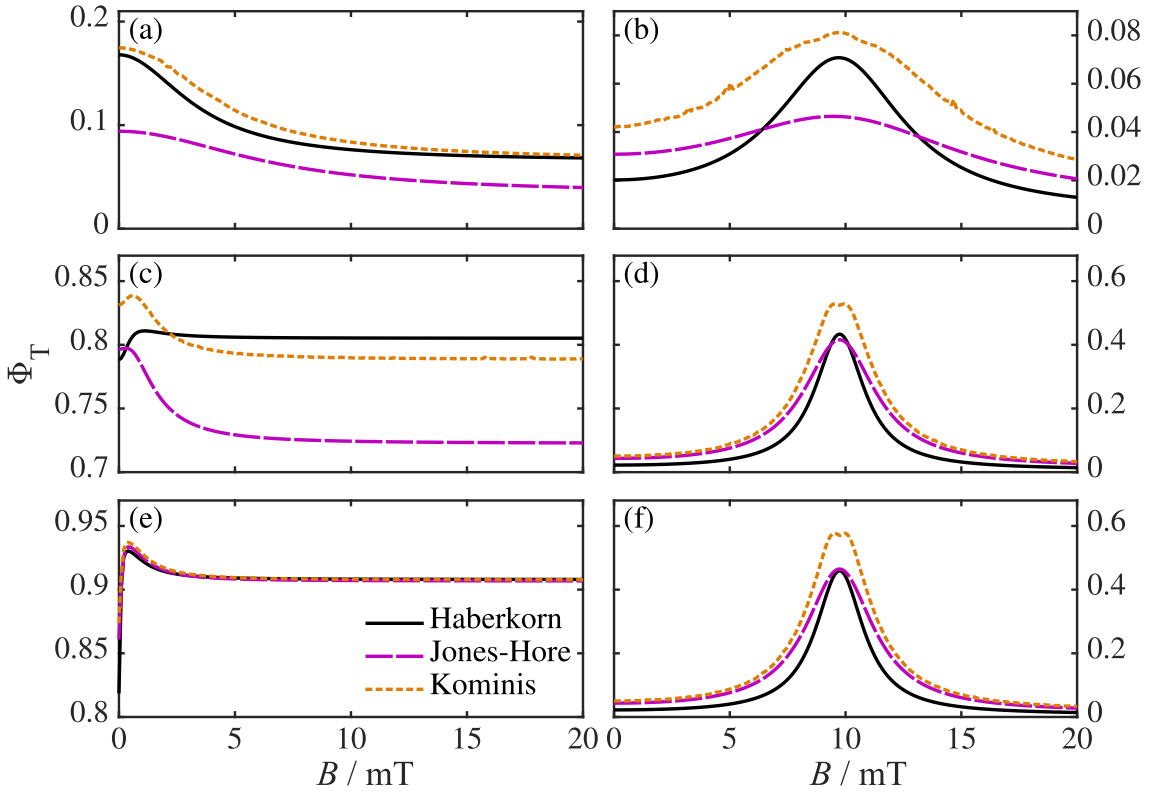

Figure 3.1: A comparison of triplet quantum yields of a radical pair reaction calculated with different radical pair quantum master equations. In (a), (c) and (e) the scalar coupling between the radical electron spins is $J = 0$, in (b), (d) and (f) the coupling is $J/\hbar\gamma_e = -5$ mT. The spin selective recombination rate constants are $k_S = k_T/10 = 100\ \mu s^{-1}$ (a) and (b), $k_S = k_T/10 = 10\ \mu s^{-1}$ in (c) and (d), and $k_S = k_T/10 = 1\ \mu s^{-1}$ in (e) and (f).

contrast the $J \neq 0$ results (the right hand column of Fig. 3.1) all show resonance effects, where there is an enhancement of singlet to T_--triplet state transfer when the Zeeman energy of the T_- state matches the energy shift between the singlet and triplet states induced by the scalar coupling.[3] In both sets of models, the differences between the different reaction terms become more pronounced as the recombination rate constants increase. In particular the broadening of magnetic field effects in the measurement based approaches, which arises due to the additional decoherence term that appears in these theories, becomes more pronounced as the rates increase. One stark example of the differences between the different master equations can be seen in panel (c), where the Haberkorn, Jones-Hore and Kominis master equations all predict qualitatively different magnetic field effects. Furthermore the Kominis master equation predicts some different features in the triplet quantum yields for $J \neq 0$ models to the other master equations, such as a small splitting of the resonance peak in

panels (d) and (f) and some additional small peaks in panel (b).

From these simple models we see that the different radical pair master equations can predict very different magnetic field effects in quantum yields of radical pair reactions, and this has also been shown to extend to predictions of other spin chemical effects, such as nuclear spin polarisation in NMR spectra,[111] electron spin polarisation in EPR spectra,[33] and dynamics of the radical pair survival probability.[33,35,37] This demonstrates the importance of knowing the correct quantum master equation for describing radical pair reactions for interpretation of experimental results. The rest of this chapter will be devoted to finding the correct master equation from a general starting point, motivated by a first principles description of the radical pair reaction.

3.2 The radical pair model

In this section I outline how to obtain a radical pair master equation which is applicable to spin-selective electron transfer reactions of radical pairs. I will start by describing the model for the radical pair electron transfer reactions, to which Nakajima-Zwanzig theory is then applied in order to obtain the radical pair QME.

3.2.1 The radical pair Hamiltonian

Here I will outline the starting point for deriving the radical pair master equation: the full molecular Hamiltonian. The focus here will be on the formal theory, and we will not concern ourselves with the details of actually calculating any of the actual Hamiltonian matrix elements that appear here, which is a formidable task. Our ultimate aim is to split the total molecular Hamiltonian into a reference part $\hat{H}_0$ and a perturbation $\hat{V}$, so this will motivate all the manipulations of the Hamiltonian we make.

The full Hilbert space for the system $\mathcal{H}$ consists of the electronic spin and spatial degrees of freedom Hilbert space $\mathcal{H}_\mathrm{e}$, the Hilbert space for the nuclear spatial degrees of freedom $\mathcal{H}_\mathrm{n}$, which is spanned by the nuclear configuration states $|\mathbf{R}\rangle$, and the Hilbert space for the nuclear spin degrees of freedom $\mathcal{H}_I$ which is spanned by the nuclear spin projection states

$|\mathbf{M}\rangle = |I_1, M_1\rangle \otimes \cdots \otimes |I_N, M_N\rangle$,

$$\mathcal{H} = \mathcal{H}_\mathrm{e} \otimes \mathcal{H}_\mathrm{n} \otimes \mathcal{H}_I. \tag{3.17}$$

Now we will consider the full Hamiltonian for the molecular system, including all N_e electrons, and all N nuclei,[40,116–118]

$$\hat{H} = \underbrace{\hat{T}_\mathrm{n} + \hat{T}_\mathrm{e} + \hat{V}_\mathrm{en} + \hat{V}_\mathrm{ee} + \hat{V}_\mathrm{nn}}_{\text{Spin preserving terms, } \hat{H}_1.} + \underbrace{\hat{H}_\mathrm{soc} + \hat{H}_\mathrm{zee} + \hat{H}_\mathrm{hfc} + \hat{H}_\mathrm{dip}}_{\text{Spin mixing terms, } \hat{H}_2.}. \tag{3.18}$$

The first six terms, $\hat{H}_1$, are all spin state preserving terms, which means each of these terms commutes with each vector component of the total electron spin operator $\hat{S}_\alpha = \sum_{i=1}^{N_\mathrm{e}} \hat{s}_{i\alpha}$, i.e. $[\hat{S}_\alpha, \hat{A}] = 0$. From left to right these spin-preserving terms are: the total nuclear kinetic energy $\hat{T}_\mathrm{n}$, the total electronic kinetic energy $\hat{T}_\mathrm{e}$, the electron-nuclear $\hat{V}_\mathrm{en}$, electron-electron $\hat{V}_\mathrm{ee}$, and nuclear-nuclear $\hat{V}_\mathrm{nn}$ coulomb interactions.[40,116,117] The remaining four terms, $\hat{H}_2$, are terms that act explicitly on the spin degrees of freedom, and as such do not commute with the total electron spin operators. Again from left to right these terms are: the spin-orbit coupling term $\hat{H}_\mathrm{soc}$, the Zeeman interaction term of all particles in the system with an external magnetic field $\hat{H}_\mathrm{zee}$, the nuclear hyperfine coupling term $\hat{H}_\mathrm{hfc}$, which includes all Fermi contact and dipolar interactions between electron and nuclear spins, and the dipolar coupling term $\hat{H}_\mathrm{dip}$, which includes all other dipolar interactions between pairs of electron spins and pairs of nuclear spins.[40,116,117] Additional spin-dependent relativistic terms also appear, but in the context of spin chemical effects in organic radical pairs, these are the most important terms.[40,116,117]

3.2.2 Radical pair reaction diabatic states

We will start by considering how to manipulate the spin preserving terms $\hat{H}_1$ to find a useful representation for describing spin-selective electron transfer reactions. These terms can be split into a total electronic Hamiltonian $\hat{H}_\mathrm{e}$ and the nuclear kinetic energy term $\hat{T}_\mathrm{n}$,

$$\hat{H}_1 = \hat{T}_\mathrm{n} + \hat{H}_\mathrm{e}. \tag{3.19}$$

The electronic Hamiltonian $\hat{H}_\mathrm{e}$ is the standard Born-Oppenheimer Hamiltonian.[119–123] This term is diagonal in the position representation of the nuclei $|\mathbf{R}\rangle$, where $\mathbf{R}$ is a position vector for all of the nuclei $\mathbf{R} = (\mathbf{R}_1, \mathbf{R}_2, \ldots, \mathbf{R}_N)$, and therefore its eigenstates can be written as

$$\hat{H}_\mathrm{e} \, |\psi_i(\mathbf{R})\rangle \, |\mathbf{R}\rangle = E_{\mathrm{e},i}(\mathbf{R}) \, |\psi_i(\mathbf{R})\rangle \, |\mathbf{R}\rangle \,, \tag{3.20}$$

where $|\psi_i(\mathbf{R})\rangle$ is an electronic wave-function, which depends parametrically on the nuclear configuration $\mathbf{R}$. These are called the *adiabatic* electronic states, because they adiabatically follow the nuclear configuration. Because the total electron spin operators commute with $\hat{H}_\mathrm{e}$, these states can be chosen to be eigenstates of the total electron spin angular momentum $\hat{S}^2 = \hat{\mathbf{S}} \cdot \hat{\mathbf{S}}$, and one of its vector components, normally chosen to be the z component,

$$\hat{S}^2 \, |\psi_i(\mathbf{R})\rangle = S(S+1) \, |\psi_i(\mathbf{R})\rangle \tag{3.21}$$

$$\hat{S}_z \, |\psi_i(\mathbf{R})\rangle = M_S \, |\psi_i(\mathbf{R})\rangle \,. \tag{3.22}$$

For reasons explained in appendix 3.A, these states can be difficult to work with when considering electron transfer reactions.[123,124] So instead we will work in the quasi-diabatic representation of the electronic states, where these states correspond to different electron transfer states of the system.[119–124] A quasi-diabatic representation can formally be obtained from the adiabatic representation by a unitary transformation of the adiabatic basis states, and the resulting Hamiltonian can be written as

$$\hat{H}_1 = \hat{T}_\mathrm{n} + \sum_a |a\rangle\langle a| \, V_a(\hat{\mathbf{R}}) + \sum_{a,b\neq a} |a\rangle\langle b| \, \hat{V}_{ab}, \tag{3.23}$$

where the states $|a\rangle$ are quasi-diabatic electronic states, $V_a(\hat{\mathbf{R}})$ is the quasi-diabatic potential energy for state a and $\hat{V}_{ab}$ is the quasi-diabatic coupling operator between two states a and b, which couples these states. These states can also be chosen to be eigenstates of $\hat{S}^2$ and $\hat{S}_z$, in which case the coupling $\hat{V}_{ab}$ only couples states of with same S and M_S quantum numbers. More details of this transformation are given in appendix 3.A.

For a strictly diabatic representation, as opposed to a quasi-diabatic representation, the coupling term $\hat{V}_{ab}$ is just a function of $\hat{\mathbf{R}}$, i.e. $\hat{V}_{ab} = V_{ab}(\hat{\mathbf{R}})$. In practice it is not always possible to construct strictly diabatic representations,[120,121,123] at least from a finite

set of adiabatic potential energy surfaces,[125] but normally one can find a quasi-diabatic representation in which the the coupling is approximately of the form $V_{ab}(\hat{\mathbf{R}})$.[121,123] The precise details of how one would construct these states from an *ab initio* electronic structure calculation are unimportant here. In what follows we will make additional approximations to the forms of the important quasi-diabatic states, and we will only require that the coupling $\hat{V}_{ab}$ can be treated as a perturbation.

From here onwards, we will consider radical pair reactions where the radical pair is a long-range charge transfer state of the molecule, and the spin selective reactions are spin-selective electron transfers, as illustrated in Fig. 1.1. In this case we assume that there exist separate diabatic states for each of the relevant electron transfer states. We denote the singlet radical pair diabatic state, the ${}^{\mathrm{S}}[\mathrm{D}^{\bullet+}\,\mathrm{A}^{\bullet-}]$ state, as $|1,\mathrm{S}\rangle$ and the triplet radial pair diabatic states, ${}^{\mathrm{T}}[\mathrm{D}^{\bullet+}\,\mathrm{A}^{\bullet-}]$, as $|1,\mathrm{T}_m\rangle$ where $m = -,0,+$ denotes the projection of the total electron spin onto the z axis. For simplicity we will only consider one singlet product, ${}^{\mathrm{S}}[\mathrm{D\,A}]$, and one triplet product, ${}^{\mathrm{T}}[\mathrm{D\,A}]$, the diabatic states for which are denoted $|2,\mathrm{S}\rangle$ and $|3,\mathrm{T}_m\rangle$, although the discussion generalises straightforwardly to include more product states.

If the two radicals are well separated, then the radical pair diabatic potential energy surfaces $V_{1,\mathrm{S}}(\mathbf{R})$ and $V_{1,\mathrm{T}_m}(\mathbf{R})$ will lie very close in energy, at least at all thermally accessible configurations, so we assume that

$$V_{1,\mathrm{S}}(\mathbf{R}) = V_{1,\mathrm{T}_m}(\mathbf{R}) \equiv V_1(\mathbf{R}). \tag{3.24}$$

We denote the singlet product surface by $V_{2,\mathrm{S}}(\mathbf{R}) \equiv V_2(\mathbf{R})$, the three degenerate triplet product surfaces by $V_{3,\mathrm{T}_m}(\mathbf{R}) \equiv V_3(\mathbf{R})$. This diabatic state picture of the radical pair reaction is illustrated graphically in Fig. 3.2 for diabatic surfaces projected onto two coordinates. The radical pair states lie on top of each other in energy, but the product surfaces are displaced significantly from each other and from the radical pair surface. Within this model, we can

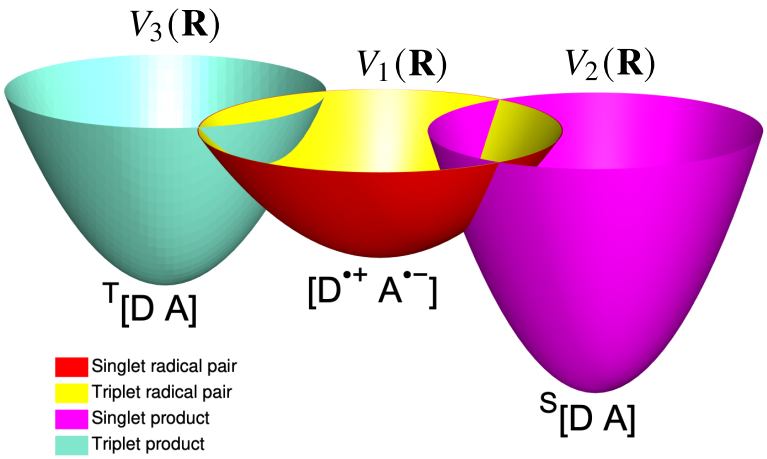

Figure 3.2: A sketch of the diabatic state model showing the diabatic potential energy surfaces in two coordinates. The radical pair states lie on top of each other, but the product states deviate significantly from each other and the radical pair state.

disregard all other states, and the diabatic state Hamiltonian we use is of the form

$$\begin{aligned}\hat{H}_1 = &\sum_{\substack{n\in\\ \{\mathrm{S},\mathrm{T}_+,\mathrm{T}_0,\mathrm{T}_-\}}} |1,n\rangle\langle 1,n|\,\hat{H}_{1\mathrm{n}} + |2,\mathrm{S}\rangle\langle 2,\mathrm{S}|\,\hat{H}_{2\mathrm{n}} + \sum_{\substack{n\in\\ \{\mathrm{T}_+,\mathrm{T}_0,\mathrm{T}_-\}}} |3,n\rangle\langle 3,n|\,\hat{H}_{3\mathrm{n}} \\ &+\left(\hat{\Delta}_\mathrm{S}\,|1,\mathrm{S}\rangle\langle 2,\mathrm{S}| + \hat{\Delta}_\mathrm{S}^\dagger\,|2,\mathrm{S}\rangle\langle 1,\mathrm{S}|\right) + \sum_{n\in\{\mathrm{T}_+,\mathrm{T}_0,\mathrm{T}_-\}}\left(\hat{\Delta}_\mathrm{T}\,|1,n\rangle\langle 3,n| + \hat{\Delta}_\mathrm{T}^\dagger\,|3,n\rangle\langle 1,n|\right)\end{aligned} \tag{3.25}$$

Here $\hat{H}_{i\mathrm{n}} = \hat{T}_\mathrm{n} + V_i(\hat{\mathbf{R}})$ is the nuclear Hamiltonian for diabatic surface i and $\hat{\Delta}_\mathrm{S}$ and $\hat{\Delta}_\mathrm{T}$ are the singlet and triplet quasi-diabatic coupling operators, which operate on the nuclear degrees of freedom. We will further assume that we can write $\hat{\Delta}_\mathrm{S} = \Delta_\mathrm{S}\hat{f}_\mathrm{S}$ where Δ_S is a real constant with units of energy, and $\hat{f}_\mathrm{S}$ is unitless operator, and likewise for $\hat{\Delta}_\mathrm{T}$. Within the Condon approximation, we assume that $\hat{f}_\mathrm{S} = \hat{f}_\mathrm{T} = 1$,[55], an approximation which is used in the Marcus-Hush theory of electron transfer rates.[126,127] In what follows I will only explicitly consider this truncated model Hamiltonian, but the generalisation of the resulting master equations to the inclusion of more product states is relatively straightforward.

This diabatic state model is a simple extension of the diabatic state model employed in standard two-state electron transfer rate theory,[123,124] which forms the basis of well established theories of electron transfer rates, such as Marcus-Hush theory.[126,127] The only additional approximation made in this extension is that the singlet and triplet radical pair potential energy surfaces can be treated as identical. The master equation derived from this model can thus be regarded as being consistent with the well-established theory of electron transfer reactions.

3.2.3 The spin density operators

Having defined the Hamiltonian for the radical pair reaction, and identified a set of relevant diabatic states, we can now define precisely what is meant by the radical pair spin density operator in this model. Because the radical pair electron spin states all lie close in energy, we need to include coherences between these states in our description of the radical pair reaction. Similarly we also need to include coherences with the spin degrees of freedom of the nuclei, because again these spin coherences will be long-lived because the interactions in $\hat{H}_2$ that couple them to the nuclear spatial degrees of freedom are typically weak. So this motivates finding a radical pair master equation for the spin density operators of the radical pair and the products, $\hat{\rho}_{i\mathrm{s}}(t)$, as defined by

$$\hat{\rho}_{1\mathrm{s}}(t) = \sum_{\substack{n,m\in \\ \{\mathrm{S},\mathrm{T}_+,\mathrm{T}_0,\mathrm{T}_-\}}} |1,n\rangle\langle 1,m| \,\mathrm{Tr}_{\mathrm{n}}[\,\langle 1,n|\hat{\rho}(t)|1,m\rangle_{\mathrm{e}}] \tag{3.26a}$$

$$\hat{\rho}_{2\mathrm{s}}(t) = |2,\mathrm{S}\rangle\langle 2,\mathrm{S}| \,\mathrm{Tr}_{\mathrm{n}}[\,\langle 2,\mathrm{S}|\hat{\rho}(t)|2,\mathrm{S}\rangle_{\mathrm{e}}] \tag{3.26b}$$

$$\hat{\rho}_{3\mathrm{s}}(t) = \sum_{\substack{n,m\in \\ \{\mathrm{T}_+,\mathrm{T}_0,\mathrm{T}_-\}}} |3,n\rangle\langle 3,m| \,\mathrm{Tr}_{\mathrm{n}}[\,\langle 3,n|\hat{\rho}(t)|3,m\rangle_{\mathrm{e}}], \tag{3.26c}$$

Here $\mathrm{Tr}_{\mathrm{n}}[\,\cdot\,]$ denotes the trace with respect to the nuclear spatial degrees of freedom and $\langle\,\cdot\,\rangle_{\mathrm{e}}$ denotes integrating just over the electronic degrees of freedom. Here $\hat{\rho}_{1\mathrm{s}}(t)$ just operates on the radical pair spin degrees of freedom, so we can identify this radical pair spin density operated denoted by $\hat{\rho}_{\mathrm{s}}(t)$ above. The other two operators act on the spin degrees of freedom of the singlet and triplet products, so these correspond to spin density operators for the products. We note that taking the trace over the electronic and other spin degrees of freedom of these operators gives the population of each of the diabatic states.

We can condense the expressions above by defining the state projection operators $\hat{\Pi}_i$ and spin projection operators $\hat{P}_S = \hat{P}_{\mathrm{T}}$ or $\hat{P}_{\mathrm{S}}$ (using the labels S and $S = 0$ interchangeably

and likewise for T and $S = 1$) as follows,

$$\hat{P}_S = \sum_{i \in \mathcal{I}_S} \sum_{M_S=-S}^{S} |i, S, M_S\rangle\langle i, S, M_S| \tag{3.27}$$

$$\hat{\Pi}_i = \sum_{S \in \mathcal{S}_i} \sum_{M_S=-S}^{S} |i, S, M_S\rangle\langle i, S, M_S| \tag{3.28}$$

where $|i, S_i, M_S\rangle$ denotes the diabatic state i with spin state $|S, M_S\rangle$. The set $\mathcal{I}_S$ denotes the set of diabatic state indices associated with total spin quantum number S, i.e. the indices i for which the $|i, S, M_S\rangle$ exists, and similarly $\mathcal{S}_i$ denotes the set of total spin quantum numbers associated with with diabatic state i, i.e the spin quantum numbers S for which $|i, S, M_S\rangle$ exists. Specifically we have $\mathcal{S}_1 = \{0, 1\}$, $\mathcal{S}_2 = \{0\}$ and $\mathcal{S}_3 = \{1\}$, and $\mathcal{I}_\mathrm{S} = \{1, 2\}$ and $\mathcal{I}_\mathrm{T} = \{1, 3\}$. With this we can more succinctly write $\hat{\rho}_{i\mathrm{s}}(t)$ as

$$\hat{\rho}_{i\mathrm{s}}(t) = \mathrm{Tr}_\mathrm{n}[\hat{\Pi}_i \hat{\rho}(t) \hat{\Pi}_i]. \tag{3.29}$$

With the above definitions, we note that $\hat{\rho}_{2\mathrm{s}}(t)$ is equal to its singlet projection $\hat{P}_\mathrm{S}\hat{\rho}_{2\mathrm{s}}(t)\hat{P}_\mathrm{S}$ and likewise $\hat{\rho}_{3\mathrm{s}}(t)$ is equal to its triplet projection $\hat{P}_\mathrm{T}\hat{\rho}_{3\mathrm{s}}(t)\hat{P}_\mathrm{T}$.

3.2.4 Initial conditions

We assume that the diabatic coupling, $\hat{\Delta}_\mathrm{S}$ and $\hat{\Delta}_\mathrm{T}$, between all states is weak, and that after any photoexcitation process to form the radical pair, its vibrational degrees of freedom rapidly relax to local equilibrium on the radical pair diabatic surface. With these assumptions, the initial state of the total system can be written as

$$\hat{\rho}(0) = \sum_i \hat{\rho}_{i\mathrm{s}}(0)\hat{\rho}_{i\mathrm{n}} \tag{3.30}$$

where $\hat{\rho}_{i\mathrm{s}}(0)$ is the initial spin state in diabatic state i, and $\hat{\rho}_{i\mathrm{n}}$ is given by

$$\hat{\rho}_{i\mathrm{n}} = \frac{\exp\left(-\beta \hat{H}_{i\mathrm{n}}\right)}{Z_{i\mathrm{n}}}, \tag{3.31}$$

in which $Z_{i\mathrm{n}} = \mathrm{Tr}_\mathrm{n}[\exp\left(-\beta \hat{H}_{i\mathrm{n}}\right)]$. This is just the thermal state, given by Eq. (2.24), for the nuclear Hamiltonian on diabat i.

3.3 Derivation of radical pair quantum master equations

Having outlined the model of the radical pair reaction, I will now show how to use this to derive quantum master equations for the radical pair spin density operator using the Nakajima-Zwanzig equation. I will start by describing the required projection superoperators, and then I will explain how to find approximate expressions for the Nakajima-Zwanzig memory kernel, from which the radical pair master equation can be derived.

3.3.1 Projection superoperators

In order to use the Nakajima-Zwanzig equation to obtain master equations for the spin density operators, we must define the projection superoperator $\mathcal{P}$. The definition of these spin density operators, Eq. (3.29), and the initial condition for the full density operator, Eq. (3.30), motivates defining the following projection superoperator

$$\mathcal{P} = \sum_{i=1,2,3} \mathcal{P}_i \tag{3.32}$$

where $\mathcal{P}_i$ are projection superoperators onto each of the diabatic states given by,

$$\mathcal{P}_i = \hat{\rho}_{i\mathrm{n}} \mathrm{Tr}_{\mathrm{n}}[\hat{\Pi}_i \ \cdot \ \hat{\Pi}_i], \tag{3.33}$$

where $\cdot$ is a placeholder for the operator on which $\mathcal{P}_i$ acts. By virtue of the fact that the set of operators $\hat{\Pi}_i$ are projection operators onto orthogonal subspaces of the Hilbert space, i.e. $\hat{\Pi}_i\hat{\Pi}_j = \delta_{ij}\hat{\Pi}_i$, these projection superoperators project onto orthogonal subspaces of Liouville space, $\mathcal{P}_i\mathcal{P}_j = \delta_{ij}\mathcal{P}_i$. From the projected density operator $\mathcal{P}\hat{\rho}(t)$, we can extract the spin density operators using Eq. (3.29) replacing $\hat{\rho}(t)$ with $\mathcal{P}\hat{\rho}(t)$.

We can bring these definitions in line with the concept of the reduced set of observables $\hat{A}_n$ discussed in the previous chapter by noting the that observables of interest, the matrix elements of spin density operators in Eq. (3.29), are of the form $\hat{A}_n = \left|i, S, M_S\right\rangle\!\left\langle i, S', M'_S\right| \otimes |\mathbf{M}\rangle\langle\mathbf{M}'|$, where $|\mathbf{M}\rangle$ denotes spin projection state for the coupled nuclear spins. As such we can write $\mathcal{P}$ defined above in the form of Eq. (2.42), where the $\hat{\rho}_n$ operators are $\hat{\rho}_{i\mathrm{n}}$.

We note that with this definition of the projection superoperator $\mathcal{P}$ and our assump-

tion about the initial condition, Eq. (3.30), for the total density operator, $\mathcal{P}\hat{\rho}(0) = \hat{\rho}(0)$, and therefore $\mathcal{Q}\hat{\rho}(0) = 0$. This means that the inhomogeneous term, Eq. (2.55), in the Nakajima-Zwanzig equation vanishes, which simplifies the derivation of approximate master equations.

3.3.2 The reference and perturbation Hamiltonians

Having defined the spin density operators we are interested in, and a projection superoperator which extracts these components of the full density operator, we just need to divide the Hamiltonian into a reference part $\hat{H}_0$ and a perturbation $\hat{V}$ so that the perturbative Nakajima-Zwanzig equation can be applied to find equations of motion for the spin density operators. We do this using the diabatic state projection operators $\hat{\Pi}_i$. The reference Hamiltonian $\hat{H}_0$ is defined as the block diagonal part of the spin preserving term $\hat{H}_1$ when projected by the operators $\hat{\Pi}_i$, plus the thermally averaged projected part of the spin-mixing term $\hat{H}_2$,

$$\hat{H}_0 = \sum_i \left(\hat{\Pi}_i \hat{H}_1 \hat{\Pi}_i + \mathrm{Tr_n} \left[\hat{\rho}_{i\mathrm{n}} \hat{\Pi}_i \hat{H}_2 \hat{\Pi}_i \right] \right) \tag{3.34}$$

$$= \sum_i \left(\hat{H}_{i\mathrm{n}} + \hat{H}_{i\mathrm{s}} \right) \hat{\Pi}_i . \tag{3.35}$$

Here the $\hat{H}_{i\mathrm{s}}$ operators correspond to the thermally averaged spin Hamiltonians for state i. The relationship between the terms in the full molecular spin-mixing Hamiltonian, $\hat{H}_2$, and the terms appearing in the radical pair spin Hamiltonian $\hat{H}_{1\mathrm{s}}$ is described in appendix 3.B. The perturbation $\hat{V}$ is then simply the remaining part of the full Hamiltonian,

$$\hat{V} = \sum_{i,j\neq i} \hat{\Pi}_i \hat{H}_1 \hat{\Pi}_j + \hat{H}_2 - \sum_i \hat{H}_{i\mathrm{s}} \hat{\Pi}_i \tag{3.36}$$

$$= \hat{V}_\mathrm{S} + \hat{V}_\mathrm{T} + \sum_{i,j} \hat{V}_{\mathrm{sn},ij} \tag{3.37}$$

in which $\hat{V}_\mathrm{S}$ and $\hat{V}_\mathrm{T}$ are the singlet and triplet selective diabatic coupling terms,

$$\hat{V}_\mathrm{S} = \hat{\Delta}_\mathrm{S} \left|1, \mathrm{S}\right\rangle\!\left\langle 2, \mathrm{S}\right| + \hat{\Delta}_\mathrm{S}^\dagger \left|2, \mathrm{S}\right\rangle\!\left\langle 1, \mathrm{S}\right| \tag{3.38}$$

$$\hat{V}_\mathrm{T} = \sum_{n\in\{\mathrm{T_+},\mathrm{T_0},\mathrm{T_-}\}} \left(\hat{\Delta}_\mathrm{T} \left|1, n\right\rangle\!\left\langle 3, n\right| + \hat{\Delta}_\mathrm{T}^\dagger \left|3, n\right\rangle\!\left\langle 1, n\right| \right) \tag{3.39}$$

and $\hat{V}_{\mathrm{sn},ij}$ are spin-nuclear coupling terms, which may also couple different diabatic states (i.e. when $i \neq j$),

$$\hat{V}_{\mathrm{sn},ij} = \hat{\Pi}_i \hat{H}_2 \hat{\Pi}_j - \delta_{ij} \hat{H}_{\mathrm{is}} \hat{\Pi}_i. \tag{3.40}$$

It is important to note that $\hat{V}_{\mathrm{S}} = \hat{P}_{\mathrm{S}}\hat{V}_{\mathrm{S}} = \hat{V}_{\mathrm{S}}\hat{P}_{\mathrm{S}}$, and similarly $\hat{V}_{\mathrm{T}} = \hat{P}_{\mathrm{T}}\hat{V}_{\mathrm{T}} = \hat{V}_{\mathrm{T}}\hat{P}_{\mathrm{T}}$, so the singlet and triplet diabatic coupling terms preserve the electron spin state, but this is not true of the spin-nuclear coupling terms.

Having split the Hamiltonian into reference and perturbation terms, we can define the reference and perturbation Liouvillians as

$$\mathcal{L}_0 = -\frac{i}{\hbar}[\hat{H}_0, \cdot\,] \tag{3.41}$$

$$\mathcal{L}_V = -\frac{i}{\hbar}[\hat{V}, \cdot\,]. \tag{3.42}$$

With these definitions of $\mathcal{L}_0$, $\mathcal{L}_V$ and $\mathcal{P}$, we see that all of the conditions set out in the section 2.3.4 for the application of perturbation theory are satisfied.

3.3.3 The incoherent rate approximation

The first approximation we will invoke in deriving the QME for the spin density operators in the incoherent rate approximation.[102] We assume that the that the Markovian approximation described in section 2.3.1 is valid for describing the dynamics of the projected density operator. This will be valid if the decay timescale of the kernel is short compared to the timescale of population transfer and spin dynamics. I will analyse the validity of this approximation in more detail later, but we can see that it is likely to be accurate in many problems because the timescale of the kernel is controlled by the rate of decoherence between diabatic states, which is controlled by the timescale of the nuclear dynamics, which typically occur on a timescale of femtoseconds. On the other hand spin dynamics and population transfer typically occur on a timescale of nanoseconds to microseconds, so there will typically a large separation of timescales between the kernel and projected density operator. I refer to this as the incoherent rate approximation in this context, because Markovian population transfer between different electron transfer states means the population transfer

process is equivalent to describing the population transfer as an incoherent first order rate process.

3.3.4 The field independent rate approximation

We note that the reference Liouvillian can be split into a term that acts on nuclear degrees of freedom and spin degrees of freedom,

$$\mathcal{L}_0 = \mathcal{L}_\mathrm{n} + \mathcal{L}_\mathrm{s}, \tag{3.43}$$

where $\mathcal{L}_\mathrm{n}$ is given by

$$\mathcal{L}_\mathrm{n} = -\frac{i}{\hbar}\left[\sum_i \hat{\Pi}_i \hat{H}_{i\mathrm{n}},\ \cdot\ \right], \tag{3.44}$$

and $\mathcal{L}_\mathrm{s}$ is given by

$$\mathcal{L}_\mathrm{s} = -\frac{i}{\hbar}\left[\sum_i \hat{\Pi}_i \hat{H}_{i\mathrm{s}},\ \cdot\ \right]. \tag{3.45}$$

Evaluating the full kernel $\mathcal{K}(t)$ in the Nakajima-Zwanzig equation is complicated by the fact that $\mathcal{L}_\mathrm{s}$ in $\mathcal{L}_0$ does not preserve electronic spin states. As discussed above, the timescales associated with the nuclear vibrations and rearrangements will be much shorter (on the order of 10^{-15} s to 10^{-12} s) than the timescale of the spin and population transfer dynamics (on the order of 10^{-9} s to 10^{-6} s), and therefore $e^{\mathcal{L}_0 t} = e^{\mathcal{L}_\mathrm{n} t} e^{\mathcal{L}_\mathrm{s} t}$ can be approximated just as $e^{\mathcal{L}_0 t} \approx e^{\mathcal{L}_\mathrm{n} t}$ in evaluating the kernel. For similar reasons, for now we will ignore the spin-nuclear coupling term, $\hat{V}_{\mathrm{ns},ij}$, in the perturbation. These terms give rise to spin relaxation, among other things, and we will later consider how to treat them. We denote the kernel in which these spin terms are ignored by $\mathcal{K}_\mathrm{n}(t)$, and invoking the incoherent rate approximation we define the Markovian rate superoperator $\mathcal{K}$ as

$$\mathcal{K} = \int_0^\infty \mathcal{K}_\mathrm{n}(t)\,\mathrm{d}t\,. \tag{3.46}$$

3.3.5 Perturbative expansion

The final approximation we use in order to find approximate quantum master equations for the spin density operators is the perturbative approximation. We expand the rate superoperator Eq. (3.46) as a perturbation series in the strength of the diabatic couplings, $\hat{\Delta}_{\mathrm{S}}$ and $\hat{\Delta}_{\mathrm{T}}$,

$$\mathcal{K} = \sum_{n=2}^{\infty} \mathcal{K}^{(n)}. \tag{3.47}$$

The terms in the perturbation series can be found by using the method described in section 2.3.4, combined with the incoherent rate (Markovian) and field independent rate approximations described above, so the nth order term is given by

$$\mathcal{K}^{(n)} = \lim_{\omega \to 0} \mathcal{P}[\mathcal{L}_V \tilde{\mathcal{G}}_{\mathrm{n}}(\omega) \mathcal{Q}]^{n-1} \mathcal{L}_V \mathcal{P}, \tag{3.48}$$

in which $\tilde{\mathcal{G}}_{\mathrm{n}}(\omega)$ is given by

$$\tilde{\mathcal{G}}_{\mathrm{n}}(\omega) = \int_0^{\infty} \mathrm{d}t \, e^{+i\omega t} e^{\mathcal{L}_{\mathrm{n}} t} = (-i\omega - \mathcal{L}_{\mathrm{n}})^{-1}. \tag{3.49}$$

In practice these are often simpler to evaluate by converting the $\tilde{\mathcal{G}}_{\mathrm{n}}(\omega)$ terms to time integrals using the convolution property of the Fourier-Laplace transform, Eq. (2.60). It is useful to note that $e^{\mathcal{L}_{\mathrm{n}} t}$ acts on operators of the form $\hat{A} = |i, S, M_S\rangle\langle j, S', M'_S| \otimes \hat{B}_{\mathrm{n}}$, where $\hat{B}_{\mathrm{n}}$ is an arbitrary operator on the nuclear spatial degrees of freedom, as follows,

$$e^{\mathcal{L}_{\mathrm{n}} t} \hat{A} = |i, S, M_S\rangle\langle j, S', M'_S| \otimes \left(e^{-i\hat{H}_{i\mathrm{n}} t/\hbar} \hat{B}_{\mathrm{n}} e^{+i\hat{H}_{j\mathrm{n}} t/\hbar} \right). \tag{3.50}$$

In evaluating the perturbative expansion, it is useful to rewrite $\hat{V}_{\mathrm{S}}$ as

$$\hat{V}_{\mathrm{S}} = \hat{P}_{\mathrm{S}} \left(\hat{\Delta}_{\mathrm{S}} \hat{T}_{12} + \hat{\Delta}_{\mathrm{S}}^{\dagger} \hat{T}_{21} \right) \hat{P}_{\mathrm{S}}, \tag{3.51}$$

where $\hat{T}_{ij}$ is a spin-selective transfer operator from the set of diabatic states j to the set i,

$$\hat{T}_{ij} = \sum_{S \in \mathcal{S}_i \cap \mathcal{S}_j} \sum_{M=-S}^{S} |i, S, M\rangle\langle j, S, M|, \tag{3.52}$$

The singlet projection operators are in included in Eq. (3.51) to emphasise that this term

only acts on singlet spin states. Similarly $\hat{V}_{\mathrm{T}}$ can be rewritten as

$$\hat{V}_{\mathrm{T}} = \hat{P}_{\mathrm{T}} \left(\hat{\Delta}_{\mathrm{T}} \hat{T}_{13} + \hat{\Delta}_{\mathrm{T}}^{\dagger} \hat{T}_{31} \right) \hat{P}_{\mathrm{T}}. \tag{3.53}$$

From the definition of $\hat{T}_{ij}$ in Eq. (3.52), $\hat{T}_{ii} = \hat{\Pi}_i$, and since these operators commute with the spin projection operators they have the property that

$$\hat{T}_{ij}\hat{T}_{kl} = \delta_{jk}\hat{T}_{il} \sum_{S \in \mathcal{S}_i \cap \mathcal{S}_j \cap \mathcal{S}_k \cap \mathcal{S}_l} \hat{P}_S. \tag{3.54}$$

A useful specific case of this is when $i = l$ and $j = k$,

$$\hat{T}_{ij}\hat{T}_{ji} = \hat{\Pi}_i \sum_{S \in \mathcal{S}_i \cap \mathcal{S}_j} \hat{P}_S, \tag{3.55}$$

It is also useful to know what happens to $\hat{T}_{ij}$ when it is projected by $\hat{\Pi}_k = \hat{T}_{kk}$, which also follows from Eq. (3.54),

$$\hat{T}_{ij}\hat{\Pi}_k = \hat{T}_{ij}\delta_{jk} \text{ and } \hat{\Pi}_k\hat{T}_{ij} = \delta_{ik}\hat{T}_{il}. \tag{3.56}$$

These properties of the transfer operators greatly simplify evaluation of the perturbation expansion of the rate superoperator.

We can split the rate superoperator into terms $\mathcal{K}_{ij}$ which connect different projected subspaces of Liouville space, using Eq. (3.32),

$$\mathcal{K} = \sum_{i,j=1,2,3} \mathcal{P}_i \mathcal{K} \mathcal{P}_j = \sum_{i,j=1,2,3} \mathcal{K}_{ij}. \tag{3.57}$$

Given this we can show that only even order terms in the perturbative expansion of the rate superoperator are non-zero. This follows from the fact that the projection superoperators $\mathcal{P}_i$ project onto diabatic population elements of Liouville space, i.e. elements of the form $\left|i, S, M_S\right\rangle\!\left\langle i, S', M_S'\right| \otimes |\mathbf{M}\rangle\!\langle\mathbf{M}'| \otimes \hat{B}_{\mathrm{n}}$. By the properties of the transfer operators $\hat{T}_{ij}$ given above, $\mathcal{L}_V$ can only connect diagonal diabatic population elements of Liouville space to off-diagonal diabatic coherence elements, and vice-versa. Because the projection superoperator removes all diabatic coherence elements of Liouville space, and because the transfer operators are spin state selective, only terms in the rate superoperator containing an even number of $\mathcal{L}_V$ superoperators are non-zero. This means $\mathcal{K}^{(n)}$ is non-zero only if n

is even.

3.3.6 Second order master equation

Employing the approximations described above, we can derive the second order radical pair quantum master equation. First we will consider the zeroth order term in Eq. (2.62), which is $\mathcal{P}\mathcal{L}_0\mathcal{P}$, which can be simplified to the following,

$$\mathcal{P}\mathcal{L}_0\mathcal{P} = \mathcal{L}_\mathrm{s}\mathcal{P}. \tag{3.58}$$

This follows from the fact that $[\hat{\Pi}_i\hat{H}_{i\mathrm{n}}, \hat{\rho}_{j\mathrm{n}}\,\mathrm{Tr}_\mathrm{n}[\hat{\Pi}_j\hat{A}\hat{\Pi}_j]] = 0$, and $\mathrm{Tr}_\mathrm{n}[[\hat{\Pi}_i\hat{H}_{i\mathrm{s}}, \hat{A}]] = [\hat{\Pi}_i\hat{H}_{i\mathrm{s}}, \mathrm{Tr}_\mathrm{n}[\hat{A}]]$ where $\hat{A}$ is any operator.

Now we consider the expansion of the remaining term in Eq. (2.62), the rate superoperator. The second order master equation is obtained by truncating this at its second order term, $\mathcal{K} \approx \mathcal{K}^{(2)}$, which is given by

$$\mathcal{K}^{(2)} = \int_0^\infty \mathrm{d}t\, \mathcal{P}\mathcal{L}_V e^{\mathcal{L}_\mathrm{n}t}\mathcal{L}_V\mathcal{P}. \tag{3.59}$$

First we will consider the rate superoperator term $\mathcal{K}_{11}^{(2)}$ that acts on the radical pair spin density operator $\hat{\rho}_{1\mathrm{s}}(t)$. We do this by explicitly expanding the double commutator,

$$\mathcal{K}_{11}^{(2)}\mathcal{P}_1\hat{\rho} = -\frac{1}{\hbar^2}\int_0^\infty \mathrm{d}t\, \mathcal{P}_1\left([\hat{V}, e^{\mathcal{L}_\mathrm{n}t}[\hat{V}, \mathcal{P}_1\hat{\rho}]]\right), \tag{3.60}$$

and we then use the above properties of the transfer operators to simplify the expansion. For simplicity, we start by only considering terms that depend on the singlet diabatic coupling $\hat{V}_\mathrm{S}$. The only non-zero contributions are found to be,

$$\begin{aligned}\mathcal{K}_{11}^{(2)}\mathcal{P}_1\hat{\rho} = -\frac{1}{\hbar^2}\int_0^\infty \mathrm{d}t\, \mathcal{P}_1\Big(&\hat{P}_\mathrm{S}\hat{\Delta}_\mathrm{S}\hat{T}_{12}\left(e^{\mathcal{L}_\mathrm{n}t}(\hat{T}_{21}\hat{\Delta}_\mathrm{S}^\dagger\hat{P}_\mathrm{S}(\mathcal{P}_1\hat{\rho}))\right)\\ &+\left(e^{\mathcal{L}_\mathrm{n}t}((\mathcal{P}_1\hat{\rho})\hat{P}_\mathrm{S}\hat{\Delta}_\mathrm{S}\hat{T}_{12})\right)\hat{T}_{21}\hat{\Delta}_\mathrm{S}^\dagger\hat{P}_\mathrm{S}\Big) + \text{ triplet coupling terms.}\end{aligned} \tag{3.61}$$

I will now show in detail how to evaluate the first term. We first note that the term on which $e^{\mathcal{L}_\mathrm{n}t}$ acts can be factorised into a spin/diabatic state term and a nuclear term

$$\hat{T}_{21}\hat{\Delta}_\mathrm{S}^\dagger\hat{P}_\mathrm{S}(\mathcal{P}_1\hat{\rho}) = (\hat{P}_\mathrm{S}\hat{T}_{21}\hat{\rho}_{1\mathrm{s}})(\hat{\Delta}_\mathrm{S}^\dagger\hat{\rho}_{1\mathrm{n}}), \tag{3.62}$$

and when $e^{\mathcal{L}_{\mathrm{n}}t}$ acts on this, using Eq. (3.50), we obtain

$$e^{\mathcal{L}_{\mathrm{n}}t}\left(\hat{T}_{21}\hat{\Delta}_{\mathrm{S}}^{\dagger}\hat{P}_{\mathrm{S}}(\mathcal{P}_1\hat{\rho})\right) = (\hat{P}_{\mathrm{S}}\hat{T}_{21}\hat{\rho}_{1\mathrm{s}})e^{-i\hat{H}_{2\mathrm{n}}t/\hbar}(\hat{\Delta}_{\mathrm{S}}^{\dagger}\hat{\rho}_{1\mathrm{n}})e^{+i\hat{H}_{1\mathrm{n}}t/\hbar}. \tag{3.63}$$

Using this, we can evaluate the first term in the expression for $\mathcal{K}_{11}^{(2)}$ as

$$\begin{aligned}\mathcal{P}_1\hat{P}_{\mathrm{S}}\hat{\Delta}_{\mathrm{S}}\hat{T}_{12}\left(e^{\mathcal{L}_{\mathrm{n}}t}(\hat{T}_{21}\hat{\Delta}_{\mathrm{S}}^{\dagger}\hat{P}_{\mathrm{S}}(\mathcal{P}_1\hat{\rho}))\right) &= \hat{P}_{\mathrm{S}}\hat{\rho}_{1\mathrm{s}}\hat{\rho}_{1\mathrm{n}}\,\mathrm{Tr}_{\mathrm{n}}[\hat{\Delta}_{\mathrm{S}}e^{-i\hat{H}_{2\mathrm{n}}t/\hbar}(\hat{\Delta}_{\mathrm{S}}^{\dagger}\hat{\rho}_{1\mathrm{n}})e^{+i\hat{H}_{1\mathrm{n}}t/\hbar}] \\ &= \frac{\Delta_{\mathrm{S}}^2 c_{1\mathrm{S}}^{(2)}(t)}{Z_{1\mathrm{n}}}\hat{P}_{\mathrm{S}}(\mathcal{P}_1\hat{\rho})\end{aligned} \tag{3.64}$$

where Δ_{S} is a real constant such that $\Delta_{\mathrm{S}}\hat{f}_{\mathrm{S}} = \hat{\Delta}_{\mathrm{S}}$, where $\hat{f}_{\mathrm{S}}$ is unitless, and the function $c_{1\mathrm{S}}^{(2)}(t)$ is given by

$$c_{1\mathrm{S}}^{(2)}(t) = \mathrm{Tr}_{\mathrm{n}}[e^{-\beta\hat{H}_{1\mathrm{n}}}e^{+i\hat{H}_{1\mathrm{n}}t/\hbar}\hat{f}_{\mathrm{S}}e^{-i\hat{H}_{2\mathrm{n}}t/\hbar}\hat{f}_{\mathrm{S}}^{\dagger}]. \tag{3.65}$$

We can repeat this for the second term in Eq. (3.61), which gives the following

$$\left(e^{\mathcal{L}_{\mathrm{n}}t}((\mathcal{P}_1\hat{\rho})\hat{P}_{\mathrm{S}}\hat{\Delta}_{\mathrm{S}}\hat{T}_{12})\right)\hat{T}_{21}\hat{\Delta}_{\mathrm{S}}^{\dagger}\hat{P}_{\mathrm{S}} = \frac{\Delta_{\mathrm{S}}^2 c_{1\mathrm{S}}^{(2)}(t)^*}{Z_{1\mathrm{n}}}(\mathcal{P}_1\hat{\rho})\hat{P}_{\mathrm{S}}. \tag{3.66}$$

The terms depending on the triplet coupling are easily obtained from the above by simply replacing the labels S with T and 2 with 3. Also, because the transfer operators $\hat{T}_{ij}$ are spin selective, there are no terms at second order in the perturbation that depend on both $\hat{V}_{\mathrm{S}}$ and $\hat{V}_{\mathrm{T}}$. Using this we find that $\mathcal{K}_{11}^{(2)}$ can be written as

$$\begin{aligned}\mathcal{K}_{11}^{(2)}\mathcal{P}_1\hat{\rho} = &\left(-\frac{k_{\mathrm{f,S}}^{(2)}}{2} - i\frac{2J_{\mathrm{S}}^{(2)}}{\hbar}\right)\hat{P}_{\mathrm{S}}(\mathcal{P}_1\hat{\rho}) + \left(-\frac{k_{\mathrm{f,S}}^{(2)}}{2} + i\frac{2J_{\mathrm{S}}^{(2)}}{\hbar}\right)(\mathcal{P}_1\hat{\rho})\hat{P}_{\mathrm{S}} \\ &+ \left(-\frac{k_{\mathrm{f,T}}^{(2)}}{2} - i\frac{2J_{\mathrm{T}}^{(2)}}{\hbar}\right)\hat{P}_{\mathrm{T}}(\mathcal{P}_1\hat{\rho}) + \left(-\frac{k_{\mathrm{f,T}}^{(2)}}{2} + i\frac{2J_{\mathrm{T}}^{(2)}}{\hbar}\right)(\mathcal{P}_1\hat{\rho})\hat{P}_{\mathrm{T}}\end{aligned} \tag{3.67}$$

$$= -\left\{\frac{k_{\mathrm{f,S}}^{(2)}}{2}\hat{P}_{\mathrm{S}} + \frac{k_{\mathrm{f,T}}^{(2)}}{2}\hat{P}_{\mathrm{T}}, (\mathcal{P}_1\hat{\rho})\right\} - \frac{i}{\hbar}\left[2J_{\mathrm{S}}^{(2)}\hat{P}_{\mathrm{S}} + 2J_{\mathrm{T}}^{(2)}\hat{P}_{\mathrm{T}}, (\mathcal{P}_1\hat{\rho})\right]. \tag{3.68}$$

The forward singlet rate constant $k_{\mathrm{f,S}}^{(2)}$ is given by

$$k_{\mathrm{f,S}}^{(2)} = \frac{2\Delta_{\mathrm{S}}^2}{\hbar^2 Z_{1\mathrm{n}}}\int_0^{\infty}\mathrm{Re}[c_{1\mathrm{S}}^{(2)}(t)]\,\mathrm{d}t\,, \tag{3.69}$$

and the forward triplet reaction rate constant is given by,

$$k_{\mathrm{f,T}}^{(2)} = \frac{2\Delta_{\mathrm{T}}^2}{\hbar^2 Z_{1\mathrm{n}}} \int_0^\infty \mathrm{Re}[c_{1\mathrm{T}}^{(2)}(t)]\,\mathrm{d}t \tag{3.70}$$

where $c_{1\mathrm{T}}^{(2)}(t)$ is defined similarly to $c_{1\mathrm{S}}^{(2)}(t)$,

$$c_{1\mathrm{T}}^{(2)}(t) = \mathrm{Tr}_{\mathrm{n}}[e^{-\beta\hat{H}_{1\mathrm{n}}} e^{+i\hat{H}_{1\mathrm{n}}t/\hbar} \hat{f}_{\mathrm{T}} e^{-i\hat{H}_{3\mathrm{n}}t/\hbar} \hat{f}_{\mathrm{T}}^\dagger] \tag{3.71}$$

where $\hat{\Delta}_{\mathrm{T}} = \Delta_{\mathrm{T}}\hat{f}_{\mathrm{T}}$. The energy shifts $2J_{\mathrm{S}}^{(2)}$ and $2J_{\mathrm{T}}^{(2)}$ are related to the imaginary parts of the correlation functions,

$$2J_{\mathrm{S}}^{(2)} = \frac{\Delta_{\mathrm{S}}^2}{\hbar Z_{1\mathrm{n}}} \int_0^\infty \mathrm{Im}[c_{1\mathrm{S}}^{(2)}(t)]\,\mathrm{d}t \tag{3.72}$$

$$2J_{\mathrm{T}}^{(2)} = \frac{\Delta_{\mathrm{S}}^2}{\hbar Z_{1\mathrm{n}}} \int_0^\infty \mathrm{Im}[c_{1\mathrm{T}}^{(2)}(t)]\,\mathrm{d}t\,. \tag{3.73}$$

We can also repeat this for the remaining terms in the second order rate superoperator. After some algebra, we find the diagonal terms are,

$$\mathcal{K}_{22}^{(2)}\mathcal{P}_2\hat{\rho} = -k_{\mathrm{b,S}}^{(2)}\mathcal{P}_2\hat{\rho} \tag{3.74}$$

$$\mathcal{K}_{33}^{(2)}\mathcal{P}_2\hat{\rho} = -k_{\mathrm{b,T}}^{(2)}\mathcal{P}_3\hat{\rho}, \tag{3.75}$$

and the the off-diagonal terms are

$$\mathcal{K}_{12}^{(2)}\mathcal{P}_2\hat{\rho} = k_{\mathrm{b,S}}^{(2)}\mathcal{T}_{12}\mathcal{P}_2\hat{\rho} \tag{3.76}$$

$$\mathcal{K}_{13}^{(2)}\mathcal{P}_3\hat{\rho} = k_{\mathrm{b,T}}^{(2)}\mathcal{T}_{13}\mathcal{P}_3\hat{\rho} \tag{3.77}$$

$$\mathcal{K}_{21}^{(2)}\mathcal{P}_1\hat{\rho} = k_{\mathrm{f,S}}^{(2)}\mathcal{T}_{21}\mathcal{P}_1\hat{\rho} \tag{3.78}$$

$$\mathcal{K}_{31}^{(2)}\mathcal{P}_1\hat{\rho} = k_{\mathrm{f,T}}^{(2)}\mathcal{T}_{31}\mathcal{P}_1\hat{\rho} \tag{3.79}$$

The transfer superoperator $\mathcal{T}_{ij}$ is given by

$$\mathcal{T}_{ij} = \hat{\rho}_{i\mathrm{n}}\,\mathrm{Tr}_{\mathrm{n}}[\hat{T}_{ij}\ \cdot\ \hat{T}_{ji}], \tag{3.80}$$

and $k_{\mathrm{b,S}}^{(2)}$ is the second order backwards singlet reaction rate constant, which is given by

$$k_{\mathrm{b,S}}^{(2)} = \frac{2\Delta_{\mathrm{S}}^2}{\hbar^2 Z_{2\mathrm{n}}} \int_0^\infty c_{2\mathrm{S}}^{(2)}(t)\,\mathrm{d}t\,, \tag{3.81}$$

where $c^{(2)}_{2\mathrm{S}}(t)$ is

$$c^{(2)}_{2\mathrm{S}}(t) = \mathrm{Tr}_{\mathrm{n}}[e^{-\beta\hat{H}_{2\mathrm{n}}}e^{+i\hat{H}_{2\mathrm{n}}t/\hbar}\hat{f}^{\dagger}_{\mathrm{S}}e^{-i\hat{H}_{1\mathrm{n}}t/\hbar}\hat{f}_{\mathrm{S}}]. \tag{3.82}$$

The backward second order triplet reaction rate constant $k^{(2)}_{\mathrm{b,T}}$ is given by an analogous expression.

Having obtained the rate superoperator at second order in the diabatic coupling, we can trace out the nuclear degrees of freedom to obtain quantum master equations for the spin density operators $\hat{\rho}_{i\mathrm{s}}(t)$,

$$\begin{aligned}\frac{\mathrm{d}}{\mathrm{d}t}\hat{\rho}_{1\mathrm{s}}(t) = &-\frac{i}{\hbar}\left[\hat{H}_{1\mathrm{s}} - 2J^{(2)}\hat{\mathbf{S}}_1\cdot\hat{\mathbf{S}}_2, \hat{\rho}_{1\mathrm{s}}(t)\right] - \left\{\frac{k^{(2)}_{\mathrm{f,S}}}{2}\hat{P}_{\mathrm{S}} + \frac{k^{(2)}_{\mathrm{f,T}}}{2}\hat{P}_{\mathrm{T}}, \hat{\rho}_{1\mathrm{s}}(t)\right\} \\ &+ k^{(2)}_{\mathrm{b,S}}\hat{P}_{\mathrm{S}}\left(\hat{T}_{12}\hat{\rho}_{2\mathrm{s}}(t)\hat{T}_{21}\right)\hat{P}_{\mathrm{S}} + k^{(2)}_{\mathrm{b,T}}\hat{P}_{\mathrm{T}}\left(\hat{T}_{13}\hat{\rho}_{3\mathrm{s}}(t)\hat{T}_{31}\right)\hat{P}_{\mathrm{T}}\end{aligned} \tag{3.83a}$$

$$\frac{\mathrm{d}}{\mathrm{d}t}\hat{\rho}_{2\mathrm{s}}(t) = -k^{(2)}_{\mathrm{b,S}}\hat{\rho}_{2\mathrm{s}}(t) + k^{(2)}_{\mathrm{f,S}}\hat{P}_{\mathrm{S}}\left(\hat{T}_{21}\hat{\rho}_{1\mathrm{s}}(t)\hat{T}_{12}\right)\hat{P}_{\mathrm{S}} \tag{3.83b}$$

$$\frac{\mathrm{d}}{\mathrm{d}t}\hat{\rho}_{3\mathrm{s}}(t) = -k^{(2)}_{\mathrm{b,T}}\hat{\rho}_{3\mathrm{s}}(t) + k^{(2)}_{\mathrm{f,T}}\hat{P}_{\mathrm{T}}\left(\hat{T}_{31}\hat{\rho}_{1\mathrm{s}}(t)\hat{T}_{13}\right)\hat{P}_{\mathrm{T}}. \tag{3.83c}$$

The scalar coupling term $-2J^{(2)}\hat{\mathbf{S}}_1\cdot\hat{\mathbf{S}}_2$, where $J^{(2)} = J^{(2)}_{\mathrm{S}} - J^{(2)}_{\mathrm{T}}$, was introduced in Eq. (3.83a) by noting that we can write the singlet and triplet projection operators acting on the radical pair diabatic states in terms of the effective electron spin operators (as introduced in appendix 3.B) as $\hat{P}_{\mathrm{S}}\hat{\Pi}_1 = (1/4 - \hat{\mathbf{S}}_1\cdot\hat{\mathbf{S}}_2)\hat{\Pi}_1$ and $\hat{P}_{\mathrm{T}}\hat{\Pi}_1 = (3/4 + \hat{\mathbf{S}}_1\cdot\hat{\mathbf{S}}_2)\hat{\Pi}_1$.

The first term that appears in Eq. (3.83a) corresponds to the coherent spin evolution, with a correction to the scalar coupling arising from the diabatic coupling $J^{(2)}$, the second term is a Haberkorn reaction term, and the third and fourth terms correspond to back-reaction terms. The rate constants appearing in these expressions are exactly the Fermi's golden rule rates for the electron transfers,[55,128] as would be derived by taking the weak diabatic coupling limit of any exact expression for the rate constants, so we see that this quantum master equation is consistent with reaction rate theory in the non-adiabatic (weak diabatic coupling) limit.[102,124,128] In the limit where the backward reaction rates are much slower than the forward reaction rates, i.e. $k^{(2)}_{\mathrm{f,S}} \gg k^{(2)}_{\mathrm{b,S}}$ and $k^{(2)}_{\mathrm{f,T}} \gg k^{(2)}_{\mathrm{b,T}}$, we can ignore the back reaction terms in Eq. (3.83), and this reduces to the Haberkorn quantum master equation for the radical pair spin density operator, $\hat{\rho}_{1\mathrm{s}}(t)$, with a correction to the scalar electron spin

coupling that appears in spin Hamiltonian.

The reactive contribution to the scaling coupling can be understood as arising from an average energy shift in the radical pair singlet and triplet states created by the spin state selective diabatic coupling. Because the singlet and triplet states couple to different product states, with different coupling strengths, the average energy shifts are different for the singlet and triplet radical pair states. These different energy shifts then manifest as a a correction to the scalar electron spin coupling in the radical pair master equation. The form of the scalar coupling correction obtained here can be seen as a generalisation of the well known expression for the scalar coupling,[26,67,129–132]

$$2J = \frac{\Delta_{\mathrm{T}}^2}{\Delta E_{\mathrm{T}}} - \frac{\Delta_{\mathrm{S}}^2}{\Delta E_{\mathrm{S}}}, \tag{3.84}$$

where ΔE_{S} and ΔE_{T} are the vertical energy gaps between the singlet and triplet states and the radical pair state at the minimum energy geometry for the radical pair. This expression is valid within the Condon approximation (constant diabatic coupling),[55] and the approximation that the nuclear configuration is fixed at the radical pair equilibrium geometry, whereas the expression for $J^{(2)}$, given by Eqs. (3.72) and (3.73), accounts for non-Condon effects, thermal fluctuations and nuclear quantum effects. I will expand upon this interpretation of the scalar coupling when I analyse the classical limit of the energy shift expressions in section 4.1.

3.3.7 Higher order master equations

As demonstrated above, a second order treatment of the diabatic coupling naturally yields the Haberkorn master equation for the radical pair spin density operator, with an additional correction to the scalar coupling between the electron spins, so the Haberkorn form of the master equation is the correct in this limit. It is therefore natural to ask if this still applies when higher order effects in the diabatic coupling become important. To answer this question, I will now derive the fourth order master equation, and discuss how to extend this to an arbitrarily high order.

As before, we will assume that the incoherent rate and the field independent rate approximations can be applied. As explained in section 3.3.5, all odd order terms in the

perturbative expansion of the rate superoperator vanish, so the next non-zero term is the fourth order term, which is given by

$$\mathcal{K}^{(4)} = \int_0^\infty \mathrm{d}t_1 \int_0^\infty \mathrm{d}t_2 \int_0^\infty \mathrm{d}t_3 \, \mathcal{P}\mathcal{L}_V e^{\mathcal{L}_\mathrm{n} t_1} \mathcal{L}_V e^{\mathcal{L}_\mathrm{n} t_2} \mathcal{L}_V e^{\mathcal{L}_\mathrm{n} t_3} \mathcal{L}_V \mathcal{P}. \tag{3.85}$$

Again we split the fourth order rate superoperator $\mathcal{K}^{(4)}$ into terms that connect different projected subspaces of Liouville space $\mathcal{K}^{(4)}_{ij}$. First we will consider the term that acts on the radical pair subspace, $\mathcal{K}^{(4)}_{11}$, which can be evaluated by first expanding the four nested commutators that appear,

$$\mathcal{K}^{(4)}_{11}\mathcal{P}_1\hat{\rho} = \int_0^\infty \mathrm{d}t_1 \int_0^\infty \mathrm{d}t_2 \int_0^\infty \mathrm{d}t_3 \, \frac{1}{\hbar^2}\mathcal{P}_1\left[\hat{V}, e^{\mathcal{L}_\mathrm{n} t_1}\left[\hat{V}, e^{\mathcal{L}_\mathrm{n} t_2}\left[\hat{V}, e^{\mathcal{L}_\mathrm{n} t_3}\left[\hat{V}, (\mathcal{P}_1\hat{\rho})\right]\right]\right]\right]. \tag{3.86}$$

Expanding this expression, there are non-zero terms arising from products of four transfer operators appearing either on the right or left of $\mathcal{P}_1\hat{\rho}$, e.g. terms of the form

$$\mathcal{P}_1(\hat{T}_{12}\hat{T}_{21}\hat{T}_{12}\hat{T}_{21}\hat{P}_\mathrm{S}(\mathcal{P}_1\hat{\rho})). \tag{3.87}$$

There are no cross terms between the singlet and triplet diabatic coupling of this form, because the transfer operators are spin selective (as given by Eq. (3.52)). These terms (and the triplet selective coupling analogues) give rise contributions to $\mathcal{K}^{(4)}_{11}$ of the same form as Eq. (3.68), i.e. $\{\hat{P}_\mathrm{S}, \cdot\}$ and $i[\hat{P}_\mathrm{S}, \cdot]$, but with fourth order rate constants in the Haberkorn term and fourth order corrections to the scalar coupling. There are additionally non-zero contributions arising from products of transfer operators on both the left and right of $\mathcal{P}_1\hat{\rho}$, for example terms of the the form

$$\mathcal{P}_1\left(\hat{T}_{12}\hat{T}_{21}\hat{P}_\mathrm{S}(\mathcal{P}_1\hat{\rho})\hat{P}_\mathrm{S}\hat{T}_{12}\hat{T}_{21}\right). \tag{3.88}$$

Noting that $\hat{P}_\mathrm{S} = \hat{1} - \hat{P}_\mathrm{T}$, we can write $\hat{P}_\mathrm{S}(\mathcal{P}_1\hat{\rho})\hat{P}_\mathrm{S}$ as

$$\hat{P}_\mathrm{S}(\mathcal{P}_1\hat{\rho})\hat{P}_\mathrm{S} = \frac{1}{2}\left\{\hat{P}_\mathrm{S}, (\mathcal{P}_1\hat{\rho})\right\} - \frac{1}{2}\left(\hat{P}_\mathrm{S}(\mathcal{P}_1\hat{\rho})\hat{P}_\mathrm{T} + \hat{P}_\mathrm{T}(\mathcal{P}_1\hat{\rho})\hat{P}_\mathrm{S}\right). \tag{3.89}$$

These terms (and the triplet analogues) appear with real coefficients, producing an additional fourth order correction to the rate constants appearing in the Haberkorn term, as well as a singlet-triplet decoherence term (the second term on the right hand side of Eq. (3.89)).

The final type of term that appears in the expansion of the commutators comes from mixed singlet-triplet coupling terms and are of the form

$$\mathcal{P}_1 \left(\hat{T}_{12} \hat{T}_{21} \hat{P}_\mathrm{S} (\mathcal{P}_1 \hat{\rho}) \hat{P}_\mathrm{T} \hat{T}_{13} \hat{T}_{31} \right) . \tag{3.90}$$

These terms, and their analogues with the singlet and triplet couplings swapped, appear with complex valued coefficients, but in conjugate pairs, so these can be simplified to give

$$\begin{aligned} &(a+ib) \hat{P}_\mathrm{S} (\mathcal{P}_1 \hat{\rho}) \hat{P}_\mathrm{T} + (a-ib) \hat{P}_\mathrm{T} (\mathcal{P}_1 \hat{\rho}) \hat{P}_\mathrm{S} \\ &\qquad = a \left(\hat{P}_\mathrm{S} (\mathcal{P}_1 \hat{\rho}) \hat{P}_\mathrm{T} + \hat{P}_\mathrm{T} (\mathcal{P}_1 \hat{\rho}) \hat{P}_\mathrm{S} \right) + ib \left[\hat{\mathbf{S}}_1 \cdot \hat{\mathbf{S}}_2, (\mathcal{P}_1 \hat{\rho}) \right] . \end{aligned} \tag{3.91}$$

Therefore these cross terms give rise to an additional contribution to the singlet-triplet decoherence, plus a further fourth order correction to the scalar coupling. After collecting all of these terms the final result for $\mathcal{K}_{11}^{(4)}$ is

$$\begin{aligned} \mathcal{K}_{11}^{(4)} \mathcal{P}_1 \hat{\rho} = &- \left\{ \frac{k_{\mathrm{f,S}}^{(4)}}{2} \hat{P}_\mathrm{S} + \frac{k_{\mathrm{f,T}}^{(4)}}{2} \hat{P}_\mathrm{T}, (\mathcal{P}_1 \hat{\rho}) \right\} - \frac{i}{\hbar} \left[-2 (J_\mathrm{S}^{(4)} - J_\mathrm{T}^{(4)} + J_\mathrm{ST}^{(4)}) \hat{\mathbf{S}}_1 \cdot \hat{\mathbf{S}}_2 \hat{P}_\mathrm{T}, (\mathcal{P}_1 \hat{\rho}) \right] \\ &- (k_{\mathrm{D,S}}^{(4)} + k_{\mathrm{D,T}}^{(4)} + k_{\mathrm{D,ST}}^{(4)}) \left(\hat{P}_\mathrm{S} (\mathcal{P}_1 \hat{\rho}) \hat{P}_\mathrm{T} + \hat{P}_\mathrm{T} (\mathcal{P}_1 \hat{\rho}) \hat{P}_\mathrm{S} \right) . \end{aligned} \tag{3.92}$$

Here $k_{\mathrm{f,S}}^{(4)}$ and $k_{\mathrm{f,T}}^{(4)}$ are the fourth order contributions to the singlet and triplet reaction rate constants, $J_\mathrm{S}^{(4)}$ and $J_\mathrm{T}^{(4)}$ are the fourth order contributions to the scalar coupling, which depend only on the singlet and triplet diabatic couplings respectively, and similarly $k_{\mathrm{D,S}}^{(4)}$ and $k_{\mathrm{D,T}}^{(4)}$ are fourth order contributions to the additional singlet-triplet decoherence rate that depend on the the singlet and triplet diabatic couplings respectively. $k_{\mathrm{D,ST}}^{(4)}$ and $J_\mathrm{ST}^{(4)}$ are the contributions to the additional decoherence rate and scalar coupling that originate from mixed singlet and triplet diabatic coupling terms of the form given in Eq. (3.90). These constants work out to be related to triple time integrals of three-time correlation functions of a similar form to $c_{2\mathrm{S}}^{(2)}(t)$ and $c_{2\mathrm{T}}^{(2)}(t)$, but involving more propagators. Full expressions for the fourth order reaction rates, scalar coupling contributions and decoherence rate contributions are given in appendix 3.C.

The method outlined above can be applied to evaluate the other fourth order terms, $\mathcal{K}_{ij}^{(4)}$, appearing in the rate superoperator. Because the diabatic coupling is spin-state selective,

these work out to be identical in form the second order expressions given in Eq. (3.74) to Eq. (3.79), but with the second order rate constants replaced with fourth order contributions to the rate constants. Combining this with the second order rate superoperators given in the previous section, we obtain the fourth order quantum master equation for the spin density operators by tracing out the nuclear degrees of freedom which gives

$$\begin{aligned}\frac{\mathrm{d}}{\mathrm{d}t}\hat{\rho}_{1\mathrm{s}}(t) = &-\frac{i}{\hbar}\left[\hat{H}_{1\mathrm{s}} - 2J\hat{\mathbf{S}}_1\cdot\hat{\mathbf{S}}_2, \hat{\rho}_{1\mathrm{s}}(t)\right] - \left\{\frac{k_{\mathrm{f,S}}}{2}\hat{P}_{\mathrm{S}} + \frac{k_{\mathrm{f,T}}}{2}\hat{P}_{\mathrm{T}}, \hat{\rho}_{1\mathrm{s}}(t)\right\} \\ &- k_{\mathrm{D}}\left(\hat{P}_{\mathrm{S}}(\mathcal{P}_1\hat{\rho})\hat{P}_{\mathrm{T}} + \hat{P}_{\mathrm{T}}(\mathcal{P}_1\hat{\rho})\hat{P}_{\mathrm{S}}\right) \\ &+ k_{\mathrm{b,S}}\hat{P}_{\mathrm{S}}\left(\hat{T}_{12}\hat{\rho}_{2\mathrm{s}}(t)\hat{T}_{21}\right)\hat{P}_{\mathrm{S}} + k_{\mathrm{b,T}}\hat{P}_{\mathrm{T}}\left(\hat{T}_{13}\hat{\rho}_{3\mathrm{s}}(t)\hat{T}_{31}\right)\hat{P}_{\mathrm{T}}\end{aligned} \tag{3.93a}$$

$$\frac{\mathrm{d}}{\mathrm{d}t}\hat{\rho}_{2\mathrm{s}}(t) = -k_{\mathrm{b,S}}\hat{\rho}_{2\mathrm{s}}(t) + k_{\mathrm{f,S}}\hat{P}_{\mathrm{S}}\left(\hat{T}_{21}\hat{\rho}_{1\mathrm{s}}(t)\hat{T}_{12}\right)\hat{P}_{\mathrm{S}} \tag{3.93b}$$

$$\frac{\mathrm{d}}{\mathrm{d}t}\hat{\rho}_{3\mathrm{s}}(t) = -k_{\mathrm{b,T}}\hat{\rho}_{3\mathrm{s}}(t) + k_{\mathrm{f,T}}\hat{P}_{\mathrm{T}}\left(\hat{T}_{31}\hat{\rho}_{1\mathrm{s}}(t)\hat{T}_{13}\right)\hat{P}_{\mathrm{T}}. \tag{3.93c}$$

In this quantum master equation, the rate constants, e.g. $k_{\mathrm{f,S}}$, scalar coupling correction, J, and decoherence rate, k_{D}, are the sums of all second and fourth order contributions, e.g. $J = J_{\mathrm{S}}^{(2)} - J_{\mathrm{T}}^{(2)} + J_{\mathrm{S}}^{(4)} - J_{\mathrm{T}}^{(4)} + J_{\mathrm{ST}}^{(4)}$. These equations have the same form Eqs. (3.83), apart from the additional decoherence term appearing in Eq. (3.93a). This additional decoherence term is what appears in the Jones-Hore reaction superoperator, Eq. (3.7), although $k_{\mathrm{D}} \neq (k_{\mathrm{S}} + k_{\mathrm{T}})/2$ as was originally suggested in Ref. [36].

We need not appeal to the idea of reactions acting as quantum measurements to understand the decoherence term that appears at fourth order. Instead, from the approach presented here, we can understand the decoherence as arising from two contributions. Firstly, the energy shift in the singlet and triplet radical pair states induced by the diabatic coupling at second order fluctuates with time due to the nuclear motion. These fluctuations in the energy gaps lead to the phase of coherences between singlet and triplet states evolving at fluctuating rates, which leads to dephasing between singlet and triplet states. Because the lowest order contribution to the energy shift is second order in the diabatic coupling, the variance in the energy shifts will be fourth order in the diabatic coupling, and therefore the decoherence rate must also only arise at fourth order. The second contribution to the additional decoherence is from diabatic recrossing effects. The fourth order rate kernel contains the effects of recrossing between diabatic surfaces and perturbations to the equilib-

rium density by the reaction process,[133–135] which in this case not only changes the reaction rates, but also gives rise to decoherence. This is because the diabatic coupling is spin selective, and therefore recrossing effectively projects the radical pair spin density operator either onto the singlet or triplet state. Analysis of the classical limit of the decoherence rate in the next chapter will add more detail to this interpretation of the decoherence rate.

As a final point, we can extend the arguments present above in deriving the form of the fourth order quantum master equation to *all* higher orders in the diabatic coupling, within the incoherent rate and field-independent rate approximations. Because the diabatic coupling is spin-selective, no additional types of radical pair spin superoperator appear in higher order quantum master equations, and there will only be higher order contributions to the parameters appearing in these master equations. This means that the quantum master equation accurate to all orders in the diabatic coupling is of the same form as Eqs. (3.93). We should note that the decoherence term only appears at fourth order in the coupling, so the leading order terms in the diabatic coupling are the Haberkorn rection term and the correction to the scalar coupling.

3.4 Concluding remarks

In this chapter, a derivation of the quantum master equation for the radical pair spin density operator from a first principles microscopic description of the radical pair reaction has been presented. Using the Nakajima-Zwanzig equation, coupled with some additional physically motivated approximations, the Haberkorn quantum master equation can be derived. We see from this treatment that the Haberkorn QME is only strictly valid in the limit where the electron transfer reactions can be described as completely non-adiabatic (corresponding to weak diabatic coupling, i.e. in the Fermi's Golden rule limit), and even in this limit a correction to the scalar coupling term in the spin Hamiltonian is required. This correction arises from the spin-selective diabatic coupling and the resulting average energy shift in radical pair spin states.

At higher orders in the diabatic coupling, an additional singlet-triplet decoherence term appears, akin to that which appears in the Jones-Hore quantum measurement based master

equation. This term can be understood as arising from energy gap fluctuations, the reaction process perturbing the singlet and triplet radical pair densities differently, and recrossing effects. But importantly at no point in this derivation is quantum measurement theory invoked, instead the theory is based on the established theory of electron transfer processes in molecular systems. This microscopic perspective on the radical pair master equation offers physical insight in radical pair processes, and shows unambiguously that quantum measurement based theories of radical pair reactions are mostly wrong.

The following two chapters build on this work. In chapter 4 I show how to obtain classical expressions for the radical pair QME parameters, which clarifies their physical meaning and gives a set of tools for assessing when the approximations used to derive them may breakdown. Then in chapter 5 I present a simulations on model radical pair reactions, for which numerically exact quantum dynamics can be calculated, to test the validity of the theory developed here.

Appendix

3.A Appendix: Quasidiabatic representations

In this appendix I will discuss the formal relationship between the adiabatic and quasi-diabatic representations of the total electronic-nuclear Hamiltonian, and thus show that the total system Hamiltonian describing the state population and nuclear dynamics can be written in the form stated at the beginning of this chapter. This is based on the theory presented in Refs.[123],[125] and[136]. Normally when considering a coupled electronic nuclear system, we expand the identity operator on the electronic subspace as

$$\hat{1}_{\mathrm{e}} = \sum_{a} |\varphi_a(\mathbf{R})\rangle_{\mathrm{e}} \langle \varphi_a(\mathbf{R})|_{\mathrm{e}} \tag{3.A.1}$$

where the electronic state $|\varphi_a(\mathbf{R})\rangle_{\mathrm{e}}$ is a function of the space and spin coordinates of the electrons which also depends on the nuclear coordinates $\mathbf{R}$, and the subscript e indicates that the operator only acts on the electronic coordinates. These states are assumed to satisfy

$$\langle \varphi_a(\mathbf{R}) | \varphi_b(\mathbf{R}) \rangle_{\mathrm{e}} = \delta_{ab}. \tag{3.A.2}$$

We could choose this basis to be the adiabatic basis, which satisfies

$$\hat{H}_{\mathrm{e}}(\mathbf{R}) \left| \psi_j(\mathbf{R}) \right\rangle_{\mathrm{e}} = E_{\mathrm{e},j}(\mathbf{R}) \left| \psi_j(\mathbf{R}) \right\rangle_{\mathrm{e}} \tag{3.A.3}$$

where $\hat{H}_{\mathrm{e}}(\mathbf{R})$ is the spin-preserving electronic Hamiltonian for a given nuclear configuration $\mathbf{R}$,

$$\hat{H}_{\mathrm{e}}(\mathbf{R}) = \hat{T}_{\mathrm{e}} + \hat{V}_{\mathrm{ee}} + \hat{V}_{\mathrm{en}}(\mathbf{R}) + V_{\mathrm{nn}}(\mathbf{R}), \tag{3.A.4}$$

but in what follows we will not assume this choice. We note that any set of electronic basis states can be written as

$$|\varphi_a(\mathbf{R})\rangle_{\mathrm{e}} = \sum_j U_{aj}(\mathbf{R}) \left|\psi_j(\mathbf{R})\right\rangle_{\mathrm{e}} \tag{3.A.5}$$

where the matrix formed by the elements $U_{aj}(\mathbf{R})$ is unitary for all $\mathbf{R}$. A general set of electronic basis states $|\varphi_a(\mathbf{R})\rangle_{\mathrm{e}}$ which does not satisfy Eq. (3.A.3) is called a quasi-diabatic basis. We will further assume that the matrix elements $\langle \mathbf{x}|\varphi_a(\mathbf{R})\rangle_{\mathrm{e}}$ are real valued, where $|\mathbf{x}\rangle_{\mathrm{e}} = |\mathbf{r}, \boldsymbol{\sigma}\rangle$ is an electron space-spin projection eigenstate. This is true for eigenstates of the spin preserving electronic Hamiltonian in Eq. (3.A.4), and if $U_{aj}(\mathbf{R})$ is real valued.

We can now define a set of basis functions for the full coupled nuclear-electronic system as

$$|\mathbf{R}, \varphi_a\rangle = |\mathbf{R}\rangle_{\mathrm{n}} |\varphi_a(\mathbf{R})\rangle_{\mathrm{e}} \tag{3.A.6}$$

where $|\mathbf{R}\rangle_{\mathrm{n}}$ is a nuclear position operator eigenstate so these satisfy $\langle \mathbf{R}, \varphi_a|\mathbf{R}', \varphi_b\rangle = \delta_{ab}\delta(\mathbf{R} - \mathbf{R}')$. The full nuclear-electronic system identity operator can be written as

$$\hat{1} = \sum_a \int \mathrm{d}\mathbf{R}\, |\mathbf{R}\rangle_{\mathrm{n}} |\varphi_a(\mathbf{R})\rangle_{\mathrm{e}} \langle \varphi_a(\mathbf{R})|_{\mathrm{e}} \langle \mathbf{R}|_{\mathrm{n}} \tag{3.A.7}$$

and using this we can write the full density operator $\hat{\varrho}$ as

$$\hat{\varrho} = \int \mathrm{d}\mathbf{R} \int \mathrm{d}\mathbf{R}' \sum_{a,b} |\mathbf{R}\rangle_{\mathrm{n}} |\varphi_a(\mathbf{R})\rangle_{\mathrm{e}}\, \varrho_{ab}(\mathbf{R}, \mathbf{R}')\, \langle \varphi_b(\mathbf{R}')|_{\mathrm{e}} \langle \mathbf{R}'|_{\mathrm{n}} \tag{3.A.8}$$

where the matrix elements $\varrho_{ab}(\mathbf{R}, \mathbf{R}')$ as given by

$$\varrho_{ab}(\mathbf{R}, \mathbf{R}') = \langle \mathbf{R}| \langle \varphi_a(\mathbf{R})|\, \hat{\varrho}\, |\varphi_b(\mathbf{R}')\rangle_{\mathrm{e}} |\mathbf{R}'\rangle_{\mathrm{n}}\,. \tag{3.A.9}$$

This system can be mapped onto a new representation with basis states $|a\rangle\,|\mathbf{R}\rangle = |a\rangle \otimes |\mathbf{R}\rangle$, where $|\mathbf{R}\rangle$ is a position eigenstate and $|a\rangle$ is an electronic state which is *independent* of the

nuclear configuration, and these satisfy

$$\langle a|b\rangle = \delta_{ab} \text{ and } \langle \mathbf{R}|\mathbf{R}'\rangle = \delta(\mathbf{R}-\mathbf{R}'). \tag{3.A.10}$$

Operators in the $|\mathbf{R}, \varphi_a\rangle$ basis of the form

$$\hat{\mathcal{A}} = \int \mathrm{d}\mathbf{R} \int \mathrm{d}\mathbf{R}' \sum_{a,b} |\mathbf{R}\rangle_{\mathrm{n}} \, |\varphi_a(\mathbf{R})\rangle_{\mathrm{e}} \, \mathcal{A}_{ab}(\mathbf{R},\mathbf{R}') \, \langle \varphi_b(\mathbf{R}')|_{\mathrm{e}} \, \langle \mathbf{R}'|_{\mathrm{n}} \tag{3.A.11}$$

are mapped onto operators in the new representation with nuclear configuration independent electronic states $\hat{A}$ as

$$\hat{\mathcal{A}} \rightarrow \hat{A} = \int \mathrm{d}\mathbf{R} \int \mathrm{d}\mathbf{R}' \sum_{a,b} |a\rangle\langle b| \, |\mathbf{R}\rangle\langle\mathbf{R}'| \, \mathcal{A}_{ab}(\mathbf{R},\mathbf{R}') \tag{3.A.12}$$

By construction this preserves operator products, so $\hat{\mathcal{A}}\hat{\mathcal{B}} \rightarrow \hat{A}\hat{B}$, and a matrix element of an operator in the original basis $\langle \mathbf{R}, \varphi_a|\hat{\mathcal{A}}|\mathbf{R}', \varphi_b\rangle$ is given by $\langle \mathbf{R}| \, \langle a|\hat{A}|b\rangle|\mathbf{R}'\rangle$. One point to note is that the momentum operator $\hat{\mathcal{P}}_k = (-i\hbar) \, \partial/\partial R_k$ on the original system, maps onto an operator in the new system as follows,

$$\hat{\mathcal{P}}_k \rightarrow \hat{P}_k - i\hbar \int \mathrm{d}\mathbf{R} \sum_{a,b\neq a} |a\rangle\langle b| \, |\mathbf{R}\rangle\langle\mathbf{R}| \left\langle \varphi_a(\mathbf{R}) \middle| \frac{\partial \varphi_b(\mathbf{R})}{\partial R_k} \right\rangle_{\mathrm{e}} \tag{3.A.13}$$

where, in a mild abuse of notation, $\hat{P}_k$ is a nuclear momentum operator on the new representation defined by $\hat{P}_k = (-i\hbar) \, \partial/\partial R_k$. $\langle \varphi_a(\mathbf{R})| \, \partial\varphi_a(\mathbf{R})/\partial R_k \, \rangle_{\mathrm{e}} = 0$ provided $\langle \varphi_a(\mathbf{R})|\varphi_a(\mathbf{R})\rangle_{\mathrm{e}} = 1$ and $\langle \mathbf{x}|\varphi_a(\mathbf{R})\rangle_{\mathrm{e}}$ is real valued.

With this framework, the spin-preserving Hamiltonian in the new representation can be written as

$$\hat{H}_1 = \hat{T}_{\mathrm{n}} + \sum_a V_a(\hat{\mathbf{R}}) \, |a\rangle\langle a| + \sum_{a,b\neq a} \hat{V}_{ab} \, |a\rangle\langle b| \, , \tag{3.A.14}$$

in which the diagonal potential function $V_a(\mathbf{R})$ is given by

$$V_a(\mathbf{R}) = \langle \varphi_a(\mathbf{R})|\hat{H}_{\mathrm{e}}(\mathbf{R})|\varphi_a(\mathbf{R})\rangle_{\mathrm{e}} + \sum_k \frac{\hbar^2}{2M_k} \left\langle \frac{\partial \varphi_a(\mathbf{R})}{\partial R_k} \middle| \frac{\partial \varphi_a(\mathbf{R})}{\partial R_k} \right\rangle_{\mathrm{e}} \tag{3.A.15}$$

and the couplings $\hat{V}_{ab}$ are

$$\hat{V}_{ab} = v_{ab}(\hat{\mathbf{R}}) + \frac{1}{2}\sum_k \left(d^k_{ab}(\hat{\mathbf{R}})\hat{P}_k + \hat{P}_k d^k_{ab}(\hat{\mathbf{R}}) \right) \tag{3.A.16}$$

in which $\hat{\mathbf{R}}$ is the nuclear position operator, and the scalar coupling term is just a function of position given by

$$v_{ab}(\mathbf{R}) = \langle \varphi_a(\mathbf{R}) | \hat{H}_\mathrm{e}(\mathbf{R}) | \varphi_b(\mathbf{R}) \rangle_\mathrm{e} + \sum_k \frac{\hbar^2}{2M_k} \left\langle \frac{\partial \varphi_a(\mathbf{R})}{\partial R_k} \middle| \frac{\partial \varphi_b(\mathbf{R})}{\partial R_k} \right\rangle_\mathrm{e}, \tag{3.A.17}$$

and the derivative couplings $d^k_{ab}(\mathbf{R})$ are

$$d^k_{ab}(\mathbf{R}) = -\frac{i\hbar}{M_k} \left\langle \varphi_a(\mathbf{R}) \middle| \frac{\partial \varphi_b(\mathbf{R})}{\partial R_k} \right\rangle_\mathrm{e}. \tag{3.A.18}$$

By virtue of the fact that $\partial \langle \varphi_a(\mathbf{R}) | \varphi_b(\mathbf{R}) \rangle_\mathrm{e} / \partial R_k = 0$, because $\langle \varphi_a(\mathbf{R}) | \varphi_b(\mathbf{R}) \rangle_\mathrm{e} = \delta_{ab}$, $d^k_{ab}(\mathbf{R}) = d^k_{ba}(\mathbf{R})^*$ and therefore the coupling terms are Hermitian.

If we choose to work in the adiabatic basis, where the states $\left|\psi_j(\mathbf{R})\right\rangle$ are eigenstates of $\hat{H}_\mathrm{e}(\mathbf{R})$ then these terms are divergent at crossing points between the adiabatic surfaces, i.e. when $E_{\mathrm{e},j}(\mathbf{R}) = E_{\mathrm{e},j'}(\mathbf{R})$. This follows from the Hellman-Feynman theorem, as follows

$$\begin{aligned}
0 &= \frac{\partial}{\partial R_k} \left\langle \psi_j(\mathbf{R}) \middle| \hat{H}_\mathrm{e}(\mathbf{R}) \middle| \psi_{j'}(\mathbf{R}) \right\rangle \\
&= \left\langle \psi_j(\mathbf{R}) \middle| \frac{\partial \hat{H}_\mathrm{e}(\mathbf{R})}{\partial R_k} \middle| \psi_{j'}(\mathbf{R}) \right\rangle \\
&\quad + \left\langle \frac{\partial \psi_j(\mathbf{R})}{\partial R_k} \middle| \hat{H}_\mathrm{e}(\mathbf{R}) \middle| \psi_{j'}(\mathbf{R}) \right\rangle + \left\langle \psi_j(\mathbf{R}) \middle| \hat{H}_\mathrm{e}(\mathbf{R}) \middle| \frac{\partial \psi_{j'}(\mathbf{R})}{\partial R_k} \right\rangle \\
&= \left\langle \psi_j(\mathbf{R}) \middle| \frac{\partial \hat{H}_\mathrm{e}(\mathbf{R})}{\partial R_k} \middle| \psi_{j'}(\mathbf{R}) \right\rangle - (E_{\mathrm{e},j}(\mathbf{R}) - E_{\mathrm{e},j'}(\mathbf{R})) \left\langle \psi_j(\mathbf{R}) \middle| \frac{\partial \psi_{j'}(\mathbf{R})}{\partial R_k} \right\rangle
\end{aligned} \tag{3.A.19}$$

so the overlap between $\left|\psi_j(\mathbf{R})\right\rangle$ and $\left|\partial \psi_{j'}(\mathbf{R}) / \partial R_k\right\rangle$ is

$$\left\langle \psi_j(\mathbf{R}) \middle| \frac{\partial \psi_{j'}(\mathbf{R})}{\partial R_k} \right\rangle = \frac{1}{E_{\mathrm{e},j}(\mathbf{R}) - E_{\mathrm{e},j'}(\mathbf{R})} \left\langle \psi_j(\mathbf{R}) \middle| \frac{\partial \hat{H}_\mathrm{e}(\mathbf{R})}{\partial R_k} \middle| \psi_{j'}(\mathbf{R}) \right\rangle \tag{3.A.20}$$

which is clearly divergent at a crossing point between the adiabatic energies. This poses a problem for perturbation theory, because these coupling terms become very large at certain nuclear configurations. As a result in this work we choose to formally work in a quasi-diabatic basis where it is assumed that the coupling terms $\hat{V}_{ab}$ can be treated as perturbations.

In some of the classical limit analysis, it is further assumed that a strict diabatic basis can be found, in which the derivative couplings exactly vanish, so $d^k_{ab} = 0$ (or at least there exists a quasi-diabatic basis in which this is a reasonable approximation) and the diabatic coupling is just a function of the nuclear coordinate operator $\hat{\mathbf{R}}$. The quasi-diabatic representation is not unique, and many procedures for constructing such representations from *ab initio* electronic structure calculations have been proposed[123], but for our purposes here, these details are unimportant. We only need assume that a quasi-diabatic representation exists which can be treated using the approximations outlined in this chapter.

3.B Appendix: The spin Hamiltonian

In this appendix, the origin of terms appearing in spin Hamiltonian are outlined. In particular here we will focus on how the "electron spins" are defined in the radical pair Hamiltonian and how spin mixing terms in the total molecular Hamiltonian, $\hat{H}_2$, give rise to terms in the effective spin Hamiltonian. Here I only consider important spin dependent terms in the full relativistic Hamiltonian, the Zeeman term, the electron spin dipolar term, as well as the nuclear-electron Fermi contact and magnetic dipolar interactions. The derivation of the spin Hamiltonian presented here is only a sketch, primarily based on Refs. [40, 116, 117], since calculating these parameters is not the focus of the work in this thesis. More details on the calculation of these parameters can be found in Refs. [117] and [40].

Before proceeding further, it is useful to now define what precisely is meant by the electron spin operators, $\hat{\mathbf{S}}_1$ and $\hat{\mathbf{S}}_2$, in a radical pair. We normally interpret these as being the electron spin operators for each of the unpaired electrons on the two radicals $D^{\bullet+}$ and $A^{\bullet-}$. Whilst this picture is intuitive, it at first appears to ignore the indistinguishability of the electron spins, by assigning distinguishable spin operators for each radical. This apparent contradiction is resolved by noting that the spin operators are really *effective spin operators*, which do not exactly correspond to distinguishable unpaired electrons on each radical. Instead they can be thought of in terms of the singlet and triplet radical pair states. From these coupled electron spin states, we can define "uncoupled" spin states of the radical

pair as

$$|1,\alpha_1\alpha_2\rangle = |1,\mathrm{T}_+\rangle \tag{3.B.1a}$$

$$|1,\alpha_1\beta_2\rangle = \frac{1}{\sqrt{2}}\left(|1,\mathrm{T}_0\rangle + |1,\mathrm{S}\rangle\right) \tag{3.B.1b}$$

$$|1,\beta_1\alpha_2\rangle = \frac{1}{\sqrt{2}}\left(|1,\mathrm{T}_0\rangle - |1,\mathrm{S}\rangle\right) \tag{3.B.1c}$$

$$|1,\beta_1\alpha_2\rangle = |1,\mathrm{T}_-\rangle\,. \tag{3.B.1d}$$

From these states we can then construct the radical pair spin operators $\hat{\mathbf{S}}_1$ and $\hat{\mathbf{S}}_2$ using their standard definitions in terms of the projection states $|\alpha_i\rangle$ and $|\beta_i\rangle$, for example $\hat{S}_{1z}$ is

$$\hat{S}_{1z} = \frac{1}{2}\sum_{\sigma_2=\alpha_2,\beta_2}\left(|1,\alpha_1\sigma_2\rangle\langle 1,\alpha_1\sigma_2| - |1,\beta_1\sigma_2\rangle\langle 1,\beta_1\sigma_2|\right). \tag{3.B.2}$$

First we will consider the Zeeman term in the spin-mixing Hamiltonian,

$$\hat{H}_{\mathrm{zee}} = \mu_{\mathrm{B}}\sum_{i=1}^{N_{\mathrm{e}}}\mathbf{B}\cdot\left(g_{\mathrm{e}}\hat{\mathbf{s}}_i + \hat{\mathbf{l}}_i\right) = \mu_{\mathrm{B}}\mathbf{B}\cdot\left(g_{\mathrm{e}}\hat{\mathbf{S}} + \hat{\mathbf{L}}\right) \tag{3.B.3}$$

where g_{e} is the free electron g-factor, $\hat{\mathbf{s}}_i$ is a unitless electron spin operator and $\hat{\mathbf{l}}_i$ is a unitless orbital angular momentum operator in a given reference frame, and $\hat{\mathbf{S}}$ and $\hat{\mathbf{L}}$ are the total spin and orbital angular momentum operators. Without loss of generality $\mathbf{B}$ can be chosen to lie along the z axis. Expanding this in a given basis of electronic states, which can be chosen to be eigenstates of $\mathbf{B}\cdot\hat{\mathbf{S}} = B\hat{S}_z$ with eigenvalue $M_a B$, gives

$$\begin{aligned}\hat{H}_{\mathrm{zee}} = {}& \mu_{\mathrm{B}} g_{\mathrm{e}} B\sum_a M_a\,|a\rangle\langle a| \\ & + \mu_{\mathrm{B}}\sum_{ab}\int \mathrm{d}\mathbf{R}\,|\mathbf{R}\rangle\langle\mathbf{R}|\,|a\rangle\langle b|\;\langle\varphi_a(\mathbf{R})|\mathbf{B}\cdot\hat{\mathbf{L}}|\varphi_b(\mathbf{R})\rangle_{\mathrm{e}}\,.\end{aligned} \tag{3.B.4}$$

When projected onto the radical pair diabatic states, the off-diagonal elements of the second term ($a \neq b$) vanish because $\hat{\mathbf{L}}$ only acts on orbital degrees of freedom and the spin states of the four radical pair diabats are all orthogonal. The diagonal elements also vanish because we can choose $\mathbf{B}$ to lie along the z axis, and the angular momentum operator for each electron is $\hat{l}_{iz} = \frac{\hbar}{i}\frac{\partial}{\partial\phi_i}$, but because the wavefunctions can be chosen to be real valued,[120] the expectation value of $\hat{L}_z$ must be zero. So we can neglect the second term in Eq. (3.B.4)

giving rise to a Zeeman contribution to the radical pair Hamiltonian, $\hat{H}_{1\text{s,zee}}$, of the form

$$\hat{H}_{1\text{s,zee}} = \text{Tr}_\text{n}[\hat{\Pi}_1 \hat{H}_\text{zee} \hat{\Pi}_1 \hat{\rho}_{1\text{n}}] = \mu_\text{B} g_\text{e} \mathbf{B} \cdot \hat{\mathbf{S}}_1 + \mu_\text{B} g_\text{e} \mathbf{B} \cdot \hat{\mathbf{S}}_2. \tag{3.B.5}$$

One exception to this is in highly symmetric systems like diatomic radicals (such as superoxide) where there are orbitally degenerate (or near degenerate) radical pair electronic states.[87]

Another important term is the electron spin dipolar coupling term,

$$\hat{H}_\text{dip} = 4\mu_\text{B}^2 \sum_{i=1}^{N_\text{e}} \sum_{j>i}^{N_\text{e}} \left(\frac{1}{\hat{r}_{ij}^3} \left(\hat{\mathbf{s}}_i \cdot \hat{\mathbf{s}}_j - \frac{3(\hat{\mathbf{s}}_i \cdot \hat{\mathbf{r}}_{ij})(\hat{\mathbf{s}}_j \cdot \hat{\mathbf{r}}_{ij})}{\hat{r}_{ij}^2} \right) \right), \tag{3.B.6}$$

where $\hat{\mathbf{r}}_{ij}$ is defined in terms of the electron position operators $\hat{\mathbf{r}}_i$ as $\hat{\mathbf{r}}_{ij} = \hat{\mathbf{r}}_i - \hat{\mathbf{r}}_j$, and $\hat{r}_{ij} = |\hat{\mathbf{r}}_{ij}|$. When this is projected onto the radical pair states, this becomes

$$\begin{aligned} &\hat{\Pi}_1 \hat{H}_\text{dip} \hat{\Pi}_1 = \\ &\sum_{\sigma_1\sigma_2\sigma_1'\sigma_2'} \int \text{d}\mathbf{R}\, |\mathbf{R}\rangle\langle\mathbf{R}|\, \big|1, \sigma_1\sigma_2\big\rangle\big\langle 1, \sigma_1'\sigma_2'\big|\, \left\langle \varphi_{1,\sigma_1\sigma_2}(\mathbf{R}) \middle| \hat{H}_\text{dip} \middle| \varphi_{1,\sigma_1'\sigma_2'}(\mathbf{R}) \right\rangle_\text{e}, \end{aligned} \tag{3.B.7}$$

and when the radicals have non-overlapping spin densities, this can be approximated as

$$\hat{\Pi}_1 \hat{H}_\text{dip} \hat{\Pi}_1 = \hat{\mathbf{S}}_1 \cdot \mathbf{D}(\hat{\mathbf{R}}) \cdot \hat{\mathbf{S}}_2 \tag{3.B.8}$$

where $\mathbf{D}(\hat{\mathbf{R}})$ is a nuclear configuration dependent dipolar coupling tensor (so it is an operator on the nuclear position degrees of freedom). After averaging over the thermal distribution for the radical pair state this becomes

$$\hat{H}_{1\text{s,dip}} = \text{Tr}_\text{n}[\hat{\Pi}_1 \hat{H}_\text{dip} \hat{\Pi}_1 \hat{\rho}_{1\text{n}}] = \hat{\mathbf{S}}_1 \cdot \langle \mathbf{D}(\mathbf{R}) \rangle_1 \cdot \hat{\mathbf{S}}_2. \tag{3.B.9}$$

Here $\langle \cdots \rangle_i = \text{Tr}_\text{n}[\cdots \hat{\rho}_{i\text{n}}]$. For an isotropic system, such as in a solution phase reaction, the average dipolar coupling tensor vanishes, but in anisotropic systems this is not true. For well separated radicals the coupling tensor $\langle \mathbf{D}(\mathbf{R}) \rangle_1$ can often be accurately approximated by treating the radicals as two point dipoles separated by some vector $\mathbf{R}_{12}$.

The nuclear hyperfine coupling term can be treated in much the same way as the electron

spin dipolar coupling term

$$\hat{H}_{\text{hfc}} = 4\mu_{\text{B}}^2 \sum_{i=1}^{N_{\text{e}}} \sum_A \frac{\gamma_A}{\gamma_{\text{e}}} \left(-\frac{8\pi}{3} \hat{\mathbf{s}}_i \cdot \hat{\mathbf{I}}_A \delta(\hat{\mathbf{r}}_{iA}) + \frac{1}{\hat{r}_{iA}^3} \left(\hat{\mathbf{s}}_i \cdot \hat{\mathbf{I}}_A - \frac{3(\hat{\mathbf{s}}_i \cdot \hat{\mathbf{r}}_{iA})(\hat{\mathbf{I}}_A \cdot \hat{\mathbf{r}}_{iA})}{\hat{r}_{iA}^2} \right) \right) \tag{3.B.10}$$

$$= \sum_A \sum_\alpha \hat{V}_{A\alpha}(\hat{\mathbf{R}}_A) \hat{I}_{A\alpha} \tag{3.B.11}$$

where now $\hat{\mathbf{r}}_{iA} = \hat{\mathbf{r}}_i - \hat{\mathbf{R}}_A$ where $\hat{\mathbf{R}}_A$ is the position operator of nucleus A, and $\hat{\mathbf{I}}_A$ is the nuclear spin operator for nucleus A. γ_A and γ_{e} are the gyromagnetic ratios for nucleus A and the free electron. The first term gives rise to the isotropic Fermi contact interaction, and the second term describes the anisotropic magnetic dipole interaction. When projected onto the radical pair states this can be expanded just as the electron dipolar coupling term is above. We assume that there a given nucleus will either be coupled to radical 1 or radical 2, so we can relabel $A \longrightarrow i\ k$ where i indicates the radical index and k is the nuclear index. We can now approximate the matrix elements of $\hat{V}_{ik\alpha}(\mathbf{R}_{ik})$ as

$$\left\langle \varphi_{1\sigma_1\sigma_2}(\mathbf{R}) \middle| \hat{V}_{ik\alpha}(\mathbf{R}_{ik}) \middle| \varphi_{1\sigma_1'\sigma_2'}(\mathbf{R}) \right\rangle_{\text{e}} = \sum_\beta A_{ik,\alpha\beta}(\mathbf{R}) \left\langle 1\sigma_1\sigma_2 \middle| \hat{S}_{i\beta} \middle| 1\sigma_1'\sigma_2' \right\rangle . \tag{3.B.12}$$

So we assume that a nucleus in radical 1 cannot couple different spin states in radical 2 and vice-versa. This is justified because hyperfine interaction decays with distance from the nucleus, and therefore only affects the local electron spin density, so this interaction, to a good approximation, cannot couple electron spin states of the other radical. The tensor $A_{ik,\alpha\beta}(\mathbf{R})$ is the nuclear configuration dependent hyperfine coupling tensor. As such the hyperfine coupling term can be written as

$$\hat{H}_{1\text{s,hfc}} = \sum_{i=1}^{2} \sum_{k=1}^{N_i} \hat{\mathbf{I}}_{ik} \cdot \langle \mathbf{A}_{ik}(\mathbf{R}) \rangle_1 \cdot \hat{\mathbf{S}}_i, \tag{3.B.13}$$

where $\mathbf{A}_{ik}(\hat{\mathbf{R}})$ is the nuclear configuration dependent hyperfine coupling tensor with matrix elements $A_{ik,\alpha\beta}(\mathbf{R}) \left|\mathbf{R}\right\rangle\!\left\langle\mathbf{R}\right|$. In an isotropic system this tensor is proportional to an identity matrix $\left\langle A_{ik,\alpha\beta}(\mathbf{R}) \right\rangle_1 = a_{ik}\delta_{ab}$, but in an anisotropic system this is not true and the full nine-component coupling tensor must be used. This can often be approximated by calculating the hyperfine tensor for a single radical in its equilibrium geometry.

The spin orbit coupling interaction has a more complex effect on the spin Hamiltonian.

For well-separated radicals, which do not contain any atoms with large nuclear charges, to a first approximation there is no direct spin-orbit coupling interaction between the radicals, so we can assume that $\hat{\Pi}_1 \hat{H}_{\text{soc}} \hat{\Pi}_1 = 0$.[137,138] This means that spin orbit coupling has no direct contribution to the radical pair spin Hamiltonian. The spin orbit coupling Hamiltonian does however couple different electronic states, which has two main effects. Firstly spin orbit coupling can give rise to spin orbit coupled charge transfer, where a change in spin state accompanies the electron transfer.[137] It can be shown that this has the same effect in an isotropic system as the spin selective electron transfer on the radical pair evolution, i.e. it adds spin selective reaction terms and scalar coupling terms, only now population is transferred to a different spin state.

The second effect of spin orbit coupling arises from an interplay of the spin orbit interaction and the orbital Zeeman interaction. When these mixed terms are treated at second order using the same treatment as outlined in detail in this chapter, they give rise to an additional terms which are linear in the applied field $\mathbf{B}$. Because these interactions are local, the dominant contributions are to corrections to the single radical Zeeman terms of the form

$$\Delta \hat{H}_{1\text{s,zee}} = \mu_{\text{B}} \mathbf{B} \cdot \langle \mathbf{g}_1 - g_{\text{e}} \mathbf{1} \rangle_1 \cdot \hat{\mathbf{S}}_1 + \mu_{\text{B}} \mathbf{B} \cdot \langle \mathbf{g}_2 - g_{\text{e}} \mathbf{1} \rangle_1 \cdot \hat{\mathbf{S}}_2 \tag{3.B.14}$$

the term $\mathbf{g}_i \equiv \mathbf{g}_i(\mathbf{R})$ is the nuclear configuration dependent g-tensor for radical i. As with the hyperfine interaction, this reduces to a scalar coupling term for an isotropic system, but the full tensor must be used for an anisotropic system. In addition to this contribution to the g-tensors, there are also other contributions that arise from other relativistic contributions to the electronic Hamiltonian. In practice, because the spin-orbit coupling interaction is local, these thermally averaged tensors can be approximated by the tensor in the equilibrium geometry of each radical. Similarly, there will be spin-orbit coupling and other relativistic contributions to the hyperfine coupling interaction and dipolar coupling.[40]

Finally, we can consider additional scalar coupling contributions. There may be a small average energy shift between the singlet and triplet radical pair states due to the direct exchange interaction, although for well separated radicals this will be very small. We can also apply the analysis of the diabatic coupling between the radical pair and product states

to treat the effect of diabatic coupling to other states of the molecule. For states significantly higher in energy than the radical pair state, the population transfer contributions can be ignored and these diabatic couplings give rise to additional contributions to scalar coupling between the radical electron spins, so overall there will be an additional contribution to the spin Hamiltonian of the form

$$\hat{H}_{1\mathrm{s,scal}} = -2\Delta J \hat{\mathbf{S}}_1 \cdot \hat{\mathbf{S}}_2. \tag{3.B.15}$$

Here I have sketched the origin of the important terms of the spin Hamiltonian starting from the full molecular Hamiltonian. In practice these terms are effectively impossible to calculate exactly, so instead they are treated as free parameters, or additional approximations are invoked to estimate them either from computations or available experimental data.

3.C Appendix: Fourth order rate expressions

The expressions for the fourth order contributions to the reaction rate constants, singlet-triplet dephasing rate and scalar electron spin coupling are related to the correlation functions $c^{(2)}_{i\mathrm{S}}(t)$ and $c^{(2)}_{i\mathrm{T}}(t)$, defined in Eq. (3.65) and Eq. (3.71), as well as the three-time correlation functions defined below

$$c^{(4)}_{1\mathrm{S}}(t_0,t_1,t_2) = \mathrm{Tr_n}\left[e^{-\beta\hat{H}_{1\mathrm{n}}}\hat{G}_{\mathrm{S}}(t_0)\hat{G}_{\mathrm{S}}(t_1)^{\dagger}\hat{G}_{\mathrm{S}}(t_2)\hat{G}_{\mathrm{S}}(0)^{\dagger}\right], \tag{3.C.1}$$

$$c^{(4)}_{1\mathrm{T}}(t_0,t_1,t_2) = \mathrm{Tr_n}\left[e^{-\beta\hat{H}_{1\mathrm{n}}}\hat{G}_{\mathrm{T}}(t_0)\hat{G}_{\mathrm{T}}(t_1)^{\dagger}\hat{G}_{\mathrm{T}}(t_2)\hat{G}_{\mathrm{T}}(0)^{\dagger}\right], \tag{3.C.2}$$

where $\hat{G}_{\mathrm{S}}(t) = e^{+i\hat{H}_{1\mathrm{n}}t/\hbar}\hat{f}_{\mathrm{S}}e^{-i\hat{H}_{2\mathrm{n}}t/\hbar}$ and $\hat{G}_{\mathrm{T}}(t) = e^{+i\hat{H}_{1\mathrm{n}}t/\hbar}\hat{f}_{\mathrm{T}}e^{-i\hat{H}_{3\mathrm{n}}t/\hbar}$. The fourth order contribution to the forward singlet rate constant is[135]

$$\begin{aligned} k^{(4)}_{\mathrm{f,S}} = &-\frac{2\Delta_{\mathrm{S}}^4}{\hbar^4 Z_{1\mathrm{n}}}\int_0^{\infty}\mathrm{d}t_0\int_0^{t_0}\mathrm{d}t_1\int_0^{t_1}\mathrm{d}t_2 \\ &\times\Bigg(\mathrm{Re}\left[c^{(4)}_{1\mathrm{S}}(t_0,t_1,t_2)+c^{(4)}_{1\mathrm{S}}(t_2,t_1,t_0)+c^{(4)}_{1\mathrm{S}}(t_1,t_0,t_2)+c^{(4)}_{1\mathrm{S}}(t_2,t_0,t_1)\right] \\ &-2\,\mathrm{Re}\left[c^{(2)}_{1\mathrm{S}}(t_0-t_1)\right]\mathrm{Re}\left[c^{(2)}_{1\mathrm{S}}(t_2)\right]-2\,\mathrm{Re}\left[c^{(2)}_{2\mathrm{S}}(t_0-t_1)\right]\mathrm{Re}\left[c^{(2)}_{2\mathrm{S}}(t_2)\right]\Bigg). \end{aligned} \tag{3.C.3}$$

The fourth order contribution to the back reaction rate, $k^{(4)}_{\mathrm{b,S}}$, is obtained by simply swapping the state indices 1 and 2 in the above expression, and the rate constant triplet expressions are obtained by swapping S for T and the index 2 for 3. The fourth order contribution to the electron spin coupling from the singlet pathway is

$$J^{(4)}_{\mathrm{S}} = -\frac{\Delta_{\mathrm{S}}^4}{2\hbar^3 Z_{1\mathrm{n}}} \int_0^\infty \mathrm{d}t_0 \int_0^{t_0} \mathrm{d}t_1 \int_0^{t_1} \mathrm{d}t_2 \times \left(\mathrm{Im}\left[c^{(4)}_{1\mathrm{S}}(t_0, t_1, t_2) \right] - \mathrm{Im}\left[c^{(2)}_{1\mathrm{S}}(t_0 - t_1) c^{(2)}_{1\mathrm{S}}(t_2) \right] \right). \tag{3.C.4}$$

The fourth order singlet pathway contribution to the singlet-triplet dephasing rate constant is

$$\begin{aligned} k^{(4)}_{\mathrm{D,S}} = \frac{\Delta_{\mathrm{S}}^4}{\hbar^4 Z_{1\mathrm{n}}} \int_0^\infty \mathrm{d}t_0 \int_0^{t_0} \mathrm{d}t_1 \int_0^{t_1} \mathrm{d}t_2 \\ \times \Big(\mathrm{Re}\left[c^{(4)}_{1\mathrm{S}}(t_2, t_1, t_0) + c^{(4)}_{1\mathrm{S}}(t_1, t_0, t_2) + c^{(4)}_{1\mathrm{S}}(t_2, t_0, t_1) \right] \\ - \mathrm{Re}\left[c^{(2)}_{1\mathrm{S}}(t_0 - t_1)^* c^{(2)}_{1\mathrm{S}}(t_2) \right] - 2\,\mathrm{Re}\left[c^{(2)}_{2\mathrm{S}}(t_0 - t_1) \right] \mathrm{Re}\left[c^{(2)}_{2\mathrm{S}}(t_2) \right] \Big). \end{aligned} \tag{3.C.5}$$

Again the triplet contributions can be obtained by swapping S for T in the above expressions. The rate constant expression in Eq. (3.C.3) is consistent with that obtained previously by others – e.g., Golosov and Reichman in Ref. [135]. These expressions are used to obtain numerical results for Model I in chapter 5, where the triple integrals in these expressions are evaluated numerically to calculate the parameters for the fourth order master equations.

The fourth order cross terms for the decoherence rate is given by the following expression,

$$\begin{aligned} k^{(4)}_{\mathrm{D,ST}} = -\frac{\Delta_{\mathrm{S}}^2 \Delta_{\mathrm{T}}^2}{\hbar^4} \int_0^\infty \mathrm{d}t_0 \int_0^{t_0} \mathrm{d}t_1 \int_0^{t_1} \mathrm{d}t_2 \\ \times \Big(\mathrm{Re}\left[c^{(4)}_{1\mathrm{ST}}(t_2, t_1, t_0) + c^{(4)}_{1\mathrm{ST}}(t_1, t_0, t_2) + c^{(4)}_{1\mathrm{ST}}(t_2, t_0, t_1) \right] \\ + \mathrm{Re}\left[c^{(4)}_{1\mathrm{TS}}(t_2, t_1, t_0) + c^{(4)}_{1\mathrm{TS}}(t_1, t_0, t_2) + c^{(4)}_{1\mathrm{TS}}(t_2, t_0, t_1) \right] \\ - \mathrm{Re}\left[c^{(2)}_{1\mathrm{T}}(t_0 - t_1)^* c^{(2)}_{1\mathrm{S}}(t_2) \right] - \mathrm{Re}\left[c^{(2)}_{1\mathrm{S}}(t_0 - t_1)^* c^{(2)}_{1\mathrm{T}}(t_2) \right] \Big). \end{aligned} \tag{3.C.6}$$

where $c_{1\mathrm{ST}}(t_0, t_1, t_2)$ is defined as

$$c_{1\mathrm{ST}}(t_0, t_1, t_2) = \mathrm{Tr}_\mathrm{n}\left[e^{-\beta\hat{H}_{1\mathrm{n}}}\hat{G}_\mathrm{S}(t_0)\hat{G}_\mathrm{S}(t_1)^\dagger\hat{G}_\mathrm{T}(t_2)\hat{G}_\mathrm{T}(0)^\dagger\right], \tag{3.C.7}$$

$c_{1\mathrm{TS}}(t_0, t_1, t_2)$ is obtained by simply swapping the labels S and T. Similarly the cross term contributing to the reactive electron spin coupling at fourth order is

$$\begin{aligned} J^{(4)}_{\mathrm{ST}} = {} & \frac{\Delta_\mathrm{S}^2\Delta_\mathrm{T}^2}{2\hbar^3}\int_0^\infty \mathrm{d}t_0 \int_0^{t_0}\mathrm{d}t_1\int_0^{t_1}\mathrm{d}t_2 \\ & \times\Bigg(\mathrm{Im}\left[c^{(4)}_{1,\mathrm{ST}}(t_2,t_1,t_0) + c^{(4)}_{1,\mathrm{ST}}(t_1,t_0,t_2) + c^{(4)}_{1,\mathrm{ST}}(t_2,t_0,t_1)\right] \\ & - \mathrm{Im}\left[c^{(4)}_{1,\mathrm{TS}}(t_2,t_1,t_0) + c^{(4)}_{1,\mathrm{TS}}(t_1,t_0,t_2) + c^{(4)}_{1,\mathrm{TS}}(t_2,t_0,t_1)\right] \\ & - \mathrm{Im}\left[c^{(2)}_{1,\mathrm{T}}(t_0-t_1)^* c^{(2)}_{1,\mathrm{S}}(t_2)\right] + \mathrm{Im}\left[c^{(2)}_{1,\mathrm{S}}(t_0-t_1)^* c^{(2)}_{1,\mathrm{T}}(t_2)\right]\Bigg). \end{aligned} \tag{3.C.8}$$

All of these fourth order expressions can either be obtained by brute force algebraic manipulations of the multiple commutators, or by using Liouville space diagram techniques as described by Hu & Mukamel in Ref. [139]. Using these techniques one could also obtain expressions for higher order contributions to the quantum master equation parameters, but little is learned from this but patience.

4

The Radical Pair Master Equation: The Classical Limit

In this chapter I will describe how to obtain classical expressions for the radical pair QME terms, which depend only on phase space integrals of functions of the positions and momenta of the nuclei in the radical pair and surrounding medium. These classical expressions offer insight into the physical meaning of the terms appearing in the radical pair master equation, in particular the additional decoherence and the scalar coupling correction.

4.1 The classical limit

In this section I will demonstrate how to obtain expressions for the parameters appearing in the quantum master equations which are valid when the nuclear motions can be treated classically. In this limit the nuclear properties can be described by averages of functions of the classical phase space variables, the momenta $\mathbf{p}$ and positions $\mathbf{q}$ of all nuclei in the system. These classical limit expressions offer transparent physical interpretations of the terms appearing in the spin density operator quantum master equation.

Classical expressions for the master equation parameters can be obtained by taking their expressions in terms of correlation functions of nuclear operators and replacing them with their classical analogues. The classical correlation functions are obtained by replacing the quantum mechanical position $\hat{\mathbf{R}}$ and momentum $\hat{\mathbf{P}}$ operators in the correlation functions with classical phase space variables $\hat{\mathbf{R}} \rightarrow \mathbf{q}$ and $\hat{\mathbf{P}} \rightarrow \mathbf{p}$, apart from in terms of the form $e^{-i\hat{H}_{\text{in}}t}A(\hat{\mathbf{P}},\hat{\mathbf{R}})e^{+i\hat{H}_{\text{in}}t}$ where the nuclear propagator is replaced with the classical

propagator,[140–143]

$$e^{-i\hat{H}_{in}t}A(\hat{\mathbf{P}},\hat{\mathbf{R}})e^{+i\hat{H}_{in}t} \rightarrow e^{\mathscr{L}_i t}A(\mathbf{p},\mathbf{q}). \tag{4.1}$$

The classical Liouvillian $\mathscr{L}_i$ is the Liouvillian corresponding to motion on the diabatic potential $V_i(\mathbf{q})$,

$$\mathscr{L}_i = \{\mathcal{H}_i(\mathbf{p},\mathbf{q}),\ \cdot\ \}, \tag{4.2}$$

where $\{\ \cdot\ ,\ \cdot\ \}$ denotes the classical Poisson bracket and $\mathcal{H}_i(\mathbf{p},\mathbf{q})$ is the classical Hamiltonian obtained from the Hamiltonian $\hat{H}_{in}$ by making the replacement $\hat{\mathbf{R}} \rightarrow \mathbf{q}$ and $\hat{\mathbf{P}} \rightarrow \mathbf{p}$.[140–143] We also replace the quantum mechanical trace in the correlation functions with a phase space integral,

$$\mathrm{Tr}[\ \cdot\ ] \rightarrow \frac{1}{(2\pi\hbar)^f}\int \mathrm{d}\mathbf{p}\int \mathrm{d}\mathbf{q}\,, \tag{4.3}$$

where f is the number of nuclear degrees of freedom, and we replace the nuclear density operators $\hat{\rho}_{in}$ with their classical analogues $\varrho_i(\mathbf{p},\mathbf{q})$,

$$\hat{\rho}_{in} \rightarrow \varrho_i(\mathbf{p},\mathbf{q}) = \frac{e^{-\beta\mathcal{H}_i(\mathbf{p},\mathbf{q})}}{\mathcal{Z}_i}, \tag{4.4}$$

in which the classical partition function $\mathcal{Z}_i$ is[141]

$$\mathcal{Z}_i = \frac{1}{(2\pi\hbar)^f}\int \mathrm{d}\mathbf{p}\int \mathrm{d}\mathbf{q}\, e^{-\beta\mathcal{H}_i(\mathbf{p},\mathbf{q})}. \tag{4.5}$$

For terms of the form $e^{-i\hat{H}_{in}t}A(\hat{\mathbf{P}},\hat{\mathbf{R}})e^{+i\hat{H}_{jn}t}$ where $i \neq j$, we further apply the static approximation by replacing this with[102,139]

$$e^{-i\hat{H}_{in}t}A(\hat{\mathbf{P}},\hat{\mathbf{R}})e^{+i\hat{H}_{jn}t} \rightarrow e^{i(V_j(\mathbf{q})-V_i(\mathbf{q}))t}A(\mathbf{p},\mathbf{q}). \tag{4.6}$$

These classical approximations can be arrived at in a more consistent manner by expressing the correlation functions using the Wigner transform and approximating the resulting expressions by truncating transforms of operator products at their lowest order terms in $\hbar$.[140,141,143] This is detailed in appendix 4.A. These approximations are only strictly valid in the high temperature, short time limit, but here I use them primarily as a tool to aid in

the physical interpretation of the quantum master equation parameters.

4.1.1 Classical second order QME parameters

First we will consider how to apply the classical approximations to simplify the second order parameter expressions. We can do this by approximating the correlation functions, by their classical limits for example $c^{(2)}_{1S}(t)$, is approximated as $c^{(2)}_{1S,cl}(t)$ as follows

$$\begin{aligned}\frac{\Delta_S^2}{Z_{1n}}c^{(2)}_{1S}(t) \approx \frac{\Delta_S^2}{\mathcal{Z}_1}c^{(2)}_{1S,cl}(t) &= \frac{1}{(2\pi\hbar)^f}\int d\mathbf{p}\int d\mathbf{q}\,\varrho_1(\mathbf{p},\mathbf{q})\Delta_S(\mathbf{q})^2 e^{i(V_1(\mathbf{q})-V_2(\mathbf{q}))t/\hbar} \\ &= \left\langle \Delta_S(\mathbf{q})^2 e^{i(V_1(\mathbf{q})-V_2(\mathbf{q}))t/\hbar}\right\rangle_1 .\end{aligned} \tag{4.7}$$

Here we have defined the average over the classical thermal density as

$$\langle\cdots\rangle_i = (2\pi\hbar)^{-f}\int d\mathbf{p}\int d\mathbf{q}\cdots\varrho_i(\mathbf{p},\mathbf{q}), \tag{4.8}$$

and we have further assumed that the diabatic coupling is a purely real function of position $\hat{\Delta}_S = \Delta_S(\hat{\mathbf{R}})$ for simplicity. Recalling that the integrals defining $k^{(2)}_{f,S}$ and $J^{(2)}_S$ (Eqs. (3.69) and (3.72)) implicitly come with the factor of $e^{-\eta t}$ in the integrand and the $\eta \to 0^+$ limit from the definition of the Fourier-Laplace transform, the time integral of this in the expressions for $k^{(2)}_{f,S}$ and $J^{(2)}_S$ can be evaluated analytically using[102]

$$\lim_{\eta\to 0^+}\int_0^\infty dt\, e^{izt-\eta t} = \pi\delta(z) + i\mathsf{P}\frac{1}{z}, \tag{4.9}$$

where $\delta(z)$ is the Dirac delta function, and P here denotes taking the Cauchy principal value. The time integral of $e^{i(V_1(\mathbf{q})-V_2(\mathbf{q}))t/\hbar}$ can therefore be expressed as the following

$$\int_0^\infty dt\,\Delta_S(\mathbf{q})^2 e^{i(V_1(\mathbf{q})-V_2(\mathbf{q}))t/\hbar} = \frac{\hbar^2}{2}\kappa_S(\mathbf{q}) + i2\hbar J_S(\mathbf{q}), \tag{4.10}$$

where $\kappa_S(\mathbf{q})$ is defined as

$$\kappa_S(\mathbf{q}) = \frac{2\pi\Delta_S(\mathbf{q})^2}{\hbar}\delta(V_1(\mathbf{q}) - V_2(\mathbf{q})), \tag{4.11}$$

and $2J_S(\mathbf{q})$ is defined as

$$2J_S(\mathbf{q}) = \mathsf{P}\frac{\Delta_S(\mathbf{q})^2}{V_1(\mathbf{q}) - V_2(\mathbf{q})}. \tag{4.12}$$

These expressions have clear physical interpretations. $\kappa_S(\mathbf{q})$ is just the local Fermi's golden rule transition rate at a given fixed nuclear configuration $\mathbf{q}$.[55] The $2J_S(\mathbf{q})$ term can be interpreted as a local, nuclear configuration $\mathbf{q}$ dependent, second order energy shift. This can be seen by considering a simple system with two states separated in energy by $\Delta E > 0$ and that are coupled by a perturbation of strength V; the energy eigenvalues of this two state system are $\pm\sqrt{\Delta E^2 + 4V^2}/2 \approx \pm(\Delta E/2 + V^2/\Delta E + O(V^4))$. So we see $2J_S(\mathbf{q})$ is the same as the leading order correction term in V in the energy eigenvalues.

Employing the above expression for the classical correlation function, and using Eq. (4.10), we find the classical approximation for the second order forward rate constant to be

$$k^{(2)}_{\mathrm{f,S,cl}} = \langle \kappa_S(\mathbf{q}) \rangle_1 \,. \tag{4.13}$$

The classical rate constant is the Fermi's golden rule rate averaged over nuclear configurations in the thermal equilibrium ensemble on diabatic potential $V_1(\mathbf{q})$, and as such only configurations where the energies of the two diabatic surfaces match, i.e. $V_2(\mathbf{q}) - V_1(\mathbf{q}) = 0$ contribute to the transition rate.[102,144] Similarly the classical expression for the singlet second order contribution to the scalar coupling is

$$2J^{(2)}_{\mathrm{S,cl}} = \langle 2J_S(\mathbf{q}) \rangle_1 \,. \tag{4.14}$$

We can understand the singlet contribution to the scalar coupling in the same way as the classical rate constant; it is simply the local energy shift averaged over the thermal probability density for diabatic potential $V_1(\mathbf{q})$. This shows that, at least when the nuclear motion can be treated classically, the correction to the scalar coupling in the radical pair master equation can be understood as arising from the spin-state selective diabatic coupling generating a thermally averaged shift in the singlet and triplet radical pair states. Analogous classical expressions can also by found for the for the triplet rate constant and scalar coupling contribution.

4.1.2 Classical fourth order QME parameters

This now leads us to consider the fourth order parameters in the quantum master equation. Classical expressions for the fourth order decoherence rates and corrections to the rate

constants can also be obtained in a similar way to the second order parameters. This simply involves applying the approximations given above to the fourth order parameter expressions, the algebra required however is somewhat laborious, so here I will just state the final results.

It is instructive first to analyse the fourth order corrections to the forward rate constant. After applying the classical approximations as described above, the classical fourth order term in the forward singlet rate constant is found to be a sum of two fluctuation correlation functions for $\kappa_S(\mathbf{q})$

$$\begin{aligned} k^{(4)}_{\mathrm{f,S,cl}} = &- \int_0^\infty \mathrm{d}t \left(\left\langle \kappa_S(\mathbf{q}) e^{\mathscr{L}_1 t} \kappa_S(\mathbf{q}) \right\rangle_1 - \langle \kappa_S(\mathbf{q}) \rangle_1 \langle \kappa_S(\mathbf{q}) \rangle_1 \right) \\ &- \int_0^\infty \mathrm{d}t \left(\left\langle \kappa_S(\mathbf{q}) e^{\mathscr{L}_2 t} \kappa_S(\mathbf{q}) \right\rangle_1 - \langle \kappa_S(\mathbf{q}) \rangle_2 \langle \kappa_S(\mathbf{q}) \rangle_1 \right). \end{aligned} \tag{4.15}$$

The $\kappa_S(\mathbf{q})$ arises from diabatic state transitions, and $e^{\mathscr{L}_1 t}$ generates nuclear motion on diabatic potential $V_1(\mathbf{q})$, and likewise $e^{\mathscr{L}_2 t}$ generates nuclear motion on diabatic potential $V_2(\mathbf{q})$. The first term can therefore be interpreted as arising from the process of the diabatic transition removing density from the region where the diabatic surfaces intersect, and the subsequent finite time it takes for nuclear motion driven density fluctuations to replenish the density in the intersection region. The second term represents a transition from diabatic surface 1 to 2, followed by nuclear motion on diabat 2, and then transition back to diabat 1. So the second term in Eq. (4.15) is the recrossing contribution from diffusion back into the intersection region on diabat 2.

We can also apply the classical approximation to derive the classical fourth order contribution to the decoherence rate. For simplicity here I will only consider the singlet contribution and ignore any triplet or mixed singlet-triplet contributions. The classical fourth order decoherence rate is given by

$$\begin{aligned} k^{(4)}_{\mathrm{D,S,cl}} = &\frac{1}{4} \int_0^\infty \mathrm{d}t \left(\left\langle \kappa_S(\mathbf{q}) e^{\mathscr{L}_1 t} \kappa_S(\mathbf{q}) \right\rangle_1 - \langle \kappa_S(\mathbf{q}) \rangle_1 \langle \kappa_S(\mathbf{q}) \rangle_1 \right) \\ &+ \frac{1}{2} \int_0^\infty \mathrm{d}t \left(\left\langle \kappa_S(\mathbf{q}) e^{\mathscr{L}_2 t} \kappa_S(\mathbf{q}) \right\rangle_1 - \langle \kappa_S(\mathbf{q}) \rangle_2 \langle \kappa_S(\mathbf{q}) \rangle_1 \right) \\ &+ \frac{4}{\hbar^2} \int_0^\infty \mathrm{d}t \left(\left\langle J_S(\mathbf{q}) e^{\mathscr{L}_1 t} J_S(\mathbf{q}) \right\rangle_1 - \langle J_S(\mathbf{q}) \rangle_1 \langle J_S(\mathbf{q}) \rangle_1 \right). \end{aligned} \tag{4.16}$$

The first two terms in Eq. (4.16) depend on the local reaction rate, so these can be thought of

as reactive contributions to the decoherence. The first term is $1/4$ of the density fluctuation term in the fourth order rate constant Eq. (4.15). This arises because the reaction process at the intersection of the diabatic surfaces perturbs the singlet nuclear density, but leaves the triplet density unchanged. The result of the different evolution of the singlet and triplet nuclear distributions is that coherence between singlet and triplet states is lost in a time-scale characteristic of the density fluctuations in the intersection region. The second term appearing is $1/2$ of the recrossing term in Eq. (4.15). This appears because the transition projects the density operator onto the singlet spin state, and therefore recrossing cannot restore coherence between singlet and triplet states that is lost in the initial transition. The third term in Eq. (4.16) originates from instantaneous fluctuations in the local energy shift in the singlet radical pair state due to the diabatic coupling, which lead to dephasing between singlet and triplet radical pair states.

4.1.3 The slow energy gap fluctuation approximation

Finally, I will introduce one more approximation, which enables us to analytically sum all order contributions to the rate constant, as well as the reactive contributions to the decoherence rate for a given spin selective pathway. This additional approximation is to assume the energy gap fluctuations and relaxation are much slower the rest of the nuclear degrees of freedom. This is often true when outer-sphere solvent contributions to the energy gap between diabats dominate.[102] As such we can assume that all degrees of freedom other than the energy gap equilibrate rapidly on a given diabatic surface, and thus we can approximate the classical diabatic propagators $e^{\mathscr{L}_i t}$ as

$$e^{\mathscr{L}_i t} \approx \int \mathrm{d}x \, e^{\mathscr{L}_i t} \mathscr{P}_i(x). \tag{4.17}$$

Here $\mathscr{P}_i(x)$ is an operator which acts on functions of the phase space variables $f(\mathbf{p}, \mathbf{q})$ according to

$$\mathscr{P}_i(x) f(\mathbf{p}, \mathbf{q}) = \delta(U_\mathrm{S}(\mathbf{q}) - x) \varrho_i(\mathbf{p}, \mathbf{q}|x) \frac{1}{(2\pi\hbar)^f} \int \mathrm{d}\mathbf{p}' \int \mathrm{d}\mathbf{q}' \, \delta(U_\mathrm{S}(\mathbf{q}') - x) f(\mathbf{p}', \mathbf{q}') \tag{4.18}$$

where $U_S(\mathbf{q})$ is the diabatic energy gap $U_S(\mathbf{q}) = V_1(\mathbf{q}) - V_2(\mathbf{q})$, and $\varrho_i(\mathbf{p},\mathbf{q}|x)$ is $\varrho_i(\mathbf{p},\mathbf{q}|x) = \varrho_i(\mathbf{p},\mathbf{q})/\langle\delta(U_S(\mathbf{q})-x)\rangle_i$.

We can understand this approximation as follows. If $f(\mathbf{p},\mathbf{q})$ is a normalised phase space distribution, then $\frac{1}{(2\pi\hbar)^f}\int d\mathbf{p}'\int d\mathbf{q}'\,\delta(U_S(\mathbf{q}')-x)f(\mathbf{p}',\mathbf{q}')$ is the probability density for observing the energy gap to have a value x given the distribution $f(\mathbf{p},\mathbf{q})$. The term $\delta(U_S(\mathbf{q})-x)\varrho_i(\mathbf{p},\mathbf{q}|x)$ is simply the thermal equilibrium density on diabatic surface i with the energy gap constrained to a value x, so the projection operator $\int dx\,\mathscr{P}_i(x)$ projects a distribution onto a new distribution where all degrees of freedom other than the energy gap are equilibrated. It is straightforward to verify that $\int dx\,\mathscr{P}_i(x)\varrho_i(\mathbf{p},\mathbf{q}) = \varrho_i(\mathbf{p},\mathbf{q})$ and that $\int dx\,\mathscr{P}_i(x)$ is idempotent as required for this projection operator.

This slow energy gap fluctuation approximation is exactly the approximation proposed by Sparpaglione & Mukamel in Ref. [102], which has previously been used to obtain expressions for electron transfer rates interpolating between the non-adiabatic limit, and the limit of high friction along the energy gap coordinate. This is also equivalent to the Zusman theory of electron transfer in the high friction limit.[145–147]

Using this approximation, and after some algebra (outlined in appendix 4.A), we obtain the following expression for the forward singlet rate constant[102]

$$k_{\mathrm{f,S,cl}} = \frac{k^{(2)}_{\mathrm{f,S,cl}}}{1 + k^{(2)}_{\mathrm{f,S,cl}}\tau_{S,1} + k^{(2)}_{\mathrm{b,S,cl}}\tau_{S,2}}. \tag{4.19}$$

$k^{(2)}_{\mathrm{f,S,cl}}$ and $k^{(2)}_{\mathrm{b,S,cl}}$ are the second order classical forward and backward singlet reaction rates. The $\tau_{S,i}$ parameters are given by

$$\tau_{S,i} = \int_0^\infty dt\left(\frac{\left\langle\kappa_S(\mathbf{q})e^{\mathscr{L}_i t}\delta(U_S(\mathbf{q}))\right\rangle_i}{\langle\kappa_S(\mathbf{q})\rangle_i\,\langle\delta(U_S(\mathbf{q}))\rangle_i} - 1\right), \tag{4.20}$$

so these characterise how quickly the nuclear configuration fluctuates on a given diabatic potential around the intersection of the diabatic surfaces. This is the trivial generalisation of the rate constant obtained in Ref. [102] to the case where the diabatic coupling is a function of $\mathbf{q}$. As in the analysis of the fourth order rate above, we can understand the $k^{(2)}_{\mathrm{f,S,cl}}\tau_{S,1}$ term as originating from the finite time it takes fluctuations in the nuclear configuration to give a reactive configuration where $U_S(\mathbf{q}) = 0$, and the $k^{(2)}_{\mathrm{b,S,cl}}\tau_{S,2}$ term can be interpreted

as arising from diabatic recrossing. These effects can be regarded as the result of friction along the energy gap coordinate.[102]

The decoherence rate contains terms, when evaluated in the classical limit, which depend on multi-time correlation functions of the the local reaction rate $\kappa_S(\mathbf{q})$, the local energy shift $\jmath_S(\mathbf{q})$, or some combination of the these. As a simplification, here we ignore the triplet reaction pathway, so we can ignore cross singlet-triplet contributions to decoherence. The purely reactive contribution, which has no dependence on $\jmath_S(\mathbf{q})$, can be analytically summed just like the rate constant using Eq. (4.17). This contribution to the decoherence rate from the singlet pathway is given by

$$k^{\mathrm{r}}_{\mathrm{D,S,cl}} = \frac{k^{(2)}_{\mathrm{f,S,cl}}}{2}\left(\frac{1}{1+\frac{1}{2}k^{(2)}_{\mathrm{f,S,cl}}\tau_{\mathrm{S},1}} - \frac{1}{1+k^{(2)}_{\mathrm{f,S,cl}}\tau_{\mathrm{S},1}+k^{(2)}_{\mathrm{b,S,cl}}\tau_{\mathrm{S},2}}\right). \tag{4.21}$$

This approaches zero in the non-adiabatic limit, $k^{(2)}_{\mathrm{f,S,cl}}\tau_{\mathrm{S},1} \ll 1$ and $k^{(2)}_{\mathrm{b,S,cl}}\tau_{\mathrm{S},2} \ll 1$, and it is bounded above by $k^{(2)}_{\mathrm{f,S,cl}}/2$. In order to assess the relationship between this theory and the Jones-Hore master equation, Eq. (3.7), we should consider the ratio of this term to the forward rate constant,

$$\frac{k^{\mathrm{r}}_{\mathrm{D,S,cl}}}{k_{\mathrm{f,S,cl}}} = \frac{1}{2}\left(\frac{\frac{1}{2}k^{(2)}_{\mathrm{f,S,cl}}\tau_{\mathrm{S},1}+k^{(2)}_{\mathrm{b,S,cl}}\tau_{\mathrm{S},2}}{1+\frac{1}{2}k^{(2)}_{\mathrm{f,S,cl}}\tau_{\mathrm{S},1}}\right). \tag{4.22}$$

As expected, in the non-adiabatic limit, where $k^{(2)}_{\mathrm{f,S,cl}}\tau_{\mathrm{S},1} \ll 1$ and $k^{(2)}_{\mathrm{b,S,cl}}\tau_{\mathrm{S},2} \ll 1$, $k^{\mathrm{r}}_{\mathrm{D,S,cl}}/k_{\mathrm{f,S,cl}}$ approaches zero. In the adiabatic limit, where the timescale of fluctuations in the energy gap controls the rate, so $k^{(2)}_{\mathrm{f,S,cl}}\tau_{\mathrm{S},1} \gg 1$, this becomes

$$\frac{k^{\mathrm{r}}_{\mathrm{D,S,cl}}}{k_{\mathrm{f,S,cl}}} \simeq \frac{1}{2}\left(1+\frac{2k^{(2)}_{\mathrm{b,S,cl}}\tau_{\mathrm{S},2}}{k^{(2)}_{\mathrm{f,S,cl}}\tau_{\mathrm{S},1}}\right). \tag{4.23}$$

In this limit the additional decoherence rate is bounded below by $1/2$, which is the Jones-Hore prediction. When recrossing effects are small, corresponding to when $k^{(2)}_{\mathrm{b,S,cl}}\tau_{\mathrm{S},2} \ll k^{(2)}_{\mathrm{f,S,cl}}\tau_{\mathrm{S},1}$, the reactive contribution to the decoherence rate is exactly the Jones-Hore prediction. In this limit only fluctuations in the density on the radical pair diabatic surface created by the reaction contribute to the decoherence, and there are no recrossing effects. However recrossing effects and fluctuations in the local energy shift will mean that in this limit the

Jones-Hore prediction of $k_{\mathrm{D}} = k_{\mathrm{f,S}}/2$ will be a lower bound on the full decoherence rate in the adiabatic limit.

4.2 The harmonic approximation

In the previous sections I have derived the general form of the radical pair quantum master equation, and given expressions for the parameters appearing in this expression which are valid when the nuclear motion can be treated classically. To gain further insight, we can apply the Marcus-Hush theory for the electron transfer rate,[126,127] and Zusman theory, its extension to the high friction adiabatic limit,[102,145–147] to obtain approximate expressions for the energy shift contributions, e.g. $2J_{\mathrm{S}}$, and reactive contributions to the decoherence rate e.g. $k^{\mathrm{r}}_{\mathrm{D,S}}$. This theory is expected to be valid when the outer-sphere contribution to the reorganisation energy of the electron transfer is dominant, since this is normally controlled by low frequency collective motions of the solvent, or when the dominant inner-sphere contributions to the reorganisation energy come from vibrational modes which can be treated classically, i.e. when $\hbar\omega < k_{\mathrm{B}}T$.[126,127,145,146]

4.2.1 Marcus-Hush theory

Here we only consider contributions from the singlet reaction path, but the results generalise trivially to the triplet reaction path contributions. Within Marcus-Hush theory, we treat the diabatic potentials for the radical pair and product electron transfer states as a set of shifted Harmonic oscillator potentials,[148]

$$V_1(\mathbf{q}) = \sum_{k=1}^{f} \frac{1}{2} m_k \omega_k^2 q_k^2 + c_k q_k \tag{4.24a}$$

$$V_2(\mathbf{q}) = \sum_{k=1}^{f} \frac{1}{2} m_k \omega_k^2 q_k^2 - c_k q_k - \epsilon_{\mathrm{S}}, \tag{4.24b}$$

where m_k and ω_k are the mass and angular frequency of oscillator k, c_k is the strength of the coupling for a particular oscillator to the electron transfer process. ϵ_{S} is the bias of the electron transfer, which for this model is the negative of the free energy change of reaction $\Delta_{\mathrm{r}}G$. The reorganisation energy for the electron transfer is the difference in energy

is defined as

$$\lambda_{\mathrm{S}} = \sum_{k=1}^{f} \frac{2c_k^2}{m_k \omega_k^2}. \tag{4.25}$$

We further make the Condon approximation, within which the diabatic coupling is treated as a constant $\Delta_{\mathrm{S}}(\mathbf{q}) \equiv \Delta_{\mathrm{S}}$. From this, we arrive at the following expression for the classical correlation function,[148]

$$\frac{\Delta_{\mathrm{S}}^2}{\mathcal{Z}_1} c_{1\mathrm{S,cl}}^{(2)}(t) = \Delta_{\mathrm{S}}^2 e^{i(\epsilon_{\mathrm{S}} - \lambda_{\mathrm{S}})t/\hbar - \lambda_{\mathrm{S}} k_{\mathrm{B}} T (t/\hbar)^2}. \tag{4.26}$$

This gives the second order rate constant,[126,127,148]

$$k_{\mathrm{f,S,cl}}^{(2)} = \frac{\Delta_{\mathrm{S}}^2}{\hbar} \sqrt{\frac{\pi}{\lambda_{\mathrm{S}} k_{\mathrm{B}} T}} e^{-(\lambda_{\mathrm{S}} - \epsilon_{\mathrm{S}})^2 / 4\lambda_{\mathrm{S}} k_{\mathrm{B}} T} \tag{4.27}$$

which is well-know Marcus-Hush expression for the electron transfer rate constant. The corresponding expression for the second order energy shift is[34]

$$2J_{\mathrm{S,cl}}^{(2)} = \frac{\Delta_{\mathrm{S}}^2}{\sqrt{\lambda_{\mathrm{S}} k_{\mathrm{B}} T}} D_+ \left(\frac{\epsilon_{\mathrm{S}} - \lambda_{\mathrm{S}}}{\sqrt{4\lambda_{\mathrm{S}} k_{\mathrm{B}} T}} \right), \tag{4.28}$$

where $D_+(x)$ is the Dawson function, which is defined as

$$D_+(x) = e^{-x^2} \int_0^x e^{z^2} \, \mathrm{d}z \, . \tag{4.29}$$

$D_+(x)$ is an odd function which is positive for $x > 0$, so in the Marcus normal regime, where $\epsilon_{\mathrm{S}} < \lambda_{\mathrm{S}}$ the energy shift is negative, but it changes sign in the inverted regime where $\epsilon_{\mathrm{S}} > \lambda_{\mathrm{S}}$. This is because in the normal regime, the singlet product diabat is above the radical pair diabat at the radical pair minimum energy geometry, so the singlet radical pair energy is shifted down. In the inverted regime, this situation is reversed, and therefore so is the energy shift.

In the high activation energy limit, $E_{\mathrm{a}}/k_{\mathrm{B}}T = (\lambda_{\mathrm{S}} - \epsilon_{\mathrm{S}})^2 / 4\lambda_{\mathrm{S}} k_{\mathrm{B}} T \gg 1$, this is asymptotically equal to

$$2J_{\mathrm{S,cl}}^{(2)} = \frac{\Delta_{\mathrm{S}}^2}{\epsilon_{\mathrm{S}} - \lambda_{\mathrm{S}}} + \frac{2\Delta_{\mathrm{S}}^2 \lambda_{\mathrm{S}} k_{\mathrm{B}} T}{(\epsilon_{\mathrm{S}} - \lambda_{\mathrm{S}})^3} + O((E_{\mathrm{a}}/k_{\mathrm{B}}T)^{-5/2}). \tag{4.30}$$

The first term is just the second order energy shift evaluated at the minimum energy

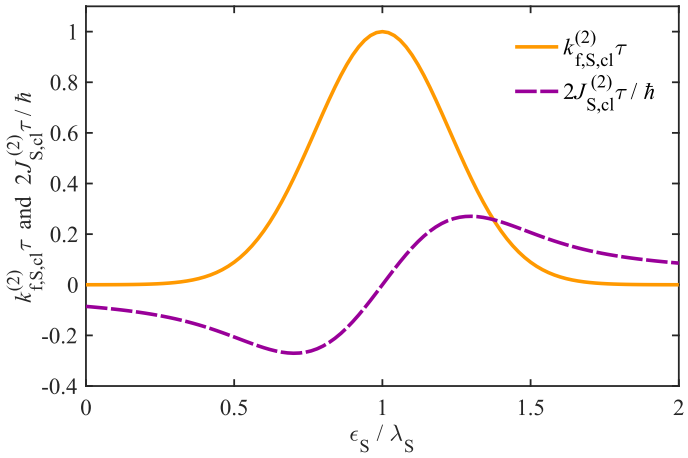

Figure 4.1: An illustration of the Marcus-Hush theory singlet rate constant and singlet contribution to the scalar coupling as a function of ϵ_S/λ_S for $\lambda_S = 1$ eV and $T = 300$ K. Here $\tau^{-1} = \Delta_S^2\sqrt{\pi/(\hbar^2\lambda_S k_B T)}$.

geometry of $V_1(\mathbf{q})$ where the energy gap is $\epsilon_S - \lambda_S$, and the second term gives a correction from thermal fluctuations around the minimum energy geometry. It should be noted that the first term corresponds exactly to the well known form Eq. (3.84) for $2J$.[26,67,129–132] In the highly activated limit, the energy shift term remains finite, so this term will dominate over the decay rate in the spin dynamics. In the activationless limit $E_a/k_BT \ll 1$, i.e. when the reaction rate constant is near its maximum, we have the following asymptotic expansion of $2J^{(2)}_{\mathrm{S,cl}}$,

$$2J^{(2)}_{\mathrm{S,cl}} = \frac{\Delta_S^2(\epsilon_S - \lambda_S)}{2\lambda_S k_B T} + O((E_a/k_BT)^2) \tag{4.31}$$

We see that when the crossing point of the diabatic surfaces is within the thermal fluctuation $\sqrt{2}\lambda_S k_B T$ in the energy gap from the minimum energy on diabat 1, there is a cancellation of positive and negative energy shifts. So when the activation energy is exactly zero, the net energy shift will also be zero.

To illustrate this behaviour of the Marcus-Hush theory expressions for the rate constant and energy shift, in Fig. 4.1 I show the behaviour of these parameters as a function of ϵ_S/λ_S, as discussed above close to the maximum in the rate constant, the energy shift is zero, but the rate constant drops rapidly as ϵ_S/λ_S moves away from 1, whereas $2J^{(2)}_{\mathrm{S,cl}}$ decays much more slowly.

The Marcus-Hush expression for the correlation function, Eq. (4.26), can also be used to derive a criterion for when the incoherent rate approximation is likely to break down. Based on the analysis of the Markovian approximation in the previous chapter, the Markovian

approximation breaks down when $\int_0^\infty t\mathcal{K}(t)\,\mathrm{d}t$ becomes large (remembering this is overall a unitless quantity). The terms in this that act on the radical pair density operator are proportional to

$$\begin{aligned}\frac{\Delta_{\mathrm{S}}^2}{\hbar^2\mathcal{Z}_1}\int_0^\infty t c_{1\mathrm{S,cl}}^{(2)}(t)\,\mathrm{d}t = \frac{\Delta_{\mathrm{S}}^2}{2\lambda_{\mathrm{S}}k_{\mathrm{B}}T}\left(1-\frac{\epsilon_{\mathrm{S}}-\lambda_{\mathrm{S}}}{\sqrt{\lambda_{\mathrm{S}}k_{\mathrm{B}}T}}D_+\left(\frac{\epsilon_{\mathrm{S}}-\lambda_{\mathrm{S}}}{\sqrt{4\lambda_{\mathrm{S}}k_{\mathrm{B}}T}}\right)\right)\\ + i\frac{\Delta_{\mathrm{S}}^2\sqrt{\pi}(\epsilon_{\mathrm{S}}-\lambda_{\mathrm{S}})}{4\sqrt{(\lambda_{\mathrm{S}}k_{\mathrm{B}}T)^3}}e^{-(\epsilon_{\mathrm{S}}-\lambda_{\mathrm{S}})^2/4\lambda_{\mathrm{S}}k_{\mathrm{B}}T}.\end{aligned} \tag{4.32}$$

If the absolute value of this is small, then the incoherent rate approximation will be valid. Using this, in the highly activated limit the incoherent rate approximation will be valid if

$$\left|\frac{\Delta_{\mathrm{S}}^2}{(\epsilon_{\mathrm{S}}-\lambda_{\mathrm{S}})^2}\right| \ll 1, \tag{4.33}$$

and in the activationless limit the validity criterion for the incoherent rate approximation is

$$\left|\frac{\Delta_{\mathrm{S}}^2}{4\lambda_{\mathrm{S}}k_{\mathrm{B}}T}\left(2+\frac{i\sqrt{\pi}(\epsilon_{\mathrm{S}}-\lambda_{\mathrm{S}})}{\sqrt{\lambda_{\mathrm{S}}k_{\mathrm{B}}T}}\right)\right| \ll 1. \tag{4.34}$$

In both limits, the approximation breaks down if $\Delta_{\mathrm{S}}/\lambda_{\mathrm{S}}$ becomes large. This makes physical sense, because when the diabatic coupling strength becomes larger than the reorganisation energy, the coherences between different electron transfer states become larger and longer lived, and because these are discarded by the projection superoperator $\mathcal{P}$ in this treatment, the dynamics of $\mathcal{P}\hat{\rho}(t)$ become increasingly non-Markovian.

Using the Marcus-Hush expression for $c_{1\mathrm{S,cl}}^{(2)}(t)$, we can also assess when the field-independent rate approximation may break down. This approximation relies on the time-scale of spin dynamics generated by $\hat{H}_{1\mathrm{s}}$ being much longer than the time-scale of the nuclear motion, which in the second order case, corresponds to the decay time of $c_{1\mathrm{S}}^{(2)}(t)$ being much shorter than the spin dynamics time-scale $\hbar/\|\hat{H}_{1\mathrm{s}}\|$. The decay time of the Marcus-Hush expression for $c_{1\mathrm{S,cl}}^{(2)}(t)$ is $\hbar/\sqrt{\lambda_{\mathrm{S}}k_{\mathrm{B}}T}$, so the field-independent rate approximation will be valid if,

$$\frac{\|\hat{H}_{1\mathrm{s}}\|}{\sqrt{\lambda_{\mathrm{S}}k_{\mathrm{B}}T}} \ll 1. \tag{4.35}$$

This criterion will almost invariably hold true.

4.2.2 Zusman theory

We can also apply the Marcus-Hush model for the potential energies, together with the Zusman theory approximation that the thermal fluctuations and dissipation of the energy gap are Markovian and the correlation function decays exponentially,[102,145–147]

$$\left\langle U_{\mathrm{S}}(\mathbf{q}) e^{\mathscr{L}_i t} U_{\mathrm{S}}(\mathbf{q}) \right\rangle_i = \left(\left\langle U_{\mathrm{S}}(\mathbf{q})^2 \right\rangle_i - \langle U_{\mathrm{S}}(\mathbf{q}) \rangle_i^2 \right) e^{-t/\tau_{\mathrm{S}}} + \langle U_{\mathrm{S}}(\mathbf{q}) \rangle_i^2 , \tag{4.36}$$

to evaluate approximate expressions for the rate constants and decoherence rates. This approximation is valid when the energy gap coordinate can be treated as an over-damped harmonic oscillator, such as when the solvent can be treated as a continuum dielectric with a Debye type dielectric response.[102] When this is combined with the slow energy gap fluctuation approximation, Eq. (4.17), we obtain the Zusman theory expression for the rate constants. Within this theory we can also find expressions for the decoherence rate contributions, which only depend on the Marcus-Hush theory parameters, $\epsilon_{\mathrm{S}}, \lambda_{\mathrm{S}}$ and Δ_{S}, and one additional parameter, the energy gap fluctuation correlation time τ_{S}.

The reactive contributions to the decoherence rate, and the higher order contributions to the rate constant depend on the parameters $\tau_{\mathrm{S},i}$ defined in Eq. (4.20), which within the above approximations are given by[146,147]

$$\tau_{\mathrm{S},i} = \tau_{\mathrm{S}} \left(\ln(2) + \frac{(\epsilon_{\mathrm{S}} + (-1)^i \lambda_{\mathrm{S}})^2}{2\lambda_{\mathrm{S}} k_{\mathrm{B}} T} {}_2F_2 \left(1, 1; \frac{3}{2}, 2; \frac{(\epsilon_{\mathrm{S}} + (-1)^i \lambda_{\mathrm{S}})^2}{4\lambda_{\mathrm{S}} k_{\mathrm{B}} T} \right) \right), \tag{4.37}$$

where ${}_2F_2(a_1, a_2; b_1, b_2; x)$ is a generalised hypergeometric function. The derivation of this is given in Refs. [146] and [147]. This is shows that $\tau_{\mathrm{S},1}$ ($\tau_{\mathrm{S},2}$) is just a function of the the activation energy for the forward (backward) reaction relative to thermal energy $k_{\mathrm{B}}T$. In the high activation energy limit the parameter $k^{(2)}_{\mathrm{f,S,cl}} \tau_{\mathrm{S},1}$ is given by

$$k^{(2)}_{\mathrm{f,S,cl}} \tau_{\mathrm{S},1} = \frac{2\pi \Delta_{\mathrm{S}}^2 \tau_{\mathrm{S}}}{\hbar} \frac{1}{|\epsilon_{\mathrm{S}} - \lambda_{\mathrm{S}}|} + O((E_{\mathrm{a}}/k_{\mathrm{B}}T)^{-3/2}) \tag{4.38}$$

and in the low activation energy limit this is given by

$$k^{(2)}_{\mathrm{f,S,cl}} \tau_{\mathrm{S},1} = \frac{\Delta_{\mathrm{S}}^2 \tau_{\mathrm{S}}}{\hbar} \sqrt{\frac{\pi}{\lambda_{\mathrm{S}} k_{\mathrm{B}} T}} \left(\ln(2) + (2 - \ln(2)) \frac{(\epsilon_{\mathrm{S}} - \lambda_{\mathrm{S}})^2}{4\lambda_{\mathrm{S}} k_{\mathrm{B}} T} \right) + O((E_{\mathrm{a}}/k_{\mathrm{B}}T)^2). \tag{4.39}$$

The expressions for $k^{(2)}_{\mathrm{b,S,cl}}\tau_{\mathrm{S},2}$ in these limits can be found by replacing ϵ_{S} with $-\epsilon_{\mathrm{S}}$ in the above expressions. It can be shown numerically that the function

$$f(x) = e^{-x}\left(\ln(2) + 2x\ {}_2F_2\left(1, 1; 3/2, 2; x\right)\right)$$

has a maximum at $x_0 \approx 1.41769$ with a value of $f(x_0) \approx 1.35136$, so $k^{(2)}_{\mathrm{f,S,cl}}\tau_{\mathrm{S},1}$ and $k^{(2)}_{\mathrm{b,S,cl}}\tau_{\mathrm{S},2}$ are bounded above by

$$k^{(2)}_{\mathrm{f,S,cl}}\tau_{\mathrm{S},1}, k^{(2)}_{\mathrm{b,S,cl}}\tau_{\mathrm{S},2} \leq \frac{\Delta_{\mathrm{S}}^2\tau_{\mathrm{S}}}{\hbar}\sqrt{\frac{\pi}{\lambda_{\mathrm{S}}k_{\mathrm{B}}T}}f(x_0). \tag{4.40}$$

These expressions give simple criteria for when we expect to see large reactive contributions to the decoherence rates within the Zusman theory of electron transfer.

Zusman theory can also be used to evaluate the fourth order local energy shift fluctuation contribution to the decoherence rate, which I denote $k^{J(4)}_{\mathrm{D,S,cl}}$. It is possible to evaluate this in two cases: the activationless case and the limit of high activation energy. In the activationless case, using the results in Refs. [102], [146] and [147], $k^{J(4)}_{\mathrm{D,S,cl}}$ can be evaluated as

$$k^{J(4)}_{\mathrm{D,S,cl}} = \frac{G}{2}\frac{\Delta_{\mathrm{S}}^4\tau_{\mathrm{S}}}{\hbar^2\lambda_{\mathrm{S}}k_{\mathrm{B}}T}, \tag{4.41}$$

where G is Catalan's constant, which has a numerical value of $G \approx 0.915966$. In the high activation energy limit we can approximate $2J(\mathbf{q})$ in Eq. (4.16) by

$$2J(\mathbf{q}) \approx \frac{\Delta_{\mathrm{S}}^2}{\langle U_{\mathrm{S}}(\mathbf{q})\rangle_1}\left(1 - \frac{\left(U_{\mathrm{S}}(\mathbf{q}) - \langle U_{\mathrm{S}}(\mathbf{q})\rangle_1\right)}{\langle U_{\mathrm{S}}(\mathbf{q})\rangle_1}\right), \tag{4.42}$$

if the mean fluctuation in the energy gap is much smaller than the average energy gap. From this we obtain the following approximation for $k^{J(4)}_{\mathrm{D,S,cl}}$,

$$k^{J(4)}_{\mathrm{D,S,cl}} = \frac{2\Delta_{\mathrm{S}}^4\lambda_{\mathrm{S}}k_{\mathrm{B}}T\tau_{\mathrm{S}}}{\hbar^2(\epsilon_{\mathrm{S}} - \lambda_{\mathrm{S}})^4}. \tag{4.43}$$

Interestingly in the activationless case, fluctuations in the energy gap, $\left\langle\left(U_{\mathrm{S}}(\mathbf{q}) - \langle U_{\mathrm{S}}(\mathbf{q})\rangle_1\right)^2\right\rangle_1 = 2\lambda_{\mathrm{S}}k_{\mathrm{B}}T$, decrease the energy shift fluctuation contribution to the decoherence rate. This is because in this case the average energy gap is zero, so larger fluctuations in the energy gap lead to a smaller fluctuation in the energy shift, because the local energy shift depends on $1/U_{\mathrm{S}}(\mathbf{q})$. Conversely in the high activation limit, larger energy gap fluctuations mean

smaller $U_S(\mathbf{q})$ are sampled, and therefore larger fluctuations in the energy gap lead to larger fluctuations in the local energy shift, giving rise to a faster decoherence rate.

4.3 Discussion

The classical limit analysis presented here offers clear physical insight into the origins of the terms appearing in the radical pair quantum master equations. For example the origin of the second order scalar coupling correction can be understood as a thermally averaged local second order energy shift. Similarly the classical analysis of the decoherence term shows that the singlet-triplet decoherence rate has three different contributions: 1) the reaction spin-selectively perturbs the nuclear distribution, 2) dynamical recrossing projects the spin density onto a particular spin state, and 3) fluctuations in the local energy shift lead to singlet-triplet dephasing. This analysis showed that in the limit of high friction along the energy gap coordinate, the decoherence rate will be bounded below by the Jones-Hore prediction, although due to recrossing effects and local energy shift fluctuations, the real decoherence rate in this limit will almost always be higher than this bound.

In the previous two sections I have also presented expressions for contributions to the scalar coupling and decoherence rate from reactive pathways, derived from the Marcus-Hush and Zusman theories of electron transfer rates. Owing to the simplicity of the underlying theory, it is unreasonable to expect that these theories will be quantitatively predictive of these terms in the quantum master equation. However, they do provide a simple tool for qualitative examination of the relative importance of different contributions to the decoherence rate and scalar coupling. In particular they predict that Jones-Hore-like decoherence will occur when the energy gap fluctuations become slower. For example, for reactions in water we can use this theory to predict when this occurs. In liquid water, energy gap fluctuations do decay approximately exponentially in time according to continuum dielectric theory,[102,145] with a time constant $\hbar/\tau_S \approx 10\ \mathrm{cm}^{-1} hc$,[149] and therefore, according to Eq. (4.40), we would expect fourth order effects to become important when $\Delta_S^2/\sqrt{\lambda_S k_B T} \gtrsim 20\ \mathrm{cm}^{-1} hc$.

In certain well-controlled experiments it may be possible to test the predictions of

Marcus-Hush and Zusman theory for the radical pair QME parameters. For example in rigid donor-acceptor dyads which form radical pairs on photo-excitation, with one dominant spin-selective recombination pathway. To date, many such examples of molecules with these properties have been synthesised.[26,27,48,66,67,131,150] In these systems the decoherence rate, spin state lifetime and scalar coupling can be measured by EPR spectroscopy[109,151] or magnetic field effects in transient absorption measurements.[48,51,150] For a molecule with a rigid molecular structure, in which outer-sphere contributions dominate the electron transfer reorganisation energies, the Marcus-Hush and Zusman theories can be expected to give accurate predictions,[126,127,145] and the recombination rate, decoherence rate and scalar coupling can all be predicted using the above formulae. In particular the scalar coupling and decoherence rates have particular functional dependences on temperature and the reorganisation energies, both of which can be controlled experimentally by changing the experimental temperature or changing solvent polarity.[102,145]

Typically the solvent viscosity, and therefore τ_S has an inverse Arrhenius dependence on temperature Ae^{+E_a/k_BT},[152] so for an activated electron transfer, one may expect a transition from Marcus-Hush behaviour of the decoherence rate $(A/\sqrt{T})e^{-E_a/k_BT}$ at high temperatures, where the non-adiabatic rate dominates decoherence, to a situation where energy gap fluctuations dominate, which would have a ATe^{+E_a/k_BT} type temperature dependence. Similarly Marcus-Hush theory predicts that $2JT^{1/2}$ would be proportional to $T^{-1/2}$ at high temperatures and $T^{1/2}$ at low temperatures.

The Marcus-Hush theory also suggests when the incoherent rate, and field independent rate approximations may break down, at which point any master equation resembling the Haberkorn master equation can be expected to break down. The criteria for these break downs are given in Eq. (4.32) and Eq. (4.35). In both cases for very large diabatic couplings, or very low temperatures and reorganisation energies one may see these approximations failing. It should be noted that for most condensed phase electron transfer reactions, the reorganisation energy will be between ~ 0.1 eV and ~ 2 eV,[124] whilst the diabatic coupling will be around $\sim 10^{-2}$ eV for short range electron transfers, and much smaller for longer range electron transfer reactions mediated by superexchange interactions.[124] So based on Eq. (4.32) we can expect the incoherent rate approximation to be valid almost universally

for electron transfer reactions in solution at room temperature.

Let us now consider the possibility of the field independent rate approximation breaking down. At large applied field strengths the Δg mechanism dominates, causing transitions between S and T_0 states at a frequency of $\Delta g B \mu_B / 2\hbar$, and if this frequency is larger than $\sqrt{\lambda_S k_B T}/\hbar$ then the field-independent rate approximation will break down. For a reaction at 300 K with a (relatively low) reorganisation energy of $\lambda_S = 0.1$ eV, this occurs when $\Delta g B \gtrsim 1000$ T. For organic radicals $\Delta g \sim 10^{-3}$, so this breakdown would occur at large field strengths larger than 10^6 T. This is far beyond the maximum fields used in experiments of around 10 T, so the field independent rate approximation is likely to hold universally.

A final comment that I will make here is that the classical QME parameter expressions given here involve simple thermal averages of position dependent observables, and their time correlation functions. This means that these can in principle be calculated from classical molecular dynamics simulations, given some model for the potential energy surfaces, in exactly the same way as electron transfer rate constants are routinely calculated.[123,124,153–156] This opens the doorway to investigating radical pair reactions using *ab initio* methods, which may offer new insights into radical pair processes that are difficult to investigate experimentally.

4.4 Concluding remarks

In the next chapter, these expressions for the validity of the perturbative radical pair master equations will be used to rationalise the results of numerical tests on models of radical pair reactions where the potential energy surfaces are treated as harmonic. In such models it is possible to perform numerically exact quantum dynamical simulations for comparison.

Appendix

4.A Appendix: Classical rate expressions

Here a derivation of the classical spin coupling parameter expressions will be presented, based primarily on Refs. [102] and [140–143]. I will start by introducing the Wigner transform for the nuclear degrees of freedom. For an operator on the nuclear degrees of freedom $\hat{A}$ the Wigner transform is a mapping from the quantum mechanical operator to a function $A^{\mathrm{W}}(\mathbf{p}, \mathbf{q})$ of classical phase space variables, defined by

$$A^{\mathrm{W}}(\mathbf{p}, \mathbf{q}) = \mathrm{Tr}_{\mathrm{n}}[\hat{\Delta}(\mathbf{p}, \mathbf{q})\hat{A}], \tag{4.A.1}$$

where the operator $\hat{\Delta}(\mathbf{p}, \mathbf{q})$ is given by

$$\hat{\Delta}(\mathbf{p}, \mathbf{q}) = \int \mathrm{d}\mathbf{y}\, e^{-i\mathbf{p}\cdot\mathbf{y}/\hbar} \left|\mathbf{q} + \frac{\mathbf{y}}{2}\right\rangle\!\left\langle \mathbf{q} - \frac{\mathbf{y}}{2}\right|, \tag{4.A.2}$$

where the integral is over all positions $\mathbf{y}$, and $|\mathbf{x}\rangle$ denotes a position state for all f nuclear degrees of freedom, in which the nuclear configuration is described by the vector $\mathbf{x}$. It is straightforward to show that the Wigner transform maps traces of products of operators $\hat{A}$ and $\hat{B}$ onto phase space integrals of the Wigner functions $A^{\mathrm{W}}(\mathbf{p}, \mathbf{q})$ and $B^{\mathrm{W}}(\mathbf{p}, \mathbf{q})$,

$$\mathrm{Tr}\left[\hat{A}\hat{B}\right] = \frac{1}{(2\pi\hbar)^f} \int \mathrm{d}\mathbf{p} \int \mathrm{d}\mathbf{q}\, A^{\mathrm{W}}(\mathbf{p}, \mathbf{q}) B^{\mathrm{W}}(\mathbf{p}, \mathbf{q}). \tag{4.A.3}$$

The Wigner transform is linear, and it transforms operators which are functions just of the momentum operators $\hat{\mathbf{P}}$ or the position operators $\hat{\mathbf{Q}}$ as follows,

$$\hat{A} = f(\hat{\mathbf{P}}) \rightarrow A^{\mathrm{W}}(\mathbf{p}, \mathbf{q}) = f(\mathbf{p}) \tag{4.A.4a}$$

$$\hat{A} = f(\hat{\mathbf{Q}}) \rightarrow A^{\mathrm{W}}(\mathbf{p}, \mathbf{q}) = f(\mathbf{q}). \tag{4.A.4b}$$

The Wigner transform can also be used to map superoperators $\mathcal{A}$ onto operators on phase space functions $\mathcal{A}^{\mathrm{W}}$ which satisfy

$$(\mathcal{A}\rho)^{\mathrm{W}}(\mathbf{p}, \mathbf{q}) = \mathcal{A}^{\mathrm{W}}\rho^{\mathrm{W}}(\mathbf{p}, \mathbf{q}). \tag{4.A.5}$$

This is done by using the fact the Wigner transform of a product of operators is given by[143]

$$\begin{aligned}(AB)^{\mathrm{W}}(\mathbf{p}, \mathbf{q}) &= A^{\mathrm{W}}(\mathbf{p}, \mathbf{q}) \exp\left[\frac{i\hbar}{2}\sum_{k=1}^{f}\left(\overleftarrow{\partial_{q_k}}\overrightarrow{\partial_{p_k}} - \overleftarrow{\partial_{p_k}}\overrightarrow{\partial_{q_k}}\right)\right] B^{\mathrm{W}}(\mathbf{p}, \mathbf{q}) \\ &= B^{\mathrm{W}}(\mathbf{p}, \mathbf{q}) \exp\left[-\frac{i\hbar}{2}\sum_{k=1}^{f}\left(\overleftarrow{\partial_{q_k}}\overrightarrow{\partial_{p_k}} - \overleftarrow{\partial_{p_k}}\overrightarrow{\partial_{q_k}}\right)\right] A^{\mathrm{W}}(\mathbf{p}, \mathbf{q})\end{aligned} \tag{4.A.6}$$

where the operators $\overrightarrow{\partial_{p_k}}$ and $\overleftarrow{\partial_{p_k}}$ are defined by $f\overrightarrow{\partial_{p_k}}g = f(\partial_{p_k}g)$ and $f\overleftarrow{\partial_{p_k}}g = (\partial_{p_k}f)g$ in which ∂_{p_k} is the partial derivative with respect to p_k, and the operators $\overrightarrow{\partial_{q_k}}$ and $\overleftarrow{\partial_{q_k}}$ are defined similarly. This means a superoperator of the form,

$$\mathcal{A}\hat{\rho} = \hat{A}\hat{\rho} \ - \hat{\rho}\hat{B} \tag{4.A.7}$$

transforms to an operator on phase space functions given by

$$\mathcal{A}^{\mathrm{W}}\rho^{\mathrm{W}}(\mathbf{p}, \mathbf{q}) = \left(A^{\mathrm{W}}(\mathbf{p}, \mathbf{q}) \exp\left[\frac{i\hbar}{2}\mathcal{J}\right] - B^{\mathrm{W}}(\mathbf{p}, \mathbf{q}) \exp\left[-\frac{i\hbar}{2}\mathcal{J}\right]\right)\rho^{\mathrm{W}}(\mathbf{p}, \mathbf{q}), \tag{4.A.8}$$

in which $\mathcal{J} = \sum_{k=1}^{f}\left(\overleftarrow{\partial_{q_k}}\overrightarrow{\partial_{p_k}} - \overleftarrow{\partial_{p_k}}\overrightarrow{\partial_{q_k}}\right)$.

The expressions for the parameters in the spin density operator master equations involve operators of the form

$$\mathcal{G}_{ij}(t)\hat{\rho} = e^{\mathcal{L}_{ij}t}\hat{\rho} = e^{-i\hat{H}_{\mathrm{n}i}t/\hbar}\hat{\rho}e^{-i\hat{H}_{\mathrm{n}j}t/\hbar}, \tag{4.A.9}$$

where $\mathcal{L}_{ij} = -(i/\hbar)(\hat{H}_{\mathrm{n}i} \cdot - \cdot \hat{H}_{\mathrm{n}j})$. The Wigner transform of this can be found using

$$\frac{\mathrm{d}}{\mathrm{d}t}\mathcal{G}_{ij}^{\mathrm{W}}(t)\rho^{\mathrm{W}}(\mathbf{p},\mathbf{q}) = \mathcal{G}_{ij}^{\mathrm{W}}(t)\mathcal{L}_{ij}^{\mathrm{W}}\rho^{\mathrm{W}}(\mathbf{p},\mathbf{q}). \tag{4.A.10}$$

The classical approximation to this equation is found by truncating $\mathcal{L}_{ij}^{\mathrm{W}}$ at lowest order in $\hbar$, the $\hbar^{-1}$ term. For $i \neq j$, this becomes

$$\frac{\mathrm{d}}{\mathrm{d}t}\mathcal{G}_{ij}^{\mathrm{W}}(t)\rho^{\mathrm{W}}(\mathbf{p},\mathbf{q}) \approx \mathcal{G}_{ij}^{\mathrm{W}}(t)\left[-\frac{i}{\hbar}(V_i(\mathbf{q}) - V_j(\mathbf{q}))\right]\rho^{\mathrm{W}}(\mathbf{p},\mathbf{q}). \tag{4.A.11}$$

which can be solved to give

$$\mathcal{G}_{ij}^{\mathrm{W}}(t) \approx \exp\left[-\frac{i}{\hbar}(V_i(\mathbf{q}) - V_j(\mathbf{q}))t\right]. \tag{4.A.12}$$

For $i = j$, $(V_i(\mathbf{q}) - V_j(\mathbf{q})) = 0$ and therefore the $\hbar^{-1}$ term vanishes and $\mathcal{L}_{ii}^{\mathrm{W}}$ must be truncated at the $\hbar^0$ term instead. This gives the following equation for $\mathcal{G}_{ii}^{\mathrm{W}}(t)$

$$\frac{\mathrm{d}}{\mathrm{d}t}\mathcal{G}_{ii}^{\mathrm{W}}(t)\rho^{\mathrm{W}}(\mathbf{p},\mathbf{q}) \approx \mathcal{G}_{ii}^{\mathrm{W}}(t)\left\{H_{\mathrm{in}}^{\mathrm{W}}(\mathbf{p},\mathbf{q}), \rho^{\mathrm{W}}(\mathbf{p},\mathbf{q})\right\}, \tag{4.A.13}$$

in which $\{\cdot, \cdot\} = \cdot\, \mathcal{J} \cdot$ here denotes the classical Poisson bracket. This can be solved to give

$$\mathcal{G}_{ii}^{\mathrm{W}}(t) \approx \exp[t\mathscr{L}_i], \tag{4.A.14}$$

where $\mathscr{L}_i = \left\{H_{\mathrm{in}}^{\mathrm{W}}(\mathbf{p},\mathbf{q}), \cdot\right\}$ is the classical Liouvillian for motion in a potential $V_i(\mathbf{q})$ (we note that the Wigner transform of the nuclear Hamiltonian $H_{\mathrm{in}}^{\mathrm{W}}(\mathbf{p},\mathbf{q})$ is simply the classical Hamiltonian $\mathcal{H}_i(\mathbf{p},\mathbf{q})$).

In a similar spirit to the classical approximation for $\mathcal{G}_{ij}^{\mathrm{W}}(t)$, we will further approximate the superoperator corresponding to left and right multiplication by the diabatic coupling $\hat{\Delta}_{\mathrm{S}}$ by the leading order term in $\hbar$, in Eq. (4.A.8),

$$\begin{aligned}(\Delta_{\mathrm{S}}\rho)^{\mathrm{W}}(\mathbf{p},\mathbf{q}) &= \Delta_{\mathrm{S}}^{\mathrm{W}}(\mathbf{p},\mathbf{q})\rho^{\mathrm{W}}(\mathbf{p},\mathbf{q}) + O(\hbar^1)\\ (\rho\Delta_{\mathrm{S}})^{\mathrm{W}}(\mathbf{p},\mathbf{q}) &= \Delta_{\mathrm{S}}^{\mathrm{W}}(\mathbf{p},\mathbf{q})\rho^{\mathrm{W}}(\mathbf{p},\mathbf{q}) + O(\hbar^1).\end{aligned} \tag{4.A.15}$$

We will also make the same approximation for the triplet diabatic coupling. This approximation is exact within the Condon approximation, when the diabatic coupling can be treated as a constant i.e. $\hat{\Delta}_{\mathrm{S}} = \Delta_{\mathrm{S}}$ and $\hat{\Delta}_{\mathrm{T}} = \Delta_{\mathrm{T}}$. Finally we can approximate the Wigner trans-

formed nuclear densities, by their classical values, which is valid in the high temperature limit, using the following

$$[\exp(-\beta H_{in})]^{\mathrm{W}}(\mathbf{p},\mathbf{q}) = \exp\Big(-\beta H_{in}^{\mathrm{W}}(\mathbf{p},\mathbf{q})\Big) + O(\beta^2). \tag{4.A.16}$$

From this we can obtain the second and fourth order classical QME parameters as given in section 4.1. This can be done by either a brute-force expansion of the rate expressions, using the classical approximation, or by using Liouville space diagrams as in Ref. [139] to evaluate the expressions. Either way, one arrives at the expressions given in the main text for the second and fourth order QME parameters.

4.B Appendix: The slow energy gap fluctuation limit

The slow energy gap approximation, Eq. (4.17), can be used to obtain an approximate rate expression which is valid at all Δ_{S}, within the approximations that underpin this treatment of the radical pair reaction. This result was originally derived by Sparpaglione & Mukamel in Ref. [102], and a sketch of their derivation is given here. First we note that the order $2n$ component of the Fourier-Laplace transform of the full field-independent rate kernel can be written as[102]

$$\tilde{\mathcal{K}}_{\mathrm{n}}^{(2n)}(\omega) = \tilde{\mathcal{T}}_{\mathrm{n}}^{(2n)}(\omega) - \frac{i}{\omega}\sum_{m=1}^{n-1}\tilde{\mathcal{K}}_{\mathrm{n}}^{(2n-2m)}(\omega)\tilde{\mathcal{T}}_{\mathrm{n}}^{(2m)}(\omega) \tag{4.B.1}$$

where the superoperator $\tilde{\mathcal{T}}_{\mathrm{n}}^{(2n)}(\omega)$ is

$$\tilde{\mathcal{T}}_{\mathrm{n}}^{(2n)}(\omega) = \mathcal{P}[\mathcal{L}_V\tilde{\mathcal{G}}_{\mathrm{n}}(\omega)\mathcal{L}_V\tilde{\mathcal{G}}_{\mathrm{n}}(\omega)]^{n-1}\mathcal{L}_V\tilde{\mathcal{G}}_{\mathrm{n}}(\omega)\mathcal{L}_V\mathcal{P}. \tag{4.B.2}$$

Because the kernel is diagonal in the singlet-triplet diabatic state basis, this can be used to find the order $2n$ rate kernel $\tilde{\mathbf{K}}^{(2n)}(\omega)$ (2×2 matrix of forward and backward singlet rate kernels, where for simplicity we assume there is no triplet reaction pathway) can be written as

$$\tilde{\mathbf{K}}^{(2n)}(\omega) = \tilde{\mathbf{T}}^{(2n)}(\omega) - \frac{i}{\omega}\sum_{m=1}^{n-1}\tilde{\mathbf{K}}^{(2n-2m)}(\omega)\tilde{\mathbf{T}}^{(2m)}(\omega). \tag{4.B.3}$$

The full rate matrix is obtained as $\mathbf{K} = \lim_{\omega\to 0}\sum_{n=1}^{\infty}\tilde{\mathbf{K}}^{(2n)}(\omega)$, and the matrix $\tilde{\mathbf{T}}^{(2n)}(\omega)$ is given by

$$[\tilde{\mathbf{T}}^{(2n)}(\omega)]_{ij} = \mathrm{Tr}\big[\hat{\Pi}_{i\mathrm{S}}[\mathcal{L}_V\tilde{\mathcal{G}}_{\mathrm{n}}(\omega)\mathcal{L}_V\tilde{\mathcal{G}}_{\mathrm{n}}(\omega)]^{n-1}\mathcal{L}_V\tilde{\mathcal{G}}_{\mathrm{n}}(\omega)\mathcal{L}_V\hat{\Pi}_{j\mathrm{S}}\hat{\rho}_{j\mathrm{n}}\big] \tag{4.B.4}$$

where $\hat{\Pi}_{i\mathrm{S}} = \hat{\Pi}_i\hat{P}_{\mathrm{S}}$, and the trace here implicitly ignores any nuclear spin degrees of freedom, so is only over nuclear vibrational and diabatic state degrees of freedom. Invoking the classical static approximation for the coherences, Eq. (4.6), we can approximate $\mathcal{L}_V\tilde{\mathcal{G}}_{\mathrm{n}}(\omega)\mathcal{L}_V\hat{\Pi}_{j\mathrm{S}}\hat{\rho}_{j\mathrm{n}}$ in the $\omega\to 0$ limit as

$$\mathcal{L}_V\tilde{\mathcal{G}}_{\mathrm{n}}(\omega\to 0)\mathcal{L}_V\hat{\Pi}_{j\mathrm{S}}\hat{\rho}_{j\mathrm{n}} \to \sum_{k=1,2}(-1)^{k+j+1}\hat{\Pi}_{k\mathrm{S}}\kappa_{\mathrm{S}}\varrho_j, \tag{4.B.5}$$

where I have suppressed the explicit dependence on $\mathbf{p}$ and $\mathbf{q}$ for compactness. Then using this and the slow energy gap coordinate approximation, Eq. (4.17), we can show that $[\mathcal{L}_V\tilde{\mathcal{G}}_{\mathrm{n}}(\omega)\mathcal{L}_V\tilde{\mathcal{G}}_{\mathrm{n}}(\omega)]\mathcal{L}_V\tilde{\mathcal{G}}_{\mathrm{n}}(\omega)\mathcal{L}_V\hat{\Pi}_{j\mathrm{S}}\hat{\rho}_{j\mathrm{n}}$ can be approximated as follows in the $\omega\to 0$ limit,

$$\begin{aligned}
&\lim_{\omega\to 0}[\mathcal{L}_V\tilde{\mathcal{G}}_{\mathrm{n}}(\omega)\mathcal{L}_V\tilde{\mathcal{G}}_{\mathrm{n}}(\omega)]\mathcal{L}_V\tilde{\mathcal{G}}_{\mathrm{n}}(\omega)\mathcal{L}_V\hat{\Pi}_{j\mathrm{S}}\hat{\rho}_{j\mathrm{n}}\\
&\to \lim_{\omega\to 0}\int_0^\infty \mathrm{d}t\, e^{i\omega t}\int \mathrm{d}x\sum_{l,k}(-1)^{l+j+1}\hat{\Pi}_{l\mathrm{S}}\kappa_{\mathrm{S}}e^{\mathscr{L}_k t}\delta(U_{\mathrm{S}}-x)\frac{\varrho_k}{\langle\delta(U_{\mathrm{S}}-x)\rangle_k}\langle\delta(U_{\mathrm{S}}-x)\kappa_{\mathrm{S}}\rangle_j\\
&= \lim_{\omega\to 0}\int_0^\infty \mathrm{d}t\, e^{i\omega t}\sum_{l,k}(-1)^{l+j+1}\hat{\Pi}_{l\mathrm{S}}\kappa_{\mathrm{S}}e^{\mathscr{L}_k t}\delta(U_{\mathrm{S}})\frac{\varrho_k}{\langle\delta(U_{\mathrm{S}})\rangle_k}\langle\kappa_{\mathrm{S}}\rangle_j\,.
\end{aligned} \tag{4.B.6}$$

Using this we find $[\tilde{\mathbf{T}}^{(4)}(\omega\to 0)]_{ij}$ to be

$$[\tilde{\mathbf{T}}^{(4)}(\omega\to 0)]_{ij} = (-1)^{i+j}\lim_{\omega\to 0}\int_0^\infty \mathrm{d}t\, e^{i\omega t}\sum_{k=1,2}\frac{\big\langle\kappa_{\mathrm{S}}e^{\mathscr{L}_k t}\delta(U_{\mathrm{S}})\big\rangle_k}{\langle\delta(U_{\mathrm{S}})\rangle_k}\langle\kappa_{\mathrm{S}}\rangle_j \tag{4.B.7}$$

by iterating the above argument one finds that $\tilde{\mathbf{T}}^{(2n)}(\omega\to 0)$ is

$$\tilde{\mathbf{T}}^{(2n)}(\omega\to 0) = (-1)^{n-1}\lim_{\omega\to 0}\tilde{g}(\omega)^{n-1}\tilde{\mathbf{T}}^{(2)}(\omega\to 0), \tag{4.B.8}$$

where the factor $\tilde{g}(\omega) = \tilde{g}_1(\omega) + \tilde{g}_2(\omega)$ is given by

$$\tilde{g}_k(\omega) = \int_0^\infty \mathrm{d}t\, e^{i\omega t}\frac{\big\langle\kappa_{\mathrm{S}}e^{\mathscr{L}_k t}\delta(U_{\mathrm{S}})\big\rangle_k}{\langle\delta(U_{\mathrm{S}})\rangle_k}. \tag{4.B.9}$$

It is also straightforward to show that

$$\tilde{\mathbf{T}}^{(2)}(\omega \to 0)^n = (-1)^{n-1} \left(\langle \kappa_S \rangle_1 + \langle \kappa_S \rangle_2\right)^{n-1} \tilde{\mathbf{T}}^{(2)}(\omega \to 0) \tag{4.B.10}$$

and $\tilde{\mathbf{T}}^{(2)}(\omega \to 0) = \mathbf{K}^{(2)}$ is the second order rate matrix,

$$\tilde{\mathbf{T}}^{(2)}(\omega \to 0) = \begin{pmatrix} -\langle \kappa_S \rangle_1 & \langle \kappa_S \rangle_2 \\ \langle \kappa_S \rangle_1 & -\langle \kappa_S \rangle_2 \end{pmatrix} \tag{4.B.11}$$

It is then straightforward to show using Eq. that $\tilde{\mathbf{K}}^{(2n)}(\omega \to 0)$ is given by

$$\tilde{\mathbf{K}}^{(2n)}(\omega \to 0) = \lim_{\omega \to 0} \left[-\Delta\tilde{g}(\omega)\right]^{n-1} \mathbf{T}^{(2)}(\omega \to 0), \tag{4.B.12}$$

where $\Delta\tilde{g}(\omega) = \Delta\tilde{g}_1(\omega) + \Delta\tilde{g}_2(\omega)$ is

$$\Delta\tilde{g}_k(\omega) = \int_0^\infty \mathrm{d}t\, e^{i\omega t} \langle \kappa_S \rangle_k \left(\frac{\left\langle \kappa_S e^{\mathscr{L}_k t} \delta(U_S) \right\rangle_k}{\langle \kappa_S \rangle_k \langle \delta(U_S) \rangle_k} - 1 \right) \tag{4.B.13}$$

and therefore the rate matrix, $\mathbf{K} = \tilde{\mathbf{K}}(\omega \to 0)$, is

$$\mathbf{K} = \frac{1}{1 + \Delta\tilde{g}(0)} \mathbf{K}^{(2)}. \tag{4.B.14}$$

From this the Eq. (4.19) follows immediately, by identifying $\Delta\tilde{g}(0) = \tau_{S,1} k^{(2)}_{f,S,cl} + \tau_{S,2} k^{(2)}_{b,S,cl}$.

Using this same approach we can exactly sum the purely reactive contributions to the additional singlet-triplet decoherence rate. First we note that within the field independent rate approximation, the kernel $\mathcal{K}_n(t)$ does not couple singlet-triplet coherences to any other element of Liouville space, as was shown earlier, and we will denote the term acting on the singlet-triplet coherences as $K_{ST}(t)$. The Fourier-Laplace transform of this can be expanded just like the rate matrix in Eq. (4.B.3),

$$\tilde{K}^{(2n)}_{ST}(\omega) = \tilde{T}^{(2n)}_{ST}(\omega) - \frac{i}{\omega} \sum_{m=1}^{n-1} \tilde{K}^{(2n-2m)}_{ST}(\omega) \tilde{T}^{(2m)}_{ST}(\omega) \tag{4.B.15}$$

where $\tilde{T}_{ST}(\omega)^{(2n)}$ is given by

$$\tilde{T}^{(2n)}_{ST}(\omega) = \mathrm{Tr}\left[\hat{\Pi}_{1ST} \left[\mathcal{L}_V \tilde{\mathcal{G}}_n(\omega) \mathcal{L}_V \tilde{\mathcal{G}}_n(\omega)\right]^{n-1} \mathcal{L}_V \tilde{\mathcal{G}}_n(\omega) \mathcal{L}_V \hat{\Pi}_{1ST} \hat{\rho}_{1n}\right] \tag{4.B.16}$$

where $\hat{\Pi}_{1ST}$ is a projection operator onto any radical pair singlet-triplet coherence element

of the diabatic state Liouville space, and again the trace is understood as only being over diabatic state and nuclear degrees of freedom. Using the classical static approximation for the action of $\tilde{\mathcal{G}}_{\mathrm{n}}(\omega)$ on coherence elements of Liouville space between diabatic states 1 and 2, we can retain only terms containing the local Fermi's Golden rule rate κ_{S}, which defines the purely reactive contribution to the singlet-triplet coherence decay. Then using the slow energy gap coordinate approximation for the elements on the same potential energy surface, i.e. for the radical pair singlet-triplet coherences, it can be shown that the $\tilde{T}_{\mathrm{ST}}^{(2n)}(\omega \to 0)$ is given by

$$\tilde{T}_{\mathrm{ST}}^{(2n)}(\omega \to 0) = -\frac{1}{2}\left(-\frac{\tilde{g}_1(\omega)}{2}\right)^{n-1} \langle \kappa_{\mathrm{S}} \rangle_1 \tag{4.B.17}$$

and

$$\tilde{T}_{\mathrm{ST}}^{(2)}(\omega \to 0)^n = \left(-\frac{\langle \kappa_{\mathrm{S}} \rangle_1}{2}\right)^n, \tag{4.B.18}$$

and using this with Eq. (4.B.15) the total decoherence term in the kernel is

$$\tilde{K}_{\mathrm{ST}}(\omega \to 0) = -\frac{1}{1 + \frac{\Delta \tilde{g}_1(0)}{2}} \frac{\langle \kappa_{\mathrm{S}} \rangle_1}{2}. \tag{4.B.19}$$

From this Eq. (4.21) for the reactive contribution to the additional decoherence rate immediately follows.

5 The Radical Pair Master Equation: Testing the Theory

In this final chapter on the radical pair master equation, I will present simulation results for a model radical pair reaction for which exact quantum dynamics and perturbative QME parameters can be calculated. This allows us to investigate the validity of the approximations made in deriving the master equations, for a realistic model of spin selective electron transfers in radical pairs.

5.1 Validation of the radical pair QME

The theory of the radical pair spin density quantum master equation presented in chapter 3 relies on certain approximations, and therefore it important to assess the validity of these approximations, ideally by comparison with numerically exact calculations. For harmonic potential energy surfaces, such numerically exact calculations of spin system observables can be performed with the hierarchical equations of motion (HEOM) method. In this section I will describe the model calculations performed, demonstrating the accuracy of the quantum master equations derived above, as well as their short-comings.

5.1.1 Model systems

In general the potential energy surfaces of radical pair systems are highly complex and solving the Liouville–von Neumann equation for the full radical pair for arbitrary potential energy surfaces is generally not tractable. However, for small systems and for certain

potential energy surfaces methods exist that can produce numerically exact results for the quantum dynamics. We consider one such exactly soluble system – the spin-boson model, in which the electronic system is coupled to an infinite bath of harmonic oscillators.[157,158] The spin-boson model has been applied extensively as a model of condensed phase electron transfer.[56,134,159–162] In these examples we will only consider the case where there is a single singlet state product, where the potential energy surfaces are given by Eq. (4.24). In this case the potential energy surfaces are fully specified by the spectral density $\mathcal{J}(\omega)$, which is related to the frequencies ω_k, masses m_k and coupling constants c_k of the harmonic bath by

$$\mathcal{J}(\omega) = \frac{\pi}{2}\sum_{k=1}^{N}\frac{c_k^2}{m_k\omega_k}\delta(\omega-\omega_k). \tag{5.1}$$

In these models, a Debye spectral density is used, in which $\mathcal{J}(\omega)$ is given by

$$\mathcal{J}(\omega) = \frac{\lambda_\mathrm{D}}{2}\frac{\omega_\mathrm{D}\omega}{\omega_\mathrm{D}^2+\omega^2}, \tag{5.2}$$

in which $\lambda_\mathrm{D} = \lambda_\mathrm{S}$ is the reorganisation energy, as in Eq. (4.25), and ω_D is the Debye cut-off frequency. This spectral density serves as a model of potential energy surface for an electron transfer in a solvent with a Debye type dielectric response, within the dielectric continuum model. In the model systems, the Condon approximation is also made, so the diabatic coupling operator is set to a constant $\hat{\Delta}_\mathrm{S} = \Delta_\mathrm{S}$.

In these tests, two models for the radical pair spin Hamiltonian $\hat{H}_\mathrm{1s}$ with two sets of initial conditions for the density operator are considered. In Model I $\hat{H}_\mathrm{1s} = 0$, and the initial density operator is set to

$$\hat{\rho}(0) = \frac{1}{2}(|1,\mathrm{S}\rangle\langle 1,\mathrm{S}| + |1,\mathrm{T}\rangle\langle 1,\mathrm{T}| + |1,\mathrm{S}\rangle\langle 1,\mathrm{T}| + |1,\mathrm{T}\rangle\langle 1,\mathrm{S}|)\hat{\rho}_\mathrm{1n}, \tag{5.3}$$

where $|1,\mathrm{T}\rangle$ refers to any of the three triplet radical pair states. Because the Hamiltonian in this model cannot mix triplet states, we need not specify which triplet state we are considering. This initial condition corresponds to a coherent superposition of singlet and triplet radical pair states, so with this we can analyse the dynamics of the singlet-triplet coherences in the presence of a singlet-selective recombination pathway.

In Model II, we consider a more complex (and more realistic) model of the radical pair, which includes a Zeeman interaction between the electron spins and an external field, as well as a single $I = 1/2$ nuclear spin coupled by an isotropic hyperfine interaction to the electron spin in radical 1, so the radical pair spin Hamiltonian $\hat{H}_{1s}$ is

$$\hat{H}_{1s} = \omega_0 \hat{S}_{1z} + \omega_0 \hat{S}_{2z} + a\hat{\mathbf{S}}_1 \cdot \hat{\mathbf{I}}. \tag{5.4}$$

ω_0 is the electron Zeeman frequency, $\omega_0 = g_e \mu_B B_0/\hbar = \gamma_e B_0$ where g_e is the free electron g-factor, μ_B is the Bohr magneton (and γ_e is the absolute value of the gyromagnetic ratio for a free electron spin), B_0 is the applied magnetic field strength, a is the isotropic hyperfine coupling constant, and $\hat{\mathbf{I}}$ is the $I = 1/2$ nuclear spin operator. In this case we take the initial condition to be

$$\hat{\rho}(0) = \frac{1}{2} |1, \mathrm{S}\rangle\langle 1, \mathrm{S}| \hat{\rho}_{1n}, \tag{5.5}$$

which corresponds to a radical pair formed by spin selective photo-excitation from a singlet ground-state precursor which has vibrationally relaxed to local equilibrium on the singlet radical pair diabatic surface. With Model II, we can assess the validity of the field-independent rate approximation for a simple model of a radical pair reaction including hyperfine coupling induced spin-state mixing.

5.1.2 Model parameters

In all simulations, the temperature is set to 300 K, and the Debye cut-off frequency ω_D for the bath is set to $\hbar\omega_D = 10\ \mathrm{cm}^{-1}\ hc$. This value is characteristic of the Debye dielectric response of liquid water at approximately 300 K, which is given in terms of the relaxation time τ_{rel} of the Debye component of the dielectric relaxation[149] and the static and optical permittivities, ε_0 and ε_∞, by $\omega_D \tau_{rel} = \varepsilon_0/\varepsilon_\infty$[102]. A relatively low value of $\hbar\omega_D/k_B T$ also significantly improves the efficiency of the exact calculations, which is important for reaching the long time-scales that we need to examine.

In Model I the bias for the forward reaction ϵ_S is set to 0 eV, and in order to test the limits of the perturbative master equations, the reorganisation energy λ_D is varied between 0.1 meV and 0.25 eV, and diabatic coupling Δ_S is varied between 0.1 meV and 10 meV.

In Model II the bias ϵ_S is set to 0.1 eV, the reorganisation energy λ_D is set to 0.5 eV, and the diabatic coupling Δ_S is set to 0.1 meV. The spin system parameters are set to $B_0 = \omega_0/g_e\mu_B = 0.5$ mT and $a/g_e\mu_B = 1.5$ mT. These parameters are chosen as a realistic set of parameters for a radical ion pair undergoing a long range electron transfer in solution, in order to examine the validity of the field independent rate approximation.

5.1.3 Exact calculations

For this model, the well-established Hierarchical Equations of Motion (HEOM) method is applied to obtain numerically exact diabatic state populations and coherences.[158,163] These calculations were performed using an early development version of the HEOMTN code, written by Lachlan Lindoy. A Matsubara expansion of the bath correlation functions is used along with a frequency based truncation scheme[164] to construct the hierarchy of auxiliary density operators required for this method.

Using this truncation scheme, results converged to graphical accuracy (less than 0.1% change) for Model I and Model II were obtained using a maximum frequency of 250 ω_D. This corresponds to a hierarchy of 369 auxiliary density operators, including contributions from the first two Matsubara modes. In order to efficiently integrate over the long timescales required here, it is necessary to use an adaptive order and time step Taylor series integrator, where the scaling scheme of Shi *et al.*[165] is used in order to allow for effective control of the errors in the integrator.

5.1.4 Approximate QME calculations

The second and fourth order rate constants, $k_{f,S}$ and $k_{b,S}$, electron spin couplings, J, and dephasing rates, k_D, are obtained using the analytic expressions for the spin-boson model which are given in appendix 5.A. The parameters are calculated by discretising the spectral density into a finite set of modes using the standard procedure.[159–161] A discretization into 1000 modes gives converged results for all parameters. The sets of calculated master equation parameters for both models are given in the following section.

For Model I the master equations, Eq. (3.83) and Eq. (3.93), are analytically soluble.

The resulting expressions for the matrix elements of $\hat{\rho}_{1s}(t)$ and $\hat{\rho}_{2s}(t)$ are

$$\begin{aligned}
\rho_{1SS}(t) &= \langle 1,S|\hat{\rho}_{1s}(t)|1,S\rangle = \frac{1}{2}\frac{k_{b,S}+k_{f,S}e^{-(k_{f,S}+k_{b,S})t}}{k_{f,S}+k_{b,S}},\\
\rho_{1ST}(t) &= \langle 1,S|\hat{\rho}_{1s}(t)|1,T\rangle = \frac{1}{2}e^{-2iJt/\hbar-(k_{f,S}/2+k_D)t},\\
\rho_{1TS}(t) &= \langle 1,T|\hat{\rho}_{1s}(t)|1,S\rangle = \rho_{1ST}(t)^*,\\
\rho_{1TT}(t) &= \langle 1,T|\hat{\rho}_{1s}(t)|1,T\rangle = \frac{1}{2},\\
\rho_{2}(t) &= \langle 2,S|\hat{\rho}_{2s}(t)|2,S\rangle = \frac{1}{2}-\rho_{1SS}(t).
\end{aligned} \tag{5.6}$$

In Model I $k_{f,S} = k_{b,S}$ because in this model $\epsilon_S = 0$. In the second order master equation k_D is zero and for the Haberkorn master equation, with the reaction term given by Eq. (3.3), $J = k_D = 0$ (i.e. we still account for the back-reaction in the way predicted by the second order master equation).

For Model II the master equations, when expanded in a basis of uncoupled spin projection states, $|\sigma_1,\sigma_2,M\rangle$, form a set of linear equations which can be solved numerically using standard techniques. Due to the non-zero bias, the three-time fourth order correlation functions are highly oscillatory, and therefore the fourth order QME parameters, which are triple integrals of these correlation functions, are very computationally expensive to evaluate accurately. Therefore for Model II we only compare the second order QME to the exact results.

5.2 Results and discussion

5.2.1 Model I

First, we will use Model I to analyse the accuracy of the incoherent rate approximation, and the perturbative treatment of the diabatic coupling. In Fig. 5.1 the time evolution of the

$\hbar^2 k^{(2)}_{f,S}/2\Delta_S^2$	$2\hbar J^{(2)}/\Delta_S^2$	$\hbar^4 k^{(4)}_{f,S}/2\Delta_S^4$	$2\hbar^3 J^{(4)}/\Delta_S^4$	$\hbar^4 k^{(4)}_{D}/\Delta_S^4$
0.66094 ns	−2.0789 ns	-1.0634×10^{-5} ps^3	2.4370×10^{-6} ps^3	1.0447×10^{-5} ps^3

Table 5.1: Second and fourth order parameters for the master equations for Model I with $\lambda_D = 0.25$ meV, calculated using expressions given in the appendix. Note that $k^{(n)}_{b,S} = k^{(n)}_{f,S}$ when $\epsilon_S = 0$.

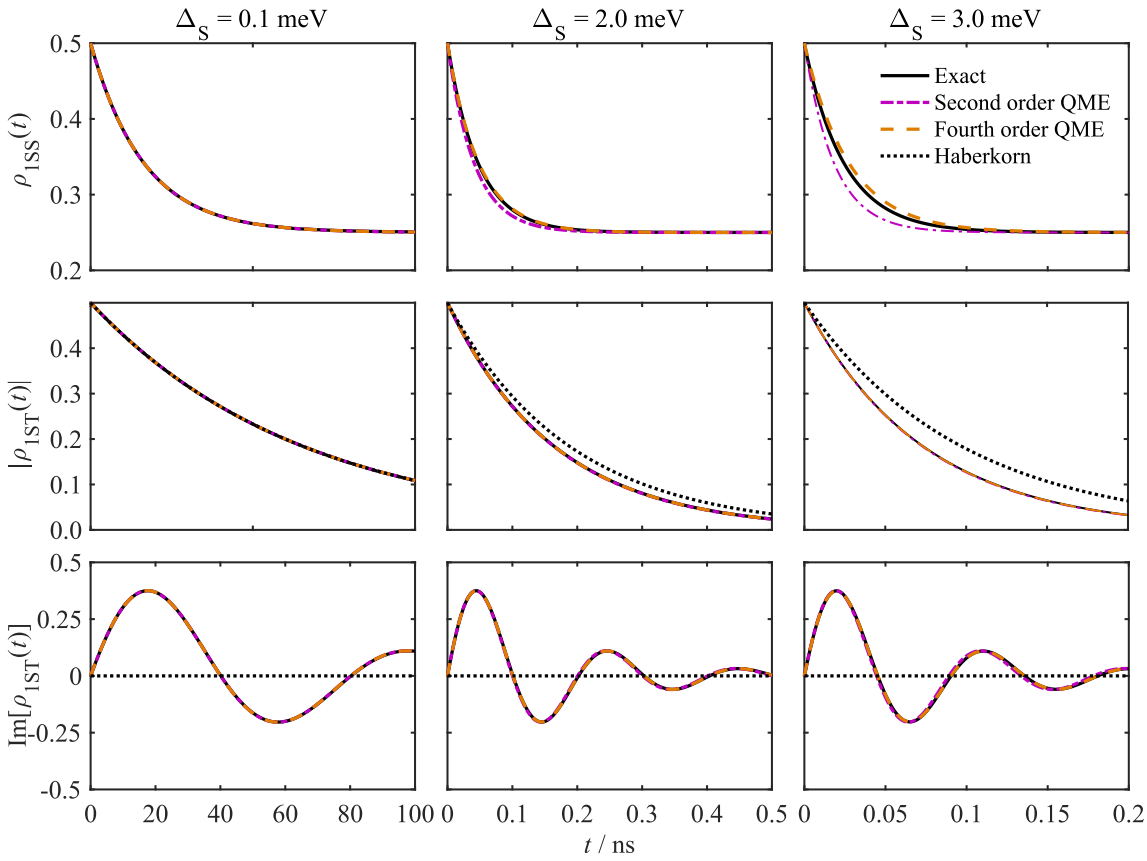

Figure 5.1: The time evolution of the singlet radical pair populations $\rho_{1SS}(t)$ (top row), the absolute value of the singlet-triplet radical pair coherence $|\rho_{1ST}(t)|$ (middle row) and the imaginary part of this coherence $\mathrm{Im}[\rho_{1ST}(t)]$ (bottom row), for three different values of the diabatic coupling Δ_S: 0.1 meV (left column), 2 meV (middle column) and 3 meV (right column). The predictions of the second and fourth order QMEs and the Haberkorn QME are also shown.

singlet radical pair populations $\rho_{1SS}(t)$, the absolute value of the singlet-triplet radical pair coherence $|\rho_{1ST}(t)|$ and the imaginary part of this coherence $\mathrm{Im}[\rho_{1ST}(t)]$ are displayed for three different values of Δ_S: 0.1 meV, 2 meV and 3 meV. The second and fourth order master equation predictions for these were calculated using Eq. (5.6) using the parameters given in Table 5.1. The Haberkorn master equation results are calculated using Eq. (5.6), setting $k_D = 0$ and $J = 0$, and using the numerically exact rate constants $k_{f,S} = k_{b,S}$ (because the bias ϵ_S is 0) obtained by fitting $k_{f,S}$ in the equation for $\rho_{1SS}(t)$ to the HEOM results.

The radical pair singlet population, $\rho_{SS}(t)$, shown in the top row of Fig 5.1, is captured qualitatively for all values of Δ_S by both the second and fourth order master equations. The Haberkorn fit to $\rho_{1SS}(t)$, using Eq. (5.6), is numerically exact ($R^2 = 1$), which demonstrates the validity of incoherent recombination approximation for this model. The fitted rate

constants are $k_{f,S} = 0.03054\ \text{ns}^{-1}, 10.63\ \text{ns}^{-1},$ and $20.58\ \text{ns}^{-1}$ for $\Delta = 0.1, 2.0$ and 3.0 meV respectively. This is in agreement with the prediction of the incoherent rate criterion for the activated limit given in Eq. (4.33). The largest value $|\Delta_S/(\epsilon_S - \lambda_S)|^2$ takes in these examples is for $\Delta_S = 3$ meV where $|\Delta_S/(\epsilon_S - \lambda_S)|^2 = 1.44 \times 10^{-4} \ll 1$, so , as is borne out by the HEOM results, we expect the incoherent rate approximation to be valid for all of these examples.

As Δ_S increases the agreement between the exact results and the master equation results decreases, with the second order quantum master equation (QME) increasingly overestimating the forward and backward rate constants and the fourth order QME increasingly underestimating them. This is of course unsurprising given that our master equations are derived from perturbation theory. For the Debye spectral density in the classical limit, the energy gap correlation function decays exponentially with a time constant $\tau_S = 1/\omega_D$, so this breakdown can be understood using Eq. (4.38). As Δ_S increases from 0.1 meV to 3 meV, $k_{f,S,cl}\tau_{S,1}$ increases from 6×10^{-3}, which is much less than 1, to 0.18, which is not significantly smaller than 1, so the breakdown of perturbation theory is expected. Improvements to perturbation theory can be made using the Padé-approximant $k \approx k^{(2)}/(1 - k^{(4)}/k^{(2)})$ for the rate constant,[102,134,135,162,166] as has been explored in work by other authors, or using the Zusman expressions given in Eq. (4.19).

The absolute value of the singlet-triplet coherence, $|\rho_{1ST}(t)|$, is shown in the middle row of Fig. 5.1. For the master equations, $|\rho_{1ST}(t)| = (1/2)e^{-(k_{f,S}/2+k_D)t}$, which depends only on k_D and $k_{f,S}$ and not on J. The fourth order QME provides as good a description of the evolution of the coherences as it does for $\rho_{1SS}(t)$. It is at first surprising that the second order QME provides an equally good description of the evolution of $|\rho_{1ST}(t)|$. This is because for the parameters in Model I $k^{(4)}_{f,S}/2 + k^{(4)}_D \approx 0$, see Table. 5.1, and therefore the total decay rate of $|\rho_{1ST}(t)|$ for both the second and fourth order QMEs is approximately $k^{(2)}_{f,S}$. In other words, because the second order QME overestimates $k_{f,S}$ for larger Δ_S, it coincidentally describes $|\rho_{1ST}(t)|$ very well for all values of Δ_S examined here. The Haberkorn prediction for the evolution of $|\rho_{1ST}(t)|$, which uses the value of $k_{f,S}$ fitted from $\rho_{1SS}(t)$ but which does not include any additional decoherence, increasingly underestimates the decay rate as Δ_S increases, which shows that there is in fact additional singlet-triplet decoherence for larger

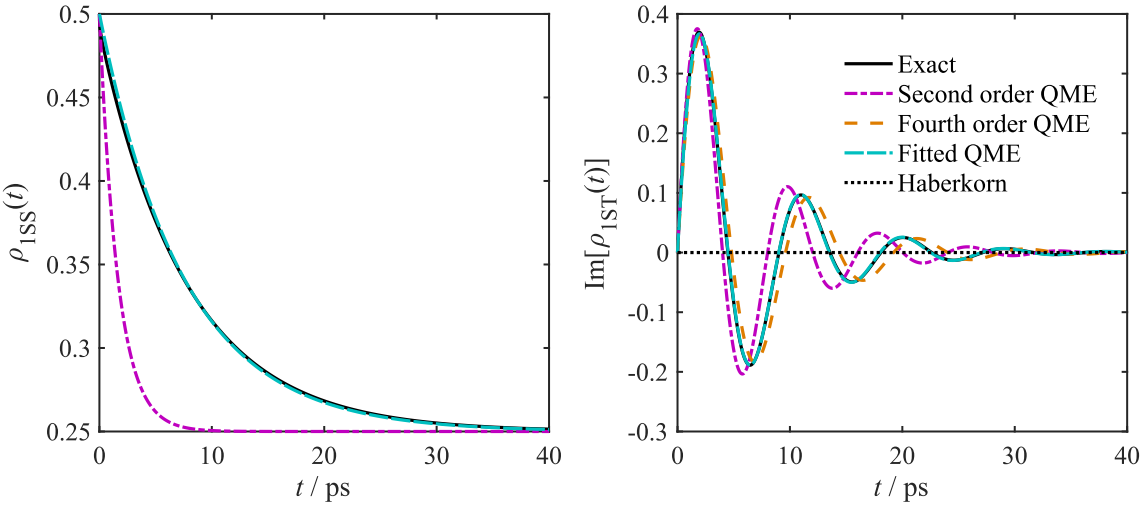

Figure 5.2: The time evolution of the singlet radical pair populations $\rho_{1SS}(t)$ (left), and the imaginary part of the singlet-triplet radical pair coherence $\mathrm{Im}[\rho_{1ST}(t)]$ (right), calculated with the exact HEOM method, second and fourth order QMEs, the Haberkorn QME and the general form of the QME in Eq. (3.93), with a fitted rate constant, scalar coupling and decoherence rate. Note that the fourth order prediction for $k_{f,S} < 0$ so this is not included on the $\rho_{1SS}(t)$ plot, and the Haberkorn and fitted curves are identical for $\rho_{1SS}(t)$.

values of the diabatic coupling strength.

Furthermore, the Haberkorn master equation, which does not include a reactive electron spin coupling term, fails to capture the evolution of the imaginary part of the singlet-triplet coherences, $\mathrm{Im}[\rho_{1ST}(t)]$, which is shown in the bottom row of Fig. 5.1. The second and fourth order equations capture the oscillation frequency, which arises due to the reactive scalar electron spin coupling J, exceptionally well in these examples. The most significant deviation is for $\Delta_S = 3.0$ meV, where the second order master equation slightly overestimates the oscillation frequency.

This model demonstrates that the conventional Haberkorn reaction operator provides an accurate description of the reduced density operators in the small Δ_S limit, provided the second order correction to the scalar electron spin coupling is included. The additional singlet-triplet dephasing term becomes more significant for larger values of Δ. However in the non-adiabatic limit, $\Delta_S \to 0$, the most important terms are the Haberkorn reaction term and the reactive electron spin coupling, which provide a sufficient description of the dynamics.

In order to illustrate that the general form of the radical pair QME proposed in Eq. (3.93)

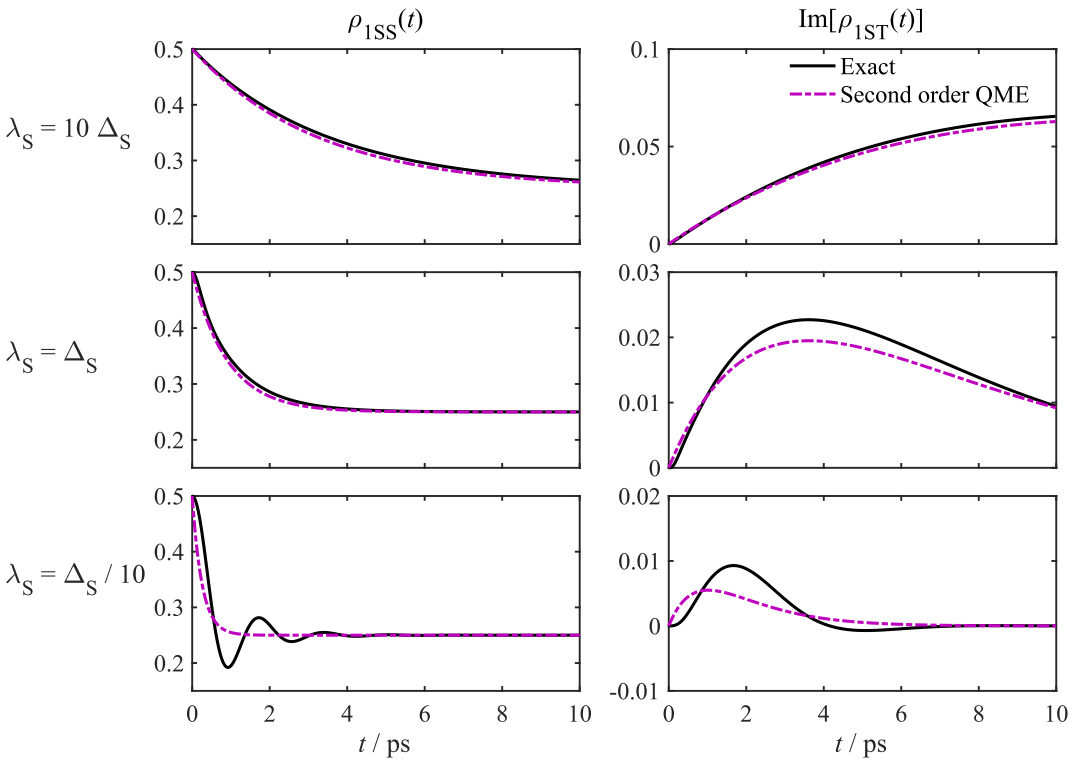

Figure 5.3: The time evolution of the singlet radical pair populations $\rho_{1SS}(t)$ (left), and the imaginary part of the singlet-triplet radical pair coherence $\mathrm{Im}[\rho_{1ST}(t)]$ (right), calculated with the exact HEOM method, and second order QME. From top to bottom the reorganisation energy in the model decreases from 10 meV (top row), to 1 meV (middle row) to 0.1 meV (bottom row).

gives a correct description of the radical pair spin dynamics, $\rho_{1SS}(t)$ and $\mathrm{Im}[\rho_{1ST}(t)]$ are shown for Model I with $\Delta_S = 10$ meV in Fig. 5.2. In this case second order perturbation theory fails to capture the population decay and spin coherence dynamics, and fourth order perturbation theory breaks down completely, predicting negative rate constants (and therefore exponential growth of the populations). However, the numerically exact HEOM results can be fitted very accurately, $R^2 > 0.99$, to the predictions of Eq. (3.93), by treating $k_{f,S} = k_{b,S}$, J and k_D as free parameters. The fitted values of these parameters are $k_{f,S} = k_{b,S} = 0.06666\ \mathrm{ps}^{-1}$, $k_D = 0.1142\ \mathrm{ps}^{-1}$ and $J/\hbar = -0.3487\ \mathrm{ps}^{-1}$. The only small deviations occur at short times $t < 5$ ps where there is some short time transient, non-Markovian behaviour in the dynamics. It should be noted that approximate resummations of the higher order terms in the rate kernel, such as the Padé approximant, could probably be used to extend the accuracy of the master equations,[134,135,162,167] but this is not the main focus of this work.

Using Model I we can also consider when the incoherent rate approximation will break down. Eq. (4.32) suggests that this will occur for very low reorganisation energies, in which case coherences between singlet radical pair and product states will be large and long-lived and therefore the incoherent rate approximation will break down. This is demonstrated in Fig. 5.3, in which the exact HEOM and second order QME dynamics of $\rho_{1SS}(t)$ and $\mathrm{Im}[\rho_{1ST}(t)]$ are shown for $\Delta_S = 1$ meV and λ_D is varied from 10 meV to 0.1 meV. The parameters used in the second order QME are given in Table 5.2. It can be seen that as the reorganisation energy decreases, the population decay and coherence dynamics become increasingly non-Markovian. For such low reorganisation energies, these examples are in the low activation energy limit, so Eq. (4.34) can be used to predict the breakdown of the incoherent rate approximation, which is expected to occur if $\Delta_S^2/2\lambda_D k_B T \gtrsim 1$. For $\lambda_D = 10$ meV, $\Delta_S^2/2\lambda_D k_B T = 0.020$, for $\lambda_D = 1$ meV, $\Delta_S^2/2\lambda_D k_B T = 0.20$, and for $\lambda_D = 10$ meV, $\Delta_S^2/2\lambda_D k_B T = 2.0$, so this criterion correctly predicts the observed non-Markovian behaviour at low reorganisation energies. It should be noted that these reorganisation energies are exceptionally low. For solution phase electron transfer reactions, the reorganisation energy will normally be > 0.1 eV, so for long range electron transfer reactions, with effective diabatic couplings ≤ 1 meV, the incoherent rate approximation is expected to be valid.

5.2.2 Model II

In all of the tests of the quantum master equations with Model I, $\hat{H}_{1s} = 0$, so we cannot assess the validity of the field-independent rate approximation. Model II however does include a non-zero $\hat{H}_{1s}$, with spin coupling parameters chosen to be comparable to those in a typical organic radical pair, in a typical magnetic field effect experiment. In Fig. 5.4 the

	$\lambda_D = 10$ meV	$\lambda_D = 1$ meV	$\lambda_D = 0.1$ meV
$\hbar^2 k_{f,S}^{(2)}/2\Delta_S^2$	0.0334807 ps	0.119184 ps	0.425478 ps
$2\hbar J^{(2)}/\Delta_S^2$	−0.0119447 ps	−0.0126490 ps	−0.0127222 ps

Table 5.2: Second order master equation parameters for Model I with $\lambda_D = 10$ meV, 1 meV and 0.1 meV calculated using expressions given in the appendix. Note that $k_{b,S}^{(n)} = k_{f,S}^{(n)}$ when $\epsilon_S = 0$.

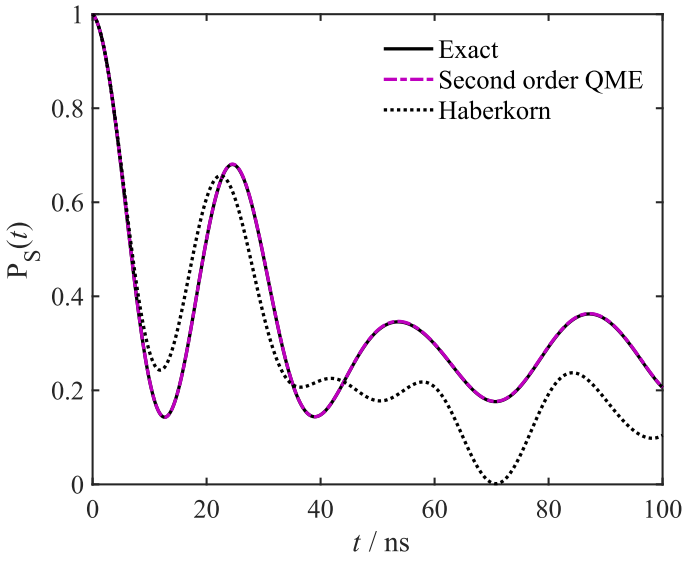

Figure 5.4: The radical pair singlet survival probability as a function of time for radical pair Model II, calculated with the exact HEOM method, the second order radical pair QME and the Haberkorn QME.

dynamics total singlet radical pair survival probability, $P_S(t) = \mathrm{Tr}_s[\hat{P}_S\hat{\rho}_{1s}(t)]$, for Model II is displayed, calculated using HEOM, the second order QME and the Haberkorn QME, in which the scalar coupling J is set to 0 and the second order forward and backward rate constants are used. The second order QME parameters calculated for this model are $\hbar^2 k^{(2)}_{f,S}/2\Delta_S^2 = 0.24057$ ns, $\hbar^2 k^{(2)}_{b,S}/2\Delta_S^2 = 5.0270 \times 10^{-3}$ ns, and $2\hbar J^{(2)}/\Delta_S^2 = -2.0789$ ns.

We see that in this realistic model of a radical pair undergoing a long range electron transfer, the second order QME agrees quantitatively with the exact HEOM results for all times. By contrast, the Haberkorn QME, which ignores the scalar coupling introduced by the presence of the singlet electron transfer pathway, is only accurate for times less than 10 ns, after which it predicts different spin dynamics for the radical pair. This illustrates two important points. Firstly, the field independent rate approximation gives very accurate predictions for spin coupling parameters expected for a typical radical pair reaction. This is in line with Eq. (4.35), because in this example $\|\hat{H}_{1s}\|/\sqrt{k_B T \lambda_D} \approx 10^{-6} \ll 1$. Secondly, ignoring the scalar coupling introduced by the spin selective reactions is not negligible, so the Haberkorn master equation without this term cannot be expected to be accurate in general, even if the electron transfers are strongly non-adiabatic.

5.3 Concluding remarks

In this chapter I have presented simulations that validate the approximations made in deriving the radical pair quantum master equation. This has confirmed that in the non-adiabatic limit the radical pair reaction is well described by the Haberkorn master equation with a correction to the scalar coupling, and beyond this limit additional decoherence appears. In all of this analysis, I have ignored the role of spin relaxation, but having established how to model radical pairs undergoing spin-selective electron transfer without spin relaxation, in the next chapter I will explore how to generalise this to include relaxation effects through the formalism of the Stochastic Liouville equation.

Appendix

5.A Appendix: Harmonic oscillator correlation functions

Analytic expressions for the spin-boson correlation functions can be obtained using harmonic oscillator coherent states.[162] Suppressing the S or T label for simplicity, these expressions are

$$c_1^{(2)}(t) = \exp(\zeta(t) + i\epsilon t/\hbar), \tag{5.A.1}$$

$$\begin{aligned} c_1^{(4)}(t_0, t_1, t_2) = \exp\big(&\zeta(t_1) + \zeta(t_0 - t_2) - \zeta(t_0) \\ &- \zeta(t_2) - \zeta(t_0 - t_1) - \zeta(t_1 - t_2) + i\epsilon(t_0 + t_2)/\hbar\big). \end{aligned} \tag{5.A.2}$$

where the function $\zeta(t)$ is given by

$$\zeta(t) = -\kappa(t) + i\phi(t). \tag{5.A.3}$$

in which $\kappa(t)$ and $\phi(t)$ are related to the spectral density by

$$\kappa(t) = \frac{4}{\pi\hbar}\int_0^\infty \mathrm{d}\omega\, \frac{\mathcal{J}(\omega)}{\omega^2} \coth\left(\frac{\beta\hbar\omega}{2}\right)(1 - \cos(\omega t)) \tag{5.A.4}$$

$$\phi(t) = -\frac{4}{\pi\hbar}\int_0^\infty \mathrm{d}\omega\, \frac{\mathcal{J}(\omega)}{\omega^2} \sin(\omega t). \tag{5.A.5}$$

The equivalent expressions for $c_2^{(2)}(t)$ and $c_2^{(4)}(t_0, t_1, t_2)$ are obtained by changing ϵ in the above expressions to $-\epsilon$. These expressions give rate constants consistent with those obtained previously.[162] These functions were numerically integrated to calculate the rate

constants, dephasing rates and scalar electron spin coupling strengths appearing in the QMEs for Models I and II.

6 The Stochastic Liouville Equation

In Chapter 3 I described how to obtain a quantum master equation for the spin degrees of freedom in a spin selective radical pair reaction. One approximation that was made in this derivation was to ignore the dependence of the spin coupling parameters on the nuclear motion. However it has long been understood in the context of EPR and NMR that fluctuations in spin coupling parameters with nuclear configuration lead to spin relaxation,[3,62,168] which gives rise to transitions between different spin states of the system. This also applies to radical pair spin dynamics, where spin relaxation can make a significant contribution to the degree of singlet-triplet mixing in radical pairs, and therefore have a large effect on various experimental observables such as quantum yields of competing reaction pathways. As a result it is important to understand how to incorporate spin relaxation into the radical pair master equation derived in chapter 3. Therefore here I will describe the framework used to do this, the *Stochastic Liouville Equation* (SLE),[169–174] and how to find approximate solutions to this using the perturbation theory based quantum master equations described in Chapter 2.

6.1 Background

As discussed briefly in section 3.3.2, the spin mixing terms in the radical pair Hamiltonian $\hat{H}_2$ in general depend on the the nuclear position degrees of freedom, which introduces a coupling between the bath of nuclear degrees of freedom and the spin system. This coupling will in general perturb the spin dynamics and enables a direct exchange of energy between

bath and spin degrees of freedom, which causes transitions between spin states.[3,62,168] This process is generally referred to as spin relaxation, because this coupling normally relaxes an initial non-equilibrium spin state to the thermal equilibrium state. The efficiency of relaxation depends on the timescale of the fluctuations of the spin system-bath coupling compared to the frequencies of the unperturbed spin dynamics, and because the spin dynamics are typically much slower than the nuclear dynamics, it is normally the slowest nuclear degrees of freedom, evolving on timescales closest to the spin evolution, that induce the most efficient spin relaxation.

In the Stochastic Liouville equation approach, we explicitly treat the slow nuclear degrees of freedom in addition to the spin degrees of freedom, in order to account for this important coupling.[169–174] Before considering the complication of introducing spin-selective electron transfer reactions, we will first consider the case of a spin system and a generic bath of nuclear bath of nuclear degrees of freedom. The Hamiltonian for this system can be decomposed into three terms,

$$\hat{H} = \hat{H}_\mathrm{s} + \hat{H}_\mathrm{sb} + \hat{H}_\mathrm{b}, \tag{6.1}$$

where $\hat{H}_\mathrm{s}$ is the system Hamiltonian, $\hat{H}_\mathrm{sb}$ is the Hamiltonian describing the coupling between the spins and the bath and $\hat{H}_\mathrm{b}$ is the Hamiltonian describing the bath of nuclear degrees of freedom. We further assume that the initial condition can be factorised into an initial system density operator $\hat{\rho}_\mathrm{s}(0)$ and an initial bath density operator $\hat{\rho}_\mathrm{b}$,

$$\hat{\rho}(0) = \hat{\rho}_\mathrm{s}(0)\hat{\rho}_\mathrm{b} \tag{6.2}$$

and the bath is assumed to initially be at thermal equilibrium

$$\hat{\rho}_\mathrm{b} = \frac{1}{Z} e^{-\beta \hat{H}_\mathrm{b}}. \tag{6.3}$$

The next sections discuss two very closely related forms of the Stochastic Liouville equation for this type of system, where the relevant slow degrees of freedom correspond to either interconversion between different molecular conformations (or sites), or some set of slowly evolving coordinates.

6.2 The *N* site Stochastic Liouville Equation

Here it will be assumed that the relevant slow degrees of freedom modulating the spin Hamiltonian correspond to a slow interconversion between different nuclear configurations. In this case, we divide the bath configurations into a set of N states (or sites), and the position space projection operators $\hat{P}_n = P_n(\hat{\mathbf{Q}})$ project onto each of these N states, and we assume the bath identity operator can be written as $\hat{1}_\mathrm{b} = \sum_{n=1}^{N} \hat{P}_n$, so each $\hat{P}_n$ projects onto a different orthogonal subspace of the bath Hilbert space. In the stochastic Liouville equation, the variables we treat explicitly are the system density operators $\hat{\rho}_{\mathrm{s},n}(t)$ for each site n,

$$\hat{\rho}_{\mathrm{s},n}(t) = \mathrm{Tr}_\mathrm{b}[\hat{P}_n \hat{\rho}(t)]. \tag{6.4}$$

In what follows I will use the Nakajima-Zwanzig approach to derive a master equation for the density operators for each site, and show that with certain additional approximations this reduces to the standard N site Stochastic Liouville equation, which has been used extensively to understand relaxation phenomena in EPR, NMR and spin chemistry. This derivation is based on the Zwanzig projection technique described in chapter 2, which has been used extensively to derive this type of master equation.[57–59,175]

6.2.1 Projection superoperator

In order to find a master equation for the density operators $\hat{\rho}_{\mathrm{s},n}(t)$, we will use the following projection superoperator

$$\mathcal{P} = \sum_{n=1}^{N} \frac{1}{Z_n} \hat{P}_n^\beta \, \mathrm{Tr}_\mathrm{b}[\hat{P}_n \cdot \,] = \sum_{n=1}^{N} \mathcal{P}_n, \tag{6.5}$$

in which $Z_n = \mathrm{Tr}_\mathrm{b}[\hat{P}_n e^{-\beta \hat{H}_\mathrm{b}}]$ is the partition function for state n and for an operator $\hat{A}$, $\hat{A}^\beta$ is

$$\hat{A}^\beta = \frac{1}{2}\left(\hat{A} e^{-\beta \hat{H}_\mathrm{b}} + e^{-\beta \hat{H}_\mathrm{b}} \hat{A}\right). \tag{6.6}$$

This choice of projection operator satisfies $\mathcal{P}^2 = \mathcal{P}$ and $\mathcal{P}\hat{\rho}(0) = \hat{\rho}(0)$ and also by construction if $\hat{\rho}(t)$ is Hermitian then $\mathcal{P}\hat{\rho}(t)$ will also be Hermitian.[a] This choice of superoperator also clearly satisfies $\mathrm{Tr}\left[\hat{P}_n \mathcal{P}\hat{\rho}(t)\right] = \hat{\rho}_{\mathrm{s},n}(t)$, so we can use this to obtain a quantum master equation for the spin density operators for each site.

6.2.2 The final master equation

If we assume also that the spin system-bath coupling is just a function of the bath position operators $\hat{H}_{\mathrm{sb}} = \hat{H}_{\mathrm{sb}}(\hat{\mathbf{Q}})$, then we can divide $\hat{H}_{\mathrm{s}} + \hat{H}_{\mathrm{sb}}$ into a sum of average couplings in state n, $\hat{H}_{\mathrm{s},n}$, and a perturbation $\hat{V}_{\mathrm{sb}}$ as

$$\hat{H}_{\mathrm{s}} + \hat{H}_{\mathrm{sb}} = \sum_{n=1}^{N} \hat{P}_n \hat{H}_{\mathrm{s},n} + \hat{V}_{\mathrm{sb}}(\hat{\mathbf{Q}}) \tag{6.7}$$

where $\hat{H}_{\mathrm{s},n}$ is given by

$$\hat{H}_{\mathrm{s},n} = \hat{H}_{\mathrm{s}} + \frac{1}{Z_n} \mathrm{Tr}_{\mathrm{b}}[\hat{H}_{\mathrm{sb}} \hat{P}_n e^{-\beta \hat{H}_{\mathrm{b}}}]. \tag{6.8}$$

Combining this with $\mathcal{P}$ as defined above, the first term in the Nakajima-Zwanzig equation (Eq. (2.53)), $\mathcal{P}\mathcal{L}\mathcal{P}$, can be simplified to

$$\mathcal{P}\mathcal{L}\mathcal{P} = -\frac{i}{\hbar} \sum_{n=1}^{N} [\hat{H}_{\mathrm{s},n}, \mathcal{P}_n \cdot \,]. \tag{6.9}$$

The term involving $\mathcal{L}_{\mathrm{b}} = -(i/\hbar)[\hat{H}_{\mathrm{b}}, \cdot\,]$ vanishes, so we see from this that transitions between different sites n are entirely described by the kernel $\mathcal{K}(t)$ in the Nakajima-Zwanzig equation. Furthermore if $\hat{H}_{\mathrm{b}}$ does not cause transitions between the different sites, and if $\hat{V}_{\mathrm{sb}}(\hat{\mathbf{Q}})$ is negligible, then each $\hat{\rho}_{\mathrm{s},n}(t)$ would evolve independently under $\hat{H}_{\mathrm{s},n}$, but in general $\hat{H}_{\mathrm{b}}$ does cause transitions between different states, and therefore mixes different $\hat{\rho}_{\mathrm{s},n}(t)$. This will be considered in the next section.

Now applying the Nakajima-Zwanzig equation with the above projection superoperator,

[a] We could define $\hat{P}_n^{\beta} = \int_0^{\beta} \mathrm{d}\lambda\, f(\lambda) e^{-\lambda \hat{H}_{\mathrm{b}}} \hat{P}_n e^{-(\beta-\lambda)\hat{H}_{\mathrm{b}}}$ for any $f(\lambda) > 0$ which satisfies $\int_0^{\beta} \mathrm{d}\lambda\, f(\lambda) = 1$. Any choice of this form reduces to $P_n(\mathbf{q}) e^{-\beta \mathcal{H}_{\mathrm{b}}(\mathbf{p},\mathbf{q})}$ in the classical limit, but this choice ensures that $\mathcal{P}\hat{\rho}(t)$ is Hermitian, and also it simplifies the resulting leading order terms in the Stochastic Liouville equation that we derive, compared to other choices such as the symmetric case $f(\lambda) = \delta(\lambda - \beta/2)$, or the Kubo transformed case $f(\lambda) = 1/\beta$.

and then projecting this onto site n and tracing out the bath gives the following master equation for $\hat{\rho}_{\mathrm{s},n}(t)$,

$$\frac{\mathrm{d}}{\mathrm{d}t}\hat{\rho}_{\mathrm{s},n}(t) = -\frac{i}{\hbar}\left[\hat{H}_{\mathrm{s},n}, \hat{\rho}_{\mathrm{s},n}(t)\right] + \sum_{m=1}^{N}\int_0^t \mathcal{K}_{nm}(t-\tau)\hat{\rho}_{\mathrm{s},m}(\tau)\,\mathrm{d}\tau \tag{6.10}$$

where kernel $\mathcal{K}_{nm}(t)$ is a superoperator given by

$$\mathcal{K}_{nm}(t) = \frac{1}{Z_m}\mathrm{Tr}_{\mathrm{b}}[\hat{P}_n\mathcal{L}e^{\mathcal{Q}\mathcal{L}t}\mathcal{Q}\mathcal{L}\hat{P}_m^{\beta}]. \tag{6.11}$$

Because $\mathcal{L}$ contains the system and system-bath coupling Hamiltonians, this will in general be a superoperator on the spin degrees of freedom. Whilst this is formally exact, it is of little use in constructing models to describe spin relaxation, owing to the complexity of these kernels. So in order to obtain a simpler equation we need to approximate the kernels somehow.

The simplest approximation to make in the kernels is to ignore all spin system dependent terms, so

$$\mathcal{K}_{nm}(t) \approx \kappa_{nm}(t) = \frac{1}{Z_m}\mathrm{Tr}_{\mathrm{b}}[\hat{P}_n\mathcal{L}_{\mathrm{b}}e^{\mathcal{Q}\mathcal{L}_{\mathrm{b}}t}\mathcal{Q}\mathcal{L}_{\mathrm{b}}\hat{P}_m^{\beta}]. \tag{6.12}$$

This will be valid if the spin system energies are very small compared to the nuclear bath energies. Note that $\kappa_{nm}(t)$ does not affect the spin degrees of freedom. The second approximation we make is to invoke the Markovian approximation, and with this the master equation for $\hat{\rho}_{\mathrm{s},n}(t)$ becomes,

$$\frac{\mathrm{d}}{\mathrm{d}t}\hat{\rho}_{\mathrm{s},n}(t) = -\frac{i}{\hbar}\left[\hat{H}_{\mathrm{s},n}, \hat{\rho}_{\mathrm{s},n}(t)\right] + \sum_{m=1}^{N} k_{nm}\hat{\rho}_{\mathrm{s},m}(t) \tag{6.13}$$

where the rate constant $k_{nm} = \int_0^{\infty}\kappa_{nm}(t)\,\mathrm{d}t$. This approximation will be valid for the steady state, and it will be valid for dynamics if the kernels $\kappa_{nm}(t)$ decay on a faster timescale than the population and spin system dynamics. This final master equation is the N site Stochastic Liouville equation.

The kernels $\kappa_{nm}(t)$ can be expressed in terms of side-side, flux-side or flux-flux correlation functions of the bath which are defined as follows.[176] First let us define the flux

operators $\hat{F}_n$ as

$$\hat{F}_n = \frac{i}{\hbar}\left[\hat{H}_\mathrm{b}, \hat{P}_n\right], \tag{6.14}$$

which give the flux into state n, and let us also define the side-side correlation functions

$$c^{\mathrm{ss}}_{nm}(t) = \mathrm{Tr}_\mathrm{b}[\hat{P}_n(t)\hat{P}^\beta_m], \tag{6.15}$$

the flux-side correlation functions,

$$c^{\mathrm{fs}}_{nm}(t) = \mathrm{Tr}_\mathrm{b}[\hat{F}_n(t)\hat{P}^\beta_m] \tag{6.16}$$

and finally the flux-flux correlation functions,

$$c^{\mathrm{ff}}_{nm}(t) = \mathrm{Tr}_\mathrm{b}[\hat{F}_n(t)\hat{F}^\beta_m] \tag{6.17}$$

where $\hat{A}(t) = e^{i\hat{H}_\mathrm{b}t/\hbar}\hat{A}e^{-i\hat{H}_\mathrm{b}t/\hbar}$. Let us also define the side-side kernel as

$$\mathcal{K}^{\mathrm{ss}}(t) = \sum_{n,m=1}^{N} \frac{\hat{P}^\beta_n}{Z_n} c^{\mathrm{ss}}_{nm}(t)\,\mathrm{Tr}_\mathrm{b}[\hat{P}_m\,\cdot\,], \tag{6.18}$$

and the flux-side kernel $\mathcal{K}^{\mathrm{fs}}(t)$ and the flux-flux kernel $\mathcal{K}^{\mathrm{ff}}(t)$ are defined similarly with the side-side correlation functions replaced with the flux-side and flux-flux correlation functions respectively. These kernels can also be written as

$$\mathcal{K}^{\mathrm{ss}}(t) = \mathcal{P}e^{\mathcal{L}_\mathrm{b}t}\mathcal{P} \tag{6.19}$$

$$\mathcal{K}^{\mathrm{fs}}(t) = \mathcal{P}\mathcal{L}_\mathrm{b}e^{\mathcal{L}_\mathrm{b}t}\mathcal{P} \tag{6.20}$$

$$\mathcal{K}^{\mathrm{ff}}(t) = \mathcal{P}\mathcal{L}_\mathrm{b}e^{\mathcal{L}_\mathrm{b}t}\mathcal{L}_\mathrm{b}\mathcal{P}. \tag{6.21}$$

Our aim is to write the Nakajima-Zwanzig kernel $\mathcal{K}(t)$ (with the approximation that the spin system terms are negligible) in terms of these kernels. We do this by noting that $\mathcal{P}\mathcal{L}_\mathrm{b}\mathcal{P} = 0$ and using the Shi & Geva identity,[177]

$$e^{\mathcal{Q}\mathcal{L}_\mathrm{b}t} = e^{\mathcal{L}_\mathrm{b}t} - \int_0^t \mathrm{d}\tau\, e^{\mathcal{L}_\mathrm{b}(t-\tau)}\mathcal{P}\mathcal{L}_\mathrm{b}e^{\mathcal{Q}\mathcal{L}_\mathrm{b}\tau} \tag{6.22}$$

so we can write

$$\mathcal{K}(t) = \mathcal{K}^{\mathrm{ff}}(t) - \int_0^t \mathrm{d}\tau\, \mathcal{K}^{\mathrm{fs}}(t-\tau)\mathcal{K}(\tau) \tag{6.23}$$

and therefore the Markovian limit of the kernel, $\lim_{\omega\to 0}\tilde{\mathcal{K}}(\omega)$, the matrix elements of which are the rate constants $k_{nm} = \lim_{\omega\to 0}\mathrm{Tr}\left[\hat{P}_n\tilde{\mathcal{K}}(\omega)\hat{P}_m^{\beta}\right]/Z_m$, can be written as

$$\lim_{\omega\to 0}\tilde{\mathcal{K}}(\omega) = \lim_{\omega\to 0}[\mathcal{P} + \tilde{\mathcal{K}}^{\mathrm{fs}}(\omega)]^{-1}\tilde{\mathcal{K}}^{\mathrm{ff}}(\omega) \tag{6.24}$$

and using the relations $\mathcal{K}^{\mathrm{fs}}(t) = \frac{\mathrm{d}}{\mathrm{d}t}\mathcal{K}^{\mathrm{ss}}(t)$ and $\mathcal{K}^{\mathrm{ff}}(t) = \frac{\mathrm{d}}{\mathrm{d}t}\mathcal{K}^{\mathrm{fs}}(t)$, as well as the fact that $\mathcal{K}^{\mathrm{ss}}(0) = \mathcal{P}$, and applying the derivative relationship for Fourier-Laplace transforms, this can also be written as

$$\lim_{\omega\to 0}\tilde{\mathcal{K}}(\omega) = \lim_{\omega\to 0}[\tilde{\mathcal{K}}^{\mathrm{ss}}(\omega)]^{-1}\tilde{\mathcal{K}}^{\mathrm{fs}}(\omega). \tag{6.25}$$

This gives formally exact expressions for the rate constants appearing the N site Stochastic Liouville equation.[b] In practice when using the Stochastic Liouville equation, we rarely know *a priori* what the rate constants k_{nm} are, since these expressions are impossible to evaluate exactly for real systems. Instead we use some simple, physically motivated model for the different sites and the rates at which they interconvert, so these expressions for the rate constants are given simply to illustrate their formal connection with the exact underlying quantum dynamics.

6.2.3 Thermal equilibrium

Before proceeding, it is worth discussing the long time limit of the Stochastic Liouville equation, Eq. (6.13), to examine the state to which $\hat{\rho}_{n,\mathrm{s}}(t)$ relaxes. It is relatively straightforward

[b] It should be noted that one could instead apply the weak system interaction approximation to the time convolutionless master equation generator $\mathcal{K}_{\mathrm{TCL}}(t)$ and evaluate this in the long-time limit to obtain the N-site Stochastic Liouville equation instead. In this case the rate constants are given by $k_{nm} = \lim_{t\to\infty}\mathrm{Tr}\left[\hat{P}_n\mathcal{K}^{\mathrm{fs}}(t)[\mathcal{K}^{\mathrm{ss}}(t)]^{-1}\hat{P}_m^{\beta}\right]/Z_m = \lim_{t\to\infty}\mathrm{Tr}\left[\hat{P}_n\mathcal{K}^{\mathrm{ff}}(t)[\mathcal{K}^{\mathrm{fs}}(t)]^{-1}\hat{P}_m^{\beta}\right]/Z_m$, which is a generalisation of the form given in[178]. These two definitions of the rate constants are not strictly the same, but become equivalent if the population dynamics become rate-like in a very short time with no significant transient behaviour.

to show that the rate constants k_{nm} satisfy,

$$k_{nm} = \frac{Z_n}{Z_m} k_{mn} \tag{6.26}$$

$$k_{nn} = -\sum_{m \neq n} k_{mn}. \tag{6.27}$$

With this we deduce that the equilibrium populations, $p_n^{\text{eq}} = Z_n/Z$, where $Z = \sum_{m=1}^{N} Z_m$, satisfy

$$\sum_{m=1}^{N} k_{nm} p_m^{\text{eq}} = 0. \tag{6.28}$$

It can therefore be shown that the steady state solution of the N site Stochastic Liouville equation, denoted by $\hat{\rho}_{\text{s},n}^{\text{eq}}$, which satisfies

$$0 = -\frac{i}{\hbar}\left[\hat{H}_{\text{s},n}, \hat{\rho}_{\text{s},n}^{\text{eq}}\right] + \sum_{m=1}^{N} k_{nm} \hat{\rho}_{\text{s},n}^{\text{eq}} \tag{6.29}$$

is given by

$$\hat{\rho}_{\text{s},n}^{\text{eq}} = \frac{p_n^{\text{eq}}}{d_{\text{s}}} \hat{1}_{\text{s}}. \tag{6.30}$$

where d_{s} is the dimensionality of the spin system Hilbert space. When this is averaged over all sites, we obtain the equilibrium spin system reduced density operator,

$$\hat{\rho}_{\text{s}}^{\text{eq}} = \frac{1}{d_{\text{s}}} \hat{1}_{\text{s}}. \tag{6.31}$$

This is the maximally mixed, infinite temperature thermal equilibrium state of the spin system. Due to the approximation made in obtaining the SLE that we completely ignore the spin interactions in evaluating Nakajima-Zwanzig kernel, the equilibrium state is the infinite temperature equilibrium state. In reality, in the limit of weak system-bath coupling we would expect the spin system to relax to the equilibrium state $e^{-\beta\langle \hat{H}_{\text{s}} \rangle_{\text{eq}}}/Z_{\text{s}}$, where $\left\langle \hat{H}_{\text{s}} \right\rangle_{\text{eq}} = \sum_n p_n^{\text{eq}} \hat{H}_{\text{s},n}$. There are ways to modify the SLE so that in the limit of weak system-bath interactions its steady state is the finite temperature system equilibrium state,[171] but in many radical pair experiments, $k_{\text{B}}T$ is significantly larger than the spin system energies, so $e^{-\beta\langle \hat{H}_{\text{s}} \rangle_{\text{eq}}} \approx \hat{1}_{\text{s}}$ and the spin system steady state of the SLE becomes the correct steady state.

6.3 The slow motion Stochastic Liouville Equation

Another commonly encountered mechanism for spin relaxation is modulation of spin coupling parameters by some set of slowly varying coordinates in the system, for example the anisotropic spin couplings depend on the orientation of the radical, which fluctuates as the molecule tumbles in solution.[57–59] The derivation of a Stochastic Liouville equation to describe this type of relaxation is very similar to the case where the nuclear configuration space is divided into a discrete set of states, so here I will only briefly describe how to apply this approach to describe slow diffusive motion which modulates spin couplings.

The Stochastic Liouville equation is now for a density operator which is a function of the set of slow coordinates $\hat{\rho}_\mathrm{s}(t, \mathsf{X})$, where X denotes the set of slowly varying coordinates. Two common examples of such a set of coordinates X are some vibrational coordinate Q for example a coordinate describing the separation of two radicals in space in a flexible molecular radical pair, or the set of Euler angles describing the orientation of a molecular radical pair in space $\Omega = (\alpha, \beta, \gamma)$. We define the projection operator $\hat{P}(\mathsf{X})$ as a nuclear bath coordinate projection operator onto the state X, and we assume these form a complete set so

$$\hat{1}_\mathrm{b} = \int \mathrm{d}\mathsf{X}\, \hat{P}(\mathsf{X}), \tag{6.32}$$

and we assume these projection operators project onto orthogonal subspaces of the bath Hilbert space. The integral is over all possible values of the set of coordinates, for example if $\mathsf{X} = \Omega$, the set of Euler angles describing the orientation of a molecular, then $\int \mathrm{d}\Omega = \int_0^{2\pi} \mathrm{d}\alpha \int_0^{\pi} \sin\beta\, \mathrm{d}\beta \int_0^{2\pi} \mathrm{d}\gamma$.[43] The density operator $\hat{\rho}_\mathrm{s}(t, \mathsf{X})$ for which we seek an equation of motion can be related to the full density operator by

$$\hat{\rho}_\mathrm{s}(t, \mathsf{X}) = \mathrm{Tr}_\mathrm{b}[\hat{P}(\mathsf{X})\hat{\rho}(t)]. \tag{6.33}$$

In what follows we once again assume that the initial condition factorises into a bath equilibrium part and a system density operator as in Eq. (6.2).

6.3.1 Projection superoperators

We can construct a projection superoperator for which $\hat{\rho}_{\mathrm{s}}(t,\mathsf{X}) = \mathrm{Tr}_{\mathrm{b}}[\hat{P}(\mathsf{X})\mathcal{P}\hat{\rho}(t)]$ and $\mathcal{P}\hat{\rho}(0) = \hat{\rho}(0)$ in an analogous way to the case of a discrete set of states,

$$\mathcal{P} = \int \mathrm{d}\mathsf{X}\, \mathcal{P}(\mathsf{X}) \tag{6.34}$$

where $\mathcal{P}(\mathsf{X})$ is given by

$$\mathcal{P}(\mathsf{X}) = \frac{1}{Z(\mathsf{X})}\hat{P}^{\beta}(\mathsf{X})\,\mathrm{Tr}_{\mathrm{b}}[\hat{P}(\mathsf{X})\,\cdot\,], \tag{6.35}$$

where $\hat{P}^{\beta}(\mathsf{X}) = (\hat{P}(\mathsf{X})e^{-\beta\hat{H}_{\mathrm{b}}} + e^{-\beta\hat{H}_{\mathrm{b}}}\hat{P}(\mathsf{X}))/2$ and $Z(\mathsf{X}) = \mathrm{Tr}_{\mathrm{b}}[\hat{P}^{\beta}(\mathsf{X})]$. We can now plug this into the Nakajima-Zwanzig equation and from that obtain a master equation for $\hat{\rho}_{\mathrm{s}}(t,\mathsf{X})$.

6.3.2 The final master equation

In order to derive the full master equation, we first need to find $\mathcal{P}\mathcal{L}\mathcal{P}$. We assume that $\mathcal{P}\mathcal{L}_{\mathrm{b}}\mathcal{P} = 0$ and therefore $\mathcal{P}\mathcal{L}\mathcal{P}$ becomes

$$\mathcal{P}\mathcal{L}\mathcal{P} = -\frac{i}{\hbar}\int \mathrm{d}\mathsf{X}\,[\hat{H}_{\mathrm{s}}(\mathsf{X}), \mathcal{P}(\mathsf{X})\,\cdot\,], \tag{6.36}$$

in which $\hat{H}_{\mathrm{s}}(\mathsf{X})$ is

$$\hat{H}_{\mathrm{s}}(\mathsf{X}) = \hat{H}_{\mathrm{s}} + \frac{1}{Z(\mathsf{X})}\,\mathrm{Tr}_{\mathrm{b}}[\hat{H}_{\mathrm{sb}}\hat{P}(\mathsf{X})e^{-\beta\hat{H}_{\mathrm{b}}}], \tag{6.37}$$

is the average system Hamiltonian in state X.

Once again to simplify the kernel term we invoke the Markovian approximation and we ignore all spin system dependent terms in evaluating the kernel. As such we can now write the SLE for the X dependent spin density operator as

$$\frac{\partial}{\partial t}\hat{\rho}_{\mathrm{s}}(t,\mathsf{X}) = -\frac{i}{\hbar}[\hat{H}_{\mathrm{s}}(\mathsf{X}), \hat{\rho}_{\mathrm{s}}(t,\mathsf{X})] + \int \mathrm{d}\mathsf{X}'\, k(\mathsf{X},\mathsf{X}')\hat{\rho}_{\mathrm{s}}(t,\mathsf{X}'). \tag{6.38}$$

Here the transition kernel $k(\mathsf{X},\mathsf{X}')$ is given by

$$k(\mathsf{X},\mathsf{X}') = \int_0^{\infty} \mathrm{d}t\,\mathrm{Tr}_{\mathrm{b}}[\hat{P}(\mathsf{X})\mathcal{L}_{\mathrm{b}}e^{\mathcal{Q}\mathcal{L}_{\mathrm{b}}t}\mathcal{Q}\mathcal{L}_{\mathrm{b}}\hat{P}^{\beta}(\mathsf{X}')]. \tag{6.39}$$

In practice this is impossible to calculate *a priori* so we instead use some model for the transition kernel between the different X states. Two important examples are given in the next sections: an overdamped vibrational coordinate and rotational diffusion. For all models of slow motion used in this work, the transition kernel is local, so instead we can write the SLE as

$$\frac{\partial}{\partial t}\hat{\rho}_{\mathrm{s}}(t,\mathsf{X}) = -\frac{i}{\hbar}[\hat{H}_{\mathrm{s}}(\mathsf{X}),\hat{\rho}_{\mathrm{s}}(t,\mathsf{X})] + \Gamma\hat{\rho}_{\mathrm{s}}(t,\mathsf{X}), \tag{6.40}$$

where Γ is some differential operator on X. In the classical limit, this is equivalent to the Smoluchowski operator appearing in the Smoluchowski equation for the evolution of the conditional probability $p(\mathsf{X},t|\mathsf{X}_0,t_0)$ for finding observing X at time t given that X_0 was observed at time t_0,[63,179]

$$\frac{\partial}{\partial t}p(\mathsf{X},t|\mathsf{X}_0,t_0) = \Gamma p(\mathsf{X},t|\mathsf{X}_0,t_0). \tag{6.41}$$

As a result of this we can use classical theories to obtain models for Γ.

Before continuing, we should briefly note that the analysis in section 6.2.3 applies to this equation as well, and this form of the SLE also relaxes the system to its infinite temperature equilibrium state. As discussed above this is normally valid because $k_{\mathrm{B}}T$ is much larger than the spin system energies, and therefore the system's equilibrium state is effectively the infinite temperature equilibrium state.

6.3.3 Example: overdamped vibrational motion

Here I will briefly outline how to obtain the Smoluchowski operator Γ for the case of the slow coordinate being an overdamped classical vibrational degree of freedom Q. In this case we can describe the motion of $Q(t)$ with the Langevin equation,[63,179]

$$m\frac{\mathrm{d}^2Q(t)}{\mathrm{d}t^2} = -\gamma\frac{\mathrm{d}Q(t)}{\mathrm{d}t} + F(Q(t)) + \xi(t), \tag{6.42}$$

where m is the mass associated with this vibrational mode, γ is the friction coefficient and $F(Q)$ is the conservative force acting on the mode and $\xi(t)$ is a randomly fluctuating force. This force at time t is assumed to be uncorrelated with $Q(t)$, it is also assumed to have a

zero mean value and correlation given by

$$\langle \xi(t) \rangle = 0 \tag{6.43}$$

$$\langle \xi(t)\xi(t') \rangle = 2\gamma k_{\mathrm{B}} T \delta(t - t'). \tag{6.44}$$

In the overdamped limit it is assumed that $|m\frac{\mathrm{d}^2 Q(t)}{\mathrm{d}t^2}| \ll |\gamma \frac{\mathrm{d}Q(t)}{\mathrm{d}t}|$, so we neglect the term on the left hand side of this equation, and thus obtain the overdamped Langevin equation

$$\frac{\mathrm{d}Q(t)}{\mathrm{d}t} = \frac{1}{\gamma} F(Q(t)) + \frac{1}{\gamma} \xi(t). \tag{6.45}$$

The time evolution of the expectation value of an arbitrary function of Q, $f(Q)$, in a short time δt is given by[179]

$$\langle \delta f(Q(t)) \rangle = \langle f(Q(t) + \delta Q(t)) - f(Q(t)) \rangle \tag{6.46}$$

$$= \langle f'(Q(t)) \delta Q(t) \rangle + \frac{1}{2} \left\langle f''(Q(t)) \delta Q(t)^2 \right\rangle + \cdots, \tag{6.47}$$

where the $Q(t_0)$ is sampled from some initial distribution $p_0(Q)$ and where $\delta Q(t)$ is given by

$$\delta Q(t) = \int_t^{t+\delta t} \frac{\mathrm{d}Q(t')}{\mathrm{d}t'} \, \mathrm{d}t' = \int_t^{t+\delta t} \frac{1}{\gamma} F(Q(t)) \, \mathrm{d}t' + \int_t^{t+\delta t} \frac{1}{\gamma} \xi(t') \, \mathrm{d}t' \,. \tag{6.48}$$

Using the fact that the force $\xi(t)$ is uncorrelated with $Q(t)$, $\langle \delta f(Q(t)) \rangle$ can be expanded to first order in δt as

$$\begin{aligned} \langle \delta f(Q(t)) \rangle &= \left\langle f'(Q(t)) \frac{1}{\gamma} F(Q(t)) \right\rangle \delta t \\ &\quad + \frac{1}{2} \left\langle f''(Q(t)) \int_t^{t+\delta t} \frac{1}{\gamma} \xi(t') \, \mathrm{d}t' \int_t^{t+\delta t} \frac{1}{\gamma} \xi(t'') \, \mathrm{d}t'' \right\rangle + O(\delta t^2) \end{aligned} \tag{6.49}$$

$$\begin{aligned} &= \left\langle f'(Q(t)) \frac{1}{\gamma} F(Q(t)) \right\rangle \delta t \\ &\quad + \frac{1}{2} \left\langle f''(Q(t)) \frac{1}{\gamma^2} \right\rangle \int_t^{t+\delta t} \int_t^{t+\delta t} \mathrm{d}t' \, \mathrm{d}t'' \, \langle \xi(t') \xi(t'') \rangle + O(\delta t^2) \end{aligned} \tag{6.50}$$

$$= \left\langle f'(Q(t)) \frac{1}{\gamma} F(Q(t)) \right\rangle \delta t + \left\langle f''(Q(t)) \frac{k_{\mathrm{B}} T}{\gamma} \right\rangle \delta t + O(\delta t^2). \tag{6.51}$$

We can equivalently write $\langle \delta f(Q(t)) \rangle$ in terms of the conditional probability

$$\langle \delta f(Q(t)) \rangle = \int_{-\infty}^{\infty} \int_{-\infty}^{\infty} f(Q) \frac{\partial}{\partial t} p(Q, t|Q_0, t_0) p_0(Q_0) \, \mathrm{d}Q \, \mathrm{d}Q_0 \, \delta t + O(\delta t^2) \tag{6.52}$$

and assuming $p(Q, t|Q_0, t_0) \to 0$ as $|Q| \to \infty$, the expectation values on the right hand side of Eq. (6.51) can be re-written using integration by parts as

$$\begin{aligned} \langle \delta f(Q(t)) \rangle = \int_{-\infty}^{\infty} \int_{-\infty}^{\infty} f(Q) \frac{\partial}{\partial Q} \left(\frac{k_\mathrm{B} T}{\gamma} \frac{\partial}{\partial Q} - \frac{1}{\gamma} F(Q) \right) \\ \times p(Q, t|Q_0, t_0) p_0(Q_0) \, \mathrm{d}Q \, \mathrm{d}Q_0 \, \delta t + O(\delta t^2). \end{aligned} \tag{6.53}$$

Noting that this is true for any function $f(Q)$ we deduce that the conditional probability evolves according to

$$\frac{\partial}{\partial t} p(Q, t|Q_0, t_0) = \frac{\partial}{\partial Q} \left(\frac{k_\mathrm{B} T}{\gamma} \frac{\partial}{\partial Q} - \frac{1}{\gamma} F(Q) \right) p(Q, t|Q_0, t_0). \tag{6.54}$$

Therefore the Smoluchowski operator is

$$\Gamma = D \frac{\partial}{\partial Q} \left(\frac{\partial}{\partial Q} - \frac{1}{k_\mathrm{B} T} F(Q) \right), \tag{6.55}$$

where the diffusion constant D is defined as $D = k_\mathrm{B} T / \gamma$.

6.3.4 Example: rotational diffusion

Another important source of spin relaxation a molecular radical in solution is modulation of anisotropic spin coupling terms by rotational diffusion of radicals. The slow variables we need to treat for this mechanism of relaxation are the Euler angles describing the orientation of the molecule Ω. In this case we can approximate the rotational motion as that of a rigid body experiencing frictional drag and a randomly fluctuating torque, so we can use the same ideas as in the case of an overdamped vibrational mode to obtain the Smoluchowski operator for rotational diffusion. Here I will simply state the result for the Smoluchowski operator[43,180,181]

$$\Gamma = -\mathbf{L} \cdot \mathbf{D} \cdot \left(\mathbf{L} + \mathbf{L} \frac{V(\Omega)}{k_\mathrm{B} T} \right), \tag{6.56}$$

in which $\mathbf{D}$ is the rotational diffusion tensor (a 3×3 matrix), $V(\Omega)$ is the potential energy of a given orientation and $\mathbf{L} = (\mathsf{L}_X, \mathsf{L}_Y, \mathsf{L}_Z)^\mathsf{T}$ is a vector of unitless, body-fixed angular momentum operators. In the absence of an aligning potential $V(\Omega)$, as is the case for free rotational diffusion in solution, and by choosing the body fixed axes to correspond to the eigenvectors (principal axes) of $\mathbf{D}$, this simplifies to

$$\Gamma = -\left(D_X \mathsf{L}_X^2 + D_Y \mathsf{L}_X^2 + D_Z \mathsf{L}_Z^2\right), \tag{6.57}$$

where D_X, D_Y, D_Z are the principal components of $\mathbf{D}$ i.e. its eigenvalues.

6.4 The radical pair Stochastic Liouville Equation

Having discussed how to obtain the Stochastic Liouville equation appropriate for describing spin relaxation in the absence of electron transfer reactions, we will now turn to the problem of spin relaxation in recombining radical pairs. The solution will be to combine the Nakajima-Zwanzig equation based methods used in chapter 3 to obtain the radical pair master equation in the absence of relaxation, and the approach taken above in sections 6.2 and 6.3 to derive the Stochastic Liouville equation for a spin system without including recombination processes.

In the spirit of the Stochastic Liouville equation, we will treat the slow degrees of freedom X which cause relaxation explicitly, so we seek a master equation for the set of density operators $\hat{\rho}_{i\mathrm{s}}(t, \mathsf{X})$ which are spin system density operators, for each set of electronic states i, which also depend on the slow degrees of freedom X. The slow coordinate dependent density operators $\hat{\rho}_{i\mathrm{s}}(t, \mathsf{X})$ are defined in terms of the full density operator $\hat{\rho}(t)$ by combining Eq. (3.29) for the electronic state spin density operators $\hat{\rho}_{i\mathrm{s}}(t)$, with Eq. (6.33) for the X dependent spin density operator $\hat{\rho}_{\mathrm{s}}(t, \mathsf{X})$ (we now switch from using b to denote the nuclear bath degrees of freedom to n as in chapter 3)

$$\hat{\rho}_{i\mathrm{s}}(t, \mathsf{X}) = \hat{\Pi}_i \, \mathrm{Tr}_\mathrm{n}[\hat{P}(\mathsf{X})\hat{\rho}(t)]\hat{\Pi}_i, \tag{6.58}$$

where $\hat{P}(\mathsf{X})$ are nuclear coordinate dependent projection operators, and $\hat{\Pi}_i$ are the electron state projection operators defined in Eq. (3.28). In what follows the slow "coordinates"

X could refer to a continuous set of coordinates as in section 6.33 or they could refer to a discrete set of states as in section 6.2, or some combination of these.

As in the previous chapter, we will assume the radical pair system is described by a Hamiltonian of the form given in Eq. (3.18), and for simplicity we will only consider three sets of quasi-diabatic electron transfer states as in Eq. (3.25). Using this framework and the ideas discussed earlier in this chapter, we will now derive the radical pair SLE using the Nakajima-Zwanzig approach.

6.4.1 Projection superoperators

The Zwanzig projection superoperator which can be used in the Nakajima-Zwanzig equation to obtain a master equation for $\hat{\rho}_{is}(t, \mathsf{X})$ combines the projection operators given in Eq. (3.32) and Eq. (6.34),

$$\mathcal{P} = \sum_i \int \mathrm{d}\mathsf{X}\, \mathcal{P}_i(\mathsf{X}), \tag{6.59}$$

where $\mathcal{P}_i(\mathsf{X})$ is

$$\mathcal{P}_i(\mathsf{X}) = \frac{1}{Z_i(\mathsf{X})} \hat{P}_i^{\beta}(\mathsf{X}) \hat{\Pi}_i \,\mathrm{Tr}_{\mathrm{n}}[\hat{P}(\mathsf{X}) \cdot]\hat{\Pi}_i. \tag{6.60}$$

The operator $\hat{P}_i^{\beta}(\mathsf{X})$ is given by

$$\hat{P}_i^{\beta}(\mathsf{X}) = \frac{1}{2}\left(\hat{P}(\mathsf{X}) e^{-\beta \hat{H}_{i\mathrm{n}}} + e^{-\beta \hat{H}_{i\mathrm{n}}} \hat{P}(\mathsf{X})\right), \tag{6.61}$$

We see that for the initial condition given by Eq. (3.30), $\mathcal{P}\hat{\rho}(0) = \hat{\rho}(0)$, and we can replace $\hat{\rho}(t)$ with $\mathcal{P}\hat{\rho}(t)$ in Eq. (6.58) to obtain $\hat{\rho}_{is}(t, \mathsf{X})$.

6.4.2 The reference and perturbation Hamiltonians

As before we can split the Hamiltonian into a reference part $\hat{H}_0$ and a perturbation $\hat{V}$. Here we will use the same notation for the components of the radical pair Hamiltonian as given in section 3.2, namely $\hat{H}_1$ is the spin preserving term of the Molecular Hamiltonian given by Eq. (3.25), and $\hat{H}_2$ is the spin-mixing term. The reference Hamiltonian $\hat{H}_0$ here is given

by

$$\hat{H}_0 = \sum_i \hat{\Pi}_i \hat{H}_1 \hat{\Pi}_i + \sum_i \int \mathrm{d}\mathsf{X}\, \hat{P}(\mathsf{X}) \hat{\Pi}_i \,\mathrm{Tr}_\mathrm{n}[\hat{P}(\mathsf{X}) \hat{H}_2 e^{-\beta \hat{H}_{i\mathrm{n}}}] \hat{\Pi}_i \tag{6.62}$$

$$= \sum_i \hat{\Pi}_i \hat{H}_{i\mathrm{n}} + \sum_i \int \mathrm{d}\mathsf{X}\, \hat{P}(\mathsf{X}) \hat{\Pi}_i \hat{H}_{i\mathrm{s}}(\mathsf{X}), \tag{6.63}$$

where $\hat{H}_{i\mathrm{n}}$ is the nuclear diabatic state Hamiltonian given by Eq. (3.25), and $\hat{H}_{i\mathrm{s}}(\mathsf{X})$ is the spin Hamiltonian for state i in configuration X, which is analogous to $\hat{H}_\mathrm{s}(\mathsf{X})$ given in Eq. (6.37) in the previous section. The perturbation $\hat{V}$ is given by

$$\hat{V} = \hat{V}_\mathrm{S} + \hat{V}_\mathrm{T} + \sum_{ij} \int \mathrm{d}\mathsf{X}\, \hat{V}_{\mathrm{sn},ij}(\mathsf{X}) \hat{P}(\mathsf{X}) \tag{6.64}$$

where $\hat{V}_\mathrm{S}$ and $\hat{V}_\mathrm{T}$ are the diabatic coupling Hamiltonians as in Eqs. (3.38) and (3.39), and $\hat{V}_{\mathrm{sn},ij}(\mathsf{X})$ is given by

$$\hat{V}_{\mathrm{sn},ij}(\mathsf{X}) = \hat{\Pi}_i \hat{H}_2 \hat{\Pi}_j \hat{P}(\mathsf{X}) - \delta_{ij} \hat{H}_{i\mathrm{s}}(\mathsf{X}) \hat{\Pi}_i. \tag{6.65}$$

This form of the perturbation assumes that the spin mixing term in the total Hamiltonian $\hat{H}_2$ depends only on the nuclear positions and not on the nuclear momenta. In a strictly diabatic representation $\hat{V}_\mathrm{S}$ is just a function of the nuclear coordinates, so these could be written as $\hat{V}_\mathrm{S} = \int \mathrm{d}\mathsf{X}\, \hat{V}_\mathrm{S}(\mathsf{X}) \hat{P}(\mathsf{X})$, and likewise for $\hat{V}_\mathrm{T}$, but for a general quasi-diabatic representation this is not true. However we can often make the Condon approximation, where the coupling operators $\hat{\Delta}_\mathrm{S}$ and $\hat{\Delta}_\mathrm{T}$ can be approximated as constants, in which case these coupling operators can be written as an integral of X dependent terms $\hat{V}_\mathrm{S}(\mathsf{X}) = \hat{V}_\mathrm{S}$.

6.4.3 The radical pair master equation

With the projection superoperators defined above, and the with the splitting of the Hamiltonian into reference and perturbation parts as above, we can apply the incoherent rate and field independent rate approximations as in chapter 3, together with a second order treatment of the diabatic coupling to obtain a master equation for the spin density operators. The terms in the kernel that cause transitions between X states in a given electron transfer state can be dealt with in the same way as in section 6.3, namely we neglect spin system terms in

evaluating these parts of the kernel and apply the Markovian approximation, and we further ignore the effect of diabatic coupling in this term. With this we obtain the following second order master equation for the radical pair spin density operator, where we ignore the back reaction terms for simplicity,

$$\begin{aligned}\frac{\partial}{\partial t}\hat{\rho}_{1\mathrm{s}}(t,\mathsf{X}) = &-\frac{i}{\hbar}\left[\hat{H}_{1\mathrm{s}}(\mathsf{X}),\hat{\rho}_{1\mathrm{s}}(t,\mathsf{X})\right]\\ &+\int \mathrm{d}\mathsf{X}'\left(-\frac{i}{\hbar}\left[-2J^{(2)}(\mathsf{X},\mathsf{X}')\hat{\mathbf{S}}_1\cdot\hat{\mathbf{S}}_2,\hat{\rho}_{1\mathrm{s}}(t,\mathsf{X}')\right]\right.\\ &\left.-\left\{\frac{k^{(2)}_{\mathrm{f,S}}(\mathsf{X},\mathsf{X}')}{2}\hat{P}_{\mathrm{S}}+\frac{k^{(2)}_{\mathrm{f,T}}(\mathsf{X},\mathsf{X}')}{2}\hat{P}_{\mathrm{T}},\hat{\rho}_{1\mathrm{s}}(t,\mathsf{X}')\right\}+k_1(\mathsf{X},\mathsf{X}')\hat{\rho}_{1\mathrm{s}}(t,\mathsf{X}')\right)\end{aligned} \tag{6.66}$$

$k_1(\mathsf{X},\mathsf{X}')$ is the transition kernel given by Eq. (6.39) with $\hat{H}_{\mathrm{b}}$ replaced with $\hat{H}_{1\mathrm{n}}$, and $J^{(2)}(\mathsf{X},\mathsf{X}')$, $k^{(2)}_{\mathrm{f,S}}(\mathsf{X},\mathsf{X}')$ and $k^{(2)}_{\mathrm{f,T}}(\mathsf{X},\mathsf{X}')$ are the second order energy shifts and singlet and triplet forward rate constants. It should be noted that these terms also give rise to transitions between different X states. The rate constants appearing in the second order Haberkorn term and the singlet and triplet contributions to the energy shifts, are given by the expressions in section 3.3.6 of the previous chapter, but with $c^{(2)}_{1\mathrm{S}}(t)$ replaced with

$$c^{(2)}_{1\mathrm{S}}(t,\mathsf{X},\mathsf{X}') = \mathrm{Tr}_{\mathrm{n}}[e^{+i\hat{H}_{1\mathrm{n}}t/\hbar}\hat{P}(\mathsf{X})\hat{f}_{\mathrm{S}}e^{-i\hat{H}_{2\mathrm{n}}t/\hbar}\hat{f}^{\dagger}_{\mathrm{S}}\hat{P}^{\beta}_{1}(\mathsf{X}')]. \tag{6.67}$$

and Z_1 replaced with $Z_1(\mathsf{X}')$.

In the classical limit, for a strictly diabatic basis (or if we can ignore any nuclear momentum dependence in $\hat{\Delta}_{\mathrm{S}}$ and $\hat{\Delta}_{\mathrm{T}}$), the off diagonal terms in $\hat{J}^{(2)}(\mathsf{X},\mathsf{X}')$, $k^{(2)}_{\mathrm{f,S}}(\mathsf{X},\mathsf{X}')$ and $k^{(2)}_{\mathrm{f,T}}(\mathsf{X},\mathsf{X}')$ vanish and these terms become local, because in this limit the correlation functions become local in X e.g.

$$c^{(2)}_{1\mathrm{S}}(t,\mathsf{X},\mathsf{X}') = \delta(\mathsf{X}-\mathsf{X}')\int \mathrm{d}\mathsf{X}''\, c^{(2)}_{1\mathrm{S}}(t,\mathsf{X}'',\mathsf{X}'). \tag{6.68}$$

Therefore we can approximate the recombination and energy shift terms in the radical pair

master equation as being local, so the master equation becomes

$$\begin{aligned}\frac{\partial}{\partial t}\hat{\rho}_{1\mathrm{s}}(t,\mathsf{X}) = &-\frac{i}{\hbar}\left[\hat{H}_{1\mathrm{s}}(\mathsf{X}) - 2J^{(2)}(\mathsf{X})\hat{\mathbf{S}}_1\cdot\hat{\mathbf{S}}_2, \hat{\rho}_{1\mathrm{s}}(t,\mathsf{X})\right] \\ &- \left\{\frac{k^{(2)}_{\mathrm{f,S}}(\mathsf{X})}{2}\hat{P}_{\mathrm{S}} + \frac{k^{(2)}_{\mathrm{f,T}}(\mathsf{X})}{2}\hat{P}_{\mathrm{T}}, \hat{\rho}_{1\mathrm{s}}(t,\mathsf{X})\right\} + \Gamma\hat{\rho}_{1\mathrm{s}}(t,\mathsf{X}),\end{aligned} \tag{6.69}$$

in which $J^{(2)}(\mathsf{X}) = \int \mathrm{d}\mathsf{X}'\, J^{(2)}(\mathsf{X}',\mathsf{X})$, and likewise for $k^{(2)}_{\mathrm{f,S}}(\mathsf{X})$ and $k^{(2)}_{\mathrm{f,T}}(\mathsf{X})$, and we have also replaced the transition kernel term with $\Gamma\hat{\rho}_{1\mathrm{s}}(t,\mathsf{X})$ for brevity.

At higher orders in the diabatic coupling, a reactive decoherence term appears, which also causes transitions between different X states. Again we can expect the dominant terms to be the diagonal terms, so we can make the same local approximation to these terms as above, so the Stochastic Liouville equation for a recombining radical pair can be written as

$$\begin{aligned}\frac{\partial}{\partial t}\hat{\rho}_{1\mathrm{s}}(t,\mathsf{X}) = &-\frac{i}{\hbar}\left[\hat{H}_{1\mathrm{s}}(\mathsf{X}) - 2J(\mathsf{X})\hat{\mathbf{S}}_1\cdot\hat{\mathbf{S}}_2, \hat{\rho}_{1\mathrm{s}}(t,\mathsf{X})\right] - \left\{\frac{k_{\mathrm{f,S}}(\mathsf{X})}{2}\hat{P}_{\mathrm{S}} + \frac{k_{\mathrm{f,T}}(\mathsf{X})}{2}\hat{P}_{\mathrm{T}}, \hat{\rho}_{1\mathrm{s}}(t,\mathsf{X})\right\} \\ &- k_{\mathrm{D}}(\mathsf{X})\left(\hat{P}_{\mathrm{S}}\hat{\rho}_{1\mathrm{s}}(t,\mathsf{X})\hat{P}_{\mathrm{T}} + \hat{P}_{\mathrm{T}}\hat{\rho}_{1\mathrm{s}}(t,\mathsf{X})\hat{P}_{\mathrm{S}}\right) + \Gamma\hat{\rho}_{1\mathrm{s}}(t,\mathsf{X}).\end{aligned} \tag{6.70}$$

To recap, the approximations necessary to obtain this form of the radical pair SLE are: the electron transfers can be described as incoherent and rate-like, the rates are independent of the spin interactions, and the electron transfer processes and spin interactions are assumed to have no effect on the transitions between different states.

Furthermore for certain relaxation mechanisms, it is also reasonable to approximate the slow coordinate dependent parameters, such as $k_{\mathrm{f,S}}(\mathsf{X})$, to be independent of the X. For example, for radical pairs rotating freely in solution, we would not expect the rate constants and energy shifts to be dependent on the orientation of the molecule in space, so we can treat these parameters as being independent of of the orientation of the radical pair Ω.

Thus far I have outlined how to treat spin relaxation processes in radical pairs using the Stochastic Liouville equation. Describing real radical pair reactions with this equation however presents difficulties due to the high computational cost of solving the SLE numerically, particularly for large spin systems, so this motivates the development of approximate radical pair master equations which account for the effects of spin relaxation. In the rest of this

chapter I examine the accuracy of perturbative master equation techniques when applied to this problem, with the aim of finding a suitable approach for modelling spin relaxation in realistic models of radical pair reactions.

6.5 Approximate relaxation master equations

In this section I will describe how to apply perturbative master equation techniques to find approximate solutions to the radical pair Stochastic Liouville equation, with the aim of finding a computationally efficient method for obtaining spin system observables, which is valid over a wide range parameters for the stochastic fluctuations.

6.5.1 Thermal averaging and fluctuation terms

In the Stochastic Liouville equation formalism, the object that contains all information about the radical pair spin system is the spin density operator $\hat{\rho}(t, \mathsf{X})$, which obeys Eq. (6.70) (dropping the 1s label[c]). Most experimental observables, for example the total radical pair concentration, or the singlet and triplet quantum yields, are independent of the slow coordinates X, so we do not need the full X dependent density operator, but instead we only need the average of this over all X, which here is denoted by $\hat{\rho}(t)$,

$$\hat{\rho}(t) = \int \mathrm{d}\mathsf{X}\, \hat{\rho}(t, \mathsf{X}). \tag{6.71}$$

In fact many experimental observables only depend on the time integrated average spin density operator, for example the singlet and triplet product quantum yields of a radical pair reaction, Φ_S and Φ_T (assuming $k_\mathrm{S}(\equiv k_{\mathrm{f,S}})$ and $k_\mathrm{T}(\equiv k_{\mathrm{f,T}})$ are independent of X),

$$\Phi_\mathrm{S} = k_\mathrm{S} \int_0^\infty \mathrm{Tr}\big[\hat{P}_\mathrm{S}\hat{\rho}(t)\big]\, \mathrm{d}t \tag{6.72a}$$

$$\Phi_\mathrm{T} = k_\mathrm{T} \int_0^\infty \mathrm{Tr}\big[\hat{P}_\mathrm{T}\hat{\rho}(t)\big]\, \mathrm{d}t\,, \tag{6.72b}$$

[c] To avoid cluttered notation, I henceforth use $\hat{\rho}$ in place of $\hat{\rho}_{1\mathrm{s}}$. We will no longer be dealing with the full density operator for all degrees of freedom of the system, and we will also ignore the back reaction processes in the radical pair reaction, so the distinction between spin system density operators for different electron transfer states is no longer required. Similarly the f subscript is dropped from $k_{\mathrm{f,S}}$ and $k_{\mathrm{f,T}}$ and $\mathrm{Tr}[\cdots]$ is now used to denote the trace over the radical pair spin Hilbert space.

and the radical pair lifetime, τ_{RP},

$$\tau_{\mathrm{RP}} = \int_0^\infty \mathrm{Tr}[\hat{\rho}(t)]\,\mathrm{d}t\,, \tag{6.73}$$

where $\mathrm{Tr}[\cdots]$ denotes the trace over the spin Hilbert space of the radical pair.

In what follows we assume that $\hat{\rho}(0,\mathsf{X})$ factorises into a product of an initial spin density operator $\hat{\rho}(0)$, and $p_0(\mathsf{X})$, an initial density for X,

$$\hat{\rho}(0,\mathsf{X}) = \hat{\rho}(0)p_0(\mathsf{X}), \tag{6.74}$$

where these are normalised such that $\mathrm{Tr}[\hat{\rho}(0)] = 1$ and $\int \mathrm{d}\mathsf{X}\, p_0(\mathsf{X}) = 1$. Furthermore we take $p_0(\mathsf{X})$ to be an equilibrium state of X so $\Gamma p_0(\mathsf{X}) = 0$.

The full X dependent Liouvillian $\mathcal{L}$, as defined by the right-hand side of Eq. (6.70), can be split into a reference part and fluctuation term, which will be treated as a perturbation. The reference part $\mathcal{L}_0$ is taken to be

$$\mathcal{L}_0 = \langle\mathcal{L}\rangle + \Gamma, \tag{6.75}$$

in which $\langle\mathcal{L}\rangle$[d] is the thermally averaged spin Liouvillian,

$$\langle\mathcal{L}\rangle = -\frac{i}{\hbar}\left[\left\langle\hat{H}\right\rangle, \cdot\,\right] - \left\{\left\langle\hat{K}\right\rangle, \cdot\,\right\} - \langle k_{\mathrm{D}}\rangle\left(\hat{P}_{\mathrm{S}}\,\cdot\,\hat{P}_{\mathrm{T}} + \hat{P}_{\mathrm{T}}\,\cdot\,\hat{P}_{\mathrm{S}}\right), \tag{6.76}$$

where $\left\langle\hat{H}\right\rangle$ is the thermal average of the full effective spin Hamiltonian, $\hat{H}(\mathsf{X})$, including the energy shift term, $\left\langle\hat{K}\right\rangle$ is the thermal average of the X dependent Haberkorn operator $\hat{K}(\mathsf{X})$, and $\langle k_{\mathrm{D}}\rangle$ is the thermal average of $k_{\mathrm{D}}(\mathsf{X})$ (*cf.* Eq. (6.70)). The thermal average $\langle\cdots\rangle$ here is defined as the average over $p_0(\mathsf{X})$

$$\langle\cdots\rangle = \int \cdots p_0(\mathsf{X})\,\mathrm{d}\mathsf{X}\,. \tag{6.77}$$

The fluctuation Liouvillian $\mathcal{L}_V = \mathcal{L} - \mathcal{L}_0$ is therefore

$$\mathcal{L}_V = -\frac{i}{\hbar}\left[\Delta\hat{H}(\mathsf{X}), \cdot\,\right] - \left\{\Delta\hat{K}(\mathsf{X}), \cdot\,\right\} - \Delta k_{\mathrm{D}}(\mathsf{X})\left(\hat{P}_{\mathrm{S}}\,\cdot\,\hat{P}_{\mathrm{T}} + \hat{P}_{\mathrm{T}}\,\cdot\,\hat{P}_{\mathrm{S}}\right). \tag{6.78}$$

[d] In a slight abuse of notation I will use angle brackets $\langle\cdots\rangle$ sometimes to represent the thermal average over the X degrees of freedom, and sometimes to denote the expectation value of a quantum operator. From the text it will be clear which is meant.

where the fluctuation terms are defined as $\Delta A(\mathsf{X}) = A(\mathsf{X}) - \langle A \rangle$.

The fluctuation Liouvillian can be re-written as a sum of fluctuating terms as,

$$\mathcal{L}_V = \sum_k f_k(\mathsf{X}) \mathcal{A}_k \tag{6.79}$$

where $f_k(\mathsf{X})$ is a scalar function of X satisfying $\langle f_k \rangle = 0$, and $\mathcal{A}_k$ is a superoperator on the spin degrees of freedom. In the case where only the Hamiltonian $\hat{H}(\mathsf{X})$ is a function of X these superoperators can be written as $\mathcal{A}_k = -(i/\hbar)[\hat{A}_k, \cdot\,]$, where $\hat{A}_k$ is some operator on the spin Hilbert space. The correlation functions $g_{jk}(t)$ of the scalar fluctuation terms $f_j(\mathsf{X})^*$ and $f_k(\mathsf{X})$ are defined as

$$g_{jk}(t) = \left\langle f_j(t)^* f_k(0) \right\rangle = \int f_j(\mathsf{X})^* e^{\Gamma t} f_k(\mathsf{X}) p_0(\mathsf{X}) \, \mathrm{d}\mathsf{X}\,, \tag{6.80}$$

and the spectral densities $J_{jk}(\omega)$ are defined as the Fourier-Laplace transforms of these (as defined in Eq. (2.57))

$$J_{jk}(\omega) = \int_0^\infty e^{i\omega t} g_{jk}(t) \, \mathrm{d}t\,. \tag{6.81}$$

These quantities will be of central importance in the development of perturbative master equations for treating spin relaxation.

I will now outline how to apply the perturbative master equations presented in chapter 2 to the radical pair SLE to obtain approximate QMEs for the averaged spin density operator $\hat{\rho}(t)$. The focus here will be on time-integrated properties of the spin system, and perturbative master equations from which these can be obtained without direct evaluation of the time evolved spin density operator $\hat{\rho}(t)$. As such we only consider master equations of the form,

$$\frac{\mathrm{d}}{\mathrm{d}t}\hat{\rho}(t) = \left[\, \langle \mathcal{L} \rangle + \mathcal{R} \,\right] \hat{\rho}(t), \tag{6.82}$$

where $\mathcal{R}$ is some relaxation superoperator. The time-integrated density operator can be obtained by inversion of $\left[\, \langle \mathcal{L} \rangle + \mathcal{R} \,\right]$,

$$\int_0^\infty \hat{\rho}(t) \, \mathrm{d}t = -\left[\, \langle \mathcal{L} \rangle + \mathcal{R} \,\right]^{-1} \hat{\rho}(0), \tag{6.83}$$

where we have used the fact that $\hat{\rho}(t \to \infty) = 0$ for a decaying radical pair. This is

equivalent to solving a linear system of equations, which is typically more computationally efficient than direct evaluation of $\hat{\rho}(t)$.

6.5.2 Redfield theory

One approach to obtaining a master equation for the ensemble averaged density operator is to apply Redfield theory (i.e. Bloch-Redfield-Wangsness theory), as described in section 2.4.3.[60–62] As discussed in chapter 2, sections 2.4.1 and 2.4.2, this is equivalent to applying to taking the long-time limit of the second order TCL master equation or the second order cumulant expansion. Applying Eqs. (2.129) and (2.130), together with the definition of $\mathcal{L}_V$ and $\mathcal{L}_0$ as above, and using Eq. (6.77) to define the bath average $\langle\cdots\rangle_{\mathrm{b}}$, we arrive at the standard Redfield equation for the spin density operator,

$$\frac{\mathrm{d}}{\mathrm{d}t}\hat{\rho}(t) = \big[\, \langle\mathcal{L}\rangle + \mathcal{R}_{\mathrm{RF}} \,\big]\hat{\rho}(t) \tag{6.84}$$

in which the Redfield superoperator can be written as

$$\mathcal{R}_{\mathrm{RF}} = \int_0^\infty \mathrm{d}\tau \int \mathrm{d}\mathsf{X}\, \mathcal{L}_V e^{\mathcal{L}_0\tau}\mathcal{L}_V e^{-\mathcal{L}_0\tau} p_0(\mathsf{X}) \tag{6.85}$$

$$= -\sum_{jk}\int_0^\infty \mathrm{d}\tau\, g_{jk}(\tau)\mathcal{A}_j^\dagger e^{\langle\mathcal{L}\rangle\tau}\mathcal{A}_k e^{-\langle\mathcal{L}\rangle\tau}, \tag{6.86}$$

where $\mathcal{A}_j^\dagger$ is the Hermitian adjoint of $\mathcal{A}_j$ in Liouville space. The last line in this equation is arrived at by using the fact that $\mathcal{L}_V = -\mathcal{L}_V^\dagger$.

It should be noted that this version of Redfield theory explicitly includes the effect of asymmetric radical pair recombination ($k_{\mathrm{S}} \neq k_{\mathrm{T}}$) on the relaxation processes, although throughout the spin chemistry literature, asymmetric recombination is normally ignored in evaluating this superoperator.[46,51,182] It can be easily verified that $\mathcal{R}_{\mathrm{RF}}$ reduces to the standard Redfield superoperator in the case of symmetric recombination ($k_{\mathrm{S}} = k_{\mathrm{T}}$), in which only the coherent evolution terms in $\langle\mathcal{L}\rangle$ are included in evaluating the Redfield superoperator. In this chapter I will refer to the Redfield theory using Eq. (6.86) as the RF theory, and the version where recombination is ignored in evaluating $\mathcal{R}_{\mathrm{RF}}$ as the RF ($\Delta k = 0$) theory.

By writing $\langle \mathcal{L} \rangle$ in terms of its eigenvalue decomposition as

$$\langle \mathcal{L} \rangle = \sum_n \Pi_n \lambda_n, \tag{6.87}$$

where Π_n is a projection superoperator and λ_n is an eigenvalue of $\langle \mathcal{L} \rangle$ (*cf.* Eq. (2.A.10)), the Redfield superoperator can be evaluated as

$$\mathcal{R}_{\mathrm{RF}} = -\sum_{jknm} J_{jk}(i(\lambda_m - \lambda_n)) \mathcal{A}_j^\dagger \Pi_n \mathcal{A}_k \Pi_m. \tag{6.88}$$

This shows that the spectral densities $J_{jk}(\omega)$ control the relaxation processes within Redfield theory.

6.5.3 Nakajima-Zwanzig theory

As an alternative to Redfield theory, we could apply the second order Markovian Nakajima-Zwanzig equation, as described in section 2.2.2, to obtain a master equation for the spin density operator. The projection operator we use is

$$\mathcal{P} = p_0(\mathsf{X}) \int \mathrm{d}\mathsf{X}\ \cdot\,, \tag{6.89}$$

and together with $\hat{\rho}(t) = \int \mathrm{d}\mathsf{X}\, \mathcal{P}\hat{\rho}(t, \mathsf{X})$ it is straightforward to obtain the following master equation for $\hat{\rho}(t)$,

$$\frac{\mathrm{d}}{\mathrm{d}t}\hat{\rho}(t) = \left[\, \langle \mathcal{L} \rangle + \mathcal{R}_{\mathrm{NZ}} \,\right]\hat{\rho}(t), \tag{6.90}$$

in which $\mathcal{R}_{\mathrm{NZ}}$ can be obtained from the second order Nakajima-Zwanzig kernel as $\mathcal{R}_{\mathrm{NZ}} = \int \mathrm{d}\mathsf{X}\, \tilde{\mathcal{K}}^{(2)}(\omega \to 0)$, and using Eqs. (2.84), (6.79) and (6.80) this can be expanded as,

$$\mathcal{R}_{\mathrm{NZ}} = \int_0^\infty \mathrm{d}\tau \int \mathrm{d}\mathsf{X}\, \mathcal{L}_V e^{\mathcal{L}_0 \tau} \mathcal{L}_V p_0(\mathsf{X}) \tag{6.91}$$

$$= -\sum_{j,k} \int_0^\infty \mathrm{d}\tau\, g_{jk}(\tau) \mathcal{A}_j^\dagger e^{\langle \mathcal{L} \rangle \tau} \mathcal{A}_k. \tag{6.92}$$

As with the Redfield relaxation superoperator, we can use the eigenvalue decomposition of $\langle\mathcal{L}\rangle$ (Eq. (6.87)), to evaluate this in terms of the spectral densities $J_{jk}(\omega)$ as

$$\mathcal{R}_{\mathrm{NZ}} = -\sum_{jkn} J_{jk}(-i\lambda_n)\mathcal{A}_j^\dagger \Pi_n \mathcal{A}_k. \tag{6.93}$$

We see that the Nakajima-Zwanzig relaxation superoperator is also determined by the spectral densities for the fluctuations in the spin Liouvillian, but in a different way to the Redfield relaxation superoperator, and as a result the two theories will in general give different predictions for the dynamics of $\hat{\rho}(t)$.

6.5.4 The extreme narrowing limit and positivity

Before comparing Redfield theory and Nakajima-Zwanzig theory for some simple models of radical pair reactions involving spin relaxation, it is worth considering the extreme narrowing limit of these two theories.[45] This is the limit where the correlation functions $g_{jk}(t)$ decay on a time-scale τ_{c} that is much shorter than the time scale of the dynamics generated by $\langle\mathcal{L}\rangle$, so in terms of the eigenvalues of $\langle\mathcal{L}\rangle$ we are considering the case $|\tau_{\mathrm{c}}\lambda_n| \ll 1$ for all λ_n. In this limit, we can set $\lambda_n, \lambda_m = 0$ in Eqs. (6.88) and (6.93), because we can approximate $g_{jk}(t)$ as being proportional to a delta function in time, so both of these relaxation superoperators reduce to $\mathcal{R}_0$,

$$\mathcal{R}_{\mathrm{NZ}}, \mathcal{R}_{\mathrm{RF}} \rightarrow \mathcal{R}_0 = -\sum_{jk} J_{jk}(0)\mathcal{A}_j^\dagger \mathcal{A}_k. \tag{6.94}$$

In the limit of very fast decaying correlations in the spin Liouvillian fluctuations, their effect becomes negligible and we also expect the perturbative approximation to become exact, so as the slowest correlation time for the fluctuations approaches zero, both the Nakajima-Zwanzig and Redfield theories, which reduce to the extreme narrowing limit result above, become exact.

When the only fluctuating terms in the spin Liouvillian are in the Hamiltonian $\hat{H}(\mathsf{X})$, the extreme narrowing limit relaxation superoperator is of Lindblad form, and as such it preserves the positivity of the spin density operator. However, beyond the extreme narrowing limit neither Redfield equation nor the perturbative Nakajima-Zwanzig equation

strictly preserves positivity of the spin density operator, which can mean populations of certain states may not be bounded between 0 and 1. This can in turn lead to predictions of quantum yields, as in Eq. (6.72), no longer being bounded between 0 and 1. In fact it is well-known that these approximate theories can suffer from this problem in the long correlation time limit (also called the static disorder limit). The extent of this problem for Redfield and Nakajima-Zwanzig theories will be evaluated in the next section.

6.6 Comparing approximate relaxation theories

Whilst the Nakajima-Zwanzig approach has been applied previously to model spin relaxation,[57,58,183,184] Redfield theory has been used much more widely in the context of spin chemistry in recent years,[44,46,51,182] with the Nakajima-Zwanzig equation being largely overlooked. A careful comparison of the application of these theories to radical pair spin dynamics therefore seems warranted. In order to test the accuracy of Redfield and Nakajima-Zwanzig theories for treating spin relaxation in radical pairs, I have simulated the triplet quantum yield Φ_{T} as a function of the fluctuation correlation time for a range of simple radical pair models using the SLE, as well as the RF and NZ master equations. The models all have X independent singlet and triplet recombination rates, and do not include the decoherence term, i.e. $k_{\mathrm{D}}(\mathrm{X}) = 0$. The thermally averaged Hamiltonian in each model is of the form

$$\left\langle \hat{H} \right\rangle = \mu_{\mathrm{B}} g_{\mathrm{e}} B(\hat{S}_{1z} + \hat{S}_{2z}) - 2J\hat{\mathbf{S}}_1 \cdot \hat{\mathbf{S}}_2 + a\hat{\mathbf{S}}_1 \cdot \hat{\mathbf{I}}, \tag{6.95}$$

which corresponds to a radical pair with a scalar coupling constant J between the radicals, in the presence of a magnetic field of strength B, containing a single $I = 1/2$ nucleus isotropically hyperfine coupled to radical 1 with a coupling constant a. In all models the radical pair is assumed to be formed in a pure singlet electronic state, and a totally mixed nuclear spin state, so $\hat{\rho}(0) = \hat{P}_{\mathrm{S}}/2$, as is often the case for radical pairs formed by photoexcitation from a singlet ground state. The spin system parameters are set to $J/g_{\mathrm{e}}\mu_{\mathrm{B}} = 5$ mT and $B = 2$ mT, and $k_{\mathrm{S}} = k_{\mathrm{T}}/100 = 1\ \mu\mathrm{s}^{-1}$ which lie in the typical range of values encountered in real experiments on radical pair reactions.

In the following we consider a two site model, in which either the hyperfine coupling constant a or the scalar coupling constant J varies between the two sites, and a model in which there is an anisotropic hyperfine coupling term between the electron spin 1 and the nuclear spin, which is modulated by free isotropic rotational diffusion of the radical pair. The details of the models used are explained alongside the results below. The exact SLE results in the two site models are obtained by treating the density operators for each site explicitly. In the models including rotational diffusion exact results are obtained by expanding $\hat{\rho}(t, \Omega)$ in a basis of Wigner functions $\mathfrak{D}^{(l)}_{ab}(\Omega)$, as described in appendix 6.A and converged results were found with a truncation of the expansion at $l = 5$.

6.6.1 Two site model

The first model we consider is a two site model with a fluctuating isotropic hyperfine constant $a(n)$, where n denotes the site index and therefore the fluctuating term in the Hamiltonian $\hat{V}(n) = \Delta\hat{H}(n)$ is

$$\hat{V}(n) = \Delta a(n)\hat{\mathbf{S}}_1 \cdot \hat{\mathbf{I}}. \tag{6.96}$$

In this model the transition kernel is just a 2×2 rate matrix composed of the two site to site transition rate constants $k_{1\to2}$ and $k_{2\to1}$. In this example these rate constants are set to $k_{1\to2} = k_{2\to1}/5 = 1/\tau_{\text{ex}}$. The predictions of Nakajima-Zwanzig and Redfield theories (with and without inclusion of the asymmetric recombination in the relaxation superoperator) for this model are shown in Fig. 6.1, along with the exact SLE results for this model. In the top panel the site specific hyperfine coupling constants of the model are $a(1)/g_{\text{e}}\mu_{\text{B}} = 0$ mT and $a(2)/g_{\text{e}}\mu_{\text{B}} = 2$ mT, which are values chosen as typical values for a real organic radical with a fluctuating conformation, and in the bottom panel $a(1)/g_{\text{e}}\mu_{\text{B}} = 0$ mT and $a(2)/g_{\text{e}}\mu_{\text{B}} = 20$ mT, which are chosen to push the limits of the perturbative theories.

First let us examine the results in the top panel of Fig. 6.1, where the model is in a physically reasonable parameter regime. As the correlation time for the fluctuations increases, there is an initial increase in the efficiency of spin relaxation, leading to an increase in the transitions from the initial electronic singlet state to triplet states, increasing the triplet yield; this effect peaks when the correlation time is on the order of time-scale of

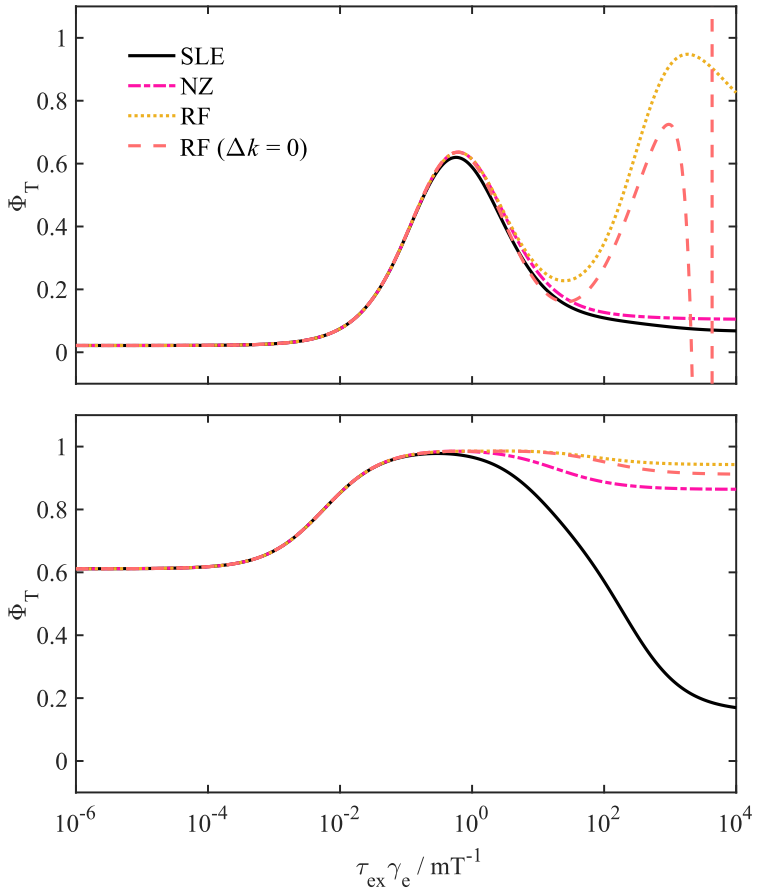

Figure 6.1: A comparison of perturbative master equations with the SLE for a two site model with asymmetric interconversion rates and a fluctuating isotropic hyperfine coupling between the two sites. In the top panel $a(1)/g_e\mu_B = 0$ mT and $a(2)/g_e\mu_B = 2$ mT, and in the bottom panel $a(1)/g_e\mu_B = 0$ mT and $a(2)/g_e\mu_B = 20$ mT.

the average spin dynamics. However as the correlation time increases further the efficiency of the relaxation induced singlet-triplet transitions decreases and the static disorder limit is approached. In this limit the system behaves as two independent ensembles, independently evolving under the spin Hamiltonians of the two sites.

As predicted above, for very short correlation times, i.e. in the extreme narrowing limit, the perturbative theories and the SLE results agree exactly in their predictions of the triplet quantum yield. The predictions of the NZ equation and RF equation then begin to differ as τ_{ex} becomes similar to the time-scale of the average dynamics, and we see that for $\tau_{ex}\gamma_e \gtrsim 10$ mT^{-1} the Redfield results diverge significantly from the exact SLE results. The full RF equation and the RF ($\Delta k = 0$) theories perform similarly in this example. The positivity problem of Redfield theory can be seen clearly in the RF($\Delta k = 0$) results, where the predicted triplet yield oscillates rapidly, going below 0 and above 1. On the other hand, the Nakajima-Zwanzig results remain relatively accurate into the static disorder limit.

Now let us examine the results for the model with significantly larger fluctuations in

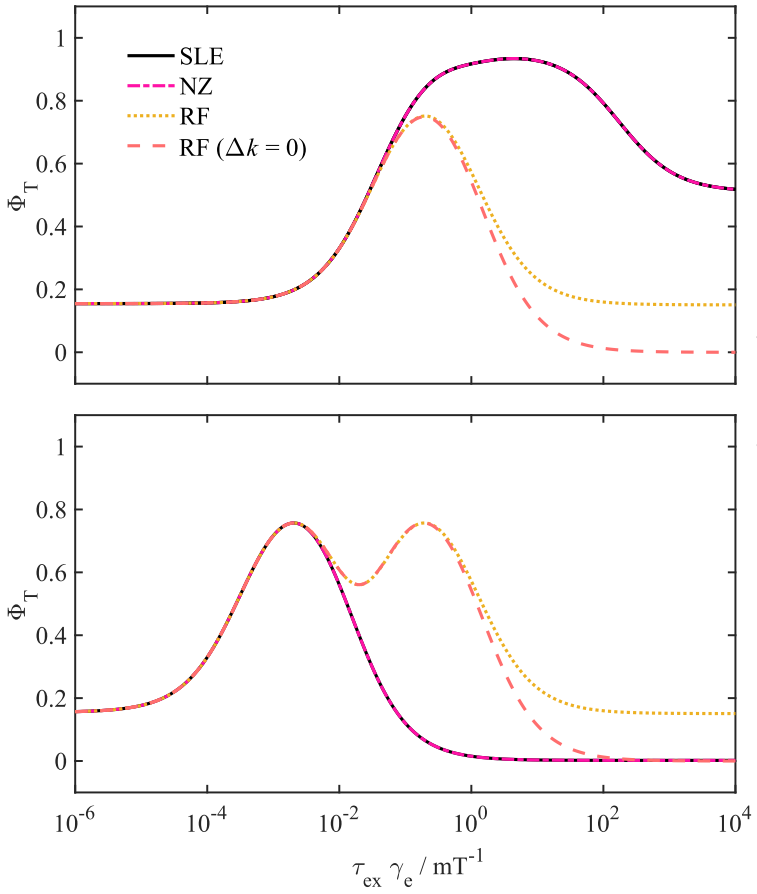

Figure 6.2: A comparison of perturbative master equations with the SLE for a two site model with symmetric interconversion rates and a fluctuating electron scalar coupling between the two sites. In the top panel $\Delta J/g_e\mu_B = 5$ mT, and in the bottom panel $\Delta J/g_e\mu_B = 50$ mT.

a in the bottom panel of Fig. 6.1. In this case the perturbative theories agree with the exact SLE results up to $\tau_{ex}\gamma_e \approx 0.1$ mT^{-1}, and after this point the perturbative theories all break down. In this example, the perturbative NZ equation predictions are marginally more accurate than those of Redfield theory, but not significantly. These results overall suggest that the NZ equation does not suffer from the same severe positivity problem of Redfield theory. It is evident that the perturbative NZ equation can be used in the long correlation time limit, provided the fluctuations are still relatively small compared to the energies of the reference thermally averaged spin dynamics, whereas Redfield theory cannot be used reliably in this limit. For large perturbations however, the perturbative master equations all break down beyond the short-correlation time, extreme narrowing limit.

As another example, in Fig. 6.2 the results of triplet yield calculations are displayed for a symmetric two-site model (in which $k_{1\to2} = k_{2\to1} = 1/\tau_{ex}$) where the scalar coupling constant varies between the sites. In this model, the site-specific scalar coupling constants are $J(1) = J + \Delta J$ and $J(2) = J - \Delta J$, where $\Delta J/g_e\mu_B = 5$ mT for the results in the top

panel of Fig. 6.2 and 50 mT for the results in the bottom panel. In this model the isotropic hyperfine coupling constant for the nuclear spin is set to $a/g_e\mu_B = 1$ mT.

In this example, fluctuations in the scalar coupling J lead to singlet-triplet dephasing, the rate of which increases with τ_{ex} initially, and then eventually the static disorder limit is reached, where the system behaves as two independent ensembles, with half the population evolving according the the spin Hamiltonian for site 1, and the other half evolving under the Hamiltonian for site 2. Increasing the singlet-triplet dephasing rate decreases the lifetime of singlet-triplet coherences, which first increases the rate of transitions from the singlet to triplet states at short correlation times, and then decreases this rate at longer correlation times. This means that the triplet quantum yield passes through a maximum.

For a symmetric two site model, where only the Hamiltonian fluctuates, the perturbative NZ equation is coincidentally exact, as can be seen in the results in Fig. 6.2. The RF equation however is not, and as in the previous example, as the correlation time increases the accuracy of RF theory deteriorates rapidly. In the large fluctuation case (bottom panel of Fig. 6.2) RF theory predicts an additional maximum in the triplet yield which is not observed in the exact SLE results.

6.6.2 Rotational diffusion model

In addition to N site models for relaxation, another important relaxation mechanism is modulation of the anisotropic spin coupling parameters by rotational Brownian motion of the radicals. In this case the slow degrees of freedom included in the SLE are the orientational degrees of freedom of the molecule, as described in 6.3.4, and in this example we include an anisotropic hyperfine coupling term between the electron spin in radical 1 and the nuclear spin, which is given by

$$\hat{V}(\Omega) = \hat{\mathbf{S}}_1 \cdot \left(\mathbf{R}(\Omega) \cdot \Delta\mathbf{A} \cdot \mathbf{R}(\Omega)^{-1}\right) \cdot \hat{\mathbf{I}}. \tag{6.97}$$

where $\mathbf{R}(\Omega)$ is the rotation matrix describing the rotation of the lab frame axes to the molecular principal axes frame at an orientation Ω (such that a vector in the molecular frame is related to the same vector in the lab frame by $\mathbf{v}_{mol} = \mathbf{R}(\Omega)^{-1}\mathbf{v}_{lab}$), and $\Delta\mathbf{A}$ is the molecular frame anisotropic coupling tensor. In the examples considered here $\Delta\mathbf{A}$ is diagonal with

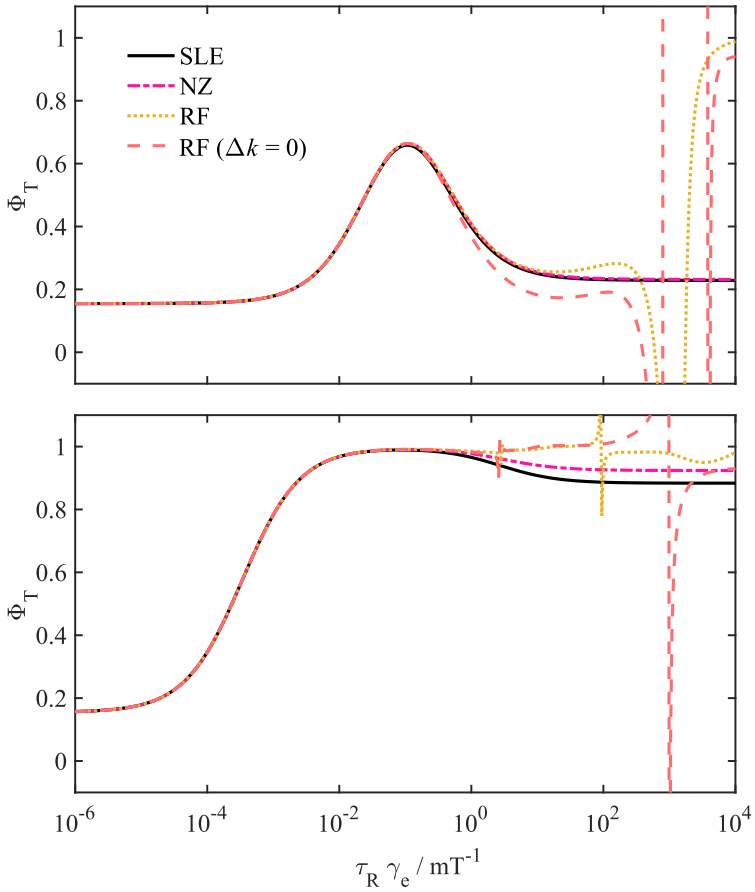

Figure 6.3: A comparison triplet quantum yields calculated with the radical pair stochastic Liouville equation and perturbative quantum master equations for a model radical pair including an anisotropic hyperfine coupling, which is modulated by rotational diffusion of the molecule. In the top panel $\Delta A/g_e\mu_B = 1$ mT and in the bottom panel $\Delta A/g_e\mu_B = 10$ mT.

diagonal elements $\Delta A_{xx} = \Delta A_{yy} = -\Delta A_{zz}/2 = -\Delta A/2$, and we only consider the case of free isotropic rotational diffusion, where the rotational correlation time is $\tau_R = 1/(6D)$, with D being the rotational diffusion constant. Here we will consider two examples, one where $\Delta A/g_e\mu_B = 1$ mT, which is representative of a relatively large anisotropic hyperfine coupling in a typical organic radical, and one where $\Delta A/g_e\mu_B = 10$ mT, which is much larger than usually observed in real organic radicals. In both examples the isotropic hyperfine coupling constant is set to $a/g_e\mu_B = 1$ mT, and all other parameters are given above.

In Fig. 6.3 the triplet yields are plotted as a function of τ_R, as calculated with the the exact SLE and the perturbative master equations. As in the examples above, the rate of relaxation induced singlet-triplet transitions passes through a maximum when the rotational correlation time is comparable to the time-scale of the thermally averaged spin dynamics, so the triplet yield passes through a maximum. In the static disorder limit (large τ_R) the system behaves like a set of independent ensembles in different orientations, so Φ_T plateaus.

In the top panel of Fig. 6.3 the results for the $\Delta A/g_e\mu_B = 1$ mT model are displayed.

As in the previous examples, the perturbative master equations agree with the exact SLE in the extreme narrowing limit, but then deviate at larger rotational correlation times. The NZ equation remains extremely accurate across all correlation times in this example, whereas the RF equation results deviate significantly from the SLE results at larger correlation times. The full RF equation breaks down when $\tau_R \gamma_e \gtrsim 10\ \mathrm{mT}^{-1}$ whereas the predictions of the RF equation with the $\Delta k = 0$ approximation used to evaluate the relaxation superoperator begins to deviate from the exact SLE results for much smaller τ_R, when $\tau_R \gamma_e \gtrsim 0.1\ \mathrm{mT}^{-1}$. Both versions of RF theory suffer from severe positivity problems at large τ_R, where they predict triplet quantum yields which exceed 1 or are below 0.

The bottom panel of Fig. 6.3 shows the results for the model with $\Delta A / g_e \mu_B = 10$ mT. Again in the short correlation time limit the perturbative master equations work extremely well, but deviations from the exact SLE results appear at longer correlation times. The Nakajima-Zwanzig equation results are not as accurate in the static disorder limit as in the example with $\Delta A / g_e \mu_B = 1$ mT, but the qualitative behaviour of Φ_T as a function of τ_R is still captured by this theory, and the error is less than 30% even in this model with such a large value of ΔA. Conversely the RF equation results deviate significant from the SLE results at long correlation times, where they suffer from the aforementioned positivity problem.

6.6.3 Discussion

In this section we have explored the use of perturbative master equations to solve the Stochastic Liouville Equation for a radical pair reaction including the effects of spin relaxation. For a range of simple models of radical pair reactions including various relaxation mechanisms we have seen that relaxation can have a large effect on the quantum yield of spin selective reactions, showing that these effects cannot in general be ignored in modelling real radical pair reactions.

The SLE is rapidly becomes very computationally expensive to solve numerically, with the computational time of a quantum yield calculation scaling as $O(N^3 d^6)$, where d is the dimensionality of the spin Hilbert space and N is the number of density operators

required in the expansion of $\hat{\rho}(t, \mathsf{X})$.[e] By contrast, the computational time of solving the perturbative master equations is $O(N^0 d^6)$, because the slow degrees of freedom X have been averaged out, so there is no need for an explicit expansion of the density operator in these coordinates. This means the perturbative master equations are significantly more efficient to use, especially in larger spin systems where multiple spin relaxation mechanism need to be considered.

The results of the previous section show that the second order Nakajima-Zwanzig equation can be used reliably to capture relaxation effects over all correlation times of the stochastic fluctuations in the spin system parameters, provided the fluctuations are relatively small and can be treated perturbatively. By contrast the commonly used Redfield approach suffers from a severe positivity problem in many of these examples when the correlation time of the stochastic fluctuations is long, which means the Redfield equation makes highly inaccurate, unphysical predictions of the reaction quantum yields. This difference can be understood by considering the approximations made in deriving the second order Markovian NZ equation and the RF equation, as described in chapter 2. The Markovian NZ equation is formally exact for time integrated properties, whereas the time-homogeneous second order TCL master equation (from which the RF equation is derived) does not possess this property. Because we are primarily interested in time-integrated observables, in using the second order Markovian NZ equation, the only approximation we are really invoking is the use of perturbation theory to evaluate the kernel, so we do not need the kernel's decay timescale to be short compared to the system dynamics. In contrast, in order to apply the RF equation, we need the second order TCL generator to reach its long-time limit on a time scale faster than the system dynamics, in addition to needing perturbation theory to be valid. This explains the difference between the NZ and RF equation results in the long correlation time limit. The Markovian NZ equation would not necessarily be more accurate for observables at intermediate times, but the only experimental observables to which this theory is applied in the next chapter are time-integrated properties, so here I have limited the analysis to this case.

[e] In practice this can be reduced by exploiting the sparsity of the total Liouvillian, but the computational time even exploiting this typically cannot go below $O(N^{5/2} d^5)$ scaling.

One commonly applied fix for the RF equation which is extensively used in the NMR and EPR literature is the secular approximation.[43,44] This has not been explored here, due to the fact that the reference dynamics are non-unitary due to the presence of radical pair recombination, which means that the secular approximation cannot be straightforwardly applied to the RF relaxation superoperator. The results in Fig. 6.3 show that the non-unitarity in the reference dynamics cannot simply be ignored in evaluating the RF relaxation superoperator, because the full RF equation results remain accurate over two orders of magnitude longer correlation times compared to the RF ($\Delta k = 0$) equation, in which the non-unitarity in the reference dynamics from asymmetric recombination rates is ignored in the construction of the relaxation superoperator. It is possible that some generalisation of the secular approximation may be as accurate, if not more accurate than the second order NZ equation, but for the purpose of modelling real radical pair reactions as explored in the next two chapters, the NZ equation is sufficient.

6.7 Conclusions

In the first part of this chapter I have described how to combine the theoretical approaches used in chapter 3 with the Stochastic Liouville equation formalism for describing relaxation, to obtain a master equation for the radical pair which can include the effects of various relaxation mechanisms. The resulting master equation is exactly what one would naïvely write down, if one wanted to combine the Haberkorn treatment of spin selective reactions with the SLE treatment of relaxation in non-recombining spin systems, but this analysis highlights the connections between these theories and approximations that are implicitly made in using the radical pair SLE to describe relaxation. The approximations used mean that the spin system relaxes to its infinite temperature equilibrium state, which clearly shows that this equation will not be valid for describing relaxation processes at very low temperatures. The derivation presented here may offer a starting point for correcting the radical pair SLE to obtain a master equation which evolves to the correct thermal equilibrium state, but this is beyond the scope of this work.

In the second part of this chapter I described how to apply approximate perturbative

master equation techniques to find approximate solutions to the radical pair SLE. Analysis of a range of different models showed that the perturbative Nakajima-Zwanzig equation is accurate over a much wider range of fluctuation correlation times than the more commonly used Redfield theory. As such this is the theory which will be applied to treat relaxation processes in modelling radical pair reactions in the next two chapters.

Appendix

6.A Appendix: Solving the rotational SLE

Here I will briefly outline the method used to numerically solve the SLE for rotational motion in the absence of an aligning potential with a symmetric rotational diffusion tensor, based on methods described in Refs. [172] and [43]. The anisotropic interactions in the spin Hamiltonian are all of the form

$$\hat{\mathbf{J}}_1 \cdot \left(\mathbf{R}(\Omega) \cdot \mathbf{C} \cdot \mathbf{R}(\Omega)^{-1}\right) \cdot \hat{\mathbf{J}}_2 \tag{6.A.1}$$

where $\hat{\mathbf{J}}_1$ and $\hat{\mathbf{J}}_1$ are spin angular momentum vector operators (or a magnetic field vector in the case of the Zeeman interaction), $\mathbf{C}$ is a traceless, real symmetric matrix and $\mathbf{R}(\Omega)$ is a rotation matrix describing the rotation from the lab frame to the molecular frame, i.e. the unit vectors defining the molecular frame axes $\mathbf{n}_{\alpha,\mathrm{mol}}(\Omega)$ in the lab frame are given by $\mathbf{R}(\Omega) \cdot \mathbf{n}_{\alpha,\mathrm{lab}}$, where $\mathbf{n}_{x,\mathrm{lab}} = (1,0,0)^\mathsf{T}$ etc.. An interaction term of the form given in Eq. (6.A.1) can be written as[43]

$$\hat{\mathbf{J}}_1 \cdot \left(\mathbf{R}(\Omega) \cdot \mathbf{C} \cdot \mathbf{R}(\Omega)^{-1}\right) \cdot \hat{\mathbf{J}}_2 = \sum_{n=-2}^{2} \sum_{m=-2}^{2} \mathfrak{D}^{(2)}_{nm}(\Omega) C^{(2)}_m T^{(2)}_n(\hat{\mathbf{J}}_1, \hat{\mathbf{J}}_2), \tag{6.A.2}$$

where $C^{(2)}_m$ is the rank 2 spherical tensor component of the coupling tensor and $T^{(2)}_n(\hat{\mathbf{J}}_1, \hat{\mathbf{J}}_2)$ is the rank 2 spherical tensor component of a pair of vector operators. This means that the

coupling part of the Hamiltonian $\Delta\hat{H}(\Omega)$ can in general be written as

$$\Delta\hat{H}(\Omega) = \sum_{n=-2}^{2}\sum_{m=-2}^{2} \mathfrak{D}^{(2)}_{nm}(\Omega)\hat{Q}^{(2)}_{mn} \tag{6.A.3}$$

where $\mathfrak{D}^{(l)}_{nm}(\Omega)$ are Wigner D-matrix elements and $\hat{Q}^{(2)}_{nm}$ are the rank 2 spherical tensor components of the couplings. Using this the coupling Liouvillian can be written as

$$\mathcal{L}_V = -\frac{i}{\hbar}\sum_{n=-2}^{2}\sum_{m=-2}^{2} \mathfrak{D}^{(2)}_{nm}(\Omega)\left[\hat{Q}^{(2)}_{mn},\ \cdot\ \right] \tag{6.A.4}$$

$$= \sum_{n=-2}^{2}\sum_{m=-2}^{2} \mathfrak{D}^{(2)}_{nm}(\Omega)\mathcal{A}^{(2)}_{mn}. \tag{6.A.5}$$

The set of Wigner D-matrices form a complete basis for functions of Ω, and therefore the density operator $\hat{\rho}(t,\Omega)$ can be expanded in this set of functions,

$$\hat{\rho}(t,\Omega) = \sum_{l=0}^{\infty}\sum_{n,m=-l}^{l}\left(\frac{2l+1}{8\pi^2}\right)^{1/2} \mathfrak{D}^{(l)}_{nm}(\Omega)\hat{\rho}^{(l)}_{nm}(t). \tag{6.A.6}$$

Observables which are orientation independent, can be obtained from this expansion as,

$$\langle O(t)\rangle = (8\pi^2)^{1/2}\,\mathrm{Tr}\left[\hat{O}\hat{\rho}^{(0)}_{00}(t)\right]. \tag{6.A.7}$$

The equations of motion for $\hat{\rho}^{(l)}_{nm}(t)$ can be found by taking the inner product with $((2l+1)/(8\pi^2))^{1/2}\mathfrak{D}^{(l)}_{nm}(\Omega)$. For symmetric rotational diffusion, where the diffusion tensors is $\mathbf{D} = D\mathbf{1}$, $\mathfrak{D}^{(l)}_{nm}(\Omega)$ is an eigenfunction of the rotational diffusion operator $-D\mathsf{L}^2$ with eigenvalue $-Dl(l+1)$ and therefore the equation of motion for $\hat{\rho}^{(l)}_{nm}(t)$ is

$$\frac{\mathrm{d}}{\mathrm{d}t}\hat{\rho}^{(l)}_{nm}(t) = (\langle\mathcal{L}\rangle - Dl(l+1))\hat{\rho}^{(l)}_{nm}(t) + \sum_{l'n'm'n''m''} C^{ln}_{2n',l'm'}C^{lm}_{2n'',l'm''}\mathcal{A}^{(2)}_{n'n''}\hat{\rho}^{(l')}_{m'm''}(t), \tag{6.A.8}$$

in which $C^{jm}_{j_1m_1,j_2m_2}$ is the Clebsch-Gordon coefficient. For free rotational diffusion, if the initial state is a steady state of $-D\mathsf{L}^2$, then the initial conditions are $\hat{\rho}^{(l)}_{nm}(t) = 0$ for $l > 0$, and

$$\hat{\rho}^{(0)}_{00}(0) = \left(\frac{1}{8\pi^2}\right)^{1/2}\hat{\rho}(0). \tag{6.A.9}$$

By truncating l in the expansion at some finite value, and expanding the operators in a

given Liouville space basis, the coefficients $\langle a|\hat{\rho}^{(l)}_{nm}(t)|b\rangle$ form a system of linear equations of the form

$$\frac{\mathrm{d}}{\mathrm{d}t}\boldsymbol{\rho}(t) = \mathbf{G}\boldsymbol{\rho}(t), \tag{6.A.10}$$

from which time integrated observables can be obtained efficiently using Eq. (6.83) by exploiting the sparsity in $\mathbf{G}$. Similarly dynamics can be obtained by solving this equation numerically, where again the sparsity in $\mathbf{G}$ can be exploited by using methods such as the Short Iterative Arnoldi method (which is employed in the dynamical SLE simulations in chapter 8).[185,186]

6.B Appendix: N site model correlation functions

In this appendix the correlation functions and spectral densities for an N site SLE are described. For an N site model, it is useful to write the set of density operators $\hat{\rho}(t,n)$ as a column vector $\hat{\boldsymbol{\rho}}(t)$ of the density operators for each site, and the SLE can be written as

$$\frac{\mathrm{d}}{\mathrm{d}t}\hat{\boldsymbol{\rho}}(t) = \sum_{n=1}^{N} \mathcal{L}_n \mathbf{P}_n \hat{\boldsymbol{\rho}}(t) + \boldsymbol{\Gamma}\hat{\boldsymbol{\rho}}(t) \tag{6.B.1}$$

$$= \langle \mathcal{L} \rangle \, \hat{\boldsymbol{\rho}}(t) + \boldsymbol{\mathcal{L}}_V \hat{\boldsymbol{\rho}}(t) + \boldsymbol{\Gamma}\hat{\boldsymbol{\rho}}(t), \tag{6.B.2}$$

where $\boldsymbol{\Gamma}$ is the N site transition matrix, and the perturbation Liouvillian $\mathcal{L}_V$ is written as a matrix $\boldsymbol{\mathcal{L}}_V$ of system Liouvillians which is of the form

$$\boldsymbol{\mathcal{L}}_V = \sum_{n=1}^{N} \mathcal{A}_n (\mathbf{P}_n - \langle p_n \rangle \, \mathbf{1}) \tag{6.B.3}$$

where $\mathcal{A}_n = \mathcal{L}_n$ is the Liouvillian corresponding to site n, $\mathbf{P}_n$ is a projection matrix onto site n, with zeros everywhere apart from the n,n element which is 1, and $\langle p_n \rangle$ is the population of site n in the steady state of the N site transition matrix $\boldsymbol{\Gamma}$. The correlation functions for the $\mathbf{P}_n - \langle p_n \rangle \, \mathbf{1}$ terms that arise in the perturbative relaxation theories are given by

$$g_{nm}(t) = \langle p_n(t) p_m(0) \rangle - \langle p_n \rangle \langle p_m \rangle \, . \tag{6.B.4}$$

The $\langle p_n(t)p_m(0)\rangle$ is the probability of finding the system in site n at time t given it started in site m, weighted by initial probability $\langle p_m\rangle$. In the long time limit $p_n(t)$ will relax to its equilibrium value, and so this must become $\langle p_n\rangle\langle p_m\rangle$ in the long time limit, so $g_{nm}(t)$ decays to zero.

We assume we can diagonalise $\mathbf{\Gamma}$ and therefore write it as $\mathbf{\Gamma} = \sum_{j=0}^{N-1} \mathbf{\Pi}_j \lambda_j$ where λ_j is an eigenvalue of $\mathbf{\Gamma}$ and $\mathbf{\Pi}_j$ is a projection matrix, and it is assumed that λ_0 satisfies $\lambda_0 = 0$, and all other λ_j are real and negative. With this the correlation function can be written as

$$g_{nm}(t) = \sum_{j=1}^{N-1} [\mathbf{\Pi}_j]_{nm} \langle p_m\rangle e^{\lambda_j t}. \tag{6.B.5}$$

and the corresponding spectral densities are

$$J_{nm}(\omega) = -\sum_{j=1}^{N-1} [\mathbf{\Pi}_j]_{nm} \langle p_m\rangle \frac{1}{\lambda_j + i\omega}. \tag{6.B.6}$$

6.C Appendix: Rotational diffusion correlation functions

In this appendix the correlation functions and spectral densities, as needed in the perturbative master equations, are given for a rotational diffusion model of relaxation. Here I will only consider the case of free diffusion of a symmetric top, in which case the rotational diffusion operator (or Smoluchowski operator) can be written as

$$\Gamma = -D_\perp(\mathsf{L}_X^2 + \mathsf{L}_Y^2) - D_\parallel \mathsf{L}_Z^2 \tag{6.C.1}$$

where $D_\perp$ is the diffusion constant for rotation about an axis perpendicular to the symmetry axis, taken to be the body fixed Z axis, and $D_\parallel$ is the diffusion constant for rotation about an axis parallel to the symmetry axis. By re-writing this operator as

$$\Gamma = -D_\perp \mathsf{L}^2 - (D_\parallel - D_\perp)\mathsf{L}_Z^2, \tag{6.C.2}$$

and therefore the eigenfunctions of this operator are the Wigner D-matrix elements,[43]

$$\Gamma \mathfrak{D}^{(l)}_{nm}(\Omega) = -[D_\perp l(l+1) + (D_\parallel - D_\perp)m^2]\mathfrak{D}^{(l)}_{nm}(\Omega). \tag{6.C.3}$$

From Eq. (6.A.3) we see that the perturbation Liouvillian can be written as a sum superoperators independent of Ω multiplied by rank 2 Wigner D-matrix elements, and the initial distribution is $p_0(\Omega) = 1/(8\pi^2)$, so with this the correlation functions we need are[43]

$$g_{nmn'm'}(t) = \left\langle \mathfrak{D}^{(2)}_{nm}(t)^* \mathfrak{D}^{(2)}_{n'm'}(0) \right\rangle \tag{6.C.4}$$

$$= \frac{1}{5} e^{-[6D_\perp + (D_\parallel - D_\perp)m^2]t} \delta_{nn'}\delta_{mm'} \tag{6.C.5}$$

$$= \frac{1}{5} e^{-t/\tau_{\mathrm{R},m}} \delta_{nn'}\delta_{mm'}, \tag{6.C.6}$$

where $1/\tau_{\mathrm{R},m} = 6D_\perp + (D_\parallel - D_\perp)m^2$. The spectral densities are therefore given by[43]

$$J_{nmn'm'}(\omega) = \delta_{nn'}\delta_{mm'} \frac{\tau_{\mathrm{R},m}}{1 - i\omega\tau_{\mathrm{R},m}}. \tag{6.C.7}$$

Note that in the case of symmetric rotational diffusion, when $D_\perp = D_\parallel = D$, $\tau_{\mathrm{R},m} = \tau_\mathrm{R} = 1/(6D)$.

7

Semiclassical Radical Pair Master Equations

Real radical pairs typically contain a large number of hyperfine coupled nuclei, and therefore modelling these systems poses a significant challenge due to the exponential scaling of the spin Hilbert space dimensionality with the number of coupled spins. This problem has motivated the development of semiclassical approximations to the spin dynamics, which remove the exponential scaling of full quantum mechanical calculations. However, the important role of relaxation processes in radical pair spin dynamics further complicates the problem of accurately modelling these systems, and as such simple phenomenological treatments of relaxation are normally used in the simulation of magnetic field effects on radical pair reactions, instead of detailed microscopic models using the Stochastic Liouville equation. Thus in order to gain more detailed insights into real radical pair reactions, we need to find a method for simulating their spin dynamics that is accurate, consistent with the radical pair Stochastic Liouville equation, simple and efficient to implement for realistically large spin systems, and compatible with a detailed microscopic model of the molecular motion of the radical pair. Computational efficiency is particularly important because radical pair models often contain several unknown parameters which must be fit to experimental data, a process that typically involves performing many consecutive simulations.

The method I present here uses the Schulten-Wolynes semiclassical approximation in combination with the use of Nakajima-Zwanzig theory to treat relaxation. The accuracy of

the method is demonstrated by numerical calculations on model radical pairs and the utility of the method is illustrated by application to DMJ-An-Ph$_n$-NDI radical pairs. In particular I focus on understanding the role of relaxation processes in these radical pairs, with the aim of going beyond simple phenomenological treatments of spin relaxation by employing microscopic models of the stochastic fluctuations in the spin Hamiltonian,

7.1 Radical pair reactions in solution

In what follows, we will consider a molecular radical pair in solution undergoing a irreversible spin-selective reactions to give some products. The ultimate aim is to simulate time-integrated electron spin observables, such as the quantum yields of competing radical pair reactions and the radical pair lifetime. Our starting point for this will be a radical pair Stochastic Liouville equation of the form,

$$\frac{\partial}{\partial t}\hat{\rho}(t,\mathsf{X}) = -\frac{i}{\hbar}\left[\left\langle\hat{H}\right\rangle + \hat{V}(\mathsf{X}), \hat{\rho}(t,\mathsf{X})\right] - \left\{\left\langle\hat{K}\right\rangle, \hat{\rho}(t,\mathsf{X})\right\} + \Gamma\hat{\rho}(t,\mathsf{X}), \tag{7.1}$$

where we assume the radical pair reactions are well described as electron transfer reactions in the non-adiabatic limit, the thermally averaged Haberkorn operator is $\left\langle\hat{K}\right\rangle = \frac{k_S}{2}\hat{P}_S + \frac{k_T}{2}\hat{P}_T$, and that the rate constants can be approximated as independent of the slow degrees of freedom X. Here k_S and k_T are the total first order singlet and triplet recombination rate constants. Here $\left\langle\hat{H}\right\rangle$ and $\hat{V}(\mathsf{X})$ are the thermally averaged and fluctuating parts of the radical pair spin Hamiltonian and Γ describes the motion of slow degrees of freedom X. For now we will not assume any particular form for X or Γ.

We will assume that the thermally averaged Hamiltonian can be divided into three terms: two singlet radical terms $\hat{H}_i$ and an coupling term $\hat{H}_{1,2}$,

$$\left\langle\hat{H}\right\rangle = \hat{H}_1 + \hat{H}_2 + \hat{H}_{1,2}. \tag{7.2}$$

In each radical, there are N_i hyperfine coupled nuclear spins, each with a total spin quantum number $I_{i,k}$, which couple via the isotropic Fermi contact interaction to the radical electron spin, and the electron spin interacts with an external magnetic field (assumed to be aligned along the z direction) via the Zeeman interaction, and therefore the single radical

Hamiltonians are

$$\hat{H}_i = g_i \mu_B B \hat{S}_{i,z} + \sum_{k=1}^{N_i} a_{i,k} \hat{\mathbf{S}}_i \cdot \hat{\mathbf{I}}_{i,k}. \tag{7.3}$$

Here g_i is the g-factor for the radical i electron spin and $a_{i,k}$ is the isotropic hyperfine coupling constant. For a molecular radical pair undergoing free rotational diffusion in solution, the anisotropic hyperfine coupling and Zeeman interaction terms average to zero, so they are not included in $\langle \hat{H} \rangle$. The radical coupling term is assumed to just contain a thermally averaged scalar coupling term,

$$\hat{H}_{1,2} = -2 \langle J \rangle \hat{\mathbf{S}}_1 \cdot \hat{\mathbf{S}}_2, \tag{7.4}$$

where this average scalar coupling constant $\langle J \rangle$ is a sum of all contributions direct and superexchange contributions, including those from the reactive pathways. Just as the anisotropic hyperfine and Zeeman terms are averaged to zero for a molecule tumbling in solution, the dipolar coupling between non-overlapping radicals also averages to zero, so only the isotropic scalar coupling term needs to be considered.

It can be assumed that the density operator is initially in a system given by

$$\hat{\rho}(0, \mathsf{X}) = \frac{1}{Z} \hat{\rho}_e(0) p_0(\mathsf{X}), \tag{7.5}$$

where $\hat{\rho}_e(0)$ is some electron spin density operator, Z is the dimensionality of the nuclear spin Hilbert space and $p_0(\mathsf{X})$ is the steady state of Γ. This corresponds to the nuclear spins initially being in a totally mixed state, i.e. the high temperature thermal equilibrium state, and the slow degrees of freedom X initially being at equilibrium. The initial condition for the electron spins $\hat{\rho}_e(0)$ will depend on how the radical pair is formed.

The hyperfine coupling terms in $\hat{H}_i$ mean that many nuclear spins have to be included in any calculation of the the radical pair spin dynamics. The dimensionality of spin Hilbert space grows exponentially with the number of coupled spins in the model, and given that typical radical pairs contain at least 20 nuclei with significant hyperfine couplings, exact numerical calculations of the radical pair spin dynamics are normally prohibitively expensive, if possible at all. The expense of such calculations is particularly problematic

when there are unknown parameters in the radical pair model, such as the spin selective reaction rate constants; these parameters normally have to be fitted by comparison of experimental data and simulated spin dynamics for many possible values of the unknown parameters. This motivates the search for accurate approximate solutions to the radical pair Stochastic Liouville equation.

In the previous chapter I demonstrated that the second order Markovian Nakajima-Zwanzig equation gives an accurate method for treating relaxation processes in radical pair reactions, but this does not circumvent the problem of the exponential scaling of the spin Hilbert space. This means some additional approximation needs to be made to the Nakajima-Zwanzig relaxation master equation in order to obtain a computationally efficient method for calculating electron spin system observables, such as the quantum yield of the radical pair reactions and the radical pair lifetime. In the next section I describe how the Schulten-Wolynes semiclassical approximation can be used to obtain a semiclassical master equation for the ensemble averaged electron spin density operator.

7.2 The Schulten-Wolynes approximation

Thus far I have demonstrated that the Nakajima-Zwanzig equation provides an accurate description of relaxation processes in radical pairs spanning the full range of fluctuation correlation times. However, solving this equation has a computational effort that increases exponentially with the size of the spin system. It is therefore fortunate that, for short-lived radical pairs and radical pairs in which the electron spin interactions are much stronger than the electron-nuclear spin interactions, the full solution of the Nakajima-Zwanzig equation is not necessary, because the Schulten-Wolynes semiclassical approximation provides a sufficiently accurate approximation to the spin dynamics.[187]

In the Schulten-Wolynes approximation, the nuclear spin operators in the Hamiltonian are replaced with static classical vectors, $\mathbf{I}_{i,k}$, of length $\sqrt{I_{i,k}(I_{i,k}+1)}$, each sampled from the surface of a sphere.[a] The reduced density operator for the electron spin subsystem is

[a] In the original formulation by Schulten and Wolynes, the central limit theorem was used to obtain the distribution of the total nuclear hyperfine field. However in the present formulation we require the orientation of each classical vector to calculate the relaxation superoperators, so we do not make this additional approximation.

approximated as the average over all orientations of the nuclear spin vectors,

$$\hat{\rho}_{\mathrm{e}}(t,\mathsf{X}) = \mathrm{Tr}_{\mathrm{b}}[\hat{\rho}(t,\mathsf{X})] \approx \int \hat{\rho}_{\mathrm{SW}}(t,\mathsf{X},\mathbf{I})P(\mathbf{I})\,\mathrm{d}\mathbf{I}\,. \tag{7.6}$$

Here $\mathrm{Tr}_{\mathrm{b}}[\cdots]$ here denotes a trace over the bath of nuclear spin degrees of freedom, $\mathbf{I} = (\mathbf{I}_{1,1}, ..., \mathbf{I}_{1,N_1}, \mathbf{I}_{2,1}, .., \mathbf{I}_{2,N_2})$ is the set of nuclear spin vectors, $\hat{\rho}_{\mathrm{SW}}(t,\mathsf{X},\mathbf{I})$ is the Schulten-Wolynes electron spin density operator for a given realisation of the nuclear spins, and $\int \mathrm{d}\mathbf{I}\cdots P(\mathbf{I})$ denotes an integral over their orientations,

$$\int \mathrm{d}\mathbf{I}\, P(\mathbf{I}) = \prod_{i=1}^{2}\prod_{k=1}^{N_i}\int \mathrm{d}\mathbf{I}_{i,k}\,\frac{\delta\left(|\mathbf{I}_{i,k}| - \sqrt{I_{i,k}(I_{i,k}+1)}\right)}{4\pi I_{i,k}(I_{i,k}+1)}. \tag{7.7}$$

We note that the integral over nuclear spin configurations can be evaluated efficiently using Monte-Carlo sampling.

The Schulten-Wolynes density operator obeys the following equation of motion,

$$\begin{aligned}\frac{\partial}{\partial t}\hat{\rho}_{\mathrm{SW}}(t,\mathsf{X},\mathbf{I}) = &-\frac{i}{\hbar}\left[\left\langle\hat{H}_{\mathrm{SW}}(\mathbf{I})\right\rangle + \hat{V}_{\mathrm{SW}}(\mathsf{X},\mathbf{I}), \hat{\rho}_{\mathrm{SW}}(t,\mathsf{X},\mathbf{I})\right]\\ &-\left\{\left\langle\hat{K}\right\rangle, \hat{\rho}_{\mathrm{SW}}(t,\mathsf{X},\mathbf{I})\right\} + \Gamma\,\hat{\rho}_{\mathrm{SW}}(t,\mathsf{X},\mathbf{I}),\end{aligned} \tag{7.8}$$

where $\left\langle\hat{H}_{\mathrm{SW}}(\mathbf{I})\right\rangle$ is $\left\langle\hat{H}\right\rangle$ with the nuclear spin operators replaced by the classical vectors ($\hat{\mathbf{I}}_{i,k} \rightarrow \mathbf{I}_{i,k}$), and likewise for $\hat{V}_{\mathrm{SW}}(\mathsf{X},\mathbf{I})$. The Schulten-Wolynes density operator is initialised in the state $\hat{\rho}_{\mathrm{SW}}(0,\mathsf{X},\mathbf{I}) = \hat{\rho}_{\mathrm{e}}(0)p_0(\mathsf{X})$. This approximation can be obtained more rigorously by taking the Stratonovich-Weyl transform of the spin density operator,[188–191] and assuming the nuclear spins static remain static throughout the dynamics, which is valid if the nuclear spin evolution is slower than the electron spin dynamics.

In order to obtain the ensemble dynamics, we can apply perturbative Nakajima-Zwanzig theory directly to this equation of motion, exactly as in the previous chapter. In this case, for each realisation $\mathbf{I}$ of the nuclear spin vectors, we evolve the ensemble averaged Schulten-Wolynes electron spin density operator $\hat{\rho}_{\mathrm{SW}}(t,\mathbf{I})$ using the Nakajima-Zwanzig equation,

$$\begin{aligned}\frac{\mathrm{d}}{\mathrm{d}t}\hat{\rho}_{\mathrm{SW}}(t,\mathbf{I}) = &-\frac{i}{\hbar}\left[\left\langle\hat{H}_{\mathrm{SW}}(\mathbf{I})\right\rangle, \hat{\rho}_{\mathrm{SW}}(t,\mathbf{I})\right]\\ &-\left\{\left\langle\hat{K}\right\rangle, \hat{\rho}_{\mathrm{SW}}(t,\mathbf{I})\right\} - \mathcal{R}_{\mathrm{NZ,SW}}(\mathbf{I})\hat{\rho}_{\mathrm{SW}}(t,\mathbf{I}),\end{aligned} \tag{7.9}$$

where $\mathcal{R}_{\mathrm{NZ,SW}}(\mathbf{I})$ is the Schulten-Wolynes Nakajima-Zwanzig relaxation superoperator for

a given $\mathbf{I}$. To construct this we simply replace the nuclear spin operators in $\mathcal{R}_{\mathrm{NZ}}$ with the corresponding nuclear spin vectors, as in constructing $\left\langle \hat{H}_{\mathrm{SW}}(\mathbf{I}) \right\rangle$. This Nakajima-Zwanzig/Schulten-Wolynes (NZ/SW) method consistently combines the Schulten-Wolynes semiclassical approximation with the second order relaxation theory provided by the Nakajima-Zwanzig equation, and so provides a way to efficiently model the spin dynamics of radical pairs containing over 20 coupled spins. With this method we can treat relaxation effects rigorously with microscopic models of the relaxation mechanisms, without resorting to phenomenological relaxation terms in the master equation.

This method is akin to the reduced density matrix hybrid approaches which have been used extensively in the study of non-adiabatic dynamics.[159,192–195] In these approaches the bath is divided into slow and fast degrees of freedom, where the slow modes are treated by performing a Wigner transform with respect to these degrees of freedom and treating them as static and the fast modes are treated using perturbative master equation approaches. The Schulten-Wolynes method described here can be obtained by performing the analogue of the Wigner transform for spin, the Stratonovich-Weyl transform,[188–191] and then treating the spins as static, so the NZ/SW method is essentially the spin dynamics analogue of the reduced density matrix hybrid approach.

7.3 Application to DMJ-NDI radical pairs

As an example application of the NZ/SW method outlined above, I will now use it to investigate the intersystem crossing and charge transfer dynamics of photoexcited dimethyljulolidine (DMJ) anthracene (An) para-oligophenylene ($\mathrm{Ph_n}$) naphthalenediimide (NDI) molecules, the chemical structure of which is shown in Fig. 7.1. These molecules have been studied experimentally by Scott *et al.*,[67] and we will use various models for the spin relaxation to interpret their experimental data for the magnetic field effects on the radical pair lifetime and triplet product quantum yields of the molecules with n=1 and n=2 para-phenylene spacers.

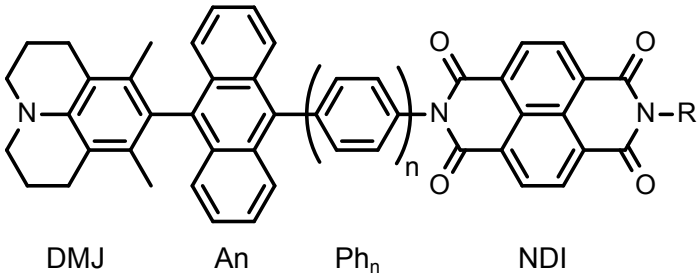

Figure 7.1: The chemical structure of the DMJ-An-Ph$_n$-NDI molecules, where R=n-C_8H_{17}. This molecule forms a radical ion pair though an electron transfer reaction initiated by photoexcitation of the DMJ-An fragment.

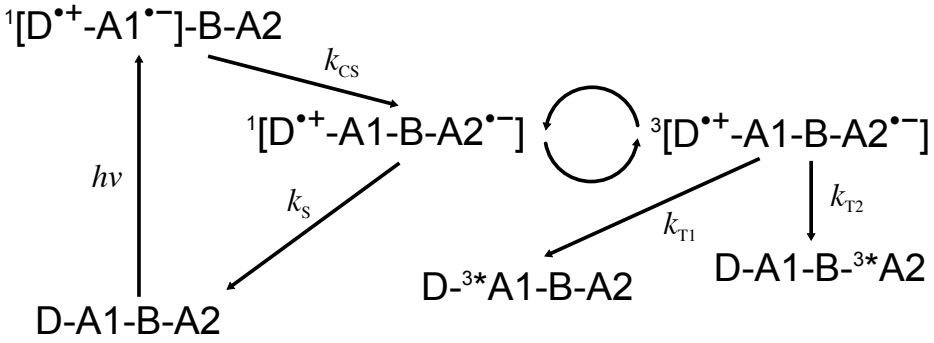

Figure 7.2: The photophysics of the DMJ-An-Ph$_n$-NDI molecule. Here D = DMJ, A1 = An, B = Ph$_n$ and A2 = NDI. The straight arrows represent incoherent processes and the curved arrows represent the radical pair spin dynamics.

7.3.1 Photophysics

Full details of Scott *et al.*'s experiments can be found in Ref. [67], where the molecule and its photophysics are fully characterised. Here it suffices to summarise the experiments on the radical pairs, which will be done with reference to Fig. 3. First the DMJ-An section of the molecule is photoexcited at the edge of its charge transfer band at 416 nm with a laser pulse at 430 nm to form a charge transfer state ^{1}[DMJ$^{\bullet+}$-An$^{\bullet-}$]. This then undergoes another charge transfer to form a radical pair state ^{1}[DMJ$^{\bullet+}$-An-Ph$_n$-NDI$^{\bullet-}$] at a rate k_{CS}. The radical pair is formed in the singlet state and undergoes charge recombination to reform the ground state molecule at a rate k_S, and hyperfine mediated intersystem crossing to form the triplet radical pair state, ^{3}[DMJ$^{\bullet+}$-An-Ph$_n$-NDI$^{\bullet-}$]. The triplet radical pair state can then convert back to the singlet radical pair state or undergo a charge transfer to form one of two triplet products. In the triplet products the electronic excitation is localised either on the anthracene, ^{3*}An, which is formed at a rate k_{T1}, or the naphthalenediimide, ^{3*}NDI,

formed at a rate k_{T2}. The total triplet recombination rate is then $k_T = k_{T1} + k_{T2}$. Both the triplet products and the radical pair state are distinguishable spectroscopically, which allows the lifetime of the radical pair state and the triplet product yields to be measured.[67]

7.3.2 Magnetic field effects

Scott *et al.*[67] measured magnetic field effects on both the lifetime of the radical pair state and the quantum yields of the triplet products relative to the zero field value. Both of these magnetic field effects exhibit a resonance centred at $B = 2J/g_e\mu_B$, where $2J$ is the average scalar coupling in the radical pair – the field at which the singlet and T_+ triplet states are degenerate in the absence of hyperfine interactions. (See Fig. 7 in section 1.2.3 for a more detailed discussion of this effect.)

The spin selective charge transfer rates k_S and k_T were estimated experimentally by fitting the kinetic traces of the radical pair state population at different applied field strengths to kinetic models of the radical pair reaction.[67] This kinetic modelling approximates the coherent intersystem crossing and incoherent relaxation effects with a simple incoherent model involving field-dependent intersystem crossing rate constants. The approximation provides estimates of recombination rate constants in a straightforward manner, but it ignores the details of the radical pair dynamics. In this work we will apply the NZ/SW method outlined above to compute the lifetimes and relative triplet yields (RTY) of the ^{3*}An products of these radical pairs. In doing so we can obtain more reliable estimates of the spin selective recombination rate constants, k_S and k_T, as well as determine the relative importance of various relaxation mechanisms and any additional mechanisms by which triplet products can be formed.

7.3.3 Relaxation mechanisms

In this modelling of magnetic field effects on DMJ$^{\bullet+}$-An-Ph$_n$-NDI$^{\bullet-}$ recombination reactions, we will consider three mechanisms of spin relaxation: rotational diffusion modulating anisotropic spin-spin couplings and the g-tensors, internal motion of the radical pair modulating the scalar electron spin coupling, and conformational changes of the radicals modulating hyperfine coupling between the nuclear and electron spins. To cover all of these

cases, the fluctuation Hamiltonian, $\hat{V}(\mathsf{X})$, is split into rotational motion and internal motion terms. The former depend on the orientation of the radical pair, Ω, and the latter on a set of reduced internal coordinates, Q, which we assume to be uncorrelated with Ω:

$$\hat{V}(\mathsf{X}) = \hat{V}_{\text{rot}}(\Omega) + \hat{V}_{\text{int}}(\mathsf{Q}). \tag{7.10}$$

In the following we will briefly discuss the rotational and internal motion relaxation mechanisms, and how the theory outlined above can be used to model them.

7.3.4 Rotational diffusion

Rotational diffusion of the radical pair leads to a fluctuation in the anisotropic parts of the spin-spin coupling tensors and the anisotropic components of the g-tensors. The overall fluctuation has the form[43,44]

$$\hat{V}_{\text{rot}}(\Omega) = \sum_{m=-2}^{2} \sum_{m'=-2}^{2} \mathfrak{D}^{(2)}_{m',m}(\Omega) \hat{Q}^{(2)}_{m,m'}, \tag{7.11}$$

where $\hat{Q}^{(2)}_{m,m'} = \hat{Q}^{(2)}_{1,m,m'} + \hat{Q}^{(2)}_{2,m,m'} + \hat{Q}^{(2)}_{\text{dip},m,m'}$. Here $\hat{Q}^{(2)}_{i,m,m'}$ is the anisotropic component of the Hamiltonian of radical i,

$$\hat{Q}^{(2)}_{i,m,m'} = \mu_{\text{B}} g^{(2)}_{i,m} T^{(2)}_{m'}(\hat{\mathbf{S}}_i, \mathbf{B}_0) + \sum_{k=1}^{N_i} A^{(2)}_{i,k,m} T^{(2)}_{m'}(\hat{\mathbf{S}}_i, \hat{\mathbf{I}}_{i,k}), \tag{7.12}$$

and $\hat{Q}^{(2)}_{\text{dip},m,m'}$ is the dipolar electron spin coupling term

$$\hat{Q}^{(2)}_{\text{dip},m,m'} = D^{(2)}_{m} T^{(2)}_{m'}(\hat{\mathbf{S}}_1, \hat{\mathbf{S}}_2). \tag{7.13}$$

In these expressions, $T^{(2)}_{m'}(\mathbf{u}, \mathbf{v})$ are rank 2 spherical tensor components for a pair of vectors $\mathbf{u}$ and $\mathbf{v}$, $A^{(2)}_{i,k,m}$, $g^{(2)}_{i,m}$ and $D^{(2)}_{m}$ are the rank 2 spherical tensor components of the hyperfine coupling tensors, g-tensors, and dipolar coupling tensor, respectively.[43] $\mathfrak{D}^{(2)}_{m',m}(\Omega)$ is the rank 2 Wigner D-matrix element for the molecule in an orientation given by Ω, which is the orientation of the principal axes of the molecule relative to the lab frame.[43]

This approximates the radical pair as a rigid body, and we will further limit our discussion to the case of symmetric top diffusion. In this case the $\mathfrak{D}^{(2)}_{m',m}(\Omega)$ matrix elements have the

following correlation functions,[196]

$$\left\langle \mathfrak{D}^{(2)}_{m,n}(t)^* \mathfrak{D}^{(2)}_{m',n'}(0) \right\rangle = \frac{\delta_{m,m'}\delta_{n,n'}}{5} e^{-(6D_\perp + (D_\parallel - D_\perp)n^2)t}, \tag{7.14}$$

where $D_\perp$ and $D_\parallel$ are the rotational diffusion constants perpendicular and parallel to the molecular symmetry axis.

7.3.5 Internal motion

Internal vibrational motion of the radical pair modulates isotropic and anisotropic coupling parameters in the radical pair Hamiltonian. Torsional motions of the radicals and the para-phenylene units modulate the superexchange coupling between radicals, leading to a fluctuation term of the form

$$\hat{V}_{\text{int}}(\mathsf{Q}) = -2\Delta J(\mathsf{Q})\hat{\mathbf{S}}_1 \cdot \hat{\mathbf{S}}_2. \tag{7.15}$$

We model the fluctuation autocorrelation function for ΔJ as a single exponential decay

$$\langle \Delta J(t)\Delta J(0)\rangle = \sigma_J^2 e^{-t/\tau_J}, \tag{7.16}$$

where σ_J^2 is the mean square fluctuation in $J(t)$ and τ_J is the correlation time of this fluctuation. This model is a significant simplification of the true molecular motion modulating the scalar coupling of the electrons, but it contains a minimal number of parameters. This type of correlation function is obtained if the dominant motion modulating $2J$ is an overdamped vibrational mode q, and if $\Delta J(q)$ is linear function of q.

The $\text{DMJ}^{\bullet+}$ radical ring system has four stable conformations, two *syn* and two *anti* (see Fig. 7.3). Each ring can flip, with an *anti* to *syn* rate constant of k_{flip}, which changes the C–H bonds in the ring hyperconjugated with the nitrogen atom p-orbital. This modulates the proton hyperfine couplings, which gives rise to spin relaxation. We assume that only one ring can flip at a time, so the model includes two rate constants: the *anti*→*syn* flip rate constant is k_{flip}, and the back flipping rate constant is k'_{flip}. With this model we ignore fluctuations of the anisotropic components of the hyperfine coupling tensor, which are at least 10 times smaller than the fluctuations in the isotropic components.

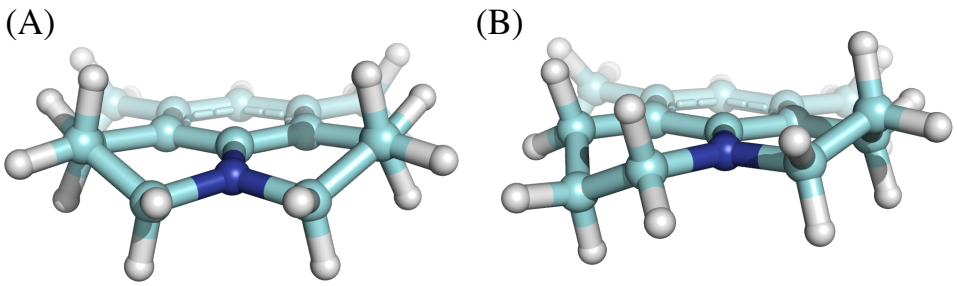

Figure 7.3: Two of the four conformations of the DMJ radical cation: (A) one of the two *syn* conformations and (B) one of the two *anti* conformations. Geometries calculated using DFT with the B3LYP functional with D3 dispersion correction and the 6-31G(d,p) basis set with Gaussian09.[197]

7.3.6 Additional triplet formation mechanisms

In addition to triplet radical pair recombination, the triplet product can be formed by other mechanisms. This may be required to explain the observed MFEs on the triplet product yield at high magnetic fields, as has been noted previously for the charge recombination along other molecular wires.[51,150,182,198]

One possibility is that spin-orbit coupling plays a role in the singlet charge recombination.[66] Some intersystem crossing will then accompany this charge recombination, yielding a triplet product from a singlet radical pair. Assuming this occurs at a rate k_{ST1} for ^{3*}An, the observed triplet yield, $\Phi_{T1,obs}$ will be related to the quantum yields defined in Eq. (6.72) by

$$\Phi_{T1,obs} = \frac{k_{T1}}{k_T}\Phi_T + \frac{k_{ST1}}{k_S}\Phi_S, \tag{7.17}$$

where k_S and k_T are the total recombination rates from the radical pair singlet and triplet states. It follows that the relative triplet yield of the DMJ-^{3*}An-Ph$_n$-NDI product state will be given by

$$\mathrm{RTY}(B) = \frac{\Phi_{T1,obs}(B)}{\Phi_{T1,obs}(0)} = \frac{\Phi_T(B) + \Phi_0}{\Phi_T(0) + \Phi_0}, \tag{7.18}$$

where

$$\Phi_0 = \frac{k_{ST1}}{k_S k_{T1}/k_T - k_{ST1}} \tag{7.19}$$

is a field-independent "background" contribution to the production of this state.

Another possibility is that in the initial charge separation step, a small fraction of triplet radical pairs are generated.[199] In this case the initial condition of the ensemble averaged

density operator becomes

$$\hat{\rho}(0) = \frac{1-\lambda_{\mathrm{T}}}{Z}\hat{P}_{\mathrm{S}} + \frac{\lambda_{\mathrm{T}}}{3Z}\hat{P}_{\mathrm{T}}, \tag{7.20}$$

where λ_{T} is the initial triplet fraction. At high fields the T_+ and T_- triplet states are well separated in energy from the singlet state, so radical pairs created in these states cannot convert to the singlet state and therefore simply recombine to give the triplet product.

The final mechanism for triplet product formation we consider is some additional relaxation not accounted for by our microscopic modelling. Any source of rapidly fluctuating magnetic fields or a mechanism which randomises the electron spin state could give rise to additional relaxation. We allow for such a contribution using the following superoperator,[45]

$$\mathcal{L}_{\mathrm{rel}}\hat{\rho}(t) = -k_{\mathrm{rel}}\left(\frac{3}{2}\hat{\rho}(t) - \sum_{\alpha=x,y,z}\hat{S}_{1,\alpha}\hat{\rho}(t)\hat{S}_{1,\alpha}\right), \tag{7.21}$$

in which we choose $\hat{S}_{1,\alpha}$ to correspond to the DMJ radical electron spin. This form of the relaxation operator arises from random fields relaxation in the extreme narrowing limit, in which case $k_{\mathrm{rel}} = 2\tau_{\mathrm{c}}\left\langle \Delta B^2 \right\rangle \gamma_{\mathrm{e}}^2$, where $\left\langle \Delta B^2 \right\rangle$ is the mean square fluctuation in the random field and τ_{c} is the correlation time of the fluctuation.[45]

7.3.7 Simulation parameters

Many of the parameters in these simulations can be determined either from existing experimental data or electronic structure calculations. The average scalar electron spin coupling can be extracted from the peaks in the relative triplet yield and radical pair lifetime curves as a function of applied magnetic field,[67] which give $2J = 170$ mT and 31 mT for the n=1 and n=2 molecules respectively. The hyperfine coupling tensors, g-tensors, and dipolar coupling tensors were obtained from available experimental data[200] and DFT calculations, and the rotational diffusion constants were estimated based on the Stokes-Einstein equation (as outlined in appendix 7.B). For simulations including the *anti-syn* ring flipping of the DMJ radical, the ratio of the flipping rates is given by $k_{\mathrm{flip}}/k'_{\mathrm{flip}} = e^{-\Delta G/RT}$. Our results were not found to be strongly dependent on ΔG so the gas phase energy difference of $\Delta G \approx 1.5$ kJ mol^{-1} was used, as calculated at the DLPNO-CCSD(T)/aug-cc-pVTZ level of

theory using the ORCA program (version 4.0.1),[201], as a simple estimate.

Given that not all parameters are known *a priori*, and that we do not even know which mechanisms of additional triplet formation may operate in these radical pairs, we shall systematically increase the complexity of our model, including more relaxation processes and additional triplet formation mechanisms as we do so. At each stage we need to determine the total spin selective recombination rates, k_S and k_T, as well as some of the relaxation parameters and additional triplet formation parameters. These are obtained by fitting each model to the experimental charge recombination rate, $k_{CR}(B) = 1/\tau_{RP}(B)$, and relative triplet yield data $\mathrm{RTY}(B)$, over a range of magnetic field strengths. For the n=1 molecule, we fit to $k_{CR}(B)$ and $\mathrm{RTY}(B)$ for magnetic field strengths between 0 mT and 500 mT, and for n=2 we fit to the available $k_{CR}(B)$ data between 0 mT and 100 mT and the $\mathrm{RTY}(B)$ data between 0 mT and 500 mT.[67] The parameters are extracted from the data by minimising an equally weighted sum of the normalised mean square errors (NMSEs) in the fits. This corresponds to minimising the following quantity with respect to the free parameters,

$$\begin{aligned}\overline{\mathrm{NMSE}} =& \frac{1}{2N_{k_{CR}}} \sum_{i=1}^{N_{k_{CR}}} \frac{(k_{CR}^{(exp)}(B_i) - k_{CR}^{(calc)}(B_i))^2}{(k_{CR,max}^{(exp)} - k_{CR,min}^{(exp)})^2} \\ &+ \frac{1}{2N_{RTY}} \sum_{i=1}^{N_{RTY}} \frac{(\mathrm{RTY}^{(exp)}(B_i) - \mathrm{RTY}^{(calc)}(B_i))^2}{(\mathrm{RTY}_{max}^{(exp)} - \mathrm{RTY}_{min}^{(exp)})^2},\end{aligned} \tag{7.22}$$

where $k_{CR}^{(exp)}(B_i)$ and $\mathrm{RTY}^{(exp)}(B_i)$ are the experimental charge recombination rate and relative triplet yield at field strength B_i and the subscripts max and min indicate the maximum and minimum values of these datasets.

7.4 Results

7.4.1 Validation of the NZ/SW method

In order to validate the NZ/SW method, it was used to simulate the relative triplet yield and the radical pair lifetime for a reduced model of the $\mathrm{DMJ^{\bullet+}}$-An-$\mathrm{Ph_n}$-$\mathrm{NDI^{\bullet-}}$ radical pairs with n=1 and n=2 containing only 15 nuclear spins. This reduced model only includes relaxation from rotational diffusion and fluctuation in the J value, which is treated using

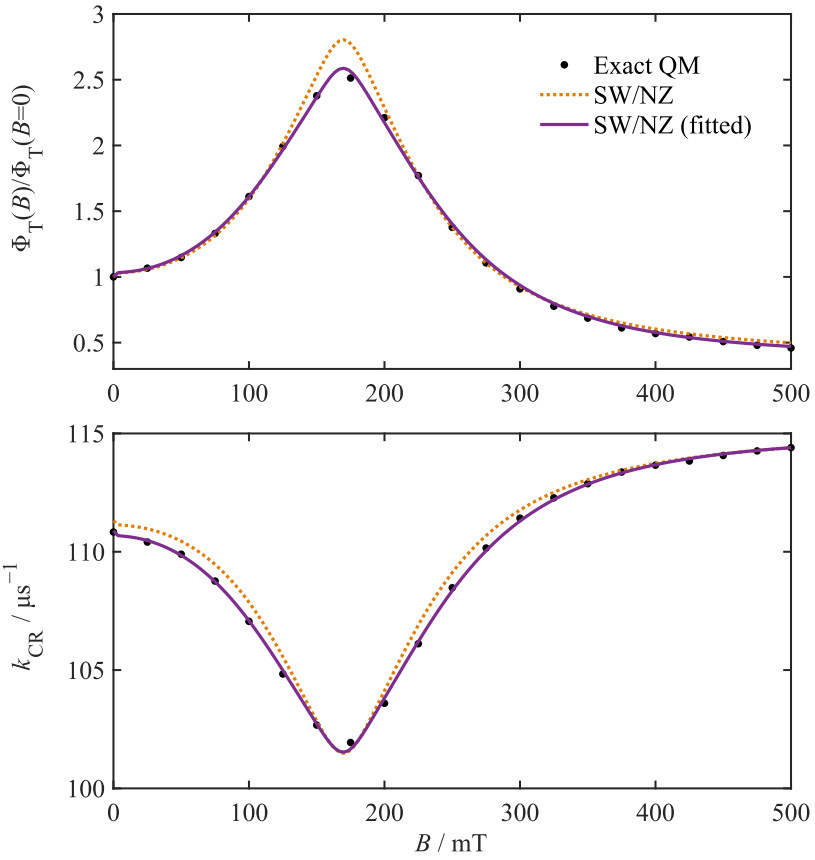

Figure 7.4: Comparison of the NZ/SW method with exact quantum mechanical simulations for the n=1 reduced model. The fitted NZ/SW results are obtained by fitting k_S, k_T, σ_J and τ_J using the NZ/SW method to the exact simulation data. Top panel: relative triplet yield data, bottom panel: $k_{CR} = 1/\tau_{RP}$ data.

a symmetric two site model. The numerically exact results were obtained by numerically propagating spin states evolving under the stochastic Schrödinger equation which generates the same dynamics as the radical pair SLE, where the full trace over nuclear spin states can be sampled efficiently using coherent spin state sampling.[185,198] These calculations were performed by Lachlan Lindoy. The numerically exact simulations took nearly a month parallelised over more than a hundred CPUs, whereas a NZ/SW calculation of an MFE curve takes less than a minute on a single CPU. This means the exact simulations cannot be used to parameter fit models to experimental data, whereas using the NZ/SW method this task is trivial, although there may be systematic errors in the fitted parameters arising from the approximations in the NZ/SW method.

The hyperfine and g-tensors used in the reduced models are detailed in appendix 7.A, and in both the n=1 and n=2 models the rotational diffusion constants are $D_{\parallel} = 3.2080\ \text{ns}^{-1}$ and $D_{\perp} = 0.11881\ \text{ns}^{-1}$. Other parameters are summarised in Table 7.1. In addition to performing a direct comparison between the exact lifetime and relative triplet yield data,

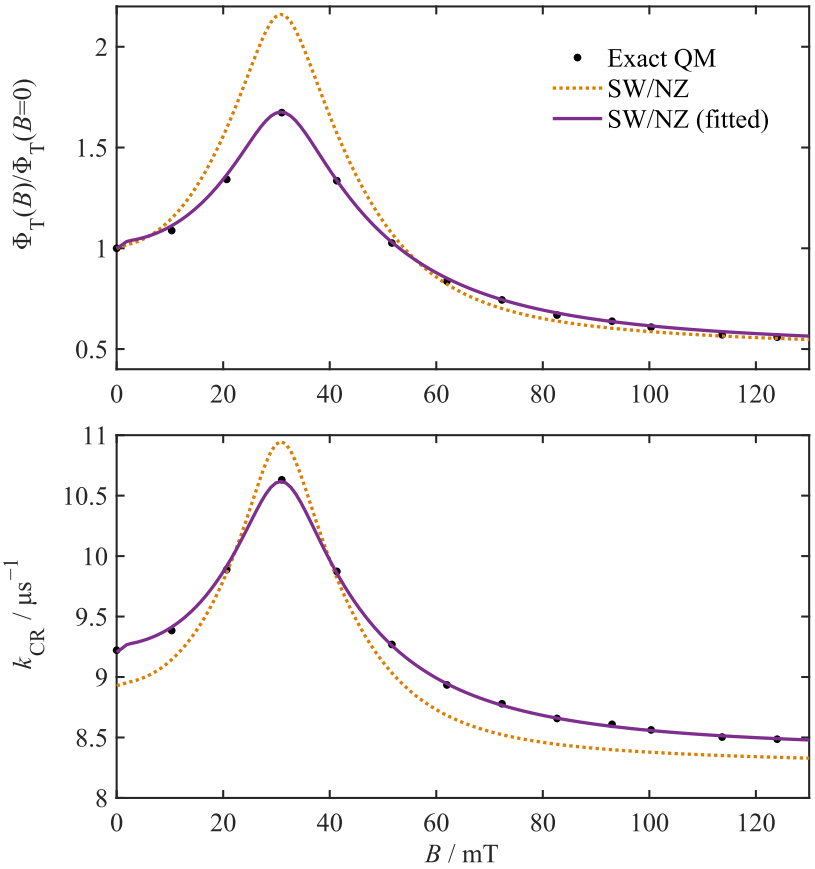

Figure 7.5: Comparison of the NZ/SW method with exact quantum mechanical simulations for the n=2 reduced model. The fitted NZ/SW results are obtained by fitting k_S, k_T, σ_J and τ_J using the NZ/SW method to the exact simulation data. Top panel: relative triplet yield data, bottom panel: $k_{CR} = 1/\tau_{RP}$ data.

the k_S, k_T, σ_J and τ_J parameters are fitted to the exact simulation data using the NZ/SW method. This numerical experiment is performed to evaluate how reliable the model parameters derived from a NZ/SW fit to available data are likely to be.

The results of these tests are shown in Fig. 7.4 for the n=1 reduced model and Fig. 7.5 for the n=2 reduced model. The NZ/SW method is more accurate for the n=1 reduced model, with a maximum error of approximately 1% in the k_{CR} data and around 10% in the relative triplet yield, than in the n=2 reduced model, where the maximum error in the k_{CR} data and

	k_S/ns^{-1}	k_T/ns^{-1}	$2\langle J\rangle/g_e\mu_B$mT	$2\sigma_J/g_e\mu_B$mT	τ_J/ns
n=1	0.11763	0.030111	170.00	200.82	0.0077085
n=1 (fitted)	0.11772†	0.029255†	170.00	145.61†	0.015711†
n=2	0.0077042	0.014657	31.000	9.3213	0.17928
n=2 (fitted)	0.0076930†	0.013854†	31.000	20.044†	0.053195†

Table 7.1: Parameters used in the reduced models. The †indicates that these parameters were treated as free parameters in fitting the NZ/SW model by minimising the $\overline{\text{NMSE}}$ in the lifetime and relative triplet yield data, using the exact simulation data as a reference.

relative triplet yield data are approximately 3% and 30% respectively. The error is worse in the n=2 case because the rate constants for the radical pair reactions and scalar electron spin coupling constants are smaller. Because both the SW and NZ approximations become exact in the limit where the isotropic hyperfine interactions and the fluctuation terms are small relative to the electron spin terms in the Liouvillian, the error can be expected to be larger in the n=2 case.

In Figs. 7.4 and 7.5 the results of fitting NZ/SW model parameters to the exact data are also shown. In this case we see that the NZ/SW model can be fitted to a very high degree of accuracy to the exact data. The resulting fitted parameters are given in Table 7.1, where we see the largest error in the fitted rate constants is less than 6%. This suggests that the systematic error introduced by using the NZ/SW method to obtain rate constants is very small. The errors in the $2\sigma_J$ and τ_J parameters are larger, but this is probably due to the fact that τ_J is much shorter than the time scale of the spin system dynamics, so the $2J$ fluctuations in this model are in the extreme narrowing limit. In this limit the $2J$ fluctuations cause singlet-triplet dephasing at a rate

$$k_{\mathrm{STD}} = \left(\frac{2\sigma_J}{\hbar}\right)^2 \tau_J, \tag{7.23}$$

and therefore the observed magnetic field effects are only really dependent on one parameter, $\sigma_J^2\tau_J$. The error in this parameter is $\sim$6% for the n=1 model and $\sim$36% for the n=2 model.

Overall the results of these numerical experiments indicate that the reaction rate constants obtained by fitting a NZ/SW model to available data are likely to be very accurate, for these molecules. The errors in the relaxation process parameters may be larger, but still in this case the errors are less than a factor of 4. This gives us some confidence in the application of the NZ/SW method to modelling MFEs in the $\mathrm{DMJ}^{\bullet+}$-An-$\mathrm{Ph_n}$-$\mathrm{NDI}^{\bullet-}$ radical pairs, although one caveat to this is that in these numerical tests the underlying relaxation model and hyperfine constants are known *a priori* with absolute certainty, which is not true of the analysis of the experimental data.

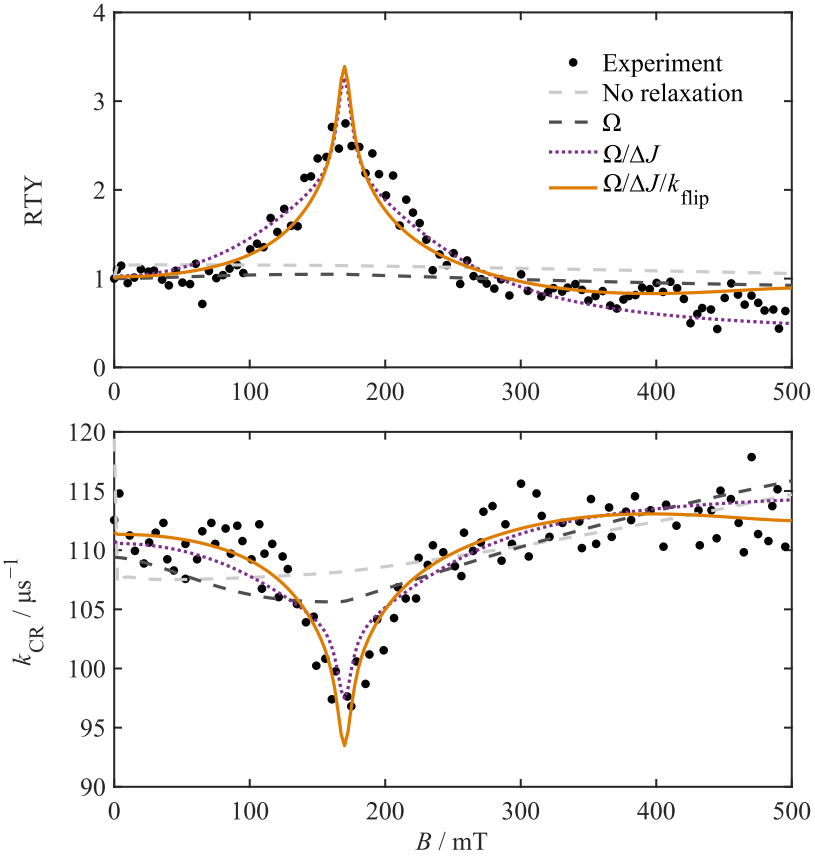

Figure 7.6: Comparison on the best fit NZ/SW results including various relaxation mechanisms with experimental data for the n=1 molecule. Ω indicates rotational diffusion is included, ΔJ indicates J fluctuations are included and k_{flip} indicates conformational changes of the DMJ radical are included. Top panel: relative triplet yield data, bottom panel: $k_{\text{CR}} = 1/\tau_{\text{RP}}$ data.

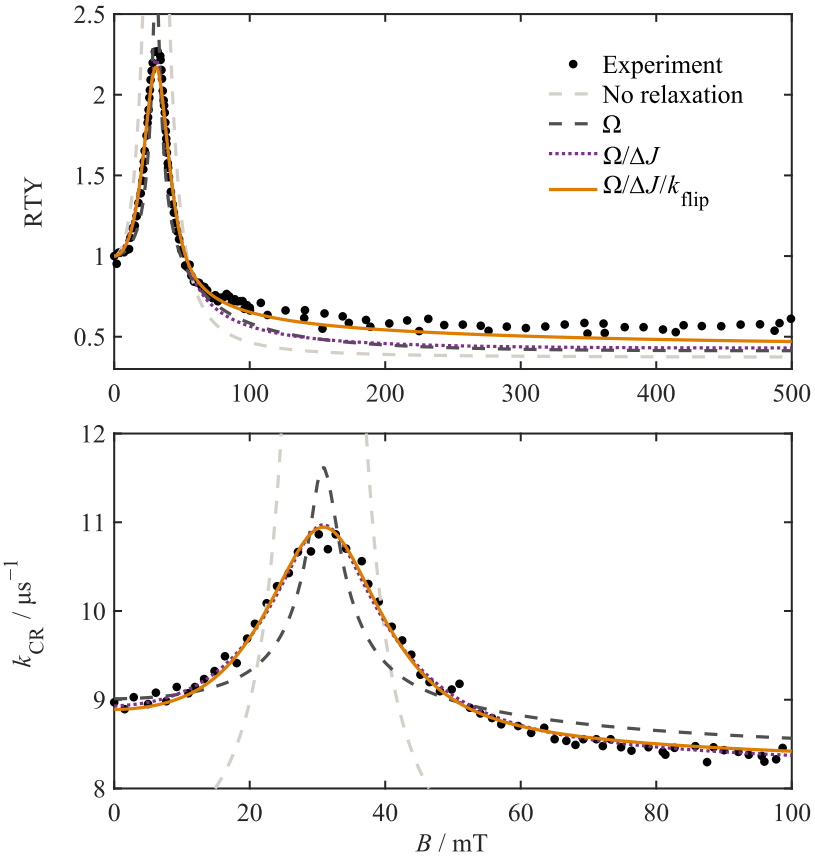

Figure 7.7: Comparison on the best fit NZ/SW results including various relaxation mechanisms with experimental data for the n=2 molecule. Ω indicates rotational diffusion is included, ΔJ indicates J fluctuations are included and k_{flip} indicates conformational changes of the DMJ radical are included. Top panel: relative triplet yield data, bottom panel: $k_{\text{CR}} = 1/\tau_{\text{RP}}$ data.

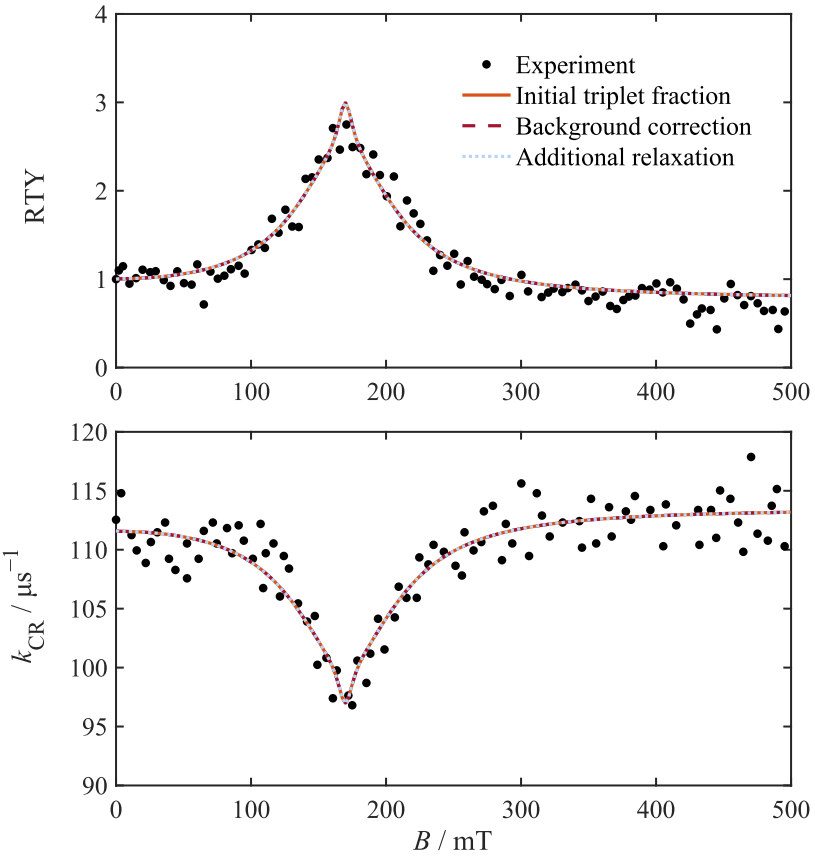

Figure 7.8: Comparison on the best fit NZ/SW results including various additional triplet formation mechanisms with experimental data for the n=1 molecule. Top panel: relative triplet yield data, bottom panel: $k_{CR} = 1/\tau_{RP}$ data.

7.4.2 Comparison with experiment

The best fits to the k_{CR} and RTY data for models of the radical pair reaction including different relaxation mechanisms are shown in Fig. 7.6 for n=1 and Fig. 7.7 for n=2, and the $\overline{\text{NMSE}}$ values for the best fit models, and the parameters obtained from them are summarised in Table 7.2. The fit quality dramatically improves as relaxation by rotational diffusion and $2J$ modulation are included for both molecules (n=1 and n=2); adding relaxation due to ring flips of the DMJ has little effect on the fit quality. However, none of the models including relaxation perfectly describe all of the features of the experimental magnetic field effect data. In particular, the k_{CR} $B = 2J/g_e\mu_B$ peak shape for the n=1 molecule and the high-field limit of the RTY for the n=2 molecule are not captured well by these models, as can be seen in panels (a) and (d) of the figure.

In Fig. 7.8 and Fig. 7.9 the best fits to the experimental data for simulations including rotational diffusion, $2J$ modulation, and one of the three proposed additional triplet formation mechanisms are displayed. The resulting best fit parameters are given in Tables

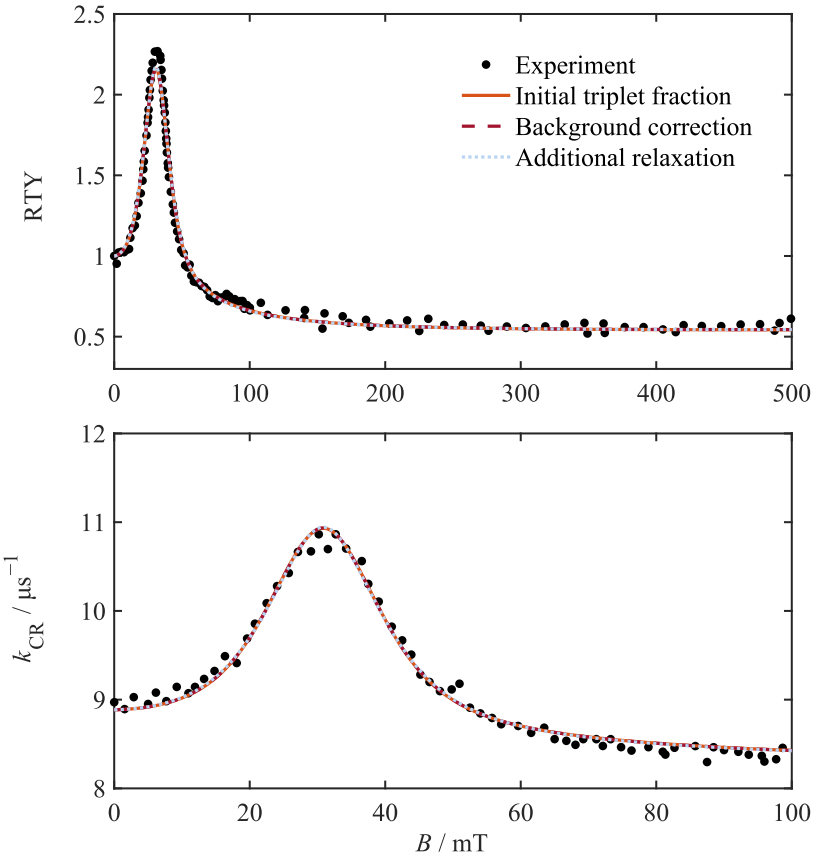

Figure 7.9: Comparison on the best fit NZ/SW results including various additional triplet formation mechanisms with experimental data for the n=2 molecule. Top panel: relative triplet yield data, bottom panel: $k_{CR} = 1/\tau_{RP}$ data.

7.2 and 7.3. Each of the additional triplet formation mechanisms improves the fit to the $B = 2J/g_e\mu_B$ peak of the n=1 k_{CR} data and the high field limit of the n=2 RTY data, although the quantitative improvement in the $\overline{\text{NMSE}}$ value for n=2 is only small. In these simulations we do not include ring flips since the results in Figs. 7.6 and 7.7 suggest they have little influence on the observed magnetic field effects. The final fit quality does not depend on the specific mechanism of additional triplet formation; to graphical accuracy they all produce identical fits. The final fitted k_S, k_T, $2\sigma_J$ and τ_J parameters, shown in Table 7.2, do not vary significantly between the models with the different additional triplet formation mechanisms.

7.5 Discussion

The fitting of various relaxation models to the experimental magnetic field effect data for the n=1 and n=2 DMJ-NDI molecules suggests that relaxation due to the modulation of anisotropic spin coupling parameters by rotational diffusion and the modulation of $2J$ by

internal motions both contribute significantly to the radical pair intersystem crossing dynamics. The analysis also strongly suggests that some additional triplet formation mechanism is required to explain the experimental magnetic field effects. In the following I will discuss the physical significance of the fitted parameters obtained in the spin dynamics models.

7.5.1 Rate constants

The best fit simulations with additional triplet formation mechanisms give a consistent set of spin-selective radical pair recombination rate constants, varying by only $\sim 5\%$. The values of the rate constants obtained from the simple kinetic model considered in Ref. [67] were $k_S = 110\ \mu s^{-1}$ and $k_T = 96\ \mu s^{-1}$ for n=1 and $k_S = 6.8\ \mu s^{-1}$ and $k_T = 15\ \mu s^{-1}$ for n=2, from which they concluded, together with data on n=3 and n=4 molecules, that the charge recombination processes occurred via a superexchange type tunnelling mechanism through the bridge, as opposed to a thermally activated hopping process. The largest deviation between the NZ/SW rate constants and those from the kinetic model is in k_T for n=1, for which the NZ/SW simulations give a value approximately three times smaller than the kinetic model prediction. Based on the numerical tests on reduced models for these radical pairs, we expect the error from using the NZ/SW method to fit k_S and k_T to be no more than $\sim 6\%$. In any case, given the relatively small differences between the new fitted rate constants and those obtained in Ref. [67], it seems likely as Scott *et al.* concluded that both the singlet and triplet charge transfers proceed via a superexchange mediated tunnelling mechanism.

7.5.2 Relaxation mechanisms

The results in Fig. 7.6 and Fig. 7.7 show that relaxation arising from rotational diffusion alone is not sufficient to account for the observed magnetic field effect curve peak shapes. The inclusion of modulation of the scalar coupling of the electron spins significantly improves the accuracy of the line shape in both molecules. In particular the widths of the observed peaks are captured well for both n=1 and n=2. Modulation of the scalar coupling gives rise primarily to singlet-triplet dephasing.[51,66,202,203] This increases the decay rate of the singlet-triplet coherences in the radical pair spin dynamics, leading to broadening

of the magnetic field effect peak. Interestingly, however, in additional tests not presented here a field-independent phenomenological dephasing term in the master equation cannot consistently explain the observed magnetic field effects, especially for n=2. This reflects the fact that the fitted $1/\tau_J$ is ≈ 4 ns^{-1}, whereas an applied field of the order of 500 mT corresponds to a Larmor frequency of the electrons of $\gamma_e B \approx 88$ ns^{-1}. The modulation of J is therefore too slow to be in the extreme narrowing limit and the field dependence of the singlet-triplet dephasing rate needs to be included properly in the calculation, for example by employing an exponential model for the J-modulation as is done here.

The inclusion of hyperfine tensor modulation by ring flips of the DMJ radical does not significantly improve the fit quality of the simulation to the magnetic field effect data for either molecule. This suggests that the relaxation induced by this hyperfine tensor modulation does not have a large effect on the spin dynamics of the radical pair. Furthermore, because the inclusion of this relaxation mechanism does not help to explain the magnetic field effect data, the k_{flip} parameters obtained from the fitting cannot be interpreted as the true physical ring flipping rate constants. In additional simulations not presented here it has been checked that this result is not dependent on the estimate of $k_{\text{flip}}/k'_{\text{flip}}$.

For the J modulation, we find that the size of the fluctuation, σ_J, scales roughly with average coupling, $\langle J \rangle$, as is expected. For n=1 the best fit value of σ_J is $\approx 1.4 \langle J \rangle$, and for n=2 it is $\approx 0.2 \langle J \rangle$. The time scales of the fluctuations, τ_J, for the n=1 and n=2 wires differ by a factor of ≈ 70. This seems a little large to be due to the torsional motions of the molecules modulating the exchange coupling, although the addition of the extra bridging para-phenylene group in the n=2 wire will clearly have some effect on this. It should also be noted that the correlation functions for the true molecular motions that modulate the scalar coupling are likely to be more complex than the simple exponential model that has been used here.

The difference in τ_J between the n=1 and n=2 wires could alternatively be explained by electron or hole hopping to a short-lived high-energy state with a larger scalar coupling to the other radical, for example with the bridge in a $\text{Ph}_n^{\bullet+}$ state or an $\text{An}^{\bullet+}$ state. The lifetime of this excited state could be very different between the n=1 and n=2 molecules, which could explain the large difference in their τ_Js. In particular, an $\text{An}^{\bullet+}$ radical intermediate

	Model	$\overline{\text{NMSE}}$	$k_{\text{S,tot}}/\mu\text{s}^{-1}$	$k_{\text{T,tot}}/\mu\text{s}^{-1}$	$2\sigma_J/g_e\mu_B\text{mT}$	τ_J/ps
n = 1	No relaxation	4.3×10^{-2}	413.0	1.178×10^{-4}	—	—
n = 1	Ω	4.3×10^{-2}	407.5	8.173×10^{-3}	—	—
n = 1	$\Omega/\Delta J$	8.6×10^{-3}	117.9	29.01	1120	0.3737
n = 1	$\Omega/\Delta J/k_{\text{flip}}$	6.9×10^{-3}	121.3	2.072	399.9	21.30
n = 1	$\Omega/\Delta J/k_{\text{rel}}$	5.8×10^{-3}	118.0	31.75	234.5	3.728
n = 1	$\Omega/\Delta J/\lambda_{\text{T}}$	5.8×10^{-3}	118.0	31.75	235.4	3.724
n = 1	$\Omega/\Delta J/\Phi_0$	5.8×10^{-3}	114.6	37.50	235.0	3.739
n = 2	No relaxation	0.4	6.536	296.8	—	—
n = 2	Ω	1.1×10^{-2}	8.009	16.05	—	—
n = 2	$\Omega/\Delta J$	2.0×10^{-3}	7.746	14.34	7.493	202.8
n = 2	$\Omega/\Delta J/k_{\text{flip}}$	1.2×10^{-3}	7.660	14.53	6.580	349.3
n = 2	$\Omega/\Delta J/k_{\text{rel}}$	1.05×10^{-3}	7.134	13.82	6.159	350.1
n = 2	$\Omega/\Delta J/\lambda_{\text{T}}$	1.05×10^{-3}	7.651	14.20	5.724	411.0
n = 2	$\Omega/\Delta J/\Phi_0$	1.05×10^{-3}	7.883	14.19	5.823	395.1

Table 7.2: Fitted parameters for the different models of DMJ-NDI radical pair spin dynamics, with the corresponding normalised mean square errors as defined in Eq. (7.22) .The models are labelled by the relaxation mechanisms/background corrections they include: Ω indicates the model includes rotational diffusion, ΔJ indicates J modulation is included, k_{flip} indicates ring flips are included, k_{rel} indicates additional field independent relaxation is included, λ_{T} indicates an initial triplet componet is included and Φ_0 indicates a background correction is included. The additional fitted parameters are given in Table 7.3.

might account for the slower time-scale and smaller variance of the n=2 J fluctuations than those for n=1, because one would expect the DMJ-An$^{\bullet+}$-Ph$_n$-NDI$^{\bullet-}$ radical pair to be less electrostatically stabilised for n=2 than for n=1.

While we cannot conclusively determine which of these mechanisms predominantly controls the $2J$ modulation, the large difference in the τ_Js of the two molecules makes electron/hole hopping to intermediate radical pair states the more likely explanation. Further experiments, complemented by an analysis of the type performed here, might help to resolve this question. One possibility would be to repeat the MFE measurements in different solvents with similar viscosities but different dielectric constants. If electron/hole hopping controls the $2J$ fluctuations, then the τ_J values would be expected to have a strong dependence on the solvent polarity, whereas if torsional motions control the $2J$ fluctuations, the solvent polarity would not be expected to have nearly such a large effect on the τ_Js.

	$k_{\mathrm{flip}}/\mathrm{ns}^{-1}$	$k_{\mathrm{rel}}/\mu\mathrm{s}^{-1}$	λ_{T}	Φ_0
n=1	2.558	3.590	0.02214	0.02462
n=2	26.04	0.6973	0.06248	0.06804

Table 7.3: Additional best fit parameters for models including ring flips, additional relaxation, an initial triplet fraction or a background correction.

7.5.3 Triplet formation mechanisms

The quality of the fit of the simulations to the experimental data improves significantly when an additional triplet formation mechanism is included in the simulations (see Figs. 7.8 and 7.9). Interestingly, the improvement is independent of the exact mechanism of triplet formation, and the fitted k_{S}, k_{T}, σ_J and τ_J parameters also agree well between the different triplet formation models. The fit quality alone cannot therefore be used to infer which additional triplet formation mechanism plays a role in these radical pairs, but we can at least speculate about which is the most plausible mechanism.

Firstly, it should be noted that the relative triplet yields measured experimentally for the ^{3*}An and ^{3*}NDI products are very similar.[67] Given that the fitted background triplet yields are small, $k_{\mathrm{ST1}} \ll k_{\mathrm{S}}$, and therefore $\Phi_0 \approx k_{\mathrm{ST1}}k_{\mathrm{T}}/k_{\mathrm{T1}}k_{\mathrm{S}}$. If the singlet radical pairs were undergoing spin-orbit coupled charge recombination to give both triplet products, then k_{ST1} and k_{ST2} would need to satisfy $k_{\mathrm{ST1}}/k_{\mathrm{T1}} \approx k_{\mathrm{ST2}}/k_{\mathrm{T2}}$. In the non-adiabatic limit, each of these ratios is proportional to a ratio of squared electron transfer Hamiltonian matrix elements, so $|\langle {}^{\mathrm{S}}\mathrm{RP}|\hat{H}|\mathrm{T1}\rangle|^2/|\langle {}^{\mathrm{T}}\mathrm{RP}|\hat{H}|\mathrm{T1}\rangle|^2 \approx |\langle {}^{\mathrm{S}}\mathrm{RP}|\hat{H}|\mathrm{T2}\rangle|^2/|\langle {}^{\mathrm{T}}\mathrm{RP}|\hat{H}|\mathrm{T2}\rangle|^2$. Given that the spin-orbit coupled charge transfer matrix elements, $\langle {}^{\mathrm{S}}\mathrm{RP}|\hat{H}|\mathrm{T}n\rangle$, depend strongly on the relative orientation of the orbitals involved in the electron transfer,[151] and in a different way to the spin-conserving matrix elements, it seems unlikely that this condition would be satisfied, and therefore this mechanism probably does not operate in these molecules under these experimental conditions.

We have also considered the inclusion of an additional relaxation mechanism in the extreme narrowing limit, with a fluctuation correlation time much shorter than the spin dynamics time scale. This produces a field-independent relaxation which has much the same effect as including a background contribution to the triplet yield, and it can also be

used to fit the experimental data (see Fig. 6). However we find that the phenomenological relaxation rates needed to fit the n=1 and n=2 data differ by more than a factor of 6 (see Table I). The length of the molecule only changes by ~10% and it is hard to imagine that such a small change in the dimensions of the molecule would produce such a large change in the relaxation rate. For example the spin-rotation interaction would most likely not display this degree of dependence on the molecular geometry. Dipolar interactions with nuclear spins in the solvent (toluene) could give rise to rapidly fluctuating fields at the radicals, but again it is not immediately clear why there would be such a large difference between in the n=1 and n=2 molecules.

This leaves initial triplet radical pair formation as the remaining possibility for the additional triplet product formation. We have shown that an initial fraction of triplet radical pairs could also explain the experimental magnetic field effect data, with similar initial triplet fractions in both the n=1 and n=2 cases ($\sim 2\%$ and $\sim 6\%$, respectively – see Table 7.3). These initial triplet fractions are relatively small and are in line with those measured in other organic linked radical pair systems.[108] The initial triplet fraction could arise from spin-orbit coupled charge transfer (SOCT) between the initial photoexcited ^{1}[DMJ$^{\bullet+}$-An$^{\bullet-}$]-Ph$_n$-NDI molecule and the triplet radical pair state. The SOCT rate, $k_{CS,T}$, would be expected to depend exponentially on the radical separation, in the same way as the spin-conserving charge separation rate constant, k_{CS}. As a result, we would expect $\lambda_T = k_{CS,T}/(k_{CS} + k_{CS,T})$ to be approximately the same in both the n=1 and n=2 molecules, which is consistent with what we find in the simulations. The small difference between λ_T for $n = 1$ and $n = 2$ might be explained by the fact that the SOCT matrix element depends strongly on the relative orientation of the orbitals involved in the electron transfer, since the angle between the DMJ and NDI groups changes by about 60° between the two molecules.

Overall, then, the simulations seem to suggest that additional intersystem crossing, most likely accompanying the initial radical pair formation step, may give rise to additional triplet product formation in these radical pairs. The available experimental data is however insufficient to establish this conclusively because the various different triplet formation mechanisms considered give rise to identical RTY curves. It may also be that all of these mechanisms operate to some small degree simultaneously to produce the observed magnetic

field effects.

7.6 Concluding remarks

In this chapter I have demonstrated how to consistently combine the Nakajima-Zwanzig theory of relaxation with the Schulten-Wolynes approximation to the electron spin dynamics of a radical pair, including the interplay of asymmetric recombination rates and electron spin relaxation. This NZ/SW method has been applied to study the spin relaxation in covalently linked DMJ-NDI radical pairs. Combining it with simple models of the internal molecular motion, it has been possible to investigate the role of different relaxation mechanisms in these radical pair reactions. In as far as possible the relaxation processes have been accounted for with microscopic models, rather than treated phenomenologically. This has proven to be important, for example in describing the singlet-triplet dephasing process in these molecules. This dephasing is not in the extreme-narrowing limit and a simple, field-independent dephasing rate would fail to describe the magnetic field effects that have been observed experimentally.

We have found that modulation of the scalar coupling between the electron spins plays a significant role in the observed magnetic field effects on these radical pairs. However this modulation alone cannot fully explain the full magnetic field dependence of the relative triplet yields and radical pair lifetimes. Another possible relaxation mechanism, ring inversions of the $DMJ^{\bullet+}$ radical modulating the hyperfine coupling constants in this radical, was found to not play any significant role in the electron spin dynamics. Alternative additional triplet formation mechanisms, involving incoherent intersystem crossing in either the charge separation or charge recombination processes, or in the radical pair state, have also been considered. Each of these possibilities was found to improve the fit to the experimental data equally well, but based on physical considerations, a small initial triplet radical pair fraction seems to provide the most plausible explanation for the additional triplet product formation.

The method presented here will hopefully prove useful in the interpretation of magnetic field effects on other radical pair reactions. It is certainly more powerful than the use of

simple kinetic models for the radical pair dynamics and phenomenological treatments of relaxation, and yet it is still relatively computationally inexpensive. Most of the parameters needed in the modelling can be obtained from DFT calculations, or EPR measurements of the constituent radicals, and the remaining parameters can be fit to experimental magnetic field effect data in a matter of minutes on a desktop computer. The NZ/SW method described here can also be straightforwardly applied to study the EPR spectra of radical pairs, and to describe other coupled spin systems such as radical triads.[70,71,85,86,204]

Appendix

7.A Reduced model parameters

Here I present the hyperfine coupling constants used in the reduced models for the n=1 and n=2 radical pairs. These are based on the full radical pair parameters with isotropic hyperfine constants rescaled to produce the same hyperfine field in each radical, $B^2_{i,\mathrm{hyp}} = \sum_{k=1}^{N_i} a_{ik}^2 I_{ik}(I_i k + 1)/g_\mathrm{e}\mu_\mathrm{B}$. These parameters are given in Tables 7.A.1, 7.A.2 and 7.A.3.

7.B DMJ$^{\bullet+}$–An–Ph$_\mathrm{n}$–NDI$^{\bullet-}$ model parameters

Here I present a summary of the spin coupling parameters used in the simulations of the DMJ$^{\bullet+}$–An–Ph$_\mathrm{n}$–NDI$^{\bullet-}$ radical pairs.

Nucleus	a_iso/mT	A^aniso_{xx}/mT	A^aniso_{yy}/mT	A^aniso_{zz}/mT	A^aniso_{xy}/mT	A^aniso_{xz}/mT	A^aniso_{yz}/mT
H1	-0.314637	0.024882	-0.036468	0.011586	-0.022270	0.096852	-0.031461
H2	-0.314637	0.024879	-0.036465	0.011586	-0.022275	-0.096854	0.031455
H3	-0.314637	0.024882	-0.036468	0.011586	-0.022270	0.096852	-0.031461
H4	-0.314637	0.024879	-0.036465	0.011586	-0.022275	-0.096854	0.031455

Table 7.A.1: Hyperfine couplings for the reduced model of the NDI radical anion. Isotropic components, $a_\mathrm{iso} = (A_{xx} + A_{yy} + A_{zz})/3$, are experimental values for the free radical and anisotropic components $A^\mathrm{aniso}_{\alpha\beta} = A_{\alpha\beta} - \delta_{\alpha\beta} a_\mathrm{iso}$. mT here is used as an abbreviation for $g_\mathrm{e}\mu_\mathrm{B}$ mT.

Nucleus	a_{iso}/mT	A_{xx}^{aniso}/mT	A_{yy}^{aniso}/mT	A_{zz}^{aniso}/mT	A_{xy}^{aniso}/mT	A_{xz}^{aniso}/mT	A_{yz}^{aniso}/mT
H1	2.309830	0.018394	-0.024143	0.005750	0.090257	0.119167	0.105530
H2	0.904158	-0.030255	-0.104512	0.134767	-0.039520	0.111178	-0.065691
H3	1.072323	0.069090	-0.014187	-0.054902	0.075976	0.013749	0.006477
H4	0.258939	0.098308	-0.057200	-0.041108	-0.013959	-0.024641	-0.002803
H5	1.074030	0.069102	-0.014201	-0.054901	0.075981	-0.014035	-0.006618
H6	0.259990	0.098464	-0.057219	-0.041245	-0.014054	0.024346	0.002814
H7	2.309280	0.017844	-0.024028	0.006183	0.090068	-0.119099	-0.105661
H8	0.902681	-0.030775	-0.104631	0.135406	-0.039322	-0.110876	0.065607
H9	-0.166635	0.036159	-0.035899	-0.000260	0.007026	0.038259	0.004047
H10	-0.166635	0.036159	-0.035899	-0.000260	0.007026	0.038259	0.004047
H11	-0.166635	0.036159	-0.035899	-0.000260	0.007026	0.038259	0.004047
H12	-0.166558	0.035983	-0.035879	-0.000104	0.007021	-0.038338	-0.004066
H13	-0.166558	0.035983	-0.035879	-0.000104	0.007021	-0.038338	-0.004066
H14	-0.166558	0.035983	-0.035879	-0.000104	0.007021	-0.038338	-0.004066
N1	0.831617	-0.772676	1.553776	-0.781100	0.061480	-0.000000	0.000443

Table 7.A.2: Hyperfine couplings for the reduced model of the DMJ radical cation. Isotropic components, $a_{\mathrm{iso}} = (A_{xx} + A_{yy} + A_{zz})/3$, are experimental values for the free radical and anisotropic components $A_{\alpha\beta}^{\mathrm{aniso}} = A_{\alpha\beta} - \delta_{\alpha\beta} a_{\mathrm{iso}}$. mT here is used as an abbreviation for $g_{\mathrm{e}}\mu_{\mathrm{B}}$ mT.

	c_{iso}/	C_{xx}^{aniso}	C_{yy}^{aniso}	C_{zz}^{aniso}	C_{xy}^{aniso}	C_{xz}^{aniso}	C_{yz}^{aniso}
NDI g-tensor	2.003900	0.000542	-0.001642	0.001100	-0.000794	0.0000	0.0000
DMJ g-tensor	2.003033	0.000667	-0.000833	0.000167	0.000000	0.0000	0.0000
D tensor/mT	0.000000	0.413380	0.413380	-0.826759	0.000000	0.0000	0.0000

Table 7.A.3: g tensors and dipolar coupling tensor used in the reduced model. Isotropic components, $c_{\mathrm{iso}} = (C_{xx} + C_{yy} + C_{zz})/3$, are experimental values for the free radical and anisotropic components $C_{\alpha\beta}^{\mathrm{aniso}} = C_{\alpha\beta} - \delta_{\alpha\beta} a_{\mathrm{iso}}$. mT here is used as an abbreviation for $g_{\mathrm{e}}\mu_{\mathrm{B}}$ mT.

7.B.1 Hyperfine coupling tensors

Isotropic components of the hyperfine coupling tensors, $a_{\text{iso}} = (A_{xx} + A_{yy} + A_{zz})/3$, for the $NDI^{\bullet-}$ radical are taken from experimental results[200] for the *N,N*-dipentyl radical anion. The signs of the isotropic components and the anisotropic components are obtained from DFT. This is done by calculating the gas phase radical ground state geometry, capped with two hydrogens (see Fig. 7.B.1), optimized with DFT using the B3LYP functional and 6-31G(d,p) basis set with the D3 dispersion correction, as implemented in Gaussian09,[197] and then calculating the hyperfine coupling tensors with the B3LYP functional and the EPR-III basis set for this optimised geometry. For the $NDI^{\bullet-}$ radical the isotropic hyperfine coupling constants are found to agree with the experimental values to within $< 10\%$. The hyperfine coupling tensor components are given in Table 7.B.1. Isotropic and anisotropic components for the syn and anti conformations of the $DMJ^{\bullet+}$ radical, capped with hydrogen (see Fig. 7.B.2), are calculated in the same way as the anisotropic values for the $NDI^{\bullet-}$ radical. We additionally average the two sets of three methyl hydrogens, H13–H15 and H16–H18, in both conformations, under the assumption that they rapidly interconvert at 295K. These are given for the syn and anti conformations in Tables 7.B.2 and 7.B.3. The hyperfine coupling tensors for the other two syn and anti conformations are obtained by inverting the molecular z axis and permuting the labels appropriately. For models which do not include ring flipping of the DMJ, hyperfine tensors for the lowest energy anti conformation are used, but the fit quality and fitted parameters are not found to be sensitive to which of the syn, anti or thermally averaged hyperfine coupling tensors are used for the $DMJ^{\bullet+}$ radical.

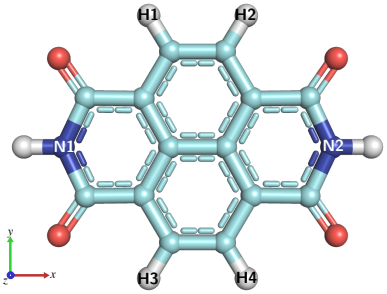

Figure 7.B.1: The NDI radical with labelled hyperfine coupled nuclei. The capping hydrogens are not included.

Nucleus	a_{iso}/mT	A_{xx}^{aniso}/mT	A_{yy}^{aniso}/mT	A_{zz}^{aniso}/mT	A_{xy}^{aniso}/mT	A_{xz}^{aniso}/mT	A_{yz}^{aniso}/mT
H1	-0.1927	0.011586	0.032114	-0.043700	-0.101834	-0.000008	0.000014
H2	-0.1927	0.011586	0.032114	-0.043700	0.101834	0.000014	0.000008
H3	-0.1927	0.011586	0.032114	-0.043700	0.101834	0.000014	0.000008
H4	-0.1927	0.011586	0.032114	-0.043700	-0.101834	-0.000008	0.000014
N1	-0.0963	0.035200	0.034000	-0.069200	0.000000	0.000000	0.000010
N2	-0.0963	0.035200	0.034000	-0.069200	0.000000	0.000000	0.000010

Table 7.B.1: Hyperfine coupling parameters for the $\text{NDI}^{\bullet-}$ radical. Isotropic components, $a_{\text{iso}} = (A_{xx}+A_{yy}+A_{zz})/3$, are experimental values for the free radical and anisotropic components $A_{\alpha\beta}^{\text{aniso}} = A_{\alpha\beta} - \delta_{\alpha\beta}a_{\text{iso}}$ in the isolated radical principal axis frame are obtained from DFT calculations as described in the text.

Nucleus	a_{iso}/mT	A_{xx}^{aniso}/mT	A_{yy}^{aniso}/mT	A_{zz}^{aniso}/mT	A_{xy}^{aniso}/mT	A_{xz}^{aniso}/mT	A_{yz}^{aniso}/mT
H1	0.486756	-0.031726	0.144387	-0.112661	0.130562	-0.015262	-0.006179
H2	2.328949	0.029447	-0.037064	0.007617	0.096496	0.115391	0.081504
H3	-0.061351	0.062467	-0.012795	-0.049672	0.044979	-0.014692	0.001259
H4	-0.060764	0.038959	-0.043062	0.004103	0.026643	-0.086679	-0.028602
H5	0.375611	0.092136	-0.037949	-0.054187	-0.025343	-0.038948	0.004200
H6	1.153098	0.082424	-0.057527	-0.024898	0.000111	0.067331	-0.006107
H7	2.329776	0.029272	-0.036836	0.007564	-0.096634	-0.115280	0.081706
H8	0.488286	-0.032014	0.144717	-0.112703	-0.130394	0.015319	-0.006342
H9	-0.060699	0.038912	-0.043011	0.004099	-0.026721	0.086652	-0.028682
H10	-0.061503	0.062395	-0.012722	-0.049673	-0.045031	0.014720	0.001226
H11	1.152785	0.082408	-0.057522	-0.024886	-0.000270	-0.067352	-0.006030
H12	0.375533	0.092205	-0.038003	-0.054202	0.025209	0.038923	0.004147
H13	-0.158930	0.035962	0.000470	-0.036432	0.037651	0.000522	0.000529
H14	-0.158930	0.035962	0.000470	-0.036432	0.037651	0.000522	0.000529
H15	-0.158930	0.035962	0.000470	-0.036432	0.037651	0.000522	0.000529
H16	-0.158931	0.035888	0.000544	-0.036432	-0.037686	-0.000526	0.000533
H17	-0.158931	0.035888	0.000544	-0.036432	-0.037686	-0.000526	0.000533
H18	-0.158931	0.035888	0.000544	-0.036432	-0.037686	-0.000526	0.000533
N1	0.835749	-0.780100	-0.737667	1.517767	0.000068	-0.000688	-0.330857

Table 7.B.2: Hyperfine coupling parameters for the $\text{DMJ}^{\bullet+}$ radical in the syn conformation, as labelled above. Isotropic components, $a_{\text{iso}} = (A_{xx} + A_{yy} + A_{zz})/3$, and anisotropic components, $A_{\alpha\beta}^{\text{aniso}} = A_{\alpha\beta} - \delta_{\alpha\beta}a_{\text{iso}}$, in the isolated radical principal axis frame are obtained from DFT calculations as described in the text.

Nucleus	a_{iso}/mT	A_{xx}^{aniso}/mT	A_{yy}^{aniso}/mT	A_{zz}^{aniso}/mT	A_{xy}^{aniso}/mT	A_{xz}^{aniso}/mT	A_{yz}^{aniso}/mT
H1	2.308839	0.018394	0.005750	-0.024144	0.119167	-0.090257	-0.105530
H2	0.903770	-0.030255	0.134767	-0.104512	0.111178	0.039520	0.065691
H3	-0.034042	0.041327	-0.039294	-0.002033	0.017961	0.078922	0.025615
H4	-0.077575	0.065617	-0.016154	-0.049462	0.036655	0.014217	0.004047
H5	1.071863	0.069089	-0.054902	-0.014187	0.013749	-0.075976	-0.006477
H6	0.258828	0.098308	-0.041108	-0.057200	-0.024641	0.013959	0.002803
H7	2.308288	0.017844	0.006183	-0.024028	-0.119099	-0.090068	0.105661
H8	0.902293	-0.030775	0.135406	-0.104631	-0.110876	0.039322	-0.065607
H9	-0.034202	0.041235	-0.039174	-0.002061	-0.018150	0.078901	-0.025838
H10	-0.077648	0.065415	-0.015957	-0.049458	-0.036874	0.014222	-0.004080
H11	1.073569	0.069102	-0.054901	-0.014201	-0.014035	-0.075981	0.006618
H12	0.259878	0.098464	-0.041245	-0.057219	0.024346	0.014054	-0.002814
H13	-0.166563	0.036159	-0.000260	-0.035899	0.038259	-0.007026	-0.004047
H14	-0.166563	0.036159	-0.000260	-0.035899	0.038259	-0.007026	-0.004047
H15	-0.166563	0.036159	-0.000260	-0.035899	0.038259	-0.007026	-0.004047
H16	-0.166487	0.035983	-0.000104	-0.035879	-0.038338	-0.007021	0.004066
H17	-0.166487	0.035983	-0.000104	-0.035879	-0.038338	-0.007021	0.004066
H18	-0.166487	0.035983	-0.000104	-0.035879	-0.038338	-0.007021	0.004066
N1	0.831260	-0.772676	-0.781100	1.553776	-0.000000	-0.061480	-0.000443

Table 7.B.3: Hyperfine coupling parameters for the DMJ$^{\bullet+}$ radical in the anti conformation, as labelled above. Isotropic components, $a_{\mathrm{iso}} = (A_{xx} + A_{yy} + A_{zz})/3$, and anisotropic components, $A_{\alpha\beta}^{\mathrm{aniso}} = A_{\alpha\beta} - \delta_{\alpha\beta} a_{\mathrm{iso}}$, in the isolated radical principal axis frame are obtained from DFT calculations as described in the text.

Radical	g_{iso}	$g_{xx} - g_{\mathrm{iso}}$	$g_{yy} - g_{\mathrm{iso}}$	$g_{zz} - g_{\mathrm{iso}}$
NDI$^{\bullet-}$	2.0040	0.0010	0.0007	-0.0020
DMJ$^{\bullet+}$	2.0031	0.0006	0.0001	-0.0009

Table 7.B.4: g tensor components used in our simulations for the radicals, with $g_{\mathrm{iso}} = (g_{xx} + g_{yy} + g_{zz})/3$.

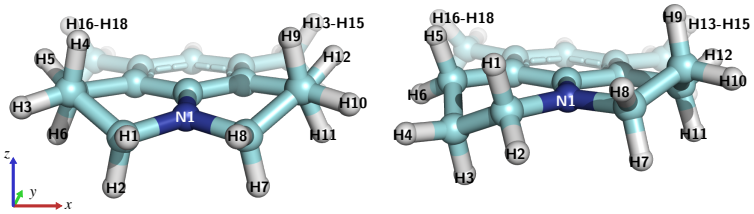

Figure 7.B.2: Syn (left) and anti (right) conformations of the DMJ radical with hyperfine coupled nuclei labelled. The capping hydrogen is not included in our simulations.

7.B.2 Dipolar coupling and g tensors

The isotropic component of the g-tensor for the $NDI^{\bullet-}$ radical is assumed to be the same as that for the *N,N*-dipentyl $NDI^{\bullet-}$ radical[200]. The anisotropic components are obtained from DFT just as the anisotropic components of the hyperfine tensors are. The isotropic and anisotropic components of the g-tensors for $DMJ^{\bullet+}$ are obtained from DFT in same way as the hyperfine coupling tensors. The same values are used for both anti and syn conformations, because the differences were found to be negligible. The off-diagonal elements for g tensors in the principal axis frame of the isolated radicals are found to be small and for simplicity are set to zero. g tensor parameters used are summarised in Table 7.B.4. Overall it was found that the simulations are not sensitive to value of the g tensors, due to the relatively low field strengths at which simulations are performed.

The dipolar coupling tensor was calculated based on the point dipole approximation, assuming the two radicals lie on the molecular z axis exactly. The isotropic value of the electron g tensors were used to calculate this coupling tensor. The radical separations used were r = 16.5 Å for the n=1 molecule and r = 20.9 Å for the n=2 molecule.[67]

7.B.3 Rotational diffusion parameters

The rotational motion of the molecule was simplified by treating it as a rigid prolate symmetric top. The isolated $DMJ^{\bullet+}$ radical y axis was taken to be parallel with the molecular $-z$ axis, and the molecular x axis was taken lie on the radical x axis (see Fig. 7.B.3 for the n=2 case). The $NDI^{\bullet-}$ x axis was taken to lie on the molecular z axis, and the isolated radical y axis was taken to be at an angle θ from the molecular x axis. This angle for the solution phase radical ion pair state was estimated from the gas phase ground state geometry,

optimized at the DFT B3LYP/6-31G(d,p) level of theory with D3 dispersion correction. For n=1 the angle was taken to be −82° and for n=2 the angle was taken to be −18°. This angle is independent of whether the $DMJ^{\bullet+}$ is in the syn or anti conformation.

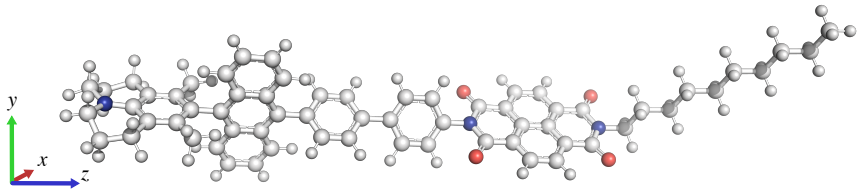

Figure 7.B.3: Example ground state geometry of the n=2 molecule with syn conformation of the $DMJ^{\bullet+}$, calculated at the DFT B3LYP/6-31G(d,p) level of theory with D3 dispersion correction. Also shown is the approximate position of the molecular axes.

The molecule was assumed to behave as a rigid rotor, with rotational diffusion constants given by the Stokes-Einstein equation,

$$D_\alpha = \frac{k_B T}{8\pi\eta r_\alpha^3} \tag{7.B.1}$$

where T is the temperature, 295K,[67], η is the bulk dynamic viscosity, taken to be 0.5812 mPa s, and r_α is the hydrodynamic radius of the molecule in the $\alpha = \parallel$ or $\perp$ direction. We estimated $r_\parallel$ as 8.50 Å, and $r_\perp$ as 15.45 Å and 17.50 Å for n=1 and n=2 molecules respectively. These estimates are based on atom-to-atom distances in the ground state gas phase geometry, adding the van der Waals radii of hydrogen of 1.2 Å and 2.8 Å for the solvent toluene,[205] ignoring the n-octyl group on the NDI, and as such these are likely to be underestimates of the true hydrodynamic radii.

This is a crude estimate based on treating the parallel and perpendicular rotational diffusion as equivalent to a sphere with a radius given by the width or length of the molecule respectively. Although crude, it likely gives a reasonable estimate, given the radical pair is not completely rigid and therefore rotation of the radicals about the inter-radical axis is likely dominated by fast internal torsional motions, which can be approximated by the diffusion of a sphere with the radius of the radical. Alternative methods for approximating rotational diffusion parameters have been used previously, by treating the entire molecule as a spherical top[51], or by treating each radical as an independently rotating spherical top[66], both of which ignore the anisotropy of the rotational diffusion in these systems, whereas

the current approach at least approximately accounts for this approximately. Furthermore, the Stokes-Einstein equation is also only approximate in this case given that the molecular volume of toluene is not significantly smaller than that of the molecule, and as a result the viscosity experienced by the molecule is likely to be smaller than that of the bulk. Given these approximations, we have tested the sensitivity of the fits and fitted parameters of our models, increasing and decreasing the diffusion constants by 50%. The fits and fitted parameters were found to not change significantly on altering the diffusion constants in this way.

8

Kinetic Master Equations for Radical Pair Intersystem Crossing

In this chapter the Nakajima-Zwanzig equation is used to explain the success of simple kinetic models in describing radical pair reactions. This offers new insights into recent experiments which have used kinetic master equations to interpret magnetic field effects on radical pair reactions, and it also gives a new tool for modelling radical pair reactions with high computational efficiency. Furthermore the kinetic master equation is employed to study magnetic field effects on the reactions of phenothiazine (PTZ), perylene-3,4:9,10-bis(dicarboximide) (PDI) radical pairs, separated by an oligo-para-phenylene bridge.

8.1 The kinetic master equation

Magnetic field effects on radical pair reactions are usually described using models that include quantum coherences between spin states, based on the radical pair master equation for the spin density operator $\hat{\rho}(t)$, which has been derived and used in the previous chapters of this thesis. The action of the effective spin Hamiltonian $\hat{H}$ on $\hat{\rho}(t)$ gives rise to coherent evolution of spins in the radical pair, as depicted in Fig. 8.1 (A). However, experiments which probe radical pair survival probabilities and the quantum yields of spin state selective recombination reactions are often interpreted using simple incoherent kinetic models for the interconversion of radical pair spin states, as depicted in Fig. 8.1 (B).[51,66,68,150,182,206]

One particular model proposed recently by Steiner *et al.* employs the following func-

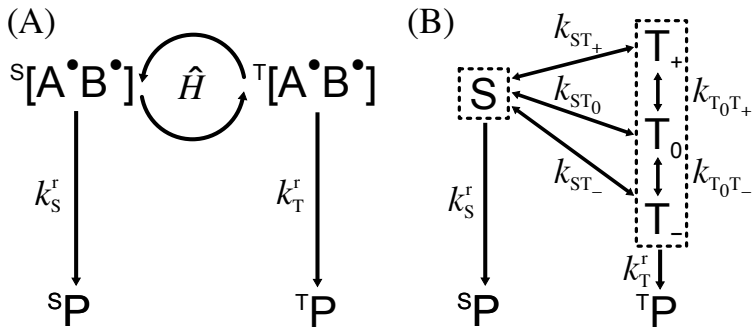

Figure 8.1: (A) A schematic picture of the radical pair mechanism with coherent quantum intersystem crossing between singlet and triplet states. (B) The incoherent kinetic scheme used to describe the radical pair mechanism.

tional form for the spin state interconversion rates,[51,150,182]

$$k_{nm} = \frac{k_{\text{hfc}}}{1 + (\epsilon_n - \epsilon_m)^2/\gamma_{\text{hfc}}^2} + \frac{k_{\text{rel}}}{1 + (\epsilon_n - \epsilon_m)^2/\gamma_{\text{rel}}^2} + k_0, \tag{8.1}$$

in which k_{hfc}, k_{rel}, k_0, γ_{hfc} and γ_{rel} are free parameters and ϵ_n is the energy of the coupled electronic spin state $|n\rangle = |\text{S}\rangle$, $|\text{T}_+\rangle$, $|\text{T}_0\rangle$, or $|\text{T}_-\rangle$ in the absence of hyperfine interactions. Here the first term represents the isotropic hyperfine contribution to the interconversion and the second represents the spin relaxation contribution. This ansatz has been used successfully to interpret the magnetic field effects on radical pair survival probabilities in several sets of experiments.[51,150,182] A similar expression for the hyperfine mediated intersystem crossing rate has previously been arrived at by applying the steady-state approximation to the coherences in a simple two-state model of the radical pair spin states.[207–210]

At a glance, the coherent quantum dynamics approach and the kinetic approach appear to be fundamentally different. But in this chapter I will show how the kinetic model can in fact be derived as an approximation to the exact quantum spin dynamics. In particular, I will show that expressions for the spin-state interconversion rate constants very similar to those in Eq. (8.1) can be obtained straightforwardly from a perturbative approximation to the solution of an appropriate Nakajima-Zwanzig equation.

8.2 Derivation of the KME

In this section I outline the derivation of the kinetic master equation (KME) for the radical pair intersystem crossing process using Nakajima-Zwanzig theory.

8.2.1 Radical pair spin dynamics

The radical pair state is described by its density operator $\hat{\rho}(t)$, which evolves according to the quantum master equation[32–34]

$$\frac{\mathrm{d}}{\mathrm{d}t}\hat{\rho}(t) = -\frac{i}{\hbar}\left[\hat{H}, \hat{\rho}(t)\right] - \left\{\frac{k_{\mathrm{S}}^{\mathrm{r}}}{2}\hat{P}_{\mathrm{S}} + \frac{k_{\mathrm{T}}^{\mathrm{r}}}{2}\hat{P}_{\mathrm{T}}, \hat{\rho}(t)\right\} - \mathcal{D}\hat{\rho}(t), \tag{8.2}$$

in which $k_{\mathrm{S}}^{\mathrm{r}}$ and $k_{\mathrm{T}}^{\mathrm{r}}$ are first-order spin selective recombination rate constants,[a] and $\hat{P}_{\mathrm{S}}$, and $\hat{P}_{\mathrm{T}}$ are projection operators onto the singlet and triplet electronic subspaces. The first term on the right-hand side of Eq. (8.2) describes the coherent spin evolution, the second describes the effect of spin-state selective radical pair recombination reactions and the third describes any additional singlet-triplet (and triplet-triplet) dephasing,

$$\mathcal{D}\hat{\rho}(t) = \sum_{n\neq m} k_{nm}^{\mathrm{d}} \hat{P}_n \,\hat{\rho}(t) \hat{P}_m, \tag{8.3}$$

in which $\hat{P}_n = |n\rangle\langle n| \otimes \hat{1}_{\mathrm{b}}$, where $\hat{1}_{\mathrm{b}}$ is a nuclear spin identity operator. Here $k_{nm}^{\mathrm{d}} = k_{mn}^{\mathrm{d}}$ is the additional dephasing rate for the n, m coherence, which arises from fluctuations in the electron spin coupling as a result of nuclear motion, as can be obtained from the extreme narrowing limit of these fluctuations (as described in section 6.5.4),[45] or strong diabatic coupling between the radical pair and product states (as described in chapter 3).[34]

The Hamiltonian $\hat{H}$ in Eq. (2) can be split into reference part $\hat{H}_0$ and a perturbation $\hat{V}$. We will take the reference part to include the average Zeeman interaction and scalar electron spin coupling, and the perturbation to include the isotropic nuclear hyperfine couplings and the difference between the Zeeman interactions of the two radicals,

$$\hat{H}_0 = \frac{\mu_{\mathrm{B}} B}{2}(g_1 + g_2)(\hat{S}_{1z} + \hat{S}_{2z}) - 2J\hat{\mathbf{S}}_1 \cdot \hat{\mathbf{S}}_2, \tag{8.4}$$

$$\hat{V} = \frac{\mu_{\mathrm{B}} B}{2}(g_1 - g_2)(\hat{S}_{1z} - \hat{S}_{2z}) + \sum_{i=1,2}\sum_{k=1}^{N_i} a_{ik}\hat{\mathbf{I}}_{ik} \cdot \hat{\mathbf{S}}_i. \tag{8.5}$$

Here $\hat{\mathbf{S}}_i$ is the unitless electron spin operator for radical i, $\hat{\mathbf{I}}_{ik}$ is the nuclear spin operator for nucleus k on radical i, a_{ik} is the isotropic hyperfine coupling constant for this nucleus, B is

[a] In this chapter the notation is changed slightly due to the large number of different rate constants appearing. A superscript r denotes a reaction rate constants and superscript d denotes a decoherence rate constant.

the applied magnetic field strength, μ_B is the Bohr magneton, g_i is the isotropic g-factor for radical i, and J is the scalar coupling constant for the electron spins.[3]

Using these definitions, we can split the full Liouvillian $\mathcal{L}$, defined by Eq. (8.2), into a reference part $\mathcal{L}_0$ and a perturbation $\mathcal{L}_V$. The perturbation is taken to only include the action of $\hat{V}$ in Liouville space, $\mathcal{L}_V = -(i/\hbar)[\hat{V}, \cdot]$, and the reference part is taken to be the remainder of the Liouvillian, $\mathcal{L}_0 = \mathcal{L} - \mathcal{L}_V$, including reaction and dephasing terms in Eq. (8.2). From the definition of $|n\rangle$ as one of the coupled electron spin states ($|\mathrm{S}\rangle$ or $|\mathrm{T}_m\rangle$), it is straightforward to show that $|n\rangle\langle m|$ is Liouville-space eigenvector of $\mathcal{L}_0$ with eigenvalue $\lambda_{nm} = -i(\epsilon_n - \epsilon_m) - \gamma_{nm}$. ϵ_n is the eigenvalue of $\hat{H}_0/\hbar$ associated with $|n\rangle$ and γ_{nm} is the total decay rate of $|n\rangle\langle m|$, $\gamma_{nm} = (k_n^{\mathrm{r}} + k_m^{\mathrm{r}})/2 + (1 - \delta_{nm})k_{nm}^{\mathrm{d}}$, which arises from the reaction and dephasing terms in Eq. (8.2) (here k_n^{r} is the reaction rate of state $|n\rangle$, either $k_{\mathrm{S}}^{\mathrm{r}}$ or $k_{\mathrm{T}}^{\mathrm{r}}$).

The initial radical pair spin density matrix for radical pair reactions can usually be written as a sum of electronic spin state projection operators,

$$\hat{\rho}(0) = \frac{1}{Z}\sum_n p_n(0)\hat{P}_n, \tag{8.6}$$

where $p_n(0)$ is the initial probability of finding the radical pair in state n and Z is the dimensionality of the nuclear spin Hilbert space, $Z = \prod_{i=1,2}\prod_{k=1}^{N_i}(2I_{ik} + 1)$.

8.2.2 The kinetic master equation

The Nakajima-Zwanzig equation (Eq. (2.53)) can be used to obtain a master equation for the populations by defining the projection superoperator as

$$\mathcal{P} = \frac{1}{Z}\sum_n \hat{P}_n \,\mathrm{Tr}\big[\hat{P}_n \cdot\,\big], \tag{8.7}$$

and then an exact equation for the populations can be obtained by taking the trace of this projected onto each of the spin states, $p_n(t) = \mathrm{Tr}\big[\hat{P}_n\mathcal{P}\hat{\rho}(t)\big]$,

$$\frac{\mathrm{d}}{\mathrm{d}t}p_n(t) = -k_n^{\mathrm{r}}p_n(t) + \sum_m \int_0^t \mathrm{d}\tau\, \kappa_{nm}(t-\tau)p_m(\tau), \tag{8.8}$$

where the rate kernels are given by $\kappa_{nm}(t) = (1/Z)\,\mathrm{Tr}\big[\hat{P}_n \mathcal{L}_V \mathcal{Q} e^{\mathcal{Q}\mathcal{L}t}\mathcal{Q}\mathcal{L}_V \hat{P}_m\big]$ and we have used the fact that $\mathcal{P}\hat{\rho}(0) = \hat{\rho}(0)$. The decay time of $\kappa_{nm}(t)$ dictates the time-scale on which short-time coherent oscillations decay. If the kernels decay on a time-scale faster than the dynamics of $p_n(t)$, we can make the incoherent rate approximation to obtain the Markovian kinetic master equation,[34,102]

$$\frac{\mathrm{d}}{\mathrm{d}t}p_n(t) = -k_n^{\mathrm{r}} p_n(t) + \sum_m k_{nm} p_m(t), \tag{8.9}$$

in which the rate constants k_{nm} are given by $k_{nm} = \int_0^\infty \mathrm{d}t\, \kappa_{nm}(t)$.

For time-integrated properties such as the singlet quantum yield, $\Phi_{\mathrm{S}} = k_{\mathrm{S}}^{\mathrm{r}} \int_0^\infty p_{\mathrm{S}}(t)\,\mathrm{d}t$, the KME in this form is exact, as discussed in chapter 2. However, in order to derive explicit expressions for the rate constants k_{nm}, we shall now treat $\hat{V}$ as a perturbation. The rate constants can be evaluated to second order in $\hat{V}$ by approximating the rate kernels as $\kappa_{nm}(t) \approx (1/Z)\,\mathrm{Tr}\big[\hat{P}_n \mathcal{L}_V \mathcal{Q} e^{\mathcal{Q}\mathcal{L}_0 t}\mathcal{Q}\mathcal{L}_V \hat{P}_m\big]$. This approximation yields a second order kinetic master equation (KME2) which rigorously gives integrated properties accurate to second order in the perturbation. From this we can also obtain a criterion of the validity of the kinetic description, using the ideas discussed in chapter 2.

8.2.3 Intersystem crossing rate constants

We can obtain the rate constants k_{nm} by integrating the second order rate kernels. Noting that $e^{\mathcal{Q}\mathcal{L}_0 t} = \mathcal{P} + \mathcal{Q}e^{\mathcal{L}_0 t}$, the second order approximation to $\kappa_{nm}(t)$ for $n \neq m$ is

$$\kappa_{nm}(t) = \frac{2}{\hbar^2 Z} e^{-\gamma_{nm}t} \cos[(\epsilon_n - \epsilon_m)t]\,\mathrm{Tr}\big[\hat{P}_n \hat{V} \hat{P}_m \hat{V}\big], \tag{8.10}$$

and $\kappa_{nn}(t) = -\sum_{m\neq n} \kappa_{mn}(t)$. Integrating this gives the following general expression for the interconversion rate constant for $n \neq m$ (with $k_{nn} = -\sum_{m\neq n} k_{mn}$),

$$k_{nm} = \frac{\mathrm{Tr}\big[\hat{P}_n \hat{V} \hat{P}_m \hat{V}\big]}{\hbar^2 Z} \frac{2\gamma_{nm}}{\gamma_{nm}^2 + (\epsilon_n - \epsilon_m)^2}. \tag{8.11}$$

This is essentially the Fermi's golden rule rate constant, where the density of states for the final state is a Lorentzian function with a width given by the decoherence rate $\hbar\gamma_{nm}$.

In order to evaluate the kernels, we need the following matrix elements of $\hat{V}$, $\langle n|\hat{V}|m\rangle \equiv$

$\hat{V}_{nm} = \hat{V}_{mn}^{\dagger}$,

$$\hat{V}_{\mathrm{ST}_{\pm}} = \mp\frac{1}{2\sqrt{2}}\left[(\hat{h}_{1x} \pm i\hat{h}_{1y}) - (\hat{h}_{2x} \pm i\hat{h}_{2y})\right] \tag{8.12a}$$

$$\hat{V}_{\mathrm{ST}_0} = \frac{1}{2}\left[\hat{h}_{1z} - \hat{h}_{2z}\right] + \frac{1}{2}\mu_{\mathrm{B}}(g_1 - g_2)B \tag{8.12b}$$

$$\hat{V}_{\mathrm{T}_0\mathrm{T}_{\pm}} = \frac{1}{2\sqrt{2}}\left[(\hat{h}_{1x} \pm i\hat{h}_{1y}) + (\hat{h}_{2x} \pm i\hat{h}_{2y})\right] \tag{8.12c}$$

$$\hat{V}_{\mathrm{T}_{\pm}\mathrm{T}_{\mp}} = 0, \tag{8.12d}$$

in which $\hat{h}_{i\alpha} = \sum_{k=1}^{N_i} a_{ik}\hat{I}_{ik\alpha}$. Taking the trace of products these as in Eq. (8.10), it is clear that the only non-vanishing terms are those proportional to an $\hat{I}_{ik\alpha}^2$ or an identity operator. The trace of $\hat{I}_{ik\alpha}^2$ is $\mathrm{Tr}_{\mathrm{b}}[\hat{I}_{ik\alpha}^2] = \frac{1}{3}I_{ik}(I_{ik}+1)Z$, which can be used to evaluate all of the terms appearing in the master equation.

The resulting kinetic master equation rate constants satisfy $k_{nm} = k_{mn}$ and they can be split into the sum of a hyperfine contribution $k_{nm}^{(\mathrm{hfc})}$ and a Δg contribution $k_{nm}^{(\Delta\mathrm{g})}$. It is clear that $k_{\mathrm{T}_{\pm}\mathrm{T}_{\mp}}^{(\mathrm{hfc})} = 0$, and that all Δg rate constants are zero other than $k_{\mathrm{ST}_0}^{(\Delta\mathrm{g})} = k_{\mathrm{T}_0\mathrm{S}}^{(\Delta\mathrm{g})}$. The non-zero rate constants are[211]

$$k_{nm}^{(\mathrm{hfc})} = \frac{\omega_{1,\mathrm{hyp}}^2 + \omega_{2,\mathrm{hyp}}^2}{6}\frac{\gamma_{nm}}{\gamma_{nm}^2 + (\epsilon_n - \epsilon_m)^2}, \tag{8.13}$$

$$k_{\mathrm{ST}_0}^{(\Delta\mathrm{g})} = \frac{1}{2}\left(\frac{\mu_{\mathrm{B}}(g_1 - g_2)B}{\hbar}\right)^2\frac{\gamma_{\mathrm{ST}_0}}{\gamma_{\mathrm{ST}_0}^2 + (\epsilon_{\mathrm{S}} - \epsilon_{\mathrm{T}_0})^2}, \tag{8.14}$$

where $\omega_{i,\mathrm{hyp}}^2 = \sum_{k=1}^{N_i} a_{ik}^2 I_{ik}(I_{ik}+1)/\hbar^2$.

The generalisation of the master equation to include electron spin relaxation arising from rotational diffusion is straightforward. Here I will simply state the additional contributions to the singlet-triplet interconversion rates for a radical pair undergoing isotropic rotational diffusion, and leave the details of the derivation to the appendix. The final expression for the relaxation-induced spin-state interconversion rates is

$$k_{nm}^{(\mathrm{hf-aniso})} = \frac{|\omega_{1,\mathrm{hyp}}^{(2)}|^2 + |\omega_{2,\mathrm{hyp}}^{(2)}|^2}{18}\frac{(\gamma_{nm} + 1/\tau_{\mathrm{R}})}{(\gamma_{nm}+1/\tau_{\mathrm{R}})^2+(\epsilon_n-\epsilon_m)^2}, \tag{8.15}$$

where τ_{R} is the isotropic rotational correlation time,[172] $|\omega_{i,\mathrm{hyp}}^{(2)}|^2 = \sum_{k=1}^{N_i}\sum_{m=-2}^{2}|A_{ik,m}^{(2)}|^2 I_{ik}(I_{ik}+1)/\hbar^2$, and $A_{ik,m}^{(2)}$ is the m^{th} rank 2 spherical tensor component of the hyperfine coupling for

nuclear spin k on radical i.[43] Analogous expressions for relaxation induced by rotational modulation of g-tensor anisotropy, and dipolar electron spin coupling, are given in the appendix, including the effect of anisotropic rotational diffusion.

Eqs. (8.13) to (8.15) are clearly very closely related to the ansatz proposed by Steiner *et al.*[51] (Eq. (8.1)). However, they have been derived here directly from the quantum mechanical description of the radical pair spin dynamics, and they do not involve any free parameters. One significant difference between our equations and Eq. (8.1) is that our width parameters γ_{nm} depend explicitly on the spin states n and m that are interconverting.

From the theory outlined above, we can find criteria for the validity of the Markovian and perturbative approximations. An approximate validity criterion can be obtained for the second order perturbative approximation by requiring that the time-scales of the unperturbed dynamics are shorter than those associated with the perturbation , i.e. for the isotropic hyperfine interactions when $(\omega_{1,\mathrm{hyp}}^2 + \omega_{2,\mathrm{hyp}}^2)/6 \ll \gamma_{nm}^2 + (\epsilon_n - \epsilon_m)^2$, for the Δg mechanism when $(\mu_\mathrm{B}(g_1 - g_2)B/\hbar)^2/2 \ll \gamma_{\mathrm{ST}_0}^2 + (\epsilon_\mathrm{S} - \epsilon_{\mathrm{T}_0})^2$, and for the anisotropic hyperfine interactions when $(|\omega_{1,\mathrm{hyp}}^{(2)}|^2 + |\omega_{2,\mathrm{hyp}}^{(2)}|^2)/18 \ll (\gamma_{nm} + 1/\tau_\mathrm{R})^2 + (\epsilon_n - \epsilon_m)^2$, where $n \neq m$.

The Markovian approximation will be valid when the decay time of the kernels is shorter than the time-scale of the population dynamics. Using Eq. (2.63) for the validity of the Markovian criterion, and Eq. (8.10) for the kernel components, we require that the maximum of $|\int_0^\infty t\kappa_{nm}(t)\,\mathrm{d}t| < 1$ for the Markovian approximation to be accurate, which reduces to

$$\frac{2\,\mathrm{Tr}\left[\hat{P}_n\hat{V}\hat{P}_m\hat{V}\right]}{\hbar^2 Z}\frac{|\gamma_{nm}^2 - (\epsilon_n - \epsilon_m)^2|}{(\gamma_{nm}^2 + (\epsilon_n - \epsilon_m)^2)^2} < 1 \tag{8.16}$$

By noting that $|\gamma_{nm}^2 - (\epsilon_n - \epsilon_m)^2| \leq \gamma_{nm}^2 + (\epsilon_n - \epsilon_m)^2$, this criterion will be satisfied when $k_{nm}^{(\mathrm{hfc}/\Delta\mathrm{g})} < \gamma_{nm}$ and equivalently for the anisotropic interactions when $k_{nm}^{(\mathrm{hf-aniso})} < \gamma_{nm} + 1/\tau_\mathrm{R}$. These criteria for Markovianity are the same as the criteria for the validity of second order perturbation theory.

Overall we see that the second order kinetic master equation (KME2) can be expected to break down when coherence decay rates energy gaps between spin states become small – these are the factors that drive spin dynamics away from the incoherent kinetic behaviour into

the coherent regime. Higher order truncations of the kernel in Eq. (2.53) and approximate resummations of these higher order terms could in principle be used to obtain master equations valid beyond the perturbative limit,[34,102] however the resulting rate constants would have a significantly more complex functional form than that proposed by Steiner *et al.* [Eq. (8.1)].

8.3 A model radical pair

In order to evaluate the accuracy of the perturbative master equation, and in particular to demonstrate where the approximations we have made in deriving it are not applicable, I will now present calculations for two example systems for which exact quantum mechanical simulations can be performed for comparison, using either the Stochastic Liouville equation[172] (as described in previous chapters) or using spin coherent state sampling to solve the Haberkorn master equation.[185,198]

As a first example, which includes the effects of electron-spin relaxation, the population dynamics for a radical pair undergoing isotropic rotational diffusion, with one radical coupled anisotropically to a single proton, have been simulated using the SLE. This model is the same as that used in section 6.6.2. Fig. 8.2 shows the singlet, triplet and total survival probabilities ($p(t) = \sum_n p_n(t)$) for this radical pair with rotational correlation times of 1 ps (top panels) and 1 ns (bottom panels), at two different applied magnetic field strengths $B = 2J/g_e\mu_B$ (left panels) and $B = 20J/g_e\mu_B$ (right panels). In this example $a = (4/3)J = \Delta A = 1\ g_e\mu_B$mT and $k_S^r = 10k_T^r = 1\ \mu s^{-1}$, so this is in a regime where the hyperfine coupling is of comparable strength to the electron spin coupling. These parameters are chosen as being representative of a real radical pair reaction in solution. In the case of only one hyperfine coupled proton, coherence effects will be highly pronounced,[53,212] making this a relatively challenging example for the KME2 method.

As the rotational correlation time decreases from 1 ns to 1 ps, it can be seen in Fig. 8.2 that the master equation becomes less accurate. When τ_R is small, isotropic hyperfine coupling dominates and the second order kinetic master equation fails to capture the coherent oscillations between the singlet and triplet states at short times. However, for longer times,

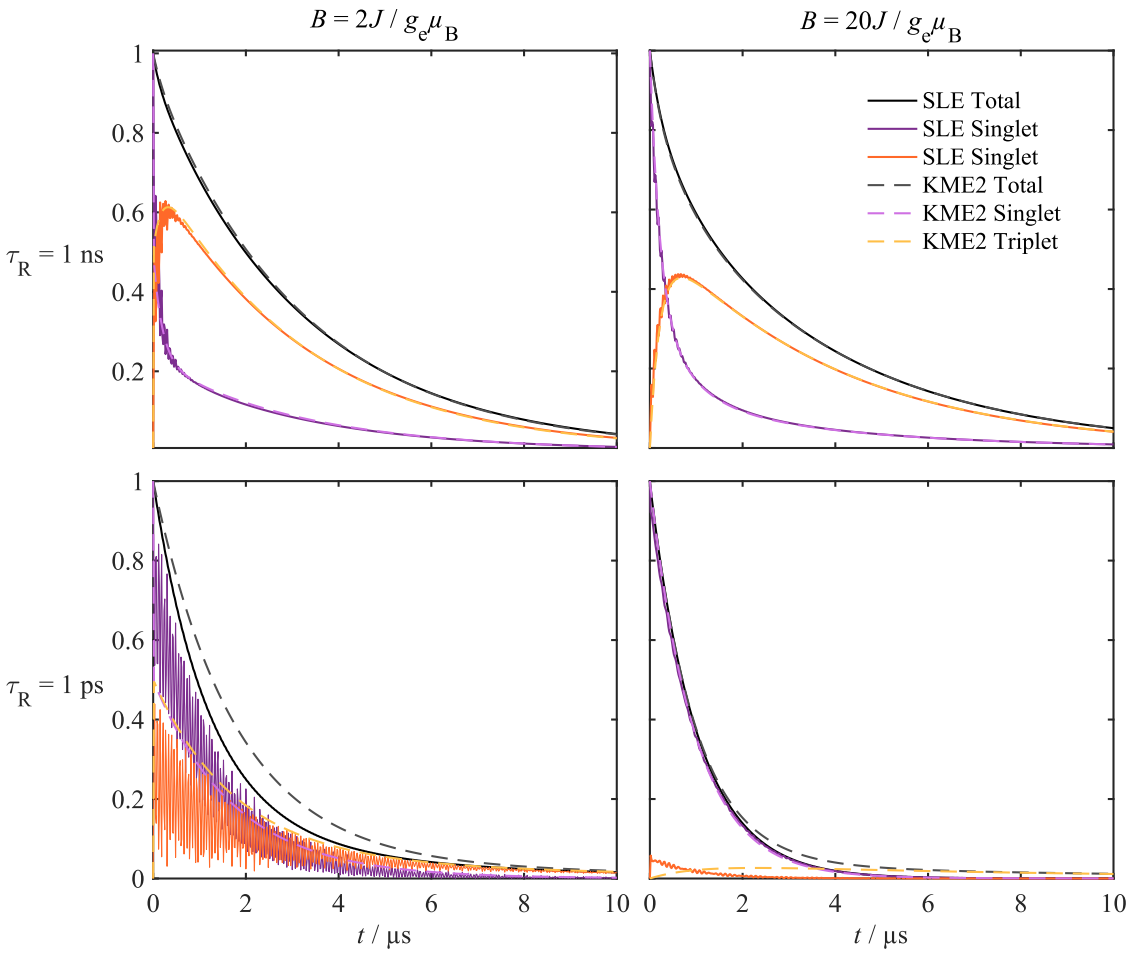

Figure 8.2: Singlet, triplet and total survival probabilities for a one proton radical pair with isotropic rotational diffusion causing relaxation. Solid lines are the exact probabilities obtained by solving the Stochastic Liouville equation and the dashed lines are the KME2 results. In the top two panels τ_R is 1 ns and in the bottom two panels τ_R is 1 ps, and in the left hand panels $B = 2J/g_e\mu_B$ and in the right hand panels $B = 20J/g_e\mu_B$. Both radicals have isotropic g-tensors with $g_i = g_e$. The scalar coupling is $J = -0.75 g_e\mu_B$ mT and the proton has a diagonal hyperfine coupling tensor with components $A_{xx} = A_{yy} = 0.5 g_e\mu_B$ mT and $A_{zz} = 2 g_e\mu_B$ mT. The radical pair reacts asymmetrically with $k_S^r = 1$ μs^{-1} and $k_T^r = 0.1$ μs^{-1}.

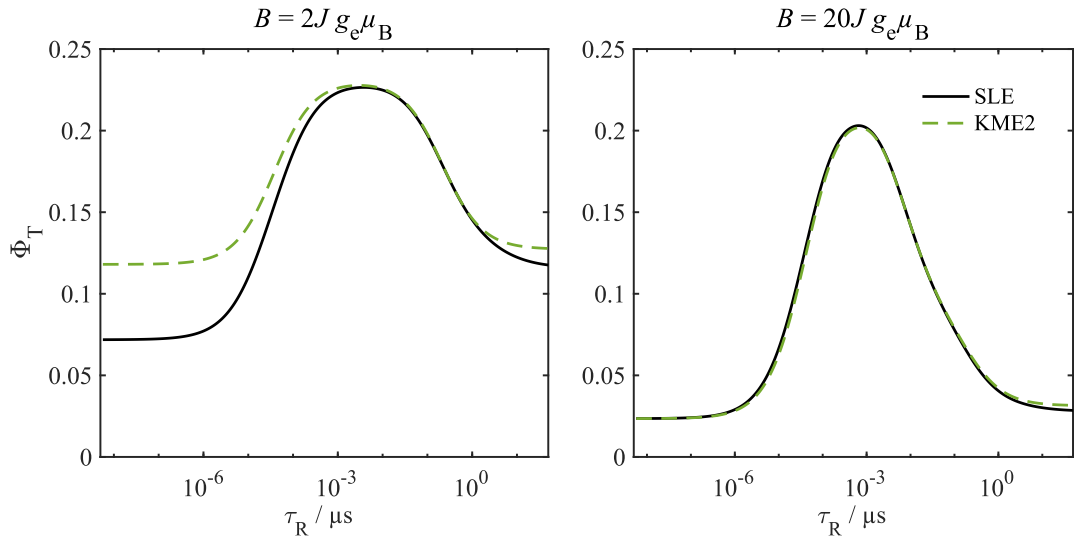

Figure 8.3: Triplet yield as a function of rotational correlation time for a one proton radical pair. The simulations in the left panel correspond to $B = 2J/g_e\mu_B$ and in the right panel they correspond to $B = 20J/g_e\mu_B$.

and when relaxation plays a significant role, as in the $\tau_R = 1$ ns case, the KME2 is very accurate. In this case it can be seen that coherent oscillations decay after $t \approx 0.5$ μs $\approx 1/\gamma_{ST_m}$, which is the decay time of the singlet-triplet rate kernels. We also see that away from the $2J$ resonance, at a high applied magnetic field strength, the KME2 is more accurate than at $B = 2J/g_e\mu_B$, where the singlet and T_+ states have equal energy, so the perturbative approximation is least accurate at this resonance.

In Fig. 8.3 we examine the accuracy of the KME2 for the triplet quantum yield of this one proton radical pair, as a function of the rotational correlation time, at the $2J$ resonance and for $B = 20J/g_e\mu_B$. Away from the $2J$ resonance, (right panel of Fig. 8.3), the KME2 is very accurate up to long correlation times, $\tau_R > 10$ μs. At the $2J$ resonance however (Fig. 8.3, left panel), the perturbative approximation to the isotropic hyperfine coupling breaks down, and when relaxation does not contribute to the radical pair intersystem crossing ($\tau_R < 1$ ps) the KME2 results no longer agree quantitatively with the exact results. This breakdown arises because the perturbation strength, $\hbar\omega_{1,\mathrm{hyp}}/\sqrt{6} = a/(2\sqrt{2}) \approx 0.35\ g_e\mu_B$ mT, is larger than the smallest unperturbed frequency, $\min_{n\neq m} \hbar[\gamma_{nm}^2 + (\epsilon_n - \epsilon_m)^2]^{1/2} \approx 0.003\ g_e\mu_B$ mT, consistent with the above discussion. The second order master equation nevertheless remains accurate when relaxation dominates (for 1 ns $< \tau_R <$ 1 μs), in spite of the strong

hyperfine coupling.

8.4 Para-phenylene molecular wires

As a second example, magnetic field effects on the recombination reactions of an homologous series of charge-separated $PTZ^{\bullet+}$–Ph_n–$PDI^{\bullet-}$ molecular wires have been simulated (the chemical structure of the molecules is shown in Fig. 8.4).[26] As demonstrated in Ref. [26], these radical pairs react spin selectively to either form the singlet ground state molecule, or an excited triplet state, where the triplet excitation is localised on the PDI fragment. Both the radical pair state and triplet product are distinguishable from the ground state spectroscopically, which enabled Weiss *et al.* to measure the radical pair survival probability $p(t, B)$ and the triplet product yield $\Phi_T(B)$, relative to the zero field values.[26] This series has also previously been studied using exact quantum mechanical simulations, as described in Ref. [198], and here the same model and parameters for the radical pair spin dynamics are used.

It has been suggested that two main mechanisms of charge transport operate in these molecules: superexchange mediated tunnelling between the two radical ions, and hopping via an intermediate state in which the Ph_n bridge is charged.[26] The dominant mechanism depends on the energetics of the states involved and the effective diabatic coupling between the states, so different mechanisms may operate for the singlet and triplet charge recombination processes. There is no direct way to determine the mechanism from magnetic field effect experiments, instead one must fit k_S^r and k_T^r using the MFE data and a model of the radical pair intersystem crossing process, and the mechanism of charge transport can be inferred from the donor-acceptor separation r_{DA} dependence of the extracted rate constants. An exponential decay of the rate constant with r_{DA} is indicative of tunnelling, whereas a rate which is constant or increases slowly with r_{DA} suggests that a hopping type mechanism operates.[26] This was originally investigated using exact quantum dynamical simulations by myself, Alan Lewis and David Manolopoulos[198], using a model of the radical pair spin dynamics which only included isotropic coupling terms. Here I will use these simulation results to benchmark the KME2 method, and then use the KME2 method with a model of

the radical pair intersystem crossing that incorporates the effects of anisotropic interactions, which cause spin relaxation, as well as isotropic couplings.

8.4.1 Isotropic coupling model

In the first model of $PTZ^{\bullet+}$–Ph_n–$PDI^{\bullet-}$ radical pairs considered, only the electronic Zeeman interaction, electronic scalar coupling and isotropic hyperfine couplings in the $PTZ^{\bullet+}$ and $PDI^{\bullet-}$ radicals are included. No relaxation contributions are present, so one may expect the Markovian and weak-coupling approximations to be less accurate than in the model considered above.

For the n=2 and n=3 radical pairs the magnetic field effect on the relative triplet yield is calculated (as was reported for the experiments by Weiss *et al.* in Ref. [26]). As was found in Ref. [198], and as discussed in chapter 7 for $DMJ^{\bullet+}$-An-Ph_n-$NDI^{\bullet-}$ radical pairs, it was necessary to add a correction to the calculated triplet yield to account for additional triplet formation, and to use the same model as in Ref. [198], here I only consider adding a background correction as in Eq. (7.18). The effect of additional relaxation or a small triplet fraction could also be included, but results in chapter 7 for a very similar radical pair show that these different additional triplet formation mechanisms yield almost identical fits to experimental data, so for simplicity here only the background correction is considered. For the n=4 and n=5 radical pairs the calculated magnetic field effect is on the survival probability of the radical pair at 55 ns after formation, as was reported in Ref. [26].

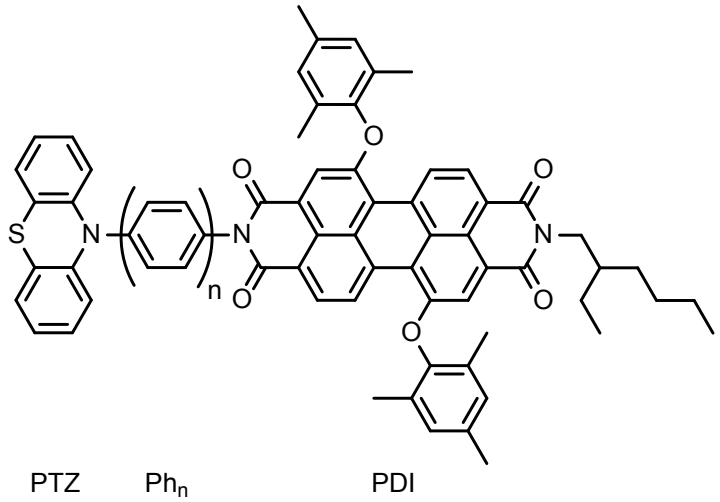

Figure 8.4: The chemical structure of the PTZ – Ph_n – PDI molecules. Photoexcitation of the PDI fragment leads to electron transfer from the PTZ to the PDI, forming a spin correlated radical ion pair.[26]

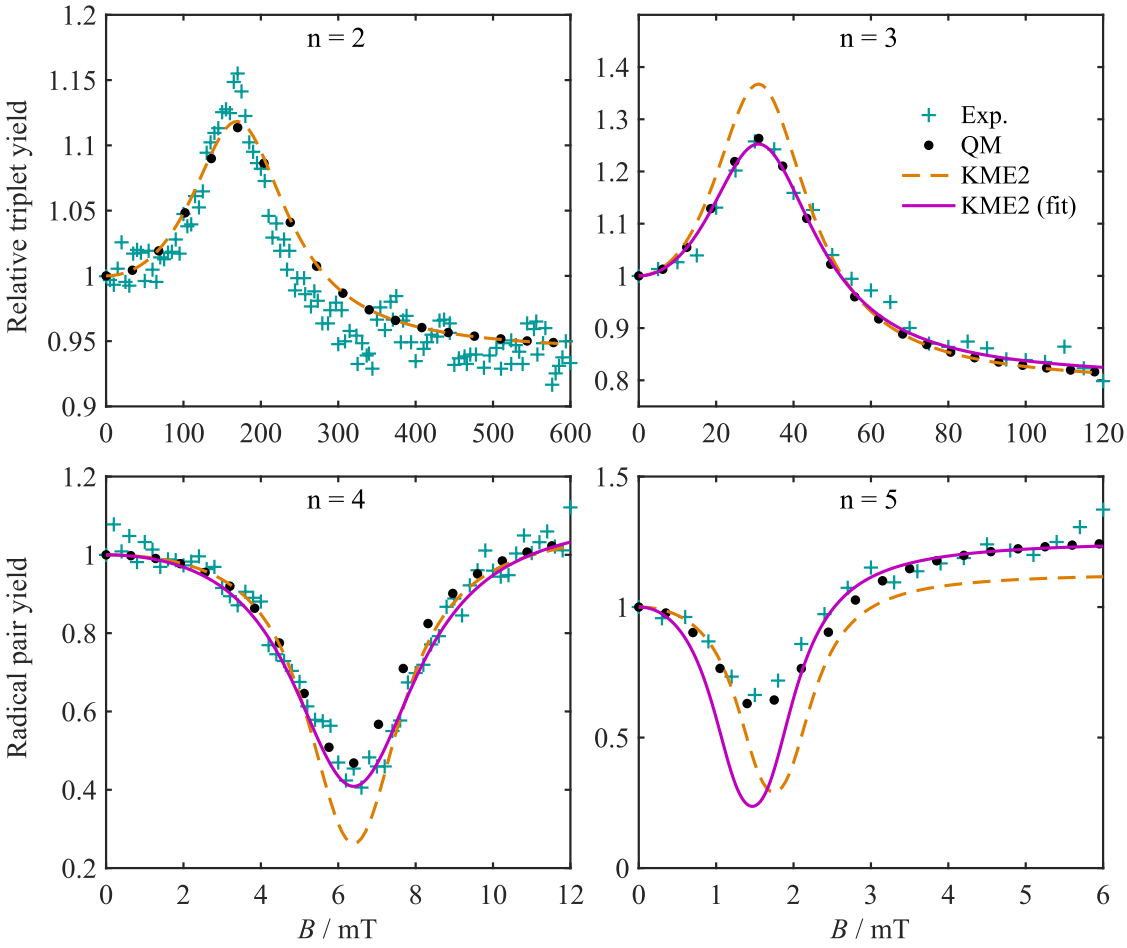

Figure 8.5: Simulated magnetic field effects for a series of $PTZ^{\bullet+}$–Ph_n–$PDI^{\bullet-}$ molecular wires. The n=2 and n=3 panels show relative triplet yields and the n=4 and n=5 panels show relative survival probabilities of the radical pair at $t = 55$ ns. The experimental data to which the quantum simulations were originally fitted are also included for comparison.[26] The QM and KME2 simulations used identical parameters, including the same background correction for the n=2 and n=3 data (see Ref. [198] for more details). The KME2 (fit) results were produced by refitting the model parameters.

From n=2 to n=5, the total scalar electron spin coupling decreases from $|2J| = 170\ g_e\mu_B$ mT to $|2J| = 1.75 g_e\mu_B$ mT, the last of which is comparable to the perturbation strength, $[(\omega_{1,\mathrm{hyp}}^2 + \omega_{2,\mathrm{hyp}}^2)/6]^{1/2} \approx 0.41 g_e\mu_B$ mT, and so treating the hyperfine interactions to lowest order in perturbation theory breaks down along the series, as can be seen from the results in Fig. 8.5. The largest deviations occur when there is a near degeneracy between the S and T_- states at the $2J$ resonance, where the perturbative approximation is least valid, and in the n=5 case where the low field effect[42] contributes significantly to the magnetic field effect on the radical pair survival probability.[198] Despite this, the errors in the KME2 results are still relatively small for the n=2–4 radical pairs.

For the n=3–5 molecular wires the kinetic master equation has been used to fit the experimental data using the same free parameters as in the quantum simulations described in Ref. [198], specifically k_S^r, k_T^r, and Φ_0 (for n=2 and n=3 only). The fitted parameters are given in Appendix 8.B. These fits are also shown in Fig. 8.5. In the n=3 and n=4 cases the data can be fit well with the KME2, with parameters differing from the QM parameters by $< 20\%$ for n=3 and $< 50\%$ for n=4. However, for the n=5 molecule, it was not possible to find k_S^r, k_T^r and J parameters for which the KME2 approximation gave a good fit to the experimental data. This is because of the importance of the low magnetic field effect in this case, and the value small of $|2J|$ and γ_{nm}. Under these circumstances the KME2 is clearly inadequate, and the only reliable way to fit the experimental data with the isotropic coupling model is to resort to a coherent quantum mechanical calculation of the type described in Ref. [198].

8.4.2 Including relaxation effects

Having demonstrated that the KME2 method can be used to reliably model magnetic field effects on the n=2–4 radical pairs, we can now use the method to include the effects of spin relaxation on the radical pair spin dynamics. Including relaxation in exact QM calculations is extremely computationally expensive, which is why these effects were ignored in the study in Ref. [198], however using the KME2 method the inclusion of electron spin relaxation is trivial. In Fig. 8.6 the magnetic field effects calculated from fitting models including relaxation using the KME2 method are shown along with the experimental data.

The model used includes relaxation from g tensor anisotropy, dipolar coupling between electron spins, and anisotropic hyperfine couplings modulated by molecular tumbling, as well as the isotropic Δg contribution. The tumbling motion is modelled using a symmetric top model, where the diffusion constants for rotation parallel and perpendicular to the symmetry axis are estimated by treating the molecule as a prolate ellipsoid, where the solvent is treated as a continuum fluid with a viscosity η, using the Stokes-Einstein equation, modified for ellipsoids.[213] This fails to account for the fact that motion about the symmetry axis for the two radicals is likely to be faster due to internal rotations of these groups, so to account for this the parallel diffusion constant $D_{\|}$ is rescaled, with the rescaled $D_{\|}$

treated as a free parameter in the model. The internal motion could be accounted for in a more sophisticated manner, but this would involve additional parameters, so for the sake of simplicity this simple rescaling of $D_{\|}$ is used. Anisotropic components of the g tensors are estimated from gas phase electronic structure calculations on the free radicals, as are the anisotropic hyperfine coupling tensors, and the angles between the radicals are estimated using the gas phase equilibrium geometries of the ground states, calculated with DFT. The dipolar coupling tensor is calculated by treating each radical as a point dipole, where the separation estimated from the gas phase equilibrium geometries. Details of the model are described in appendix 8.B.

When relaxation is also included, it is found that some additional changes need to be made to the model to obtain good least squares fits to the experimental data. Firstly for the n=4 and n=5 radical pairs it was found that an additional field-independent singlet-triplet dephasing needed to be included, with rate constant $k_{\mathrm{STD}} = k^{\mathrm{d}}_{\mathrm{ST}_m}$. For the n=2 and n=3 radical pairs, adding this relaxation mechanism into the model was not found to significantly improve the fits, so it is excluded for simplicity. Secondly, the $2J$ value was adjusted for the n=2. Since the $2J$ value was originally estimated by simply taking the magnetic field at which the MFE is maximised, this is a reasonable small adjustment to make to the model. For the n=5 molecule the original experimental $2J$ value of $-1.5 g_{\mathrm{e}} \mu_{\mathrm{B}}$ mT was used. Thirdly, as discussed in Ref. [198], the Δg value estimated by taking the isotropic g values for the free radicals is likely to be an overestimate, because in the radical pairs the local electronic environments of the radicals are altered, so for the n=2 results a rescaling of the experimental, free radical Δg value was introduced. The Δg mechanism makes effectively no contribution to the observed magnetic field effects for radical pairs with n>2, because B is much smaller in these other cases, so this rescaling is not included in the other radical pairs.

The values of the parameters $k^{\mathrm{r}}_{\mathrm{S}}$, $k^{\mathrm{r}}_{\mathrm{T}}$, $D_{\|}$, Φ_0 (for n=2 and n=3), k_{STD} (for n=4 and n=5), as well as $2J$ (for n=2 and n=5) and Δg (for n=2), were obtained by least squares fitting the KME2 model with these free parameters to the experimental MFE data, with the constraint that the zero field lifetime of the radical pair is within 5% of the experimental lifetime. The best fits are shown in Fig. 8.6 along with the experimental MFE data. The n=2 panel (top

left) includes the model without rescaling Δg and $2J$ and with these rescalings. The fitted parameters are given in appendix 8.B.

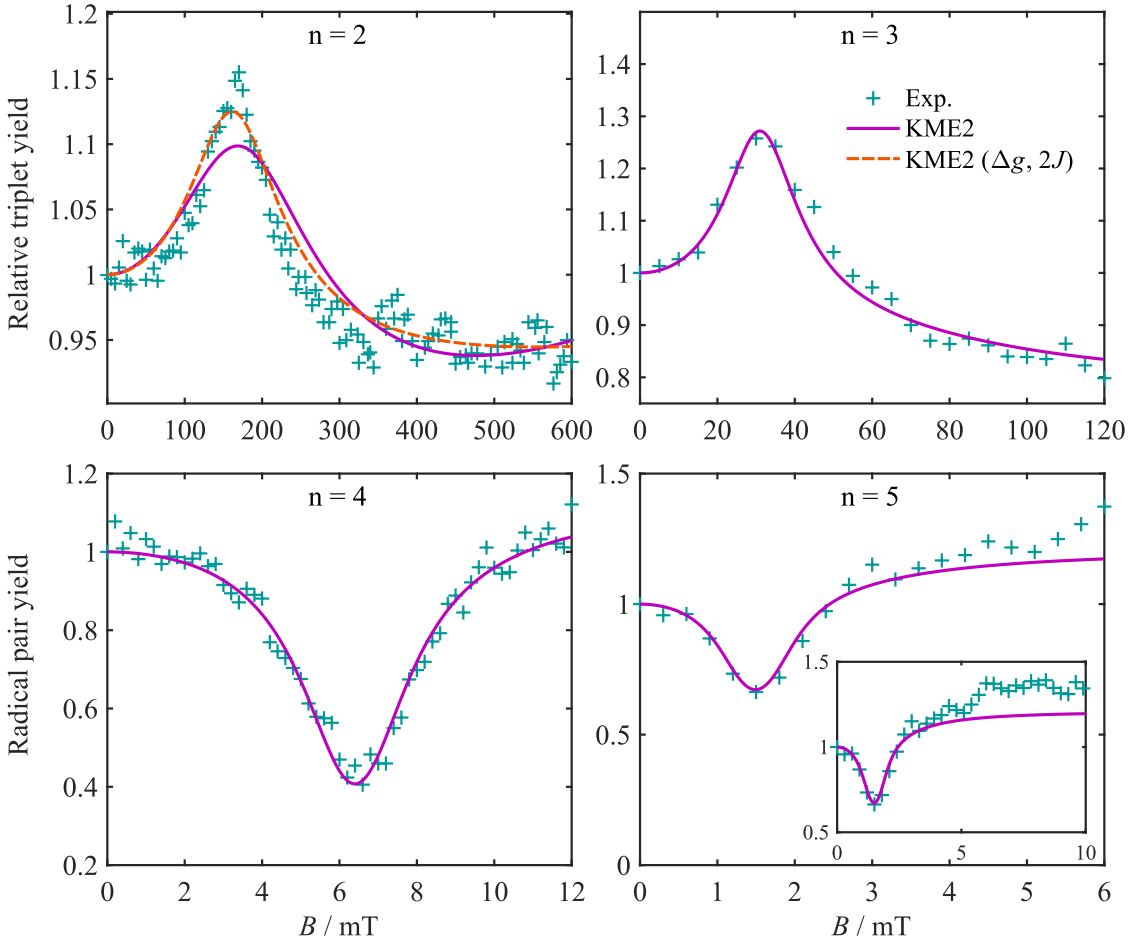

Figure 8.6: Simulated magnetic field effects for a series of $PTZ^{\bullet+}$–Ph_n–$PDI^{\bullet-}$ molecular wires. The n=2 and n=3 panels show relative triplet yields and the n=4 and n=5 panels show relative survival probabilities of the radical pair at $t = 55$ ns. The experimental data to which the models are fitted are also included for comparison.[26] As described in the text, for n=2 only the value of Δg and $2J$ were refitted, the results of which are given by the orange dashed curve. Adjusting Δg and $2J$ for the n=3–5 radical pairs did not significantly alter the fit quality or the values of parameters, so these results are not shown.

Firstly we note that including relaxation effects the KME2 models can provide very good fits to the experimental data for n=2–4 radical pairs, with some deviations at large applied magnetic fields for n=5 (as shown in the insert of the bottom right panel in Fig. 8.6). The deviations for n=5 can be explained by comparing the KME2 and QM results in Fig. 8.5, where it was found that low magnetic field effects which are not captured by second order perturbation theory play a role in the spin dynamics, leading to a breakdown

of the KME2 description in this case. The deviation for n=5 is most pronounced at high fields, which is most likely because the magnetic field effect reported is a relative magnetic field, $p(t, B)/p(t, B = 0\ \text{mT})$, so if the spin dynamics are not accurately described at zero field, e.g. if $p(t, B = 0\ \text{mT})$ is overestimated, then the high magnetic field effects may not be described accurately.

The adjusted values of $2J/g_e\mu_B$ for the n=2 is −161.9 mT, which is a relatively small shift from the experimental value.[b] Similarly the change in the Δg value is relatively small for n=2, where it is scaled down from $\Delta g = 0.0025$ based on experimental measurements of the free radical g values to $\Delta g = 0.00128$, a decrease by a factor of approximately 2. This is likely due to the different substituents on the radicals leading to a small change in the electronic structure of the radicals, which slightly shifts the g values.

The fitted values of k_{STD} for n=4 and n=5 are 145 μs^{-1} and 20.7 μs^{-1}, which are approximately equal to the fitted values of k_T^r in each case, so when relaxation is included, it appears that singlet-triplet dephasing makes a reasonable contribution to the observed magnetic field effects. These values are similar to singlet-triplet decoherence rates reported for similar rigid radical ion pairs.[48,50] Singlet-triplet dephasing is also likely present in the n=2 and n=3 radical pairs, but adding this parameter did not improve the fit quality for these radical pairs, so it is not possible to reliably fit this parameter for these molecules. From the kinetic equations, the width of the magnetic field effect peaks will be governed by $\gamma_{\text{ST}_m} = k_{\text{STD}} + (k_S^r + k_T^r)/2$, so both dephasing and lifetime broadening contribute additively to the width. This means the fitted k_T^r values for n=2 and n=3 are likely overestimates, because singlet-triplet dephasing is not included.

The rescaling of the rotational diffusion constant for motion parallel to the molecular symmetry axis, $D_{\parallel}^{\text{fitted}}/D_{\parallel}^{\text{Einstein}}$, was found to lie between 8.8 and 11.6 for these radical pairs, which suggests that faster torsional motion about the molecular symmetry axis makes a significant contribution to the modulation of anisotropic spin coupling parameters. This motion would be expected to be similar for all molecules, which is consistent with the small range of rescaling parameters found across the series of molecules.

[b] As suggested in Ref. [26] the net electron spin coupling is assumed to be anti-ferromagnetic, so $2J < 0$, although the magnetic field effects are not sensitive to the sign of $2J$. In fact within the KME2 method the observed magnetic field effect is completely independent of the sign of $2J$.

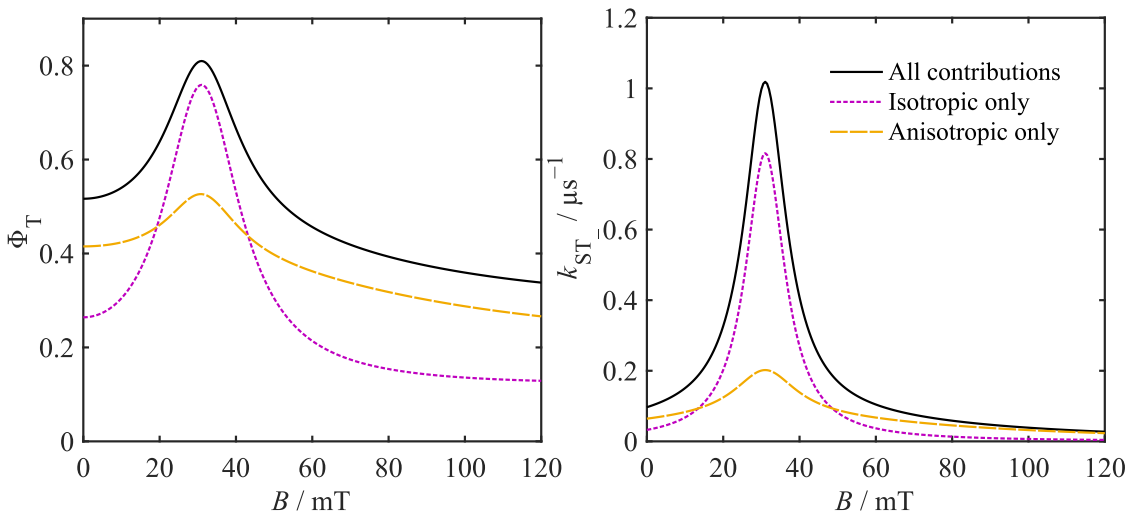

Figure 8.7: Singlet-triplet interconversion rate constants and triplet yields with and without relaxation.

The KME2 method provides a useful tool for analysing the relative contributions of isotropic coupling and anisotropic coupling contributions to the radical pair intersystem crossing process, because the kinetic rate constants at second order are a simple sum of anisotropic and isotropic terms. This means we can evaluate whether or not the inclusion of relaxation contributions to the intersystem crossing is actually important. In Fig. 8.7 the triplet quantum yield (left panel), and the total S $\rightarrow$ T_- intersystem crossing rate constant (right panel) is shown for the n=3 radical pair as a function of applied field strength. The triplet yields and rate constants including only isotropic coupling terms or only relaxation due to modulation of anisotropic coupling terms are also shown. It can be seen in the right hand panel of Fig. 8.7 that for $B < 10$ mT and $B > 50$ mT anisotropic coupling contributions dominate the intersystem crossing rate, but close to the $2J$ resonance, the isotropic contribution dominates. This means that neither isotropic nor anisotropic coupling effects can be said to dominate the entire range of observed MFEs, which is reflected in the triplet yields calculated including either both isotropic and anisotropic couplings, or just one of these, as shown in the left panel of Fig. 8.7. This clearly shows the importance of including relaxation effects in modelling the MFEs on radical pair reactions.

In the previous study of these radical pair reactions using quantum mechanical simulations[198], which ignored any anisotropic coupling/relaxation effects, the fitted spin selective rate constants along the series of molecules were used to infer the spin selective mechanisms

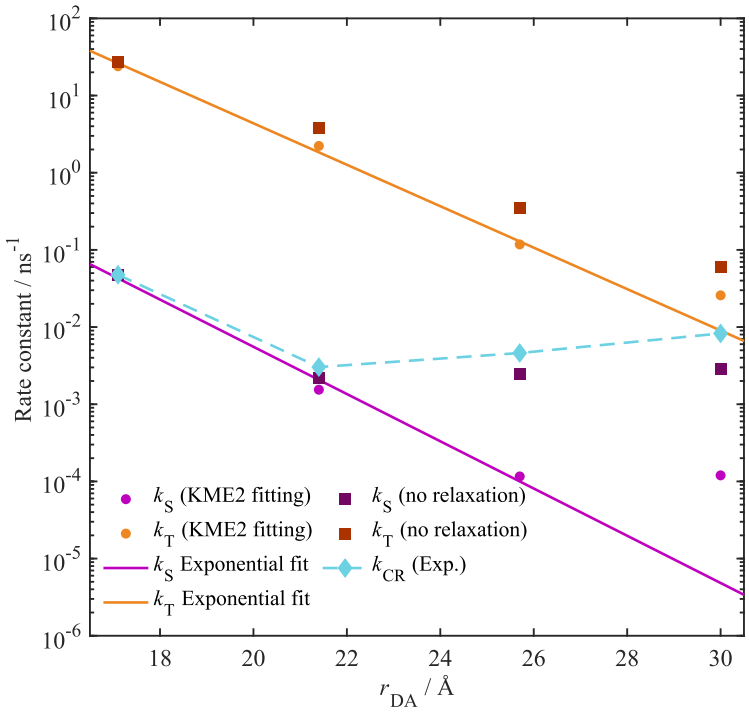

Figure 8.8: (A) A schematic picture of the radical pair mechanism with coherent quantum intersystem crossing between singlet and triplet states. (B) The incoherent kinetic scheme used to describe the radical pair mechanism.

of charge recombination. It was concluded that the triplet recombination mechanism is superexchange mediated electron tunnelling, based on the observation that the rate constant decays exponentially with radical separation, whereas for the singlet recombination for n>2 it was concluded that a hopping mechanism dominates, based on the observation that k_S^r becomes approximately independent of the donor-acceptor separation. However, in light of the fact that anisotropic coupling effects likely make a large contribution to the radical pair intersystem crossing process, we should re-evaluate these conclusions about the spin dependent charge recombination mechanisms.

The fitted values of the spin selective rate constants are plotted in Fig. 8.8 as a function of the donor-acceptor separation, r_{DA}, with circles denoting the new KME2 fitted values, where relaxation is included, and squares denoting the values obtained in Ref. [198] using the model that only includes isotropic couplings. It is clear that the experimental charge recombination rate k_{CR}, which is the inverse of the radical pair lifetime, depends on both the singlet and triplet recombination rates and the rate of intersystem crossing. Whilst the values of k_T^r obtained with relaxation included are relatively similar, the values of k_S^r are approximately an order of magnitude smaller for the n=4 and n=5 radical pairs. So whilst the triplet recombination does appear to be tunnelling dominated across the whole

series, it appears that for the singlet recombination the hopping mechanism dominates for n>4 rather than n>3. The deviation for longer wires when relaxation is included can be explained by noting that the relaxation contribution to intersystem crossing becomes larger with decreasing $2J$, because the rotational correlation times are relatively short (ranging from approximately 0.1 ns to 2 ns) and only weakly dependent on the wire length, so as the energy gaps between singlet and triplet states decrease, the rate of relaxation induced intersystem crossing increases. This gives rise to large deviations between the models with and without anisotropic coupling for longer wires.

For n=2–4 the KME2 recombination rate constants were fitted to an exponential decay with donor-acceptor separation $k = k_0 e^{-\beta r_{\mathrm{DA}}}$ (due to the fact that the KME2 method may not be reliable for n=5, the n=5 rate constants were excluded in this fitting for the triplet rate constant), which are shown as solid lines in Fig. 8.8. For the singlet recombination pathway $\beta = 0.705$ Å^{-1} for the triplet recombination pathway $\beta = 0.618$ Å^{-1}, which are relatively close to the decay constant observed for the charge separation step of $\beta = 0.46$ Å^{-1}[26]. The small differences between the decay constants could be due to errors in the model or noise in the experimental data, but they could also arise due to the differences in the superexchange diabatic coupling. Assuming the singlet and triplet electron transfers are well described by the non-adiabatic limit, the square coupling matrix elements are given approximately by[129,139]

$$\Delta^2 = \frac{V_{\mathrm{DB}_1}^2}{\Delta E_1^2} \prod_{k=1}^{n-1} \frac{V_{\mathrm{B}_k\mathrm{B}_{k+1}}^2}{\Delta E_{k+1}^2} V_{\mathrm{B}_n\mathrm{A}}^2, \tag{8.17}$$

where V_{DB_1} the diabatic coupling matrix elements between the donor (charge separated radical pair) and first bridge localised charge transfer state (a charged phenylene state), and the $V_{\mathrm{B}_n\mathrm{A}}$ is the coupling matrix element between the acceptor and the final bridge charge transfer state, $V_{\mathrm{B}_k\mathrm{B}_{k+1}}$ is the diabatic coupling between neighbouring bridge charge transfer states. ΔE_k is the energy gap between the initial state and the kth bridge charge transfer state, at lowest energy crossing point of the initial and final charge transfer states. Because for the singlet and triplet charge transfers the initial and final states have different free energy changes and reorganisation energies, the crossing points are different and therefore ΔE_k

can be expected to be different between singlet and triplet pathways, which may explain the small differences in the β values obtained.

8.5 Concluding Remarks

In this chapter, I have shown how the incoherent kinetic description of radical pair intersystem crossing can be derived from the Haberkorn quantum dynamical description. A perturbative approximation to the nuclear hyperfine coupling in the exact Nakajima-Zwanzig equation leads to a second order kinetic master equation for the electronic spin state populations. It is seen that the finite lifetime of the radical pair spin states, as well as any additional dephasing, drives the transition to incoherent kinetic behaviour. The KME2 is accurate in the long-time limit and exact for time integrated properties exactly to second order in the hyperfine interactions and in the difference between the radical g-tensors.

Tests on model systems have shown that the simple kinetic equations are remarkably accurate when the singlet-triplet coherence time is short, or when relaxation processes dominate, and when the hyperfine interaction is relatively weak compared to other spin interactions. However, the second order kinetic description obviously has some shortcomings. For example, it fails to capture the decrease in the S to T_0 interconversion rate at low applied magnetic field strengths,[42] as demonstrated by the failure of the KME2 to quantitatively capture the magnetic field effect on the survival probability of the $PTZ^{\bullet+}$–Ph_5–$PDI^{\bullet-}$ radical pair. There are however many situations in which the approximation works well, and so it can be expected that the theory developed here will prove useful in the interpretation of many future experiments on radical pair reactions (in fact it has already been used in the studies on other radical pairs presented in Refs. [31] and [48]).

As an example application of this theory, it has been applied to include the effects of relaxation induced by modulation of anisotropic spin couplings on $PTZ^{\bullet+}$–Ph_5–$PDI^{\bullet-}$ radical pairs. The new simulations with the KME2 suggest that there is a change in mechanism of singlet charge transfer in these molecules occurring at n>4 rather than n>3 as was inferred from fitted rate constants from a model excluding relaxation effects. This demonstrates the importance of including relaxation effects in simulations of radical pair

reactions, and a task for which the KME2 method is ideally suited.

Appendix

8.A The kinetic master equation with rotational diffusion

In the following we assume the radical pair is rigid, and the orientation between the radicals is fixed. The case of two independently rotating radicals is straightforward to obtain from this approach as well. Our starting point for deriving the kinetic equations for radical pair intersystem crossing including the effects of rotational diffusion is the Stochastic Liouville equation for the radical pair spin density operator, as a function of time t and orientation of the molecule Ω[172]

$$\begin{aligned}\frac{\mathrm{d}}{\mathrm{d}t}\hat{\rho}(t,\Omega) = &-\frac{i}{\hbar}\left[\hat{H}(\Omega),\hat{\rho}(t,\Omega)\right] - \left\{\frac{k_{\mathrm{S}}^{\mathrm{r}}}{2}\hat{P}_{\mathrm{S}} + \frac{k_{\mathrm{T}}^{\mathrm{r}}}{2}\hat{P}_{\mathrm{T}},\hat{\rho}(t,\Omega)\right\} \\ &- \sum_{n\neq m} k_{nm}^{\mathrm{d}}\hat{P}_n\hat{\rho}(t,\Omega)\hat{P}_m + \Gamma\hat{\rho}(t,\Omega).\end{aligned} \tag{8.A.1}$$

where D is the rotational diffusion operator

$$\Gamma = -(D_X\mathsf{L}_X^2 + D_Y\mathsf{L}_Y^2 + D_Z\mathsf{L}_Z^2) \tag{8.A.2}$$

where D_A is the rotational diffusion constant and L_A is the rotational angular momentum operator about the body-fixed axis A. Including the rotational diffusion, we take the reference part of the Hamiltonian $\hat{H}_0$ to be defined as before and now we also include the

anisotropic spin couplings in the perturbation $\hat{V}(\Omega)$, which also defines $\mathcal{L}_V$,

$$\hat{V}(\Omega) = \frac{\mu_B B}{2}(g_1 - g_2)(\hat{S}_{1z} - \hat{S}_{2z}) + \sum_{i=1,2}\sum_{k=1}^{N_i} a_{ik}\hat{\mathbf{I}}_{ik}\cdot\hat{\mathbf{S}}_i + \sum_{m=-2}^{2}\sum_{m'=-2}^{2}\mathfrak{D}^{(2)}_{m',m}(\Omega)\hat{Q}^{(2)}_{m,m'}. \tag{8.A.3}$$

$\mathfrak{D}^{(2)}_{m',m}(\Omega)$ is a Wigner D-matrix element and the operators $\hat{Q}^{(2)}_{m,m'}$ contain the anisotropic spin couplings,[43]

$$\hat{Q}^{(2)}_{m,m'} = D^{(2)}_m T^{(2)}_{m'}(\hat{\mathbf{S}}_1, \hat{\mathbf{S}}_2) + \sum_{i=1,2}\mu_B g^{(2)}_{i,m} T^{(2)}_{m'}(\hat{\mathbf{S}}_i, \mathbf{B}) + \sum_{i=1,2}\sum_{k=1}^{N_i} A^{(2)}_{i,k,m} T^{(2)}_{m'}(\hat{\mathbf{S}}_i, \hat{\mathbf{I}}_{i,k}). \tag{8.A.4}$$

$T^{(2)}_m(\hat{\mathbf{u}}, \hat{\mathbf{v}})$ is component m of a rank 2 spherical tensor for two vector operators, $A^{(2)}_{i,k,m}$ is the mth spherical tensor component m of the rank 2 hyperfine coupling tensor for nuclear spin k on radical i and similarly $g^{(2)}_{i,m}$ is a spherical tensor component of the rank 2 g-tensor for radical i. The spin density operator will initially be in a state of the form,

$$\hat{\rho}(0, \Omega) = \hat{\rho}(0) p_0(\Omega). \tag{8.A.5}$$

In solution, the initial distribution of the orientations is isotropic

$$p_0(\Omega) = \frac{1}{8\pi^2}. \tag{8.A.6}$$

As before we define a Liouville space projection operator which we can use to obtain the kinetic master equation,

$$\mathcal{P} = \frac{1}{Z}\sum_n p_0(\Omega)\,\hat{P}_n \int \mathrm{d}\Omega\ \mathrm{Tr}\big[\hat{P}_n \cdot\,\big]. \tag{8.A.7}$$

In order to evaluate the second order rate kernels, we note that the $\mathcal{L}_0$ propagator can be split into a spin part and a diffusion part

$$e^{\mathcal{L}_0 t} = e^{\mathcal{L}_s t} e^{\Gamma t}. \tag{8.A.8}$$

We will also therefore need the rank 2 Wigner D-matrix correlation functions,

$$\begin{aligned}\left\langle \mathfrak{D}^{(2)}_{a,b}(\Omega,t)^* \mathfrak{D}^{(2)}_{a',b'}(\Omega)\right\rangle &= \int \mathrm{d}\Omega\, \mathfrak{D}^{(2)}_{a,b}(\Omega)^* e^{\Gamma t} \mathfrak{D}^{(2)}_{a',b'}(\Omega) p_0(\Omega) \\ &= \frac{\delta_{a,a'}}{5} \sum_{k=1}^{5} h_{k,b} h^*_{k,b'} e^{-t/\tau_{\mathrm{R},k}} \\ &= \frac{\delta_{a,a'}}{5} c_{b,b'}(t)\end{aligned} \tag{8.A.9}$$

where the values of $1/\tau_{\mathrm{R},k}$ are given in Table 8.A.1 and the values of $h_{k,m}$ are given in Table 8.A.2. We also note that $\left\langle \mathfrak{D}^{(2)}_{n,m}(\Omega,t)\right\rangle = 0$. With this we see the terms in the second order kernel that mix isotropic and anisotropic hyperfine couplings vanish, and the anisotropic coupling terms are

$$\begin{aligned}\kappa^{(\mathrm{hf-aniso})}_{nm}(t) &= \frac{2}{\hbar^2} e^{-\gamma_{nm}t} \cos((\epsilon_n - \epsilon_m)t) \sum_{a,b,a',b'} \left\langle \mathfrak{D}^{(2)}_{a,b}(\Omega,t)^* \mathfrak{D}^{(2)}_{a',b'}(\Omega)\right\rangle \mathrm{Tr}\left[\hat{P}_n \hat{Q}^\dagger_{b,a} \hat{P}_m \hat{Q}_{b',a'}\right] \\ &= \frac{2}{\hbar^2} e^{-\gamma_{nm}t} \cos((\epsilon_n - \epsilon_m)t) \sum_{a,b,b'} \left\langle \mathfrak{D}^{(2)}_{a,b}(\Omega,t)^* \mathfrak{D}^{(2)}_{a,b'}(\Omega)\right\rangle \\ &\times \sum_{i=1,2} \sum_{k=1}^{N_i} A^{(2)*}_{i,k,b} A^{(2)}_{i,k,b'} \mathrm{Tr}\left[\hat{P}_n T^{(2)}_a(\hat{\mathbf{S}}_i, \hat{\mathbf{I}}_{i,k})^\dagger \hat{P}_m T^{(2)}_a(\hat{\mathbf{S}}_i, \hat{\mathbf{I}}_{i,k})\right] \\ &= \frac{2}{\hbar^2} e^{-\gamma_{nm}t} \cos((\epsilon_n - \epsilon_m)t) \sum_{b,b'} \frac{c_{b,b'}(t)}{5} \\ &\times \sum_{i=1,2} \sum_{k=1}^{N_i} A^{(2)*}_{i,k,b} A^{(2)}_{i,k,b'} \sum_a \mathrm{Tr}\left[\hat{P}_n T^{(2)}_a(\hat{\mathbf{S}}_i, \hat{\mathbf{I}}_{i,k})^\dagger \hat{P}_m T^{(2)}_a(\hat{\mathbf{S}}_i, \hat{\mathbf{I}}_{i,k})\right] \\ &= \frac{2}{\hbar^2} e^{-\gamma_{nm}t} \cos((\epsilon_n - \epsilon_m)t) \sum_{b,b'} \frac{c_{b,b'}(t)}{5} \sum_{i=1,2} \sum_{k=1}^{N_i} A^{(2)*}_{i,k,b} A^{(2)}_{i,k,b'} \frac{5}{36} I_{i,k}(I_{i,k}+1) \\ &= \frac{1}{18\hbar^2} e^{-\gamma_{nm}t} \cos((\epsilon_n - \epsilon_m)t) \sum_{b,b'} c_{b,b'}(t) \sum_{i=1,2} \sum_{k=1}^{N_i} A^{(2)*}_{i,k,b} A^{(2)}_{i,k,b'} I_{i,k}(I_{i,k}+1).\end{aligned}$$

Integrating this gives, for $n \neq m$ (apart from for $k^{(\mathrm{hf-aniso})}_{\mathrm{T}_\pm \mathrm{T}_\mp}$ which is zero)

$$k^{(\mathrm{hf-aniso})}_{nm} = \int_0^\infty \kappa^{(\mathrm{hf-aniso})}_{nm}(t)\, \mathrm{d}t \tag{8.A.10}$$

$$= \frac{1}{18} \sum_j \frac{\gamma_{nm} + 1/\tau_{\mathrm{R},j}}{(\gamma_{nm} + 1/\tau_{\mathrm{R},j})^2 + (\epsilon_n - \epsilon_m)^2} \sum_{b,b'} h_{j,b} h_{j,b'} \sum_{i=1,2} \sum_{k=1}^{N_i} \frac{A^{(2)*}_{i,k,b} A^{(2)}_{i,k,b'} I_{i,k}(I_{i,k}+1)}{\hbar^2}, \tag{8.A.11}$$

k	1	2	3	4	5
$1/\tau_{\mathrm{R},k}$	$4D_X + D_Y + D_Z$	$D_X + 4D_Y + D_Z$	$D_X + D_Y + 4D_Z$	$6\bar{D} - 2\Delta_D$	$6\bar{D} + 2\Delta_D$

Table 8.A.1: Table of $1/\tau_{\mathrm{R},k}$ values where $\bar{D} = (D_X + D_Y + D_Z)/3$ and $\Delta_D = \sqrt{D_X^2 + D_Y^2 + D_Z^2 - D_X D_Y - D_Y D_Z - D_Z D_X}$.

	b				
k	-2	-1	0	1	2
1	0	$1/\sqrt{2}$	0	$1/\sqrt{2}$	0
2	0	$-1/\sqrt{2}$	0	$1/\sqrt{2}$	0
3	$-1/\sqrt{2}$	0	0	0	$1/\sqrt{2}$
4	$1/\sqrt{2+\Lambda_-^2}$	0	$\Lambda_-/\sqrt{2+\Lambda_-^2}$	0	$1/\sqrt{2+\Lambda_-^2}$
5	$1/\sqrt{2+\Lambda_+^2}$	0	$\Lambda_+/\sqrt{2+\Lambda_+^2}$	0	$1/\sqrt{2+\Lambda_+^2}$

Table 8.A.2: Table of $h_{k,b}$ values where $\Lambda_\pm = \sqrt{2/3}(D_X + D_Y - 2D_Z \pm 2\Delta_D)/(D_X - D_Y)$.

apart from $k_{\mathrm{T}_\pm\mathrm{T}_\mp}^{(\mathrm{hf-aniso})}$, which are zero. In the case of symmetric top rotational diffusion, where $D_X = D_Y = D_\perp$ and $D_Z = D_\parallel$, this simplifies to

$$k_{nm}^{(\mathrm{hf-aniso})} = \frac{1}{18}\sum_b \frac{\gamma_{nm} + 1/\tau_{\mathrm{R},b}^{(\mathrm{symm})}}{(\gamma_{nm} + 1/\tau_{\mathrm{R},b}^{(\mathrm{symm})})^2 + (\epsilon_n - \epsilon_m)^2} \sum_{i=1,2}\sum_{k=1}^{N_i} \frac{|A_{i,k,b}^{(2)}|^2 I_{i,k}(I_{i,k}+1)}{\hbar^2} \tag{8.A.12}$$

where $1/\tau_{\mathrm{R},b}^{(\mathrm{symm})} = 6D_\perp + b^2(D_\parallel - D_\perp)$. This clearly reduces to the expression given above when $D_X = D_Y = D_Z$. Similar expressions can be obtained for the g-tensor anisotropy and

the dipolar coupling,

$$k_{\mathrm{ST}_0}^{(\mathrm{g-aniso/D})} = k_{\mathrm{T}_0\mathrm{S}}^{(\mathrm{g-aniso/D})} = \frac{\mu_\mathrm{B}^2 B^2}{15\hbar^2} \sum_j \frac{\gamma_{\mathrm{ST}_0} + 1/\tau_{\mathrm{R},j}}{(\gamma_{\mathrm{ST}_0} + 1/\tau_{\mathrm{R},j})^2 + (\epsilon_\mathrm{S} - \epsilon_{\mathrm{T}_0})^2} \sum_{b,b'} h_{j,b} h_{j,b'} \Delta g_b^{(2)*} \Delta g_{b'}^{(2)} \tag{8.A.13}$$

$$k_{\mathrm{ST}_\pm}^{(\mathrm{g-aniso/D})} = k_{\mathrm{T}_\pm\mathrm{S}}^{(\mathrm{g-aniso/D})} = \frac{\mu_\mathrm{B}^2 B^2}{20\hbar^2} \sum_j \frac{\gamma_{\mathrm{ST}_\pm} + 1/\tau_{\mathrm{R},j}}{(\gamma_{\mathrm{ST}_\pm} + 1/\tau_{\mathrm{R},j})^2 + (\epsilon_\mathrm{S} - \epsilon_{\mathrm{T}_\pm})^2} \sum_{b,b'} h_{j,b} h_{j,b'} \Delta g_b^{(2)*} \Delta g_{b'}^{(2)} \tag{8.A.14}$$

$$\begin{aligned} k_{\mathrm{T}_0\mathrm{T}_\pm}^{(\mathrm{g-aniso/D})} = k_{\mathrm{T}_\pm\mathrm{T}_0}^{(\mathrm{g-aniso/D})} &= \frac{1}{10\hbar^2} \sum_j \frac{\gamma_{\mathrm{T}_0\mathrm{T}_\pm} + 1/\tau_{\mathrm{R},j}}{(\gamma_{\mathrm{T}_0\mathrm{T}_\pm} + 1/\tau_{\mathrm{R},j})^2 + (\epsilon_{\mathrm{T}_0} - \epsilon_{\mathrm{T}_\pm})^2} \\ &\times \sum_{b,b'} h_{j,b} h_{j,b'} (D_b^{(2)*} \mp 2\bar{g}_b^{(2)*} \mu_\mathrm{B} B)(D_{b'}^{(2)} \mp 2\bar{g}_{b'}^{(2)} \mu_\mathrm{B} B) \end{aligned} \tag{8.A.15}$$

$$k_{\mathrm{T}_\mp\mathrm{T}_\pm}^{(\mathrm{g-aniso/D})} = k_{\mathrm{T}_\pm\mathrm{T}_\mp}^{(\mathrm{g-aniso/D})} = \frac{1}{10\hbar^2} \sum_j \frac{\gamma_{\mathrm{ST}_\pm} + 1/\tau_{\mathrm{R},j}}{(\gamma_{\mathrm{ST}_\pm} + 1/\tau_{\mathrm{R},j})^2 + (\epsilon_\mathrm{S} - \epsilon_{\mathrm{T}_\pm})^2} \sum_{b,b'} h_{j,b} h_{j,b'} D_b^{(2)*} D_{b'}^{(2)}, \tag{8.A.16}$$

in which $\Delta g_b^{(2)} = g_{2,b}^{(2)} - g_{1,b}^{(2)}$ and $2\bar{g}_b^{(2)} = g_{1,b}^{(2)} + g_{2,b}^{(2)}$.

8.B PTZ$^{\bullet+}$–Ph$_n$–PDI$^{\bullet-}$ simulation parameters

The isotropic and anisotropic hyperfine coupling parameters used in the simulations are listed in the following two tables. The isotropic hyperfine couplings are taken from EPR data on the free radicals and the anisotropic couplings are taken from calculations on the free radicals in geometries optimised using Gaussian09[197] with DFT at the B3LYP/6-31G(d,p) level of theory, with the g tensors and anisotropic hyperfine couplings obtained at the same level of theory. The listed hyperfine tensors assume the torsional angle between the PTZ and PDI groups is 0, but because a symmetric diffusion model is used where the axis separating the two radicals is taken as the symmetry axis, and because the individual radical contributions to the KME2 rate constants are independent of each other, and invariant to rotations of the tensors about the molecular z axis, we do not need to recalculate these tensors for each molecule. Here I use the same numbering scheme for the nuclei as in Ref. [198].

Nucleus	a_{iso}/mT	A_{xx}^{aniso}/mT	A_{yy}^{aniso}/mT	A_{zz}^{aniso}/mT	A_{xy}^{aniso}/mT	A_{xz}^{aniso}/mT	A_{yz}^{aniso}/mT
H1	-0.113000	-0.611434	0.006725	0.604709	0.026454	0.012482	0.650482
H2	-0.113000	-0.653329	0.006834	0.646495	0.028183	-0.013260	-0.695966
H3	-0.050000	-0.368356	0.181504	0.186852	0.019238	0.025176	0.649996
H4	-0.050000	-0.394314	0.194396	0.199918	0.020545	-0.026807	-0.694966
H5	-0.249000	-0.288490	0.934089	-0.645599	0.055556	-0.056699	-1.341588
H6	-0.249000	-0.288471	0.933899	-0.645428	0.055776	0.056722	1.341687
H7	0.050000	-0.711878	0.912091	-0.200212	0.071227	-0.021916	-0.474382
H8	0.050000	-0.711871	0.911996	-0.200125	0.071308	0.022027	0.474481
N1	0.634000	9.847802	-4.950802	-4.897000	-0.623203	0.000000	0.000000

Table 8.B.1: Hyperfine coupling parameters for the $PTZ^{\bullet+}$ radical. Isotropic components, $a_{\mathrm{iso}} = (A_{xx} + A_{yy} + A_{zz})/3$, and anisotropic components, $A_{\alpha\beta}^{\mathrm{aniso}} = A_{\alpha\beta} - \delta_{\alpha\beta} a_{\mathrm{iso}}$, in the molecular frame. mT is used as a short-hand for $g_{\mathrm{e}}\mu_{\mathrm{B}}$ mT.

Nucleus	a_{iso}/mT	A_{xx}^{aniso}/mT	A_{yy}^{aniso}/mT	A_{zz}^{aniso}/mT	A_{xy}^{aniso}/mT	A_{xz}^{aniso}/mT	A_{yz}^{aniso}/mT
H1	0.078500	-0.429000	0.118088	0.310912	0.000000	0.000000	-0.326566
H2	0.078500	-0.429000	0.118127	0.310873	0.000000	0.000000	-0.326577
H3	-0.172000	-0.363000	0.313451	0.049549	0.000000	0.000000	1.009916
H4	-0.172000	-0.363000	0.313451	0.049549	0.000000	0.000000	1.009916
H5	0.057500	-0.430000	0.219277	0.210723	0.000015	-0.000016	0.629985
H6	0.057500	-0.430000	0.219277	0.210723	-0.000015	0.000016	0.629985
N1	-0.062100	-0.439333	0.213492	0.225841	0.000000	0.000000	-0.003297
N2	-0.062100	-0.439333	0.213492	0.225841	0.000000	0.000000	-0.003297

Table 8.B.2: Hyperfine coupling parameters for the $PDI^{\bullet-}$ radical. Isotropic components, $a_{\mathrm{iso}} = (A_{xx} + A_{yy} + A_{zz})/3$, and anisotropic components, $A_{\alpha\beta}^{\mathrm{aniso}} = A_{\alpha\beta} - \delta_{\alpha\beta} a_{\mathrm{iso}}$, in the molecular frame. mT is used as a short-hand for $g_{\mathrm{e}}\mu_{\mathrm{B}}$ mT.

The experimental $\Delta g = 0.0025$ was used in the simulations where it was included (and not rescaled), whilst for simplicity the isotropic g value was taken to be the free electron g value. The dipolar coupling estimated based on treating the radical spins as point dipoles separated by a vector of length R, which for n=2-5 is estimated as 17.2 Å, 21.5 Å, 25.8 Å and 30.1 Å, from the equilibrium geometries of the radicals calculated with DFT at the ωB97XD/6-31G(d) level of theory. The g tensors were obtained from the same calculations as the hyperfine tensors. Because the **D** tensor is assumed to be diagonal in the molecular frame, with $D_{xx} = D_{yy} = -D_{zz}/2 = D$, we need only know the g tensors in the molecular frame where the torsion angle is zero, which are given in Table 8.B.2.

The rotational diffusion coefficients were estimated based on treating the molecule as a prolate spheroid for which the rotational diffusion constants for rotation about the symmetry

Radical	g_{xx}^{aniso}	g_{yy}^{aniso}	g_{zz}^{aniso}	g_{xy}^{aniso}	g_{xz}^{aniso}	g_{yz}^{aniso}
$PDI^{\bullet-}$	0.0012	0.0005	-0.0017	-0.0001	0.0000	0.0000
$PTZ^{\bullet+}$	0.0027	0.0011	-0.0038	0.0000	0.0000	0.0000

Table 8.B.3: PDI and PTZ radical g tensors. Anisotropic components, $g_{\alpha\beta}^{\text{aniso}} = g_{\alpha\beta} - \delta_{\alpha\beta} g_{\text{iso}}$, in the molecular frame, assuming a torsional angle of 0.

axis $D_{\parallel}$ and about the axes orthogonal to the symmetry axis $D_{\perp}$ are

$$D_{\parallel} = \frac{3}{4}\frac{2p^2 - S}{p^2 - 1}D \tag{8.B.1}$$

$$D_{\perp} = \frac{3}{4}\frac{2 - (2 - (1/p)^2)S}{(1/p)^2 - p^2}D, \tag{8.B.2}$$

where $p = c/a > 1$, where a is the short semi-axis and c is the long semi-axis, $S = 2\text{atanh}(\xi)/\xi$ and $\xi = \sqrt{|p^2 - 1|}/p$. D is the diffusion constant for a sphere of the same volume as the spheroid predicted by the Stokes-Einstein equation, so $D = k_{\text{B}}T/(6\eta V)$ where $V = 4\pi a^2 c/3$.[213] This assumes the solvent can be treated as a continuum fluid with stick boundary conditions, at the molecular level, and furthermore this assumes the molecule is ellipsoidal. Because these approximations break down, and because of the role of internal torsional motions about the symmetry axis of the molecule, $D_{\parallel}$ is rescaled in the model fitting. In each case a scaling of $D_{\parallel}$ by a factor of about 10 is found. The unadjusted $D_{\parallel}$ values are 0.3136, 0.2875, 0.2653 and 0.2304 ns^{-1} for n=2–5.

Here I also give the set of rate constants, $2J$ values and additional model parameters for the $PTZ^{\bullet+}$–Ph_n–$PDI^{\bullet-}$ radical pair models with the isotropic coupling model and the extended model including relaxation effects. Fitting of the free parameters in the KME2 models is done by performing a least squares fit to the experimental MFE data, subject to the constraint that the lifetime is close to the experimental lifetime. In the isotropic coupling model the lifetime is constrained to be within 1 ns of the experimental value and in the anisotropic coupling model the lifetime is constrained to be within 5% of the experimental value. For n=2-5 the experimental lifetimes are 21 ns, 330 ns, 217 ns and 121 ns.[26]

Model	k_S^r/ns^{-1}	k_T^r/ns^{-1}	$2J/g_e\mu_B$ mT	Φ_0
n=2 (original)	0.04736	27.5	−170	0.0416
n=3 (original)	0.002160	3.8	−31	0.525
n=3 (KME2 fit)	0.002013	4.517	−31	0.628
n=4 (original)	0.002449	0.35	−6.4	–
n=4 (KME2 fit)	0.001584	0.5322	−6.4	–
n=5 (original)	0.002887	0.060	−1.75	–
n=5 (KME2 fit)	0.0009665	0.07533	−1.47	–

Table 8.B.4: Rate constants, scalar coupling parameters and background corrections used in the simulations of the $PTZ^{\bullet+}$–Ph_n–$PDI^{\bullet-}$ radical pairs including only isotropic interactions. Original parameters are taken from Ref. [198].

n	k_S^r/ns^{-1}	k_T^r/ns^{-1}	$2J/g_e\mu_B$ mT	$D_\parallel/ns^{-1}$	$D_\perp/ns^{-1}$	Φ_0	k_{STD}/ns^{-1}
2	0.0496	38.5	-170.0	3.09	0.126	0.0315	–
2 ($\Delta g/2J$)	0.0497	24.0	-161.9	3.04	0.126	0.0626	–
3	0.00154	2.22	-31.0	2.52	0.100	0.562	–
4	0.000111	0.118	-6.4	3.08	0.0814	–	0.145
5	0.000120	0.0258	-1.5	2.64	0.0562	–	0.0207

Table 8.B.5: KME2 simulation parameters with the model of the $PTZ^{\bullet+}$–Ph_n–$PDI^{\bullet-}$ radical pairs including spin relaxation effects. $\Delta g/2J$ indicates the n=2 model where these parameters are rescaled.

9 Conclusions

Spin chemistry, and in particular radical pair reactions, have been of significant interest in recent years because the wide range of technological applications and biological processes in which spin chemical effects manifest. The work presented here has aimed to provide a more detailed understanding of these effects, in particular the theory of radical pair electron transfer reactions, and how to model these reactions accurately and efficiently. To conclude this thesis I will summarise the main results, and then reflect on some possible future directions for this work.

9.1 Summary

In this thesis I have described how to apply quantum master equation techniques to a range of problems in spin chemistry. This approach has given new insights into the theory of radical pair processes, as well as provided new practical tools for efficiently simulating spin chemical effects, which I will summarise below.

9.1.1 Theory

For some years there has been debate around the role of quantum measurement theory in radical pair reactions,[33,35,36,109] with a plethora of quantum measurement theory based master equations for radical pair reactions being proposed.[35,36,38] The only experiment to date to directly test which master equation provides a correct description of the radical pair spin dynamics confirmed the validity of the "traditional" Haberkorn master equation.[109] The

work in chapters 3, 4 and 5 aimed to provide a theoretical foundation to this experimental result. Using the tools of quantum master equations, in chapter 3 I derived a general radical pair master equation, starting from the well-established theory of electron transfer reactions.[123,124,126,127] This confirms the validity of the original Haberkorn master equation, with some additional corrections, and broadly refutes the quantum measurement approaches. In chapter 4 I used a set of classical approximations to obtain approximate validity criteria for the Haberkorn master equation, and the corrections to this, which can be expressed in terms of parameters in the Marcus-Hush theory[126,127] and Zusman theory[145] expressions for electron transfer rates. In chapter 5 I confirmed this radical pair master equation theory in numerical tests using an exactly soluble model of a radical pair reaction for comparison.

In chapter 6 I discussed how to extend the radical pair master equation to include spin relaxation effects through the Stochastic Liouville equation approach, and also how to use perturbative master equation techniques to obtain an efficient method for finding an approximate solution to the SLE. Here I demonstrated that the Nakajima-Zwanzig master equation yields a more accurate approximate solution than the commonly used Bloch-Redfield-Wangsness[60,61] theory for a range of model problems. The resulting master equation is still very difficult to solve numerically for realistic models of radical pair reactions, due to the exponential scaling of the Liouville space dimensionality with the number of coupled nuclear spins. To circumvent this problem, in chapter 7 the Nakajima-Zwanzig relaxation master equation was combined with the Schulten-Wolynes semiclassical approximation[187] to give an efficient and accurate method for modelling real radical pair reactions.

Although radical pair reactions are normally understood using quantum master equations for the spin density operator, recent experiments have clearly demonstrated that simple kinetic master equations can often provide a very good description of these reactions.[51] These experiments motivated the work presented in chapter 8, where the Nakajima-Zwanzig approach was employed to derive a perturbative kinetic master equation for describing radical pair reactions. This gives physical insight into the empirical kinetic master equations that have been used until now, and also provides a simple and computationally efficient tool for modelling radical pair reactions.

9.1.2 Applications

In order to demonstrate the utility of master equation approaches in describing radical pair reactions, I have applied these techniques to study two sets of donor-bridge-acceptor molecules. In chapter 7 I applied the Schulten-Wolynes/Nakajima-Zwanzig master equation to elucidate the role of different relaxation mechanisms in $DMJ^{\bullet+}-An-Ph_n-NDI^{\bullet-}$ spin dynamics.[67] In particular it was found that rotational Brownian motion and modulation of scalar coupling play significant roles in the spin dynamics of these radical pairs, and that the correlation times of these motions are sufficiently long that simple phenomenological spin relaxation models would not be able to quantitatively capture the observed magnetic field effects. From these simulations, evidence for an additional field-independent mechanism of triplet product formation is also found, and the results of these simulations and available experimental data point towards a small fraction of radical pairs being formed initially in the triplet state.

The second set of radical pairs studied in this work were $PTZ^{\bullet+}-Ph_n-PDI^{\bullet-}$ radical pairs.[26] I demonstrated that the second order perturbative kinetic master equation can be used to accurately model the magnetic field effects on various observables of these radical pair reactions provided the electron spin coupling is strong and the radical pair lifetime is sufficiently short. I then applied the kinetic master equation to include relaxation effects and showed that rotational Brownian motion can have a big influence on observed magnetic field effects. In these models of $PTZ^{\bullet+}-Ph_n-PDI^{\bullet-}$ radical pairs, the spin selective reaction rate constants have to be treated as free parameters fitted to the experimental data, and including relaxation processes significantly alters the fitted values of k_S. Interestingly, these results suggest that superexchange mediated electron tunnelling operates at larger inter-radical separations in the singlet-selective electron transfer than previously thought.[198]

9.2 Directions for further research

With more experiments probing spin chemical effects in radical pairs being performed,[25,48,50,214–216] and with interest in the radical pair mechanism as a potential physical basis for the magnetic compass sense of birds,[21,87,90,217,218] there are many avenues open for potential further

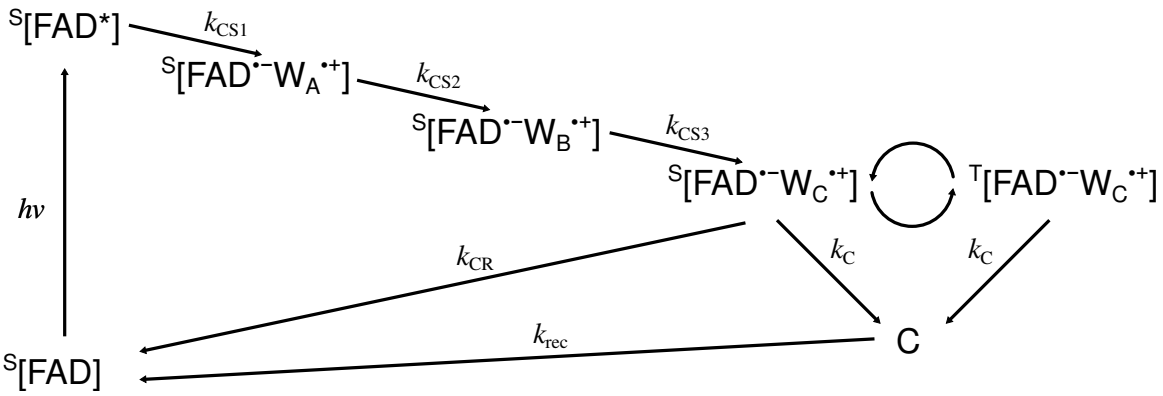

Figure 9.1: A simplified version of the proposed cryptochrome FAD Trp-triad reaction scheme which forms the basis of the radical pair hypothesis for avian magnetoreception. Here W denotes tryptophan.

research using master equation techniques to explore spin chemistry.

9.2.1 Spin coherence in cryptochrome

The spin selective charge recombination reaction of $FAD^{\bullet-}$ and $Trp^{\bullet+}$ radicals in cryptochrome proteins is currently of central interest in the quest to understand avian magnetoreception.[21,93] It has been proposed that magnetic field dependent interconversion of singlet and triplet radical pairs, and spin selective charge recombination of the radical pair, leads to an orientation dependent formation of some signalling state C, which would form the basis of the avian magnetic compass sense.[21,93] The radical pair is known to form after photo-excitation of FAD, which initiates a sequence of charge separation steps along a triad (or possibly tetrad) of tryptophan residues in the protein. The proposed reaction scheme of the FAD-Trp triad in cryptochrome is summarised in Fig. 9.1.[21]

The sensitivity of the chemical compass relies on many factors, but key factors are the lifetime of spin coherences in the radical pair state, and the strength of the scalar coupling between the radical electron spins.[219,220] The theory outlined in chapter 3 can be extended to more complex reaction schemes, involving multiple electron transfer states, to study this type of radical pair reaction scheme. Furthermore, using the models described in chapter 4 for the electron transfer processes, parametrised for the FAD-Trp triad system, it may be possible to predict the lifetimes and scalar coupling strengths in the FAD-Trp radical pair states. This type of study may provide insight into the results of previous magnetic

field effect experiments on cryptochromes.[30] This approach could also reveal interesting details about the cryptochrome electron transfers that are difficult to probe experimentally, for example one could determine whether the electron transfer reactions are dominated by hopping or superexchange mediated tunnelling processes.[124]

9.2.2 Signalling processes in cryptochrome

Most theoretical and computational studies of the cryptochrome radical pair have only examined magnetic field effects on the singlet yield of the radical pair reaction, with various models for the radical pair spin dynamics.[21,87,89,90,98,220] These studies have mostly ignored the kinetics of the photoexcitation process and the recycling of the hypothetical signalling state "C" back to the ground state of the cryptochrome, but these processes will all necessarily have some effect on the sensitivity of the compass. Quantum master equations provide a useful technique for simplifying the coupled equations of motion for the spin density operators for all of the different states in Fig. 9.1, which can give bounds on the sensitivity of the proposed mechanism. Quantum master equation techniques would also enable us to numerically solve these equations of motion for the observables of interest in a computationally efficient way, which would allow us to investigate the recycling and photoexcitation kinetics with realistic models of the radical pair spin interactions.

9.2.3 Extending the kinetic master equations

Recent experiments by Mims *et al.*[48] on donor-bridge-acceptor systems with $k_{\mathrm{T}} > k_{\mathrm{S}}$ have demonstrated that the validity conditions for the kinetic master equations breakdown in certain radical pairs at the $B = 2J/g_{\mathrm{e}}\mu_{\mathrm{B}}$ resonance, and in this case bi-exponential decay kinetics of the radical pair state are observed. This bi-exponential decay has been explained in terms of the "orphan state effect," in which a fraction of the radical pair nuclear spin states cannot couple S and T_{+} states, by the isotropic hyperfine coupling interaction.[48] This leads to a long-lived fraction of singlet radical pair states on resonance, which cannot convert to more reactive triplet states. This effect can obviously never be captured by a simple kinetic master equation of the form described in chapter 8. However, it may be possible to extend the kinetic master equation to capture the effect, for example by explicitly including

nuclear spin states in the kinetic model. Similarly the low magnetic field effect[41,42] cannot be captured by the second order kinetic master equation, but by evaluating the higher order contributions to the rate constants, it may be possible to describe these low field effects with simple kinetic master equations.

Recently there have been several experiments using chemically induced dynamic nuclear polarisation (CIDNP) to probe radical pair intermediates,[50] for example in photosynthetic reaction centres.[14] These experiments use the fact that the nuclear spins in radical pairs are polarised by the hyperfine interaction with the electron spins in the radical pair state, and this polarisation is detectable in products by NMR spectroscopy. The CIDNP signal P_{A} of a given nucleus A is the net spin polarisation generated by the radical pair spin dynamics. It is given by

$$P_{\mathrm{A}} = \int_0^\infty \mathrm{d}t\, \mathrm{Tr}\big[\hat{I}_{\mathrm{A},z}(k_{\mathrm{S}}\hat{P}_{\mathrm{S}} + k_{\mathrm{T}}\hat{P}_{\mathrm{T}})\hat{\rho}(t)\big], \tag{9.1}$$

so this is not directly obtainable from the kinetic master equation. This is because the observables of interest, $\hat{I}_{\mathrm{A},z}\hat{P}_{\mathrm{S}}$ and $\hat{I}_{\mathrm{A},z}\hat{P}_{\mathrm{T}}$, are contained in $\mathcal{Q}\hat{\rho}(t)$ and not $\mathcal{P}\hat{\rho}(t)$ as defined in deriving the KME. However it is possible to reconstruct $\mathcal{Q}\hat{\rho}(t)$ from $\mathcal{P}\hat{\rho}(t)$ using Eq. (2.49), or a perturbative expansion of this. This would enable simulations of CIDNP experiments using computationally efficient kinetic master equation techniques.

9.3 Final remarks

In this thesis I have aimed to describe how quantum master equation techniques can be applied to solve a range of problems in spin chemistry. Not only do master equations offer a rigorous route to a theoretical framework for understanding spin chemical phenomena, but they also provide a valuable tool for simulating experimental observables, and thereby gaining new insights into spin chemical effects in real systems. It is my belief that there is much more to gain from the application of quantum master equations in spin chemistry, and I hope that this work will open to door to further developments in this direction.

References

[1] L. P. Lindoy, T. P. Fay, and D. E. Manolopoulos, "Quantum mechanical spin dynamics of a molecular magnetoreceptor", J. Chem. Phys. **152**, 164107 (2020).

[2] T. P. Fay, L. P. Lindoy, and D. E. Manolopoulos, "Spin relaxation in radical pairs from the stochastic Schrödinger equation", submitted.

[3] U. E. Steiner and T. Ulrich, "Magnetic Field Effects in Chemical Kinetics and Related Phenomena", Chem. Rev. **89**, 51 (1989).

[4] K. A. McLauchlan and U. E. Steiner, "Invited article: The spin-correlated radical pair as a reaction intermediate", Mol. Phys. **73**, 241 (1991).

[5] B. Brocklehurst, "Magnetic fields and radical reactions: recent developments and their role in nature.", Chem. Soc. Rev. **31**, 301 (2002).

[6] C. R. Timmel and K. B. Henbest, "A study of spin chemistry in weak magnetic fields", Philos. Trans. R. Soc. A Math. Phys. Eng. Sci. **362**, 2573 (2004).

[7] C. T. Rodgers, "Magnetic field effects in chemical systems", Pure Appl. Chem. **81**, 19 (2009).

[8] P. J. Hore, K. L. Ivanov, and M. R. Wasielewski, "Spin chemistry", J. Chem. Phys. **152**, 120401 (2020).

[9] M. R. Wasielewski, "Energy, charge, and spin transport in molecules and self-assembled nanostructures inspired by photosynthesis", J. Org. Chem. **71**, 5051 (2006).

[10] Y. Wu, J. Zhou, J. N. Nelson, R. M. Young, M. D. Krzyaniak, and M. R. Wasielewski, "Covalent Radical Pairs as Spin Qubits: Influence of Rapid Electron Motion between Two Equivalent Sites on Spin Coherence", J. Am. Chem. Soc. **140**, 13011 (2018).

[11] J. N. Nelson, J. Zhang, J. Zhou, B. K. Rugg, M. D. Krzyaniak, and M. R. Wasielewski, "CNOT gate operation on a photogenerated molecular electron spin-qubit pair", J. Chem. Phys. **152**, 014503 (2020).

[12] R. Bittl and S. Weber, "Transient radical pairs studied by time-resolved EPR", Biochim. Biophys. Acta - Bioenerg. **1707**, 117 (2005).

[13] M. Volk, T. Häberle, R. Feick, A. Ogrodnik, and M. E. Michel-Beyerle, "What can be learned from the singlet-triplet splitting of the radical pair P+H- in the photosynthetic reaction center? Conclusions from electric field effects on the P+H- recombination dynamics", J. Phys. Chem. **97**, 9831 (1993).

[14] S. Paul, U. Roy, M. Böckers, J. Neugebauer, A. Alia, and J. Matysik, "15 N photo-CIDNP MAS NMR analysis of a bacterial photosynthetic reaction center of Rhodobacter sphaeroides wildtype", J. Chem. Phys. **151**, 195101 (2019).

[15] A. Angerhofer and R. Bittl, "Radicals and Radical Pairs in Photosynthesis", Photochem. Photobiol. **63**, 11 (1996).

[16] T. Cardona, A. Sedoud, N. Cox, and A. W. Rutherford, "Charge separation in Photosystem II: A comparative and evolutionary overview", Biochim. Biophys. Acta - Bioenerg. **1817**, 26 (2012).

[17] A. Marais, I. Sinayskiy, F. Petruccione, and R. Van Grondelle, "A quantum protective mechanism in photosynthesis", Sci. Rep. **5**, 8720 (2015).

[18] S. Prakash, Alia, P. Gast, H. J. De Groot, G. Jeschke, and J. Matysik, "Magnetic field dependence of photo-CIDNP MAS NMR on photosynthetic reaction centers of Rhodobacter sphaeroides WT", J. Am. Chem. Soc. **127**, 14290 (2005).

[19] J. Matysik, A. Diller, E. Roy, and A. Alia, "The solid-state photo-CIDNP effect", Photosynth. Res. **102**, 427 (2009).

[20] A. Alia, F. Buda, H. J. de Groot, and J. Matysik, "Solid-State NMR of Nanomachines Involved in Photosynthetic Energy Conversion", Annu. Rev. Biophys. **42**, 675 (2013).

[21] C. T. Rodgers and P. J. Hore, "Chemical magnetoreception in birds: The radical pair mechanism", Proc. Natl. Acad. Sci. U. S. A. **106**, 353 (2009).

[22] C. A. Dodson, P. J. Hore, and M. I. Wallace, "A radical sense of direction: Signalling and mechanism in cryptochrome magnetoreception", Trends Biochem. Sci. **38**, 435 (2013).

[23] H. G. Hiscock, S. Worster, D. R. Kattnig, C. Steers, Y. Jin, D. E. Manolopoulos, H. Mouritsen, and P. J. Hore, "The quantum needle of the avian magnetic compass", Proc. Natl. Acad. Sci. **113**, 4634 (2016).

[24] T. P. Fay, L. P. Lindoy, D. E. Manolopoulos, and P. J. Hore, "How quantum is radical pair magnetoreception?", Faraday Discuss. **221**, 77 (2019).

[25] C. Kerpal, S. Richert, J. G. Storey, S. Pillai, P. A. Liddell, D. Gust, S. R. Mackenzie, P. J. Hore, and C. R. Timmel, "Chemical compass behaviour at microtesla magnetic fields strengthens the radical pair hypothesis of avian magnetoreception", Nat. Commun. **10**, 3707 (2019).

[26] E. A. Weiss, M. J. Ahrens, L. E. Sinks, A. V. Gusev, M. A. Ratner, and M. R. Wasielewski, "Making a Molecular Wire: Charge and Spin Transport through para-Phenylene Oligomers", J. Am. Chem. Soc. **126**, 5577 (2004).

[27] K. Maeda, K. B. Henbest, F. Cintolesi, I. Kuprov, C. T. Rodgers, P. A. Liddell, D. Gust, C. R. Timmel, and P. J. Hore, "Chemical compass model of avian magnetoreception", Nature **453**, 387 (2008).

[28] K. Maeda, A. J. Robinson, K. B. Henbest, H. J. Hogben, T. Biskup, M. Ahmad, E. Schleicher, S. Weber, C. R. Timmel, and P. J. Hore, "Magnetically sensitive light-induced reactions in cryptochrome are consistent with its proposed role as a magnetoreceptor", Proc. Natl. Acad. Sci. **109**, 4774 (2012).

[29] E. W. Evans, D. R. Kattnig, K. B. Henbest, P. J. Hore, S. R. Mackenzie, and C. R. Timmel, "Sub-millitesla magnetic field effects on the recombination reaction of flavin and ascorbic acid radicals", J. Chem. Phys. **145**, 085101 (2016).

[30] D. M. Sheppard, J. Li, K. B. Henbest, S. R. Neil, K. Maeda, J. Storey, E. Schleicher, T. Biskup, R. Rodriguez, S. Weber, P. J. Hore, C. R. Timmel, and S. R. MacKenzie, "Millitesla magnetic field effects on the photocycle of an animal cryptochrome", Sci. Rep. **7**, 42228 (2017).

[31] S. Riese, J. S. Brand, D. Mims, M. Holzapfel, N. N. Lukzen, U. E. Steiner, and C. Lambert, "Giant magnetic field effects in donor–acceptor triads: On the charge separation and recombination dynamics in triarylamine–naphthalenediimide triads with bis-diyprrinato-palladium(II), porphodimethenato-palladium(II), and palladium(II)–porphyrin photosens", J. Chem. Phys. **153**, 054306 (2020).

[32] R. Haberkorn, "Density matrix description of spin-selective radical pair reactions", Mol. Phys. **32**, 1491 (1976).

[33] K. L. Ivanov, M. V. Petrova, N. N. Lukzen, and K. Maeda, "Consistent treatment of spin-selective recombination of a radical pair confirms the haberkorn approach", J. Phys. Chem. A **114**, 9447 (2010).

[34] T. P. Fay, L. P. Lindoy, and D. E. Manolopoulos, "Spin-selective electron transfer reactions of radical pairs: Beyond the Haberkorn master equation", J. Chem. Phys. **149**, 064107 (2018).

[35] I. K. Kominis, "Quantum Zeno effect explains magnetic-sensitive radical-ion-pair reactions", Phys. Rev. E - Stat. Nonlinear, Soft Matter Phys. **80**, 056115 (2009).

[36] J. Jones and P. Hore, "Spin-selective reactions of radical pairs act as quantum measurements", Chem. Phys. Lett. **488**, 90 (2010).

[37] J. A. Jones, K. Maeda, and P. J. Hore, "Reaction operators for spin-selective chemical reactions of radical pairs", Chem. Phys. Lett. **507**, 269 (2011).

[38] M. Kritsotakis and I. K. Kominis, "Retrodictive derivation of the radical-ion-pair master equation and Monte Carlo simulation with single-molecule quantum trajectories", Phys. Rev. E **90**, 042719 (2014).

[39] I. V. Khudyakov, Y. A. Serebrennikov, and N. J. Turro, "Spin-orbit coupling in free-radical reactions: on the way to heavy elements", Chem. Rev. **93**, 537 (1993).

[40] F. Neese, "Quantum chemistry and EPR parameters", eMagRes **6**, 1 (2017).

[41] C. R. Timmel, U. Till, B. Brocklehurst, K. A. McLauchlan, and P. J. Hore, "Effects of weak magnetic fields on free radical recombination reactions", Mol. Phys. **95**, 71 (1998).

[42] A. M. Lewis, T. P. Fay, D. E. Manolopoulos, C. Kerpal, S. Richert, and C. R. Timmel, "On the low magnetic field effect in radical pair reactions", J. Chem. Phys. **149**, 034103 (2018).

[43] M. P. Nicholas, E. Eryilmaz, F. Ferrage, D. Cowburn, and R. Ghose, "Nuclear spin relaxation in isotropic and anisotropic media", Prog. Nucl. Magn. Reson. Spectrosc. **57**, 111 (2010).

[44] S. Worster, D. R. Kattnig, and P. J. Hore, "Spin relaxation of radicals in cryptochrome and its role in avian magnetoreception", J. Chem. Phys. **145**, 035104 (2016).

[45] D. R. Kattnig, J. K. Sowa, I. A. Solov'Yov, and P. J. Hore, "Electron spin relaxation can enhance the performance of a cryptochrome-based magnetic compass sensor", New J. Phys. **18**, 063007 (2016).

[46] D. R. Kattnig, I. A. Solov'Yov, and P. J. Hore, "Electron spin relaxation in cryptochrome-based magnetoreception", Phys. Chem. Chem. Phys. **18**, 12443 (2016).

[47] M. S. Lazorski, I. Schapiro, R. S. Gaddie, A. P. Lehnig, M. Atanasov, F. Neese, U. E. Steiner, and C. M. Elliott, "Spin-chemical effects on intramolecular photoinduced charge transfer reactions in bisphenanthroline copper(i)-viologen dyad assemblies", Chem. Sci. **11**, 5511 (2020).

[48] D. Mims, A. Schmiedel, M. Holzapfel, N. N. Lukzen, C. Lambert, and U. E. Steiner, "Magnetic field effects in rigidly linked D-A dyads: Extreme on-resonance quantum coherence effect on charge recombination", J. Chem. Phys. **151**, 244308 (2019).

[49] T. P. Fay, L. P. Lindoy, and D. E. Manolopoulos, "Electron spin relaxation in radical pairs: Beyond the Redfield approximation", J. Chem. Phys. **151**, 154117 (2019).

[50] I. Zhukov, N. Fishman, A. Kiryutin, N. Lukzen, M. Panov, U. Steiner, H.-M. Vieth, J. Schäfer, C. Lambert, and A. Yurkovskaya, "Positive electronic exchange interaction and predominance of minor triplet channel in CIDNP formation in short lived charge separated states of D-X-A dyads", J. Chem. Phys. **152**, 014203 (2020).

[51] U. E. Steiner, J. Schäfer, N. N. Lukzen, and C. Lambert, "J -Resonance Line Shape of Magnetic Field-Affected Reaction Yield Spectrum from Charge Recombination in a Linked Donor-Acceptor Dyad", J. Phys. Chem. C **122**, 11701 (2018).

[52] J. E. Lawrence, A. M. Lewis, D. E. Manolopoulos, and P. J. Hore, "Magneto-electroluminescence in organic light-emitting diodes", J. Chem. Phys. **144**, 214109 (2016).

[53] A. M. Lewis, D. E. Manolopoulos, and P. J. Hore, "Asymmetric recombination and electron spin relaxation in the semiclassical theory of radical pair reactions", J. Chem. Phys. **141**, 044111 (2014).

[54] H.-P. Breuer and F. Petruccione, *The Theory of Open Quantum Systems* (Oxford University Press, 2007).

[55] V. May and O. Kühn, *Charge and Energy Transfer Dynamics in Molecular Systems* (Wiley-VCH Verlag GmbH & Co. KGaA, 2000).

[56] R. Zwanzig, *Nonequilibrium Statistical Mechanics* (Oxford University Press, 2001).

[57] S. Nakajima, "On Quantum Theory of Transport Phenomena", Prog. Theor. Phys. **20**, 948 (1958).

[58] R. Zwanzig, "Ensemble method in the theory of irreversibility", J. Chem. Phys. **33**, 1338 (1960).

[59] H. Mori, "Transport, Collective Motion, and Brownian Motion", Prog. Theor. Phys. **33**, 423 (1965).

[60] A. Redfield, in *Adv. magn. opt. reson.* Vol. 1, C (1965), pp. 1–32.

[61] R. K. Wangsness and F. Bloch, "The Dynamical Theory of Nuclear Induction", Phys. Rev. **89**, 728 (1953).

[62] M. Goldman, "Advances in magnetic resonance: Formal theory of spin-lattice relaxation", J. Magn. Reson. **149**, 160 (2001).

[63] H. P. Breuer, B. Kappler, and F. Petruccione, "The Time-Convolutionless Projection Operator Technique in the Quantum Theory of Dissipation and Decoherence", Ann. Phys. (N. Y). **291**, 36 (2001).

[64] F. Shibata, Y. Takahashi, and N. Hashitsume, "A generalized stochastic liouville equation. Non-Markovian versus memoryless master equations", J. Stat. Phys. **17**, 171 (1977).

[65] S. Chaturvedi and F. Shibata, "Time-convolutionless projection operator formalism for elimination of fast variables. Applications to Brownian motion", Zeitschrift für Phys. B Condens. Matter Quanta **35**, 297 (1979).

[66] T. Miura, A. M. Scott, and M. R. Wasielewski, "Electron spin dynamics as a controlling factor for spin-selective charge recombination in donor - Bridge - Acceptor molecules", J. Phys. Chem. C **114**, 20370 (2010).

[67] A. M. Scott, T. Miura, A. B. Ricks, Z. E. X. Dance, E. M. Giacobbe, M. T. Colvin, and M. R. Wasielewski, "Spin-Selective Charge Transport Pathways through p-Oligophenylene-Linked Donor- Bridge- Acceptor Molecules", J Am Chem Soc J. Am. Chem. Soc. **131**, 17655 (2009).

[68] A. M. Scott and M. R. Wasielewski, "Temperature dependence of spin-selective charge transfer pathways in donor-bridge-acceptor molecules with oligomeric fluorenone and p -phenylethynylene bridges", J. Am. Chem. Soc. **133**, 3005 (2011).

[69] Y. Hou, X. Zhang, K. Chen, D. Liu, Z. Wang, Q. Liu, J. Zhao, and A. Barbon, "Charge separation, charge recombination, long-lived charge transfer state formation and intersystem crossing in organic electron donor/acceptor dyads", J. Mater. Chem. C **7**, 12048 (2019).

[70] N. E. Horwitz, B. T. Phelan, J. N. Nelson, C. M. Mauck, M. D. Krzyaniak, and M. R. Wasielewski, "Spin Polarization Transfer from a Photogenerated Radical Ion Pair to a Stable Radical Controlled by Charge Recombination", J. Phys. Chem. A **121**, 4455 (2017).

[71] B. K. Rugg, B. T. Phelan, N. E. Horwitz, R. M. Young, M. D. Krzyaniak, M. A. Ratner, and M. R. Wasielewski, "Spin-Selective Photoreduction of a Stable Radical within a Covalent Donor-Acceptor-Radical Triad", J. Am. Chem. Soc. **139**, 15660 (2017).

[72] B. K. Rugg, M. D. Krzyaniak, B. T. Phelan, M. A. Ratner, R. M. Young, and M. R. Wasielewski, "Photodriven quantum teleportation of an electron spin state in a covalent donor–acceptor–radical system", Nat. Chem. **11**, 981 (2019).

[73] R. Geng, T. T. Daugherty, K. Do, H. M. Luong, and T. D. Nguyen, "A review on organic spintronic materials and devices: I. Magnetic field effect on organic light emitting diodes", J. Sci. Adv. Mater. Devices **1**, 128 (2016).

[74] R. Geng, H. M. Luong, T. T. Daugherty, L. Hornak, and T. D. Nguyen, "A review on organic spintronic materials and devices: II. Magnetoresistance in organic spin valves and spin organic light emitting diodes", J. Sci. Adv. Mater. Devices **1**, 256 (2016).

[75] P. Müller and M. Ahmad, "Light-activated Cryptochrome Reacts with Molecular Oxygen to Form a Flavin–Superoxide Radical Pair Consistent with Magnetoreception", J. Biol. Chem. **286**, 21033 (2011).

[76] R. M. Sherrard, N. Morellini, N. Jourdan, M. El-Esawi, L.-D. Arthaut, C. Niessner, F. Rouyer, A. Klarsfeld, M. Doulazmi, J. Witczak, A. D'Harlingue, J. Mariani, I. Mclure, C. F. Martino, and M. Ahmad, "Low-intensity electromagnetic fields induce human cryptochrome to modulate intracellular reactive oxygen species", PLOS Biol. **16**, edited by D. Keays, e2006229 (2018).

[77] L.-D. Arthaut, N. Jourdan, A. Mteyrek, M. Procopio, M. El-Esawi, A. D'Harlingue, P.-E. Bouchet, J. Witczak, T. Ritz, A. Klarsfeld, S. Birman, R. J. Usselman, U. Hoecker, C. F. Martino, and M. Ahmad, "Blue-light induced accumulation of reactive oxygen species is a consequence of the Drosophila cryptochrome photocycle", PLoS One **12**, edited by I. Solov'yov, e0171836 (2017).

[78] P. Pospíšil, "Production of Reactive Oxygen Species by Photosystem II as a Response to Light and Temperature Stress", Front. Plant Sci. **7**, 1621 (2016).

[79] M. El-Esawi, L.-D. Arthaut, N. Jourdan, A. D'Harlingue, J. Link, C. F. Martino, and M. Ahmad, "Blue-light induced biosynthesis of ROS contributes to the signaling mechanism of Arabidopsis cryptochrome", Sci. Rep. **7**, 13875 (2017).

[80] M. Hammad, M. Albaqami, M. Pooam, E. Kernevez, J. Witczak, T. Ritz, C. Martino, and M. Ahmad, "Cryptochrome mediated magnetic sensitivity in: Arabidopsis occurs independently of light-induced electron transfer to the flavin", Photochem. Photobiol. Sci. **19**, 341 (2020).

[81] A. J. Hoff, "Magnetic field effects on photosynthetic reactions", Q. Rev. Biophys. **14**, 599 (1981).

[82] C. B. Grissom, "Magnetic Field Effects in Biology: A Survey of Possible Mechanisms with Emphasis on Radical-Pair Recombination", Chem. Rev. **95**, 3 (1995).

[83] C. Levy, B. D. Zoltowski, A. R. Jones, A. T. Vaidya, D. Top, J. Widom, M. W. Young, N. S. Scrutton, B. R. Crane, and D. Leys, "Updated structure of Drosophila cryptochrome", Nature **495**, E3 (2013).

[84] R. Wiltschko and W. Wiltschko, "Magnetoreception in birds", J. R. Soc. Interface **16**, 20190295 (2019).

[85] D. R. Kattnig, "Radical-Pair-Based Magnetoreception Amplified by Radical Scavenging: Resilience to Spin Relaxation", J. Phys. Chem. B **121**, 10215 (2017).

[86] D. R. Kattnig and P. J. Hore, "The sensitivity of a radical pair compass magnetoreceptor can be significantly amplified by radical scavengers", Sci. Rep. **7**, 11640 (2017).

[87] T. C. Player and P. J. Hore, "Viability of superoxide-containing radical pairs as magnetoreceptors", J. Chem. Phys. **151**, 225101 (2019).

[88] E. W. Evans, C. A. Dodson, K. Maeda, T. Biskup, C. J. Wedge, and C. R. Timmel, "Magnetic field effects in flavoproteins and related systems", Interface Focus **3**, 20130037 (2013).

[89] N. S. Babcock and D. R. Kattnig, "Electron–Electron Dipolar Interaction Poses a Challenge to the Radical Pair Mechanism of Magnetoreception", J. Phys. Chem. Lett. **11**, 2414 (2020).

[90] C. Atkins, K. Bajpai, J. Rumball, and D. R. Kattnig, "On the optimal relative orientation of radicals in the cryptochrome magnetic compass", J. Chem. Phys. **151**, 065103 (2019).

[91] H. G. Hiscock, H. Mouritsen, D. E. Manolopoulos, and P. Hore, "Disruption of Magnetic Compass Orientation in Migratory Birds by Radiofrequency Electromagnetic Fields", Biophys. J. **113**, 1475 (2017).

[92] W. Wiltschko, U. Munro, H. Ford, and R. Wiltschko, "Red light disrupts magnetic orientation of migratory birds", Nature **364**, 525 (1993).

[93] T. Ritz, S. Adem, and K. Schulten, "A model for photoreceptor-based magnetoreception in birds", Biophys. J. **78**, 707 (2000).

[94] I. Chaves, R. Pokorny, M. Byrdin, N. Hoang, T. Ritz, K. Brettel, L.-O. Essen, G. T. J. van der Horst, A. Batschauer, and M. Ahmad, "The Cryptochromes: Blue Light Photoreceptors in Plants and Animals", Annu. Rev. Plant Biol. **62**, 335 (2011).

[95] T. Biskup, E. Schleicher, A. Okafuji, G. Link, K. Hitomi, E. D. Getzoff, and S. Weber, "Direct Observation of a Photoinduced Radical Pair in a Cryptochrome Blue-Light Photoreceptor", Angew. Chemie Int. Ed. **48**, 404 (2009).

[96] D. Nohr, S. Franz, R. Rodriguez, B. Paulus, L.-O. Essen, S. Weber, and E. Schleicher, "Extended Electron-Transfer in Animal Cryptochromes Mediated by a Tetrad of Aromatic Amino Acids", Biophys. J. **111**, 301 (2016).

[97] M. Liedvogel, K. Maeda, K. Henbest, E. Schleicher, T. Simon, C. R. Timmel, P. J. Hore, and H. Mouritsen, "Chemical Magnetoreception: Bird Cryptochrome 1a Is Excited by Blue Light and Forms Long-Lived Radical-Pairs", PLoS One **2**, edited by H. El-Shemy, e1106 (2007).

[98] A. A. Lee, J. C. S. Lau, H. J. Hogben, T. Biskup, D. R. Kattnig, and P. J. Hore, "Alternative radical pairs for cryptochrome-based magnetoreception", J. R. Soc. Interface **11**, 20131063 (2014).

[99] H. J. Hogben, O. Efimova, N. Wagner-Rundell, C. R. Timmel, and P. Hore, "Possible involvement of superoxide and dioxygen with cryptochrome in avian magnetoreception: Origin of Zeeman resonances observed by in vivo EPR spectroscopy", Chem. Phys. Lett. **480**, 118 (2009).

[100] I. A. Solov'yov and K. Schulten, "Magnetoreception through cryptochrome may involve superoxide", Biophys. J. **96**, 4804 (2009).

[101] J. von Neumann, "Wahrscheinlichkeitstheoretischer Aufbau der Quantenmechanik", in Nachrichten von der gesellschaft der wissenschaften zu göttingen, math. klasse (1927), pp. 245–272.

[102] M. Sparpaglione and S. Mukamel, "Dielectric friction and the transition from adiabatic to nonadiabatic electron transfer. I. Solvation dynamics in Liouville space", J. Chem. Phys. **88**, 3263 (1988).

[103] J. H. Freed, "Generalized Cumulant Expansions and Spin?Relaxation Theory", J. Chem. Phys. **49**, 376 (1968).

[104] G. T. Evans, P. D. Fleming, and R. G. Lawler, "Hydrodynamic theory of CIDEP and CIDNP", J. Chem. Phys. **58**, 2071 (1973).

[105] R. C. Johnson and R. E. Merrifield, "Effects of magnetic fields on the mutual annihilation of triplet excitons in anthracene crystals", Phys. Rev. B **1**, 896 (1970).

[106] P. A. Purtov, "To the theory of Zeno chemical effect: The exactly solvable model", Chem. Phys. Lett. **496**, 335 (2010).

[107] I. K. Kominis, "Comment on 'Spin-selective reactions of radical pairs act as quantum measurements' (Chemical Physics Letters 488 (2010) 90-93)", Chem. Phys. Lett. **508**, 182 (2011).

[108] K. Maeda, C. J. Wedge, J. G. Storey, K. B. Henbest, P. A. Liddell, G. Kodis, D. Gust, P. J. Hore, and C. R. Timmel, "Spin-selective recombination kinetics of a model chemical magnetoreceptor", Chem. Commun. **47**, 6563 (2011).

[109] K. Maeda, P. Liddell, D. Gust, and P. J. Hore, "Spin-selective recombination reactions of radical pairs: Experimental test of validity of reaction operators", J. Chem. Phys. **139**, 234309 (2013).

[110] K. M. Vitalis and I. K. Kominis, “Lamb shift in radical-ion pairs produces a singlet-triplet energy splitting in photosynthetic reaction centers”, Eur. Phys. J. Plus **129**, 187 (2014).

[111] K. Tsampourakis and I. Kominis, “Quantum trajectory tests of radical-pair quantum dynamics in CIDNP measurements of photosynthetic reaction centers”, Chem. Phys. Lett. **640**, 40 (2015).

[112] G. Jeschke, “Comment on "quantum trajectory tests of radical-pair quantum dynamics in CIDNP measurements of photosynthetic reaction centers" [Chem. Phys. Lett. 640 (2015) 40-45]”, Chem. Phys. Lett. **648**, 200 (2016).

[113] I. K. Kominis, “Reply to the comment on "quantum trajectory tests of radical-pair quantum dynamics in CIDNP measurements of photosynthetic reaction centers" by G. Jeschke”, Chem. Phys. Lett. **648**, 204 (2016).

[114] V. Weisskopf and E. Wigner, “Berechnung der natürlichen Linienbreite auf Grund der Diracschen Lichttheorie”, Zeitschrift für Phys. **63**, 54 (1930).

[115] U. Till, C. R. Timmel, B. Brocklehurst, and P. J. Hore, “The influence of very small magnetic fields on radical recombination reactions in the limit of slow recombination”, Chem. Phys. Lett. **298**, 7 (1998).

[116] J. E. Harriman, *Theoretical foundations of electron spin resonance*, Physical chemistry.v. 37 (Academic Press, New York, 1978).

[117] P. Manninen, *Breit-Pauli Hamiltonian and Molecular Magnetic Resonance Properties* (2004).

[118] W. Liu, “Essentials of relativistic quantum chemistry”, J. Chem. Phys. **152**, 180901 (2020).

[119] M. Baer, “Electronic non-adiabatic transitions derivation ofthe general adiabatic-diabatic transformation matrix”, Mol. Phys. **40**, 1011 (1980).

[120] C. A. Mead and D. G. Truhlar, “Conditions for the definition of a strictly diabatic electronic basis for molecular systems”, J. Chem. Phys. **77**, 6090 (1982).

[121] T. Pacher, C. A. Mead, L. S. Cederbaum, and H. Köppel, “Gauge theory and quasidiabatic states in molecular physics”, J. Chem. Phys. **91**, 7057 (1989).

[122] M. Baer and R. Englman, “A study of the diabatic electronic representation within the born-oppenheimer approximation”, Mol. Phys. **75**, 293 (1992).

[123] T. Van Voorhis, T. Kowalczyk, B. Kaduk, L.-P. Wang, C.-L. Cheng, and Q. Wu, “The Diabatic Picture of Electron Transfer, Reaction Barriers, and Molecular Dynamics”, Annu. Rev. Phys. Chem. **61**, 149 (2010).

[124] J. Blumberger, “Recent Advances in the Theory and Molecular Simulation of Biological Electron Transfer Reactions”, Chem. Rev. **115**, 11191 (2015).

[125] D. R. Yarkony, “Diabolical conical intersections”, Rev. Mod. Phys. **68**, 985 (1996).

[126] R. A. Marcus, “On the theory of oxidation-reduction reactions involving electron transfer. I”, J. Chem. Phys. **24**, 966 (1956).

[127] N. S. Hush, "Adiabatic rate processes at electrodes. I. Energy-charge relationships", J. Chem. Phys. **28**, 962 (1958).

[128] P. G. Wolynes, "Imaginary time path integral Monte Carlo route to rate coefficients for nonadiabatic barrier crossing", J. Chem. Phys. **87**, 6559 (1987).

[129] P. W. Anderson, "New approach to the theory of superexchange interactions", Phys. Rev. **115**, 2 (1959).

[130] Y. Kobori, S. Sekiguchi, K. Akiyama, and S. Tero-Kubota, "Chemically Induced Dynamic Electron Polarization Study on the Mechanism of Exchange Interaction in Radical Ion Pairs Generated by Photoinduced Electron Transfer Reactions", J. Phys. Chem. A **103**, 5416 (1999).

[131] E. A. Weiss, M. A. Ratner, and M. R. Wasielewski, "Direct measurement of singlet-triplet splitting within rodlike photogenerated radical ion pairs using magnetic field effects: Estimation of the electronic coupling for charge recombination", J. Phys. Chem. A **107**, 3639 (2003).

[132] E. A. Weiss, M. R. Wasielewski, and M. A. Ratner, "A general formulation for magnetic exchange coupling within long-distance radical ion pairs", J. Chem. Phys. **123**, 064504 (2005).

[133] D. G. Evans and R. D. Coalson, "Incorporating backflow into a relaxation theory treatment of the dynamics of nonequilibrium nonadiabatic transition processes", J. Chem. Phys. **102**, 5658 (1995).

[134] M. Cho and R. J. Silbey, "On the transition from nonadiabatic to adiabatic rate kernel: Schwinger's stationary variational principle and Padé approximation", J. Chem. Phys. **106**, 2654 (1997).

[135] A. A. Golosov and D. R. Reichman, "Reference system master equation approaches to condensed phase charge transfer processes. I. General formulation", J. Chem. Phys. **115**, 9848 (2001).

[136] S. Jang, "Nonadiabatic quantum Liouville and master equations in the adiabatic basis", J. Chem. Phys. **137**, 22A536 (2012).

[137] L. Salem and C. Rowland, "The Electronic Properties of Diradicals", Angew. Chemie Int. Ed. English **11**, 92 (1972).

[138] I. V. Khudyakov, Y. A. Serebrennikov, and N. J. Turro, "Spin-Orbit Coupling in Free-Radical Reactions: On the Way to Heavy Elements", Chem. Rev. **93**, 537 (1993).

[139] Y. Hu and S. Mukamel, "Tunneling versus sequential long-range electron transfer: Analogy with pump-probe spectroscopy", J. Chem. Phys. **91**, 6973 (1989).

[140] H. Weyl, "Quantenmechanik und Gruppentheorie", Zeitschrift für Phys. **46**, 1 (1927).

[141] E. Wigner, "On the quantum correction for thermodynamic equilibrium", Phys. Rev. **40**, 749 (1932).

[142] H. J. Groenewold, "On the principles of elementary quantum mechanics", Physica **12**, 405 (1946).

[143] J. E. Moyal, "Quantum mechanics as a statistical theory", Math. Proc. Cambridge Philos. Soc. **45**, 99 (1949).

[144] J. O. Richardson and M. Thoss, "Non-oscillatory flux correlation functions for efficient nonadiabatic rate theory", J. Chem. Phys. **141**, 074106 (2014).

[145] L. D. Zusman, "Outer-sphere electron transfer in polar solvents", Chem. Phys. **49**, 295 (1980).

[146] L. Hartmann, I. Goychuk, and P. Hänggi, "Controlling electron transfer in strong time-dependent fields: Theory beyond the Golden Rule approximation", J. Chem. Phys. **113**, 11159 (2000).

[147] J. Casado-Pascual, M. Morillo, I. Goychuk, and P. Hänngi, "The role of different reorganization energies within the Zusman theory of electron transfer", J. Chem. Phys. **118**, 291 (2003).

[148] A. Nitzan, *Chemical Dynamics in Condensed Phases* (Oxford University Press, 2006).

[149] R. Buchner, J. Barthel, and J. Stauber, "The dielectric relaxation of water between 0 ° C and 35 ° C", Chem. Phys. Lett. **306**, 57 (1999).

[150] J. H. Klein, D. Schmidt, U. E. Steiner, and C. Lambert, "Complete Monitoring of Coherent and Incoherent Spin Flip Domains in the Recombination of Charge-Separated States of Donor-Iridium Complex-Acceptor Triads", J. Am. Chem. Soc. **137**, 11011 (2015).

[151] Z. E. Dance, Q. Mi, D. W. McCamant, M. J. Ahrens, M. A. Ratner, and M. R. Wasielewski, "Time-resolved EPR studies of photogenerated radical ion pairs separated by p-phenylene oligomers and of triplet states resulting from charge recombination", en, J. Phys. Chem. B **110**, 25163 (2006).

[152] B. E. Poling, R. C. Reid, J. M. Prausnitz, and J. P. O'Connell, *The properties of gases and liquids*. 5th ed. (McGraw-Hill, New York ; London, 2001).

[153] R. A. Kuharski, J. S. Bader, D. Chandler, M. Sprik, M. L. Klein, and R. W. Impey, "Molecular model for aqueous ferrous–ferric electron transfer", J. Chem. Phys. **89**, 3248 (1988).

[154] A. K. Manna, D. Balamurugan, M. S. Cheung, and B. D. Dunietz, "Unraveling the mechanism of photoinduced charge transfer in carotenoid-porphyrin-C60 molecular triad", J. Phys. Chem. Lett. **6**, 1231 (2015).

[155] X. Sun, P. Zhang, Y. Lai, K. L. Williams, M. S. Cheung, B. D. Dunietz, and E. Geva, "Computational Study of Charge-Transfer Dynamics in the Carotenoid-Porphyrin-C60 Molecular Triad Solvated in Explicit Tetrahydrofuran and Its Spectroscopic Signature", J. Phys. Chem. C **122**, 11288 (2018).

[156] W. Fang, R. A. Zarotiadis, and J. O. Richardson, "Revisiting nuclear tunnelling in the aqueous ferrous-ferric electron transfer", Phys. Chem. Chem. Phys. **22**, 10687 (2020).

[157] A. O. Caldeira and A. J. Leggett, "Quantum tunnelling in a dissipative system", Ann. Phys. (N. Y). **149**, 374 (1983).

[158] A. Ishizaki and Y. Tanimura, "Quantum dynamics of system strongly coupled to low-temperature colored noise bath: Reduced hierarchy equations approach", J. Phys. Soc. Japan **74**, 3131 (2005).

[159] T. C. Berkelbach, D. R. Reichman, and T. E. Markland, "Reduced density matrix hybrid approach: An efficient and accurate method for adiabatic and non-adiabatic quantum dynamics", J. Chem. Phys. **136**, 034113 (2012).

[160] J. O. Richardson, "Ring-polymer instanton theory of electron transfer in the nonadiabatic limit", J. Chem. Phys. **143**, 134116 (2015).

[161] H. Wang and M. Thoss, "Theoretical study of ultrafast photoinduced electron transfer processes in mixed-valence systems", J. Phys. Chem. A **107**, 2126 (2003).

[162] M. G. Mavros and T. Van Voorhis, "Resummed memory kernels in generalized system-bath master equations", J. Chem. Phys. **141**, 54112 (2014).

[163] Y. Tanimura and R. Kubo, "Two-Time Correlation Functions of a System Coupled to a Heat Bath with a Gaussian-Markoffian Interaction", J. Phys. Soc. Japan **58**, 1199 (1989).

[164] A. G. Dijkstra and V. I. Prokhorenko, "Simulation of photo-excited adenine in water with a hierarchy of equations of motion approach", J. Chem. Phys. **147**, 64102 (2017).

[165] Q. Shi, L. Chen, G. Nan, R. X. Xu, and Y. Yan, "Efficient hierarchical Liouville space propagator to quantum dissipative dynamics", J. Chem. Phys. **130**, 84105 (2009).

[166] Z. Gong, Z. Tang, S. Mukamel, J. Cao, and J. Wu, "A continued fraction resummation form of bath relaxation effect in the spin-boson model", J. Chem. Phys. **142**, 084103 (2015).

[167] H.-T. Chen, T. C. Berkelbach, and D. R. Reichman, "On the accuracy of the Padé-resummed master equation approach to dissipative quantum dynamics", J. Chem. Phys. **144**, 154106 (2016).

[168] N. M. Atherton, *Principles of electron spin resonance* (Ellis Horwood Limited, New York, 1973).

[169] R. Kubo, "Statistical Physics of Random Systems", J. Phys. Soc. Japan **26**, 1 (1969).

[170] J. H. Freed, G. V. Bruno, and C. F. Polnaszek, "Electron spin resonance line shapes and saturation in the slow motional region", J. Phys. Chem. **75**, 3385 (1971).

[171] A. J. Vega and D. Fiat, "Relaxation theory and the stochastic Liouville equation", J. Magn. Reson. **19**, 21 (1975).

[172] J. C. S. Lau, N. Wagner-Rundell, C. T. Rodgers, N. J. B. Green, and P. J. Hore, "Effects of disorder and motion in a radical pair magnetoreceptor", J. R. Soc. Interface **7**, S257 (2010).

[173] J. B. Pedersen, "Theory of chemically induced dynamic electron polarization. I", J. Chem. Phys. **58**, 2746 (1973).

[174] J. Pedersen, A. Shushin, and J. S. Jørgensen, "Magnetic field dependent yield of geminate radical pair recombination in micelles", Chem. Phys. **189**, 479 (1994).

[175] E. Darve, J. Solomon, and A. Kia, "Computing generalized Langevin equations and generalized Fokker-Planck equations", Proc. Natl. Acad. Sci. U. S. A. **106**, 10884 (2009).

[176] W. H. Miller, S. D. Schwartz, and J. W. Tromp, "Quantum mechanical rate constants for bimolecular reactions", J. Chem. Phys. **79**, 4889 (1983).

[177] Q. Shi and E. Geva, "A new approach to calculating the memory kernel of the generalized quantum master equation for an arbitrary system-bath coupling", J. Chem. Phys. **119**, 12063 (2003).

[178] J. E. Lawrence, T. Fletcher, L. P. Lindoy, and D. E. Manolopoulos, "On the calculation of quantum mechanical electron transfer rates", J. Chem. Phys. **151**, 114119 (2019).

[179] M. Ceriotti, "A novel framework for enhanced molecular dynamics based on the generalized Langevin equation Molecular dynamics simulations Simulation of the trajectories of a system at the atomic level", PhD thesis (2010).

[180] M. H. Peters, "The Smoluchowski diffusion equation for structured macromolecules near structured surfaces", J. Chem. Phys. **112**, 5488 (2000).

[181] S. Delong, F. Balboa Usabiaga, and A. Donev, "Brownian dynamics of confined rigid bodies", J. Chem. Phys. **143**, 144107 (2015).

[182] N. N. Lukzen, J. H. Klein, C. Lambert, and U. E. Steiner, "The Quantum Dynamical Basis of a Classical Kinetic Scheme Describing Coherent and Incoherent Regimes of Radical Pair Recombination", Zeitschrift fur Phys. Chemie **231**, 197 (2017).

[183] C. H. Wang and D. M. Grant, "Nuclear spin?lattice relaxation of coupled spin systems in liquids", J. Chem. Phys. **64**, 1522 (1976).

[184] R. Terwiel and P. Mazur, "On the theory of spin-spin relaxation", Physica **32**, 1813 (1966).

[185] A. M. Lewis, T. P. Fay, and D. E. Manolopoulos, "An efficient quantum mechanical method for radical pair recombination reactions", J. Chem. Phys. **145**, 244101 (2016).

[186] W. T. Pollard and R. A. Friesner, "Solution of the Redfield equation for the dissipative quantum dynamics of multilevel systems", J. Chem. Phys. **100**, 5054 (1994).

[187] K. Schulten and P. G. Wolynes, "Semiclassical description of electron spin motion in radicals including the effect of electron hopping", J. Chem. Phys. **68**, 3292 (1978).

[188] H. L. Stratonovich, "On Distributions in Representation Space", J. Exptl. Theor. Phys. **4**, 1012 (1957).

[189] J. C. Várilly and J. Gracia-Bondía, "The moyal representation for spin", Ann. Phys. (N. Y). **190**, 107 (1989).

[190] A. B. Klimov and P. Espinoza, "Moyal-like form of the star product for generalized SU(2) Stratonovich-Weyl symbols", J. Phys. A. Math. Gen. **35**, 8435 (2002).

[191] F. Li, C. Braun, and A. Garg, "The Weyl-Wigner-Moyal formalism for spin", EPL (Europhysics Lett. **102**, 60006 (2013).

[192] T. C. Berkelbach, T. E. Markland, and D. R. Reichman, "Reduced density matrix hybrid approach: Application to electronic energy transfer", J. Chem. Phys. **136**, 084104 (2012).

[193] A. Montoya-Castillo, T. C. Berkelbach, and D. R. Reichman, "Extending the applicability of Redfield theories into highly non-Markovian regimes", J. Chem. Phys. **143**, 194108 (2015).

[194] J. H. Fetherolf and T. C. Berkelbach, "Linear and nonlinear spectroscopy from quantum master equations", J. Chem. Phys. **147**, 244109 (2017).

[195] A. J. Schile and D. T. Limmer, "Simulating conical intersection dynamics in the condensed phase with hybrid quantum master equations", J. Chem. Phys. **151**, 014106 (2019).

[196] R. Tarroni and C. Zannoni, "On the rotational diffusion of asymmetric molecules in liquid crystals", J. Chem. Phys. **95**, 4550 (1991).

[197] M. J. Frisch, G. W. Trucks, G. E. S. H. B. Schlegel, M. A. Robb, J. R. Cheeseman, G. Scalmani, B. M. V. Barone, G. A. Petersson, H. Nakatsuji, M. Caricato, H. P. H. X. Li, A. F. Izmaylov, J. Bloino, G. Zheng, J. L. Sonnenberg, M. Had, and D. J. Fox, "Gaussian 09", Gaussian, Inc., Wallingford CT (2009).

[198] T. P. Fay, A. M. Lewis, and D. E. Manolopoulos, "Spin-dependent charge recombination along para -phenylene molecular wires", J. Chem. Phys. **147**, 064107 (2017).

[199] K. Maeda, C. J. Wedge, J. G. Storey, K. B. Henbest, P. A. Liddell, G. Kodis, D. Gust, P. J. Hore, and C. R. Timmel, "Spin-selective recombination kinetics of a model chemical magnetoreceptor", Chem. Commun. **47**, 6563 (2011).

[200] G. Andric, J. F. Boas, A. M. Bond, G. D. Fallon, K. P. Ghiggino, C. F. Hogan, J. A. Hutchison, M. A.-P. Lee, S. J. Langford, J. R. Pilbrow, G. J. Troup, and C. P. Woodward, "Spectroscopy of Naphthalene Diimides and Their Anion Radicals", Aust. J. Chem. **57**, 1011 (2004).

[201] F. Neese, "The ORCA program system", Wiley Interdiscip. Rev. Comput. Mol. Sci. **2**, 73 (2012).

[202] T. Miura, "Studies on coherent and incoherent spin dynamics that control the magnetic field effect on photogenerated radical pairs", Mol. Phys. **118**, e1643510 (2020).

[203] H. M. Hoang, V. T. B. Pham, G. Grampp, and D. R. Kattnig, "Magnetic Field-Sensitive Radical Pair Dynamics in Polymethylene Ether-Bridged Donor-Acceptor Systems", ACS Omega **3**, 10296 (2018).

[204] C. Sampson, R. H. Keens, and D. R. Kattnig, " On the magnetosensitivity of lipid peroxidation: two- versus three-radical dynamics ", Phys. Chem. Chem. Phys. **21**, 13526 (2019).

[205] B. M. Schulze, D. L. Watkins, J. Zhang, I. Ghiviriga, and R. K. Castellano, "Estimating the shape and size of supramolecular assemblies by variable temperature diffusion ordered spectroscopy", Org. Biomol. Chem. **12**, 7932 (2014).

[206] H. Hayashi and S. Nagakura, "Theoretical Study of Relaxation Mechanism in Magnetic Field Effects on Chemical Reactions", Bull. Chem. Soc. Jpn. **57**, 322 (1984).

[207] T. Miura, K. Maeda, and T. Arai, "The spin mixing process of a radical pair in low magnetic field observed by transient absorption detected nanosecond pulsed magnetic field effect", J. Phys. Chem. A **110**, 4151 (2006).

[208] K. Maeda, T. Miura, and T. Arai, "A practical simulation and a novel insight to the magnetic field effect on a radical pair in a micelle", Mol. Phys. **104**, 1779 (2006).

[209] T. Miura and H. Murai, "Real-time observation of the spin-state mixing process of a micelttzed radical pair in weak magnetic fields by nanosecond fast field switching", J. Phys. Chem. A **112**, 2526 (2008).

[210] M. Mojaza and J. Boiden Pedersen, "Kinetic models in spin chemistry. 1. The hyperfine interaction", Chem. Phys. Lett. **535**, 201 (2012).

[211] T. P. Fay and D. E. Manolopoulos, "Radical pair intersystem crossing: Quantum dynamics or incoherent kinetics?", J. Chem. Phys. **150**, 151102 (2019).

[212] D. E. Manolopoulos and P. J. Hore, "An improved semiclassical theory of radical pair recombination reactions", J. Chem. Phys. **139**, 124106 (2013).

[213] S. H. Koenig, "Brownian motion of an ellipsoid. A correction to Perrin's results", Biopolymers **14**, 2421 (1975).

[214] S. Hagi, K. Kato, M. Hinoshita, H. Yoshino, E. Shikoh, and Y. Teki, "Low-magnetic field effect and electrically detected magnetic resonance measurements of photocurrent in vacuum vapor deposition films of weak charge-transfer pyrene/dimethylpyromellitdiimide (Py/DMPI) complex", J. Chem. Phys. **151**, 244704 (2019).

[215] J. A. Hughes, S. J. O. Hardman, N. S. Scrutton, D. M. Graham, J. R. Woodward, and A. R. Jones, "Observation of the Δ g mechanism resulting from the ultrafast spin dynamics that follow the photolysis of coenzyme B 12", J. Chem. Phys. **151**, 201102 (2019).

[216] V. A. Bagryansky, V. I. Borovkov, A. O. Bessmertnykh, I. S. Tretyakova, I. V. Beregovaya, and Y. N. Molin, "Interaction of spin-correlated radical pair with a third radical: Combined effect of spin-exchange interaction and spin-selective reaction", J. Chem. Phys. **151**, 224308 (2019).

[217] H. G. Hiscock, T. W. Hiscock, D. R. Kattnig, T. Scrivener, A. M. Lewis, D. E. Manolopoulos, and P. J. Hore, "Navigating at night: fundamental limits on the sensitivity of radical pair magnetoreception under dim light", Q. Rev. Biophys. **52**, e9 (2019).

[218] D. Kobylkov, J. Wynn, M. Winklhofer, R. Chetverikova, J. Xu, H. Hiscock, P. J. Hore, and H. Mouritsen, "Electromagnetic 0.1–100 kHz noise does not disrupt orientation in a night-migrating songbird implying a spin coherence lifetime of less than 10 μs", J. R. Soc. Interface **16**, 20190716 (2019).

[219] O. Efimova and P. J. Hore, "Role of exchange and dipolar interactions in the radical pair model of the avian magnetic compass", Biophys. J. **94**, 1565 (2008).

[220] N. S. Babcock and D. R. Kattnig, "Electron–Electron Dipolar Interaction Poses a Challenge to the Radical Pair Mechanism of Magnetoreception", J. Phys. Chem. Lett. **11**, 2414 (2020).